

Ecophysiological monitoring of native and foreign Oaks in Central Europe, introduced
in the framework of proactive climate change mitigation

Dissertation

zur Erlangung des Doktorgrades

der Naturwissenschaften

vorgelegt beim Fachbereich 15

der Johann Wolfgang Goethe-Universität

in Frankfurt am Main

von

Stefan Koller

aus Frankfurt am Main

Frankfurt 2015

(D 30)

vom Fachbereich 15 der

Johann Wolfgang Goethe - Universität als Dissertation angenommen.

Dekan:

Gutachter:

Datum der Disputation:

Table of Contents

Abstract.....	1
Zusammenfassung	5
1. Introduction.....	11
1.1. Influence of climate change on forest habitats.....	11
1.2. The role of chlorophyll in vitality monitoring	14
1.3. Research objective	21
2. Materials & Methods.....	22
2.1. Investigation area	22
2.2. Monitoring of morphological and chemical leaf traits.....	25
2.2.1. Calculation of morphological leaf traits.....	27
2.2.2. Determination of leaf pigment concentrations	28
2.2.3. Determination of leaf nitrogen concentrations.....	29
2.3. Non-invasive sensing of chemical leaf traits	30
2.3.1. Assessment of SPAD-reading variability concerning application	31
2.4. Seasonal monitoring of chlorophyll content and PS II functionality.....	33
2.5. Stress response analyses.....	36
2.5.1. Drought stress.....	36
2.5.2. Heat stress	43
2.5.3. Cold stress in <i>Q. ilex</i>	47
3. Results.....	51
3.1. Investigation area	51
3.1.1. Climate at Frankfurt Schwanheim in 2012 and 2013.....	51
3.1.2. Spatial distribution of abiotic growth factors at FR	52
3.2. Monitoring of morphological and chemical leaf traits.....	55
3.2.1. Monitoring of morphological leaf traits	55
3.2.2. Monitoring of chemical leaf traits.....	60
3.3. Non-invasive sensing of chemical leaf traits	63
3.3.1. Assessment of SPAD-reading variability concerning application	71
3.4. Seasonal monitoring of chlorophyll content and PS II functionality.....	77
3.4.1. Seasonal variability of chlorophyll content.....	77
3.4.2. Seasonal variability of photosystem II functionality	82
3.4.3. Relationship between JIP-test parameters.....	87
3.4.4. Relationship between SPAD-readings and JIP-test parameters.....	89

Table of Contents

3.5. Stress response analyses	91
3.5.1. Drought stress	91
3.5.2. Heat stress	99
3.5.3. Cold stress in <i>Q. ilex</i>	103
4. Discussion.....	111
4.1. Investigation areas	111
4.2. Monitoring of morphological and chemical leaf traits	113
4.3. Non-invasive sensing of chemical leaf traits	120
4.4. Seasonal monitoring of chlorophyll content and PS II functionality	128
4.5. Stress response analyses	140
4.5.1. Drought stress	140
4.5.2. Heat stress	145
4.5.3. Cold stress in <i>Q. ilex</i>	148
5. Conclusion and Outlook	153
References	157
List of Figures	171
List of Tables.....	173
List of abbreviations.....	174
Appendix	177
Lebenslauf	186
Danksagung.....	190

Abstract

Even for moderate future CO₂ emission scenarios, the Intergovernmental Panel on Climate Change (IPCC) predicts a high probability of a mean annual temperature increase by several degrees in Central Europe, with a higher probability of summer droughts and heat waves for the next century. These changes could have a large impact on the physiological performance, vulnerability and productivity of trees in Central Europe. Along with these climatic changes, potential ranges of European tree species are expected to shift. Less area is suspected to support optimal growth and vitality for beech, spruce and pine and may be better suited for the more drought tolerant oaks. But in some areas of Germany, where native pedunculate (*Quercus robur*) and sessile oak (*Q. petraea*) already represent a large portion of broadleaf tree vegetation, increased vitality losses are noted and expected to increase in the future. In Southern Hesse, the predicted climate change may even provide a potential habitat for Mediterranean Oak species. A passive strategy, awaiting natural seed dispersal to fill in climate change induced losses is rejected by all decision makers in favour of proactive actions to transition smoothly from prone to resilient stands in the future. However, species and species mixtures are going to be assessed, for which practical experience is currently low or missing. Tools and Methods which allow a fast and comparative evaluation of plant photosynthetic performance are valuable aids for forestry management.

Against this background, experimental forest plots have been established in Southern Hesse, where local (*Quercus robur*), Mediterranean (*Q. pubescens*, *Q. frainetto*, *Q. ilex*) and a recommended North American oak species (*Q. rubra*) have been planted. The vitality of individual trees has to be evaluated to comparatively assess how species, provenances and/or individuals cope with environmental and silvicultural induced influences at different localities, in order to provide the ability to make adjustments. Decrease of vitality is usually correlated to a decrease in photosynthetic performance on different temporal scales. If unfavourable conditions persist, adjustments are made to decrease the amount of absorbed and transferred energy, measurable as total or relative pigment decreases and/or alterations of chlorophyll (Chl) fluorescence yields. Methods to non-destructively quantify relative pigment contents and to record chlorophyll fluorescence transients have become available for field use. The application of the methods has been shown to be greatly beneficial in the estimation

of leaf chlorophyll content and compounds closely correlated to the pigments quantity (e.g. nitrogen) as well as in the assessment of plant vitality decreases in a number of species, (mostly agriculturally and horticulturally used crops) exposed to numerous abiotic and biotic stresses. However, research has shown that the radiometric signals used for the non-destructive determination of light harvesting capacity (measurement of light transmittance by a Chl-meter: SPAD-502) and photosynthetic performance [measurement of the fast Chl fluorescence transient: “Plant Efficiency Analyser (PEA)] are not readily applicable, show high species specific variability and results obtained for one species may not be simply transferred to another. Systematic investigations allowing the application of these non-destructive methods in oaks, which could serve as future forest trees in Central Europe, have not been carried out.

Within the presented thesis, oak taxa with a great variability of morphological leaf traits and life strategies were monitored in two week intervals for a duration of 2 years with the aim to enable the application of the methods in the comparative assessment of plant vitality and to detect the interspecific differences and seasonal dynamics of leaf morphological and leaf chemical traits as well as the influence of environmental stresses on the radiometric sensing of the chlorophyll content (with its associated relationship to other chemical leaf compounds like nitrogen) and the photochemical performance. Leaf samples were taken and analysed to investigate the absolute/optical (sensu PARRY *et al.* 2014) pigment relationship, the influence of morphological leaf traits on the non-destructive measurement of light transmission in the red and infrared portion of the electromagnetic spectrum and the species-specific correlation of chlorophyll to nitrogen for its indirect quantification. Controlled and semi-controlled experiments in climate chambers, climate cabinets and greenhouses were conducted to investigate if a species-specific variability in the response to heat and drought stress was present, how they affect the photosynthetic performance of the species and how they influence the recorded radiometric signals. In order to investigate the performance of the evergreen Holm Oak (*Q. ilex*) under Central European winter conditions and its response to cold stress, an additional 6 month monitoring program was conducted in the winter of 2012/2013. Measurements concerning the in-field use and applicability of optical chlorophyll sensing, providing reference values and guidelines regarding its utilisation complete the investigations.

The key morphological leaf traits, concerning the ratios of leaf mass to leaf area and leaf dry mass to its saturated fresh mass were found to significantly differ between the *Quercus* taxa planted 2011 in Southern Hesse. In order to complement the data obtained from *Q. robur*, *Q. frainetto*, *Q. ilex*, *Q. pubescens* and *Q. rubra*, morphological leaf traits of the deciduous Mediterranean Oak *Q. cerris*, the evergreen Cork Oak *Q. suber* and the two semi-evergreen hybrids *Q. x turneri* (*Q. robur* x *Q. ilex*) and *Q. x hispanica* (*Q. suber* x *Q. cerris*) were additionally included in the analysis. The key leaf morphological traits were found not to group according to their evergreen or deciduous leaf type, instead they represented a continuum spanning from the native *Q. robur* (and *Q. rubra*) on one end of the spectrum to the evergreens *Q. ilex* and *Q. suber* on the other end with the Mediterranean deciduous and semi-deciduous taxa in between. Increased ratios of leaf mass per area were accompanied by increases in leaf thickness, which was found to be assessable by its proportional ratio of saturated fresh mass to leaf area. The interspecific differences in the morphological leaf traits, which were found to reach a steady state after a leaf development in spring and early summer and no further alterations towards the end of the growing season, significantly influenced the relationship of pigment and nitrogen contents to its optical estimation by the SPAD Chl-meter, when values were mass based. Referring pigments on the base of their leaf area and correcting mass based nitrogen contents with the ratio of leaf area to leaf dry mass, resulted in absolute/optical Chl relationships with no developmental or species specific influence. The relationships were found to be non-linear (attributed to optical effects resulting from the spatial heterogeneity of Chl within the leaf), and best fit by a second order polynomial regression and a homographic model. Single species calibration equations and a global model for all taxa with its best-fit parameters and coefficients of determinations are given, allowing for the quantitative estimation of area based total chlorophyll, Chl a, Chl b, total carotenoids and total leaf nitrogen contents from non-destructively measurable SPAD-readings during all stages of leaf development in *Quercus*, which was not possible up to date. From the seasonal dynamics of leaf chlorophyll concentration, distinct phases were derived, marking the chlorophyll increase during leaf development, a steady state phase with low variability during the so called “core vegetation time” and a chlorophyll decrease during leaf senescence. Phase transitions varied between individuals of the same species and among species, leading to differences in potential annual carbon gains. Changes of fluorescence

Abstract

parameters derived from the predawn recording of fast Chl fluorescence induction transients (OJIP) were associated to developmental changes in pigment content. During leaf development and senescence, low chlorophyll contents were associated with a lower maximal fluorescence yield. Full transient analysis revealed additional fluorescence increases at ~1-9 ms, associated with a decrease of Q_A^- re-oxidation. Thus trapped energy is dissipated effectively at an early step in the electron transport chain, decreasing the risk of a high electron pressure at times of sufficient absorption by chlorophylls but low photosynthetic capacity. The plants' leaf chlorophyll concentrations during the core vegetation time were found to be significantly correlated between consecutive years, indicating conserved limitations with a spatial influence, relevant to multi-year assessments. Leaf chlorophyll concentrations differed significantly among the species, which needs to be considered in comparisons of different species. The fluorescence parameter F_v/F_m , representing the maximum quantum yield of primary photochemistry, is most often used as an indicator of decreased vitality, since it decreases under multiple stresses. A correlation of a large number of OJIP transient derived parameters, recorded over a wide range of physiological conditions, revealed a generally late response of F_v/F_m and earlier alterations of parameters that include fluorescence yields of the early rise and at the intermittent J- and I-steps of the transient. Thus changes of the shape of the induction curve, apart from decreases of maximal- or increases in ground fluorescence, may be determined by the time-resolved recording of transient data and the subsequent calculation of RC/ABS, ψ_{E0} and PI_{abs} (which are related but responded to different degrees). Stresses induced through drought, heat or cold may influence this relationship as shown for *Q. ilex* under winter conditions. Besides, alterations of Chl fluorescence yields can occur, which are decoupled from changes in total leaf chlorophyll content. Stress may further alter the relationship of Chl-meter readings and biochemical compounds which are only indirectly associated to the measured total chlorophyll content.

In the framework of this research thesis, models for the prediction of leaf pigment- and nitrogen contents from optical data, alterations of photosynthetic functionality, and reference data were provided, allowing for the use and classification of non-destructive, optical methods in *Quercus*-Taxa for the comparative assessment of plant vitality under Central European conditions.

Zusammenfassung

Der Weltklimarat (IPCC) prognostiziert bis zum Ende des Jahrhunderts eine Erhöhung der Jahresmitteltemperatur sowie eine erhöhte Wahrscheinlichkeit für das Auftreten von Wetterextremen wie Dürreperioden und Hitzewellen. Diese Veränderungen des mitteleuropäischen Klimas werden einen großen Einfluss auf die physiologische Leistungsfähigkeit, Schadanfälligkeit und Produktivität von Waldbäumen ausüben. Damit einhergehend wird eine Verschiebung von potentiellen Verbreitungsgebieten europäischer Waldbäume angenommen. Es wird erwartet, dass größere Flächenanteile, die gegenwärtig ein optimales Wachstum und eine hohe Vitalität der Buche unterstützen, in Zukunft besser für die trockenoleranteren Eichen geeignet sein werden. In einigen Gebieten Deutschlands mit trockenwarmen Regionalklima, in denen einheimische Eichenarten wie die Stieleiche (*Quercus robur*) und die Traubeneiche (*Q. petraea*) derzeit bereits einen großen Anteil von Laubbäumen stellen, treten jedoch bereits Schäden auf. Deren weitere Zunahme ist auf Basis von Klimaszenarien in der Zukunft zu erwarten. Prognosen auf der Basis moderater Klimaszenarien weisen die Region Südhessen als potentielles Verbreitungsgebiet mediterraner Eichenarten aus. Eine passive Strategie, welche den Verlust geschädigter Bäume durch eine natürliche Ausbreitung von klimatisch besser angepassten Baumarten abwartet, wird von den Entscheidungsträgern aller Bundesländer abgelehnt. Eine proaktive Handlungsweise wird empfohlen, welche Schad anfällige und leistungsschwache Waldstandorte in belastbarere Flächen umwandeln soll. Bisher gibt es jedoch kaum Erfahrungen mit Hinblick auf die prognostizierten Veränderungen des Klimas und der Einführung gebietsfremder Arten in Mischbeständen.

Methoden, die eine schnelle und vergleichbare Evaluierung der photosynthetischen Leistungsfähigkeit von Bäumen erlauben, sind für waldbauliche Steuerungen wertvolle Hilfestellungen. Vor diesem Hintergrund wurden in Südhessen experimentelle Versuchsflächen etabliert, auf denen neben der heimischen Stieleiche *Q. robur*, verschiedene mediterrane Eichen in ihrem prognostizierten potentiellen Verbreitungsgebiet sowie die nordamerikanische Roteiche (*Q. rubra*) gepflanzt wurden. Mit Hilfe von vergleichenden Vitalitätsbestimmungen an Einzelbäumen könnte die Eignung von verschiedenen Arten, Herkünften einer Art sowie individuellen Bäumen

am jeweiligen Standort, wie auch ihre jeweilige Bewältigung von Stressperioden und waldbaulichen Maßnahmen bemessen werden. Eine Vitalitätsabnahme ist in der Regel mit einer Abnahme der photosynthetischen Leistungsfähigkeit korreliert. Länger anhaltende, ungünstige Bedingungen führen daher zu Anpassungen, die die Energieaufnahme oder ihre Weiterleitung reduzieren. Dies kann anhand von Pigmentverlusten, veränderten Pigmentverhältnissen oder auch in Veränderungen der abgestrahlten Fluoreszenz von Chlorophyll (Chl) beobachtet werden. Methoden zur zerstörungsfreien, radiometrischen Bestimmung von Pigmentgehalten und zur Aufnahme von Fluoreszenztransienten sind für Messungen unter Freilandbedingungen verfügbar. Bisherige Studien zeigten, dass die Anwendung solcher Methoden für eine Bestimmung des relativen Chl Gehaltes und mit Chl assoziierten Komponenten in der Evaluierung von Vitalitätsveränderungen in einer Vielzahl von Pflanzenarten (meist landwirtschaftliche und gartenbauliche Nutzpflanzen) und diversen Umwelteinflüssen von großem Nutzwert sein kann. Die Forschungen verdeutlichen aber auch, dass die Transmissionsmessungen für die zerstörungsfreie Bestimmung der Lichtsammelkapazität eines Blattes (mittels eines Chlorophyllmeters: SPAD-502) und die Aufnahme der schnellen Fluoreszenzkinetik zur Bestimmung der Funktionalität des Photosyntheseapparates [mittels des "Plant Efficiency Analyser" (PEA)] nicht ohne weiteres anwendbar sind, oft eine hohe artspezifische und saisonale Variabilität aufzeigen und dass Ergebnisse an einer Art nicht unmittelbar auf andere Arten übertragbar sind. Untersuchungen, welche die Anwendung dieser Methoden für Eichenarten in Mitteleuropa ermöglichen könnten, wurden bisher noch nicht durchgeführt.

In der hier vorgelegten Forschungsarbeit wurden Eichentaxa mit einem hohen Maß an blattspezifischer Merkmalsvariabilität in zweiwöchigen Intervallen über eine Dauer von zwei Jahren beobachtet und beprobt. Ziel war es, die interspezifischen Unterschiede und die jahreszeitliche Dynamik von morphologischen und chemischen Blattmerkmalen sowie die Beeinflussung der radiometrischen Bestimmung des Chlorophyllgehaltes (und damit assoziierten Komponenten wie z.B. Blattstickstoffgehalt) und der photosynthetischen Funktionalität durch Umweltbelastungen in Eichen zu untersuchen. Die Analyse der Blattproben zielte neben der Bestimmung der Beziehung zwischen absoluten und optisch ermittelten Pigmentgehalten auf die Ermittlung des Einflusses der Blattstruktur auf die Lichttransmission im roten und

infrarotem Bereich des Elektromagnetischen Spektrums ab, sowie auf die artspezifische Korrelation von Blattstickstoff zu Blattchlorophyll und dessen indirekte Quantifizierung. Des Weiteren wurden Versuche zur Trocken- und Hitzestressanpassung unter kontrollierten und halbkontrollierten Bedingungen in Klimakammern, Klimaschränken und Treibhäusern durchgeführt, um eine potentiell artspezifische Stressantwort, sowie eine mögliche Beeinflussung der aufgenommenen radiometrischen Messwerte zu ermitteln. Ein zusätzliches Monitoringprogramm im Winter 2012/2013 mit einer Dauer von sechs Monaten ermöglichte die Überprüfung der Anpassungsfähigkeit der immergrünen Steineiche (*Q. ilex*) auf mitteleuropäische Winterbedingungen und die Veränderung der photosynthetischen Funktionalität unter Kältestress. Messungen im Zusammenhang mit der praktischen Anwendbarkeit der zerstörungsfreien, optischen Methode und zur Bereitstellung von Referenzdaten für zukünftige Evaluierungen komplementieren die Untersuchungen.

Signifikante, artspezifische Unterschiede wurden in den blattmorphologischen Schlüsselmerkmalen (welche das Verhältnis von Blattmasse zu Blattfläche und von Trocken- zu gesättigtem Frischgewicht quantifizieren) in den *Quercus*-Arten ermittelt, die im Jahr 2011 in Südhessen auf einer Versuchsfläche in Frankfurt Schwanheim angepflanzt worden waren. Um die Daten dieser fünf Eichenarten (*Q. robur*, *Q. frainetto*, *Q. ilex*, *Q. pubescens* und *Q. rubra*) zu ergänzen, wurden zusätzliche morphologische Analysen für die mediterran verbreitete und laubwerfende Zerreiche (*Q. cerris*), die immergrüne Korkeiche (*Q. suber*) und zwei Hybriden aus immergrünen und laubwerfenden Arten *Q. x turneri* (*Q. robur* x *Q. ilex*) und *Q. x hispanica* (*Q. suber* x *Q. cerris*) aufgenommen. Eine Auflistung der morphologischen Schlüsselmerkmale ergab keine eindeutige Gruppierung anhand der Blatt-Lebensdauer in laubwerfende und immergrüne Blatttypen. Vielmehr ordneten sich die Werte in kontinuierlichen Abstufungen zwischen den jeweiligen Extremen, d.h. den immergrünen Eichenarten und *Q. robur* / *Q. rubra*. Aus blattökonomischer Sicht nimmt der Anteil der investierten Biomasse pro lichteinfangender Fläche von der heimischen *Q. robur* und der nordamerikanischen *Q. rubra* über die mediterranen laubwerfenden Eichen zu den immergrünen Arten deutlich zu. Zunahmen im Verhältnis von Blattmasse zu Blattfläche wurden von erhöhten Blattdicken begleitet, welche durch das dazu proportionale Verhältnis von gesättigtem Frischgewicht zur Blattfläche in allen untersuchten Eichenarten bestimmt werden kann. Die artspezifischen Unterschiede in den

morphologischen Blattmerkmalen, die einen Gleichgewichtszustand im Anschluss an die Blattentwicklung im Frühling einnahmen und sich gegen Ende der Vegetationsperiode nicht weiter veränderten, beeinflussten auf signifikante Weise die Beziehung zwischen absoluten, massebasierten Pigment- und Stickstoffgehalten und deren radiometrischen Bestimmung. Wurden die Pigmentgehalte hingegen auf die Blattfläche bezogen und die Stickstoffgehalte mittels des Verhältnisses von Blattfläche zu Trockenmasse korrigiert, zeichnete sich eine Beziehung zwischen absoluten und optisch ermittelten Werten ab, der jegliche jahreszeitliche oder artspezifische morphologische Variabilität fehlte und die somit für alle *Quercus*-Taxa anwendbar ist. Der Zusammenhang zwischen den absolut gemessenen Pigment- und Stickstoffgehalten und den optisch ermittelten Werten folgte einer nicht-linearen Beziehung, welche optischen Effekten, resultierend aus der räumlichen Heterogenität von Chlorophyll im Blatt, zugeschrieben und am geeignetsten von einer polynomischen Funktion zweiter Ordnung, sowie einem homographischen Modell beschrieben wurde. Koeffizienten für die Berechnung von flächenbezogenen Gehalten von Gesamtchlorophyll, Chl a, Chl b und Carotinoiden für die jeweiligen *Quercus*-taxa, wie auch für ein artübergreifendes Modell wurden ermittelt, um die Berechnung dieser Komponenten anhand von zerstörungsfrei messbaren SPAD-Werten während aller Entwicklungsstufen zu ermöglichen. Aus der jahreszeitlichen Entwicklung der Pigmentgehalte konnten drei deutliche Phasen abgeleitet werden, die der Blattentwicklung im Frühling, einer Plateauphase mit geringen Veränderungen ("core vegetation time") und dem Pigmentabbau während der Herbstlaubfärbung entsprechen. Die jeweiligen Phasenübergänge variierten zum Teil erheblich zwischen einzelnen Individuen einer Art sowie zwischen den Arten, was Unterschiede in der potentiellen, jährlichen Kohlenstoffaufnahme nach sich zieht. Entwicklungsabhängige Veränderungen des Pigmentgehalts waren verknüpft mit Änderungen in der Ausprägung der schnellen Fluoreszenzkinetik (OJIP), welche für eine bessere Vergleichbarkeit jeweils vor Sonnenaufgang aufgezeichnet wurden. In Phasen mit geringen Blattchlorophyllgehalten wurden auch geringere Werte für die maximale Fluoreszenzausbeute aufgezeichnet. Analysen der gesamten Fluoreszenzkinetik wiesen jedoch während der Blattentwicklung und der Seneszenz zusätzliche Anstiege der Fluoreszenz in einem Bereich von ~1-9 ms auf, die mit einer Abnahme der Q_A^- Re-oxidation in Verbindung gebracht wird. Absorbierte und weitergeleitete Energie kann somit effektiv in einem

frühen Stadium des Elektronentransports abgeführt werden, was das Risiko eines erhöhten Elektronendrucks in Zeiten ausreichender Lichtaufnahme, aber geringer photosynthetischer Kapazität, verhindert. Es wurde gezeigt, dass Pigmentgehalte, die während der Plateauphase eines Jahres ermittelt wurden, signifikant mit den Pigmentgehalten aus dem Folgejahr korrelierten, was nachhaltige Limitierungen mit räumlichen Bezug vermuten lässt und für mehrjährige Evaluierungsprogramme von Relevanz ist. Absolute Pigmentkonzentrationen wiesen zudem einen signifikanten, artspezifischen Unterschied auf, was in der Bewertung artübergreifender Vergleiche berücksichtigt werden muss. Der am häufigsten genutzte Fluoreszenzparameter F_v/F_m , welcher die maximale Quantenausbreite der primären Photochemie beschreibt, wird zur Quantifizierung von Vitalitätseinbußen eingesetzt, da seine Abnahme unter einer Vielzahl von Stressbedingungen nachgewiesen wurde. Eine Korrelation unterschiedlicher Fluoreszenzparameter, die aus Veränderungen der Form des OJIP Transienten abgeleitet werden können und über einen großen Bereich physiologischer Zustände in den unterschiedlichen Eichenarten aufgezeichnet wurden, zeigte jedoch eine allgemein späte Reaktion von F_v/F_m hin, sowie auf eine höhere Sensitivität von Parametern, die Informationen aus der anfänglichen Steigung der J- und der I- Stufe des OJIP Transienten einbeziehen. Hier sind vor allem die Parameter RC/ABS, ψ_{E0} und der Performance Index PI_{abs} zu nennen, die miteinander in Beziehung stehen und in unterschiedlichem Maße einander beeinflussen. Stressbedingungen, wie Hitze-, Kälte- oder Trockenstress, können einen Einfluss auf diese Beziehung ausüben, wie anhand der Analyse der Fluoreszenztransienten von *Q. ilex* unter Kältestress beobachtet wurde. Des Weiteren können Stressbedingungen zu Veränderung von Fluoreszenzparametern ohne einer gleichzeitigen Änderung des Pigmentgehaltes führen, wie auch die indirekte Bestimmung von mit Chl assoziierten Komponenten (Carotinoide, Chl a, Chl b) mittels optischer Bestimmung (durch die Veränderungen von Pigmentverhältnissen) beeinflussen. Es konnten Modelle zur Berechnung von Blattpigmenten und Blattstickstoff aus optischem Messdaten, Veränderungen der photosynthetischen Funktionalität, sowie Referenzdaten hinsichtlich artspezifischer und jahreszeitlicher Variabilität unter mitteleuropäischen Umweltbedingungen ermittelt werden, die eine Nutzung und Einordnung von zerstörungsfreien optischen Messwerten zur Ermittlung von Vitalitätsunterschieden in Eichen ermöglichen

1. Introduction

“The greatest oak was once a little nut, which held its ground”

The greatest oaks hold their ground since the first managerial interventions were executed in the 14th century and underwent different forest (ab)uses until today, since oaks count to the long-lived species of trees. In forestry and silviculture, trees are planted for a harvest by future generations with the knowledge obtained by past generations. Only recently, tools have become available to provide sound predictions of climatic conditions of the future affecting forest health, which need to be taken into consideration, when stands are newly timbered. But the vitality of a tree is a complex trait, dependent on a number of biotic and abiotic factors, with large spatial variability and not integratively predictable. Thus different silvicultural strategies and species mixtures will be necessary to mitigate the effect of climate change on forest stands in Central Europe and to transition smoothly from today's prone to resilient stands in the future. On a number of experimental sites and stands, trees of different species, native and introduced, are planted now. Methods are needed to additionally assess the vitality of young trees and their response to environmental changes and managerial modifications to ensure that fast adjustments can be made. In order to provide a quantification of plant fitness and vitality by determining stress induced pigment changes and limitations to photosynthesis, influential factors on non-destructive, radiometric methods were investigated in today still foreign oak species, which might develop to great oaks in the future as long as they can manage to hold their ground.

1.1. Influence of climate change on forest habitats

The physiological performance, vulnerability and productivity of trees in their environment are influenced by the climate and the occurrence of environmental stresses. Different climate change scenarios are being calculated with immense effort in order to estimate abiotic factors like temperature and precipitation for the next century (CHRISTENSEN *et al.* 2013, KOVATS *et al.* 2014). Knowledge of the tendency of change and its timeframe allows for proactive actions in order to mitigate its effects. These actions are especially urgent for long living organisms like trees, for which rotation times for timber production mostly exceed 100 years. The Intergovernmental Panel on

Introduction

Climate Change (IPCC) predicts an increase in the mean annual temperature for the future Central European climate with a higher probability of summer droughts and heat waves (CHRISTENSEN *et al.* 2013). HANEWINKEL *et al.* (2013) calculated the potential ranges of European tree species on the basis of distribution data from the international monitoring network in Europe (FISCHER *et al.* 2010) as well as the expected shifts of these ranges under a moderate climate warming scenario until 2100 (Figure 1). The potential ranges are predicted to drastically change in the near future, leading to large impacts on spruce and pine in particular. The range of beech is also expected to decrease, being replaced mainly through oak, which is better adapted to drier

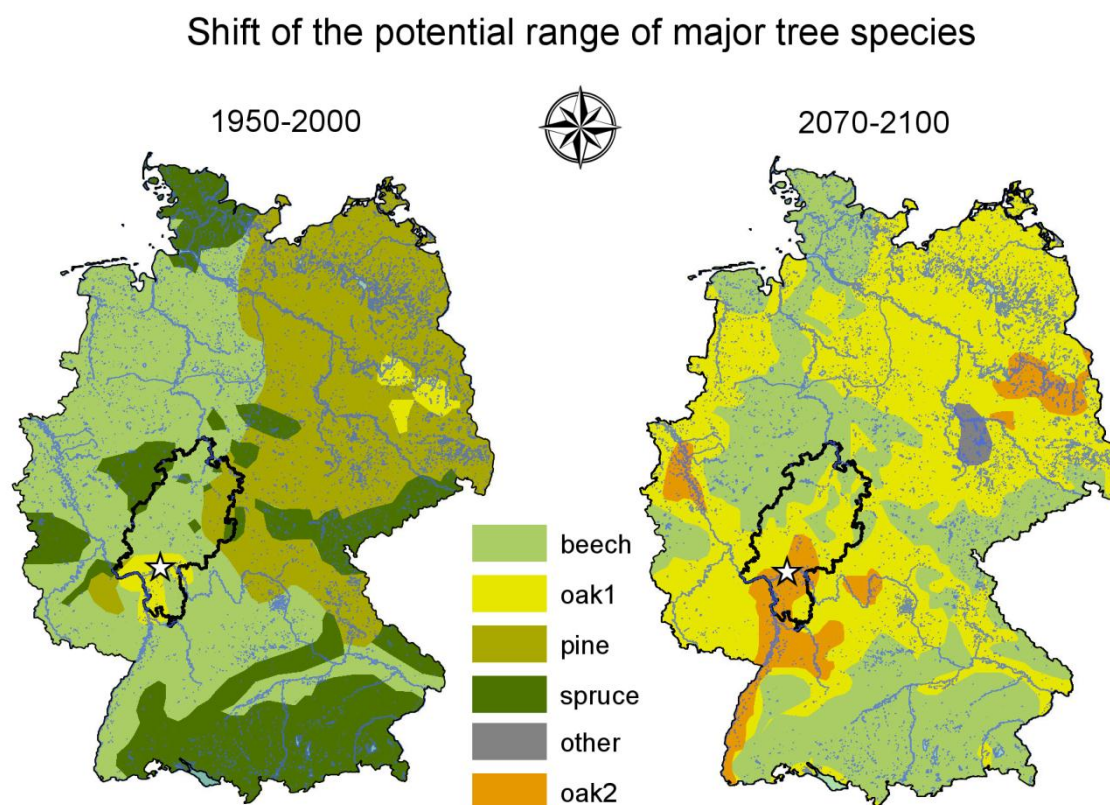


Figure 1: Shift of the potential range of major tree species in Germany. Map redrawn and modified from HANEWINKEL *et al.* 2013. Present climate envelopes for major tree species were calibrated on basis of ICP Forest plots (FISCHER *et al.* 2010) using variables derived from the WordClim climate database (HIJMANS *et al.* 2005) for the normal period of 1950-2000. Range shift in 2070-2100 was modelled for a moderate warming according to the A1B scenario (SOLOMON *et al.* 2007). Federal state of Hesse is highlighted and experimental forest plot in Frankfurt Schwanheim is indicated by a white star. Beech: *Fagus sylvatica*; Oak 1: *Quercus robur*, *Q. petraea*; Pine: *Pinus sylvestris*, *P. nigra*, *P. pinaster*; Spruce: *Picea abies*; Oak 2: *Quercus cerris*, *Q. frainetto*, *Q. ilex*, *Q. pubescens*, *Q. pyrenaica*, *Q. suber*; Other: none of the above. Modifications to HANEWINKEL *et al.* (2013) consist in showing potential range shifts for Germany only, with added state borders and water bodies from a digital landscape model (DLM) ©GeoBasis-DE BKG 2015, (<http://www.bkg.bund.de>). Map coordinate system: WGS 1984 UTM Zone 32U, Projection: Transverse Mercator. Date: WGS 1984.

conditions (ELLENBERG 1996). In parts of Germany, mainly along the Upper Rhine valley and the Rhine-Main region in southern Hesse, the predicted climate changes were found to provide a potential habitat for Mediterranean oaks, deciduous as well as evergreen (HANEWINKEL *et al.* 2013). However, the named tree species are not only viable within their potential ranges and a range shift should not be necessarily associated with a species loss. However, if trees grow on the edge or outside of their potential range, decreases in plant vigour and a higher susceptibility to abiotic and biotic stresses are probable.

Vitality losses and increased crown dieback are already occurring in southern Hesse, where the mean temperature is higher compared to other regions in Germany and the water balance in summer is found to be increasingly negative (DWD 2015, Figure 49). The Rhine-Main conurbation is seen as one of the regions in Central Europe in which forest management faces major challenges, today and in the future (NW-FVA 2013). Decreasing ground water tables and concomitant drought stress since the 1970s have gradually weakened large forest areas, in which forest dieback is now evident (NW-FVA 2013). According to the latest Hessian report on the state of the forest (HMUELV 2014), forests in the Rhine-Main region are deteriorating with a relative crown thinning in oak being twice as high as compared to other regions in Hesse. In pine, mistletoe infestations strongly increased with infestations in over one third of the pines. Further increases in drought stress were modelled for forests in southern Hesse for the near future (NW-FVA 2013), and silvicultural intervention through forest conversion, species mixture and the introduction of species, better adapted to the dry environment, were proposed for such regions (BOLTE *et al.* 2009, GLATZER & SCHRAMM 2010, BUSSOTTI *et al.* 2015). There is a significant debate in forestry, concerning the origin of the species to be introduced (KÖLLING 2007, BMUB 2008, BOLTE *et al.* 2009). Besides European species, non-native species from other continents are proposed (BOLTE *et al.* 2009, SCHMIEDINGER *et al.* 2009), with unknown impact on European ecosystems. Against this background, three experimental forest plots were established in southern Hesse (South Hesse Oak Project, cf. KOLLER *et al.* 2014), where Mediterranean Oak species (including *Quercus pubescens*, native in south-west Germany), fitting the future potential range (cf. Figure 1), were planted alongside with local *Q. robur*. In two of the three sites, *Q. rubra* of North American origin, introduced to Europe in 1724 (MORE & WHITE 2002) was added, since the species has been

Introduction

proposed in the region as a substitute species on threatened oak stands (NW-FVA 2013). These Common Garden type experimental plots allow to comparably investigate species-specific responses to Central European climate on the morphological, physiological and phenological level, to screen for well adapted species and to establish as well as to evaluate new methods in the assessment of stress and vitality decreases. BUSSOTTI *et al.* (2015) listed key functional traits to utilize in the screening for well suited species in the framework of climate change adaptations with associated increases in dry conditions. These key functional traits are, apart from growth and survival:

- morphological traits, mainly area to mass ratios
- chemical traits, mainly leaf chlorophyll and nitrogen contents
- phenological traits, like leaf flushing and senescence
- photosystem II functioning
- and photosynthetic capacity under water shortage

1.2. The role of chlorophyll in vitality monitoring

Stress is defined as an unfavourable condition (abiotic, biotic or anthropogenic in nature), which leads to a change in homeostasis, requiring a plant's stress response and restitution to avoid acute damage (LICHTENTHALER 1998). Of special interest, and also most common, are changes in photosynthetic productivity, since productivity controls long term growth, resilience and competitiveness in the field. In this context the relative amount of energy consumption and uptake must be close to equilibrium in order to avoid losses in productivity on the one hand and over-excitation on the other hand (DEMMIG-ADAMS *et al.* 2012). An over-excitation, resulting from a higher rate of energy trapping to energy consumption, bears the risk of electron donation to oxygen, leading to reactive oxygen species (ROS), with detrimental effects on photosystem function (LARCHER 2003, DEMMIG-ADAMS *et al.* 2012). The plant's photosynthetic apparatus contains numerous possibilities of regulating this important demand, which can range from long term responses like changes in chlorophyll content (i.e. HALDIMANN *et al.* 2008, BAQUEDONA & CASTILLO 2006, 2007, JALEEL *et al.* 2009) to short term responses like changes in electron transport (i.e. TACH *et al.* 2007, TOTH *et al.* 2007, VAN HEERDEN *et al.* 2007).

Chlorophylls play an active central role in the absorption and photochemical transformation of light energy in all photosynthetically active organisms (SCHREIBER 2003), thus controlling photosynthetic potential and consequently, primary production (FIELD *et al.* 1995). Many stresses manifest themselves in decreased foliar chlorophyll content or changes in pigment ratios (i.e. CARTER & KNAPP 2001, JALEEL *et al.* 2009, HALDIMANN *et al.* 2008, DEMMIG-ADAMS *et al.* 2012), and are mostly visually detectable. A decreased chlorophyll content may be seen as synonymous to a decreased light harvesting capacity, since less light energy can be absorbed and trapped per unit time by the light reaction of photosynthesis. The relative amount of leaf yellowing is (apart from crown dieback) primarily used in the assessment of tree vitality in European forest monitoring programs (ROSSINI *et al.* 2006, HMUELV 2014). Traditional quantitative methods for the determination of pigment content require their extraction from the tissue by a solvent and the subsequent photospectrometrical determination in the laboratory (i.e. LICHTENTHALER 1987, PARRY *et al.* 2014). The pigments are characterized by different peak absorption wavelengths in different solvents, empirically estimated by the photospectrometrical determination of absorption spectra of isolated pigments (LICHTENTHALER 1987). The resulting pigment specific equations allow for the determination of the single pigment concentration in solvents containing multiple pigments. This method of pigment determination is accurate, but on the other hand destructive, time-consuming and labour intensive. Deviations from the calculated pigment concentrations may occur, with the use of different types of spectrometers and/or extraction methods (WELLBURN 1994, PARRY *et al.* 2014).

When precise pigment concentrations are not necessarily obligatory, non-destructive methods for the measurement of pigment content may be sufficient, especially in the field (i.e. RICHARDSON *et al.* 2002, PARRY *et al.* 2014). In contrast to the traditional extraction method, non-invasive radiometrical measurements allow for the long-term monitoring of relative pigment contents at the same leaf. Since chlorophylls are the major light absorbing pigments in higher plants, most methods for non-invasive pigment determination focus on the determination of total chlorophyll (SIMS & GAMON 2002, PARRY *et al.* 2014). Chlorophylls have two major absorption maxima in the blue and red portion of the electromagnetic spectrum, leading to the characteristic green light reflectance and transmission, generally associated with healthy vegetation. Different amounts of carotenoids and anthocyanins can however alter the

Introduction

deceived leaf colour, with or without actual changes in the leaf's chlorophyll content (SIMS & GAMON 2002), leading to possible misinterpretations in the qualitative visual assessments of different species. The red peak of chlorophyll absorption is mostly unaffected by changes in accessory pigments (LICHTENTHALER 1987, SIMS & GAMON 2002) and therefore preferably used for the non-invasive chlorophyll determination. In most commercially available Chl-meters, two light emitting diodes with peak wavelengths in the red (high absorption of Chl) and infrared (no absorption of Chl) are contained, avoiding measurements in regions of the electromagnetic spectrum which could be affected by accessory pigments like carotenoids (SIMS & GAMON 2002). The relative Chl concentration of the sampled leaf is then calculated from the difference in light transmission of the two LEDs with and without the enclosed leaf blade (PARRY *et al.* 2014). The reference wavelength at the infrared portion of the electromagnetic spectrum is included to correct for leaf tissue related influences. Chl-meter readings are mainly dimensionless, which requires a calibration equation with the Chl extraction method to associate optical Chl-meter readings to quantified values of Chl concentration (absolute/optical Chl relationship) (i.e. MARKWELL *et al.* 1995, RICHARDSON *et al.* 2002).

The use of non-destructive optical Chl determination has been widely advocated, due to its ease and speed of application (i.e. MARKWELL *et al.* 1995, RICHARDSON *et al.* 2002, HAWKINS *et al.* 2009, SILLA *et al.* 2010). However, several constraints to the method have been observed, which may cause the method to be impracticable in the intended use: to comparably assess the vitality of different *Quercus* species. The interspecific comparability of Chl-meter readings has to be investigated by species specific calibrations, since differences in the absolute/optical Chl relationship have been repeatedly reported (i.e. MONJE & BUGBEE 1992, MARKWELL *et al.* 1995, YAMAMOTO *et al.* 2002, COSTE *et al.* 2010, SILLA *et al.* 2010, PARRY *et al.* 2014). Some authors have found leaf morphological traits (MONJE & BUGBEE 1992, YAMAMOTO *et al.* 2002, NIGAM & ARUNA 2008, MARENCO *et al.* 2009) or leaf age (SILLA *et al.* 2010) to influence the absolute/optical Chl relationship, despite of the reference wavelength in the near-infrared region (PARRY *et al.* 2014). Others have found the leaf's water content (MARTINEZ & GUIMET 2004), or the spatial distribution of chloroplasts within the cell to be significantly influential (NAUŠ *et al.* 2010). Without the analysis of influencing factors of the absolute/optical Chl relationship, the optical Chl determination cannot be

used to comparably assess and quantify changes in the Chl content of different Oaks with diverse leaf traits. If the benefits of optical Chl measurements are to be used in the monitoring of introduced *Quercus* taxa in the framework of a proactive method to supplement tree species on increasingly difficult stands in Central Europe, the influence of the above named factors must be investigated.

The proportion of light, which is neither transmitted nor reflected but absorbed by the chlorophyll in the chloroplasts of leaves, causes a transition from the ground state of the molecule to an excited state (HARBINSON & ROSENQVIST 2003). From the excited state, the molecule can relax to the ground state by a variety of routes (KLESSINGER & MICHL 1995). Since energy is a conserved property, the relaxation is always accompanied by the formation of another product, which contains the energy of the excited state. This can be the conversion to heat, the release as a photon (fluorescence),

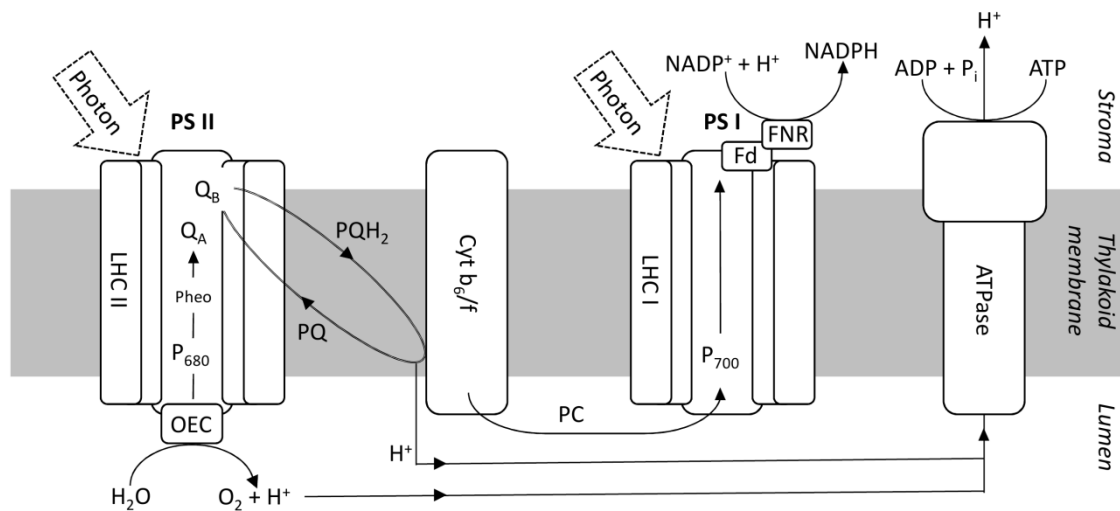


Figure 2: Schematic representation of the light reaction and its principle organization within the thylakoid membrane. Modified from ROSENQVIST & VAN KOOTEN (2003). Photosystem II (PSII) contains the Oxygen-Evolving Complex (OEC) on the lumen side of the membrane, the Reaction Centre (RC) P_{680} , the primary electron acceptor Pheophytin (Pheo) and the secondary electron acceptors Q_A and Q_B . When Q_B is reduced two times, it migrates to the lipid layer as part of the reduced Plastoquinol (PQ) pool (PQH_2). At the cytochrome b_6/f complex (Cyt b_6/f), PQH_2 is oxidized to PQ, which migrates back to the Q_B binding site at PSII. Electrons are transferred from Cyt b_6/f to the next mobile component Plastocyanin (PC), which migrates to the Lumen. Photosystem I (PSI) contains the RC P_{700} and numerous electron acceptors (not shown). The light energy is directed to the RCs by light harvesting chlorophyll protein complexes (LHCI and LHCII). The electrons are transferred from PSI to NADPH via Ferredoxin (Fd) and Ferredoxin $NADP^+$ -reductase (FNR). A pH gradient created across the Thylakoid membrane by water splitting in the OEC and by oxidation of PQH_2 constitutes the major part of the electrochemical driving force for photophosphorylation of ADP via the ATP synthase/hydrolase complex (ATPase).

Introduction

excitation transfer to another molecule or chemical change (photochemistry) (HARBINSON & ROSENQVIST 2003). If a reaction centre (RC) chlorophyll of photosystem II (PSII) (P_{680}) was excited either directly by a photon or by excitation transfer of chlorophyll of the light harvesting complex (LHC), it may be oxidized by the primary electron acceptor Pheophytin (Pheo), which leaves P_{680} oxidized and leads to a reduced electron acceptor (Figure 2). This process is known as photochemistry, a chemical change as a consequence of light absorption and the formation of an excited state (HARBINSON & ROSENQVIST 2003). Pheo is further reduced by the first stable electron acceptor: plastoquinone A (Q_A). More electron acceptors are subsequently reduced along the electron transport chain (ETC), leading eventually to the reduction of $NADP^+$ to NADPH and to a pH gradient across the thylakoid membrane that constitutes the major driving force for the phosphorylation of ADP to ATP (cf. Figure 2, LARCHER 2003). Photochemical processes, such as the oxidation of Chl in a RC, and photophysical processes like fluorescence emission, occur with certain efficiencies or yields (denoted as ϕ), which are a measure of the probability that an excited state will undergo a certain transformation (HARBINSON & ROSENQVIST 2003). The sum of all yields is one. Although the relative proportion of fluorescence emission is low (~3% of absorbed light *in vivo*), its measurement is a highly sensitive, non-invasive and reliable method for the fast measurement of photosynthetic efficiency (STIRBET & GOVINDJEE 2011). In relation to fluorescence, there are important differences between PSI and PSII. PSI has a low fluorescence yield, which is constant under physiological conditions. In contrast, PSII has a higher fluorescence yield, which changes with changing physiological conditions (KRAUSE & WEIS 1991). Thus, changes in the fluorescence yield reflect mainly changes in the rate of photochemical charge separation at the PSII RCs (KRAUSE & WEIS 1991, SCHREIBER 2003) under continuous light conditions. If the ETC becomes fully reduced, Pheo cannot be oxidized by Q_A (DUYSENS & SWEERS 1963), and a charge separation cannot take place, the excited state relaxes through the dissipation of heat or fluorescence. If the RC is not able to accept a photon or excitation energy of another chlorophyll, it is denoted as “closed” and fluorescence of the antenna is high. On the other hand, if the RC is able to accept a photon or excitation energy by another chlorophyll molecule it is denoted as “open” and the fluorescence of the antenna is low. With a saturating light pulse it is possible to “close” all open RCs in a very short time (1s) with no change in the ratio of heat dissipation and fluorescence

(SCHREIBER 2003). If all RCs are open (if the sample is dark adapted) and the ETC is fully oxidized, the fluorescence of the antenna is minimal (F_0). The saturating light pulse reduces the ETC and all RCs are subsequently closed, leading to the maximal fluorescence yield (F_m) (KAUTSKY & HIRSCH 1931). The ratio of this maximal variable fluorescence ($F_v = F_m - F_0$) to the maximal fluorescence yield (F_v/F_m) therefore equals the maximal quantum yield of primary photochemistry (ϕ_{P0}), which was found to be $\sim 0,83$ in healthy leaves of C3 plants (BJÖRKMAN & DEMMIG 1987). In stressed or damaged plants, F_v/F_m is often found to be reduced (BRESTIČ & ŽIVČÁK 2013). It is the most frequently used fluorescence parameter, often applied as an indicator of photoinhibition or other kind of injuries on PSII (BAKER 2008, BRESTIČ & ŽIVČÁK 2013). The fast increasing phase of the fluorescence transient (the increase of fluorescence from the ground state F_0 to the maximal yield F_m) is however not linear, but has distinct inflection points in semi-logarithmic plots (Figure 3). The fast phase is labelled OJIP transient with O for origin, the first measured minimum level, J (at 2 ms) and I (at 30 ms) are intermediate levels and P stands for peak ($P = F_m$ at saturating light). In heat treated samples, another intermediate step at $\sim 300 \mu\text{s}$ has been observed, which is denoted as K (GUISSÉ *et al.* 1995). It is assumed, that the fast fluorescence rise is a

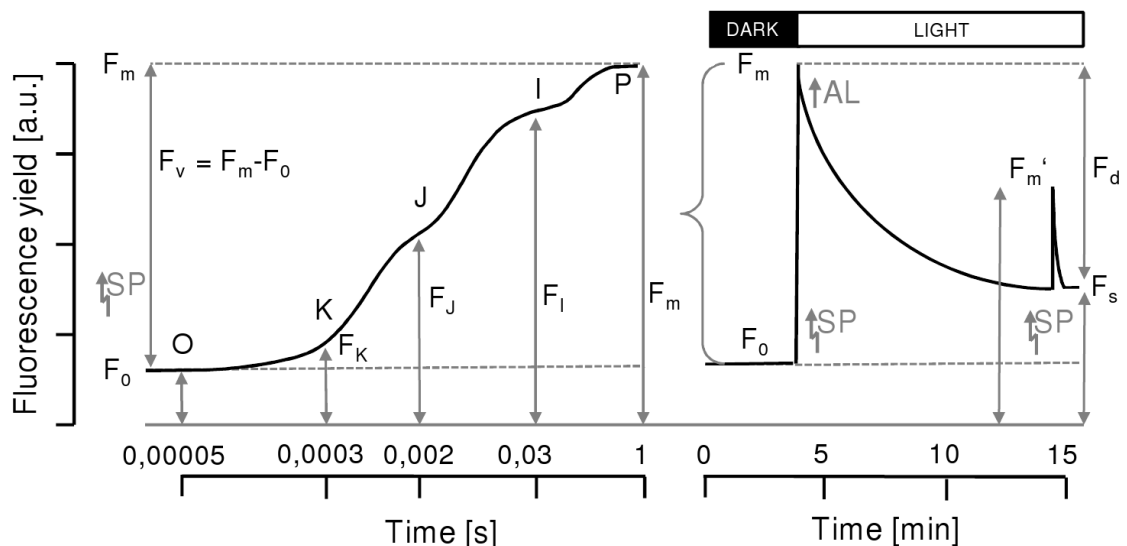


Figure 3: Fast and slow chlorophyll fluorescence transients. Upon illumination of a dark adapted sample with a saturating light pulse (SP), the fluorescence yield increases from a ground state (F_0) to a maximum (F_m). When continuous actinic light (AL) is provided, the fluorescence yield decreases (F_d) to a steady state (F_s). At this stage, a saturating light pulse given at an illuminated sample provides the maximum fluorescence in light (F_m'). A time resolved recording of the fast phase of the fluorescence induction from F_0 to F_m (on logarithmic scale) provides the OJIP transient (in some cases OKJIP transient) from which the parameters of the JIP-test can be derived (Appendix II). Figure modified from STRASSER & STRASSER (1995), ROSENQVIST & VAN KOOTEN (2003) and BRESTIČ & ŽIVČÁK (2013).

Introduction

reflection of the concentration of reduced Q_A (Q_A^-), affected by the kinetics of several different redox reactions in the photosynthetic ETC. If leaves were treated with DCMU (3-(3',4'-dichlorophenyl)-1,1'-dimethylurea), which blocks the electron transport from Q_A to Q_B , F_m was already reached at 2 ms (J-step) (STRASSER & STRASSER 1995). Thus, the fluorescence yield after the J-step is associated with a simultaneous re-oxidation of Q_A until the fluorescence yield approaches its maximum at the P-step (STRASSER *et al.* 2000, STIRBET & GOVINDJEE 2012). The OJIP transient has therefore the potential to be used for the characterization of the photochemical quantum yield of PSII photochemistry, and the electron transport activity. Further, the OJIP Chl fluorescence transient has been used as an excellent tool to monitor specific effects of various inhibitors and stressors on the photosynthetic apparatus and its function (STIRBET & GOVINDJEE 2011). Based on the analysis of the OJIP transient, the “JIP-test” has been developed as a tool to rapidly screen many samples, providing information about the structure, conformation, and function of the photosynthetic apparatus (cf. Appendix II and STRASSER & STRASSER 1995, STRASSER *et al.* 2004, STIRBET & GOVINDJEE 2011). If continuous and constant light is further provided, the fluorescence yield will slowly decline (fluorescence is “quenched”), until a steady state of fluorescence is reached (F_s), at which photochemical and non-photochemical quenching (NPQ) of fluorescence is in a state of equilibrium. A saturating light pulse at this stage yields the maximal fluorescence under steady state conditions (F_m'), which is lower than F_m , since the acceptor side of PSII is partly reduced and pH driven non-photochemical quenching occurs (STIRBET & GOVINDJEE 2011, ADAMS *et al.* 2004). In contrast to the maximum quantum yield of PSII ($F_v/F_m = \phi_{P0}$), at this stage the effective quantum yield of PSII in light [$\phi_{PSII} = (F_m' - F_s)F_m'^{-1}$] (BAKER 2008), the fluorescence decrease ratio [$R_{Fd} = (F_m - F_s)F_s^{-1}$] (LICHTENTHALER *et al.* 2005), as well as the contribution of NPQ [$= (F_m - F_m')F_m'^{-1}$] can be measured (BAKER 2008, BRESTIČ & ŽIVČÁK 2013) (cf. Figure 3).

1.3. Research objective

In order to mitigate the effects of climate change on difficult forest stands in Central Europe, plants of different species and provenances need to be considered for planting. Tools for a comparative assessment and quantification of plant's ability to cope with various stresses, which allow fast and easy operation, could provide important information on the suitability of a given species or genotype for plantation in a changing environment. Methods to non-destructively quantify light harvesting capacity and photochemical functioning through the measurement of light transmittance and chlorophyll fluorescence seem promising. However without the knowledge on species specific and temporal variability in the absolute/optical Chl relationship, the influence of leaf morphological traits and their seasonal dynamics and the influence of environmental stress such as drought, heat or cold on the photosynthetic performance of the species and on the measured signals, these methods are not readily applicable. For the first time, common garden plantations of several oak taxa with a wide range of leaf traits and leaf life strategies (deciduous, evergreen, semi-deciduous) have been established in Central Europe, which allow the monitoring and comparative assessment of morphological, chemical and phenological leaf traits and the assessment of their influence on the radiometric determination of photosynthetic functioning under Central European climate conditions. The following hypothesis was tested:

Interspecific differences and seasonal dynamics of leaf morphological and leaf chemical traits as well as environmental stresses influence the radiometric sensing of chlorophyll content (with its associated relationship to other chemical leaf compounds like nitrogen) and photochemical performance on the leaf level.

In order to test this hypothesis, radiometric Chl-meter and Chl fluorescence readings were taken from several different *Quercus* taxa in equally spaced intervals from leaf unfolding until leaf senescence in two subsequent years in a common garden type experimental forest plantation. Leaf samples were investigated in terms of relative and absolute Chl content, leaf morphological traits, pigments and nitrogen content, spanning the whole range measurable leaf ages and seasonal dynamics. An additional monitoring of *Q. ilex* under Central European winter conditions and several experiments under controlled conditions were conducted to investigate the influence of cold, heat and drought stress on pigment contents and ratios, fluorescence transients, Chl-meter readings and their relationship and provide reference data for future monitoring efforts.

2. Materials & Methods

2.1. Investigation area

The experimental plantation (~0,5 ha) at Frankfurt Schwanheim (N 50°04'24" E 08°34'06") is situated in the municipal forest of Frankfurt on the Southern Middle Terrace of the Main river valley (elevation: 95 m above sea level) in a ~140 year old *Pinus sylvestris* forest (thinned to 50 trees ha⁻¹ prior to planting). Individual adult trees of *Q. robur* and *Q. petraea* (80-125 years old) are located on the site. Natural rejuvenations of *Q. robur*, *Q. rubra*, *Rhamnus frangulae* and *Carpinus betulus* occur. The site is managed for *Rubus fruticosus* agg. and *Calamagrostis epigejos* ground cover. Within the site, a soil profile has been taken and analysed for grain size, soil type, carbon- (DIN ISO 10694) and nitrogen content (DIN ISO 13878) by the Hessian Agency for the Environment and Geology HLUG (see 3.1.2). Long-term mean annual precipitation sums to 657,8 mm and yearly average temperature was recorded to be 9,7°C (norm-period 1961-1990, data from German Meteorological Service DWD, climate station Frankfurt airport, ID 1420). Monitoring wells for ground water depth are located close to the site (G03360, G00620, operated by Hessenwasser GmbH). Since 2013 a monitoring well is situated directly on site (HLUG, station ID: "Schwanheim" 507193, see Figure 4). Mean depth of ground water table is given at 3,5 m. In spring 2011, 5 different *Quercus* species were randomly planted in "Trupp"-scheme of 21 trees of the same species in 1 m distance to each other (PETERSEN 2007), resulting in 8 Trupps each of the following species: *Q. robur* L. (n = 168, 2 years old, provenance: 81707 "Upper Rhine Valley"), *Q. pubescens* WILLD. (n = 169, 1 year old, provenance: QPU741 Languedoc, FR), *Q. frainetto* TEN. (n = 168, 3 years old, provenance: Umbria, IT), *Q. ilex* L. ssp. *ilx* (n = 168, 1 year old, provenance: QIL701 Sud-Oust, FR) and *Q. rubra* L. (n = 168, 2 years old, provenance: 81602), obtained from a tree nursery (Darmstädter Forstbaumschulen GmbH). A ring of *Carpinus betulus* was added around the Trupps as described in PETERSEN (2007), where planting locations allowed to.

The site was equipped with an on-site climate station (iMetos sm SMT280, Pessl Instruments GmbH, Weiz, AT), automatically recording the following parameters in one hour intervals: Air temperature at 2 m height (minimal, maximal, mean) [°C], soil temperature at 20 cm depth (minimal, maximal, mean) [°C], relative humidity [%], dew point temperature [°C], solar radiation [W m^{-2}], precipitation [mm], wind speed [m s^{-1}] and soil water potential at 50 cm depth [cbar].

To monitor the spatial variability of light and temperature on the site, 10 self-sufficient temperature and light data loggers (HOBO Pendant UA-002-08, Onset Computer Cooperation, Bourne, MA, USA) were installed on a 20 x 20 m raster at 1 m height in June 2013. The data loggers were set to measure at 10 min intervals and data was retrieved manually every two weeks. Soil samples were taken at 21.05.2014 with a soil probe at 30 cm depth at all 40 Trupps ($n = 1$, between trees with ID 6 and 11 cf. Figure 4). Samples were dried in an oven (T6060, Heraeus, Hanau, DE) at 40°C until constant weight was obtained and stored in 2 ml Eppendorf cups until further measurement. At the Department of Soil Zoology (Senckenberg Görlitz), soil samples were ground in a mixer mill for 7 min at 25 s^{-1} with 2 steel balls per Eppendorf cup (MM400, Retsch GmbH, Haan, DE). The pulverized leaf samples (2 aliquots of ~9 mg) were transferred to tin boats (4 x 4 x 11 mm, Elementar Analysensysteme GmbH, Hanau, DE) and weighed on a precision scale (Mettler Toledo XP6, Giessen, DE). Total nitrogen and carbon concentrations were determined against a standard (Acetanilide, Merck; cas-no. 103-84-4) on dry weight basis in an elemental analyser (vario PYRO Cube, Elementar Analysensysteme GmbH, Hanau, DE).

In order to assign measured values of installed devices, trees and samples to their distinct locations, the FR site was manually mapped by marking 10 x 10 m raster and noting the specific locations with help of a tape measure, since GPS (Global Positioning Systems) measurements were not sufficiently accurate. Hand drawn maps were digitized, merged and georeferenced (Figure 4) in a Geoinformation System (ArcGIS 10.0, Environmental Systems Research Institute Inc ESRI, Redlands, CA, US).

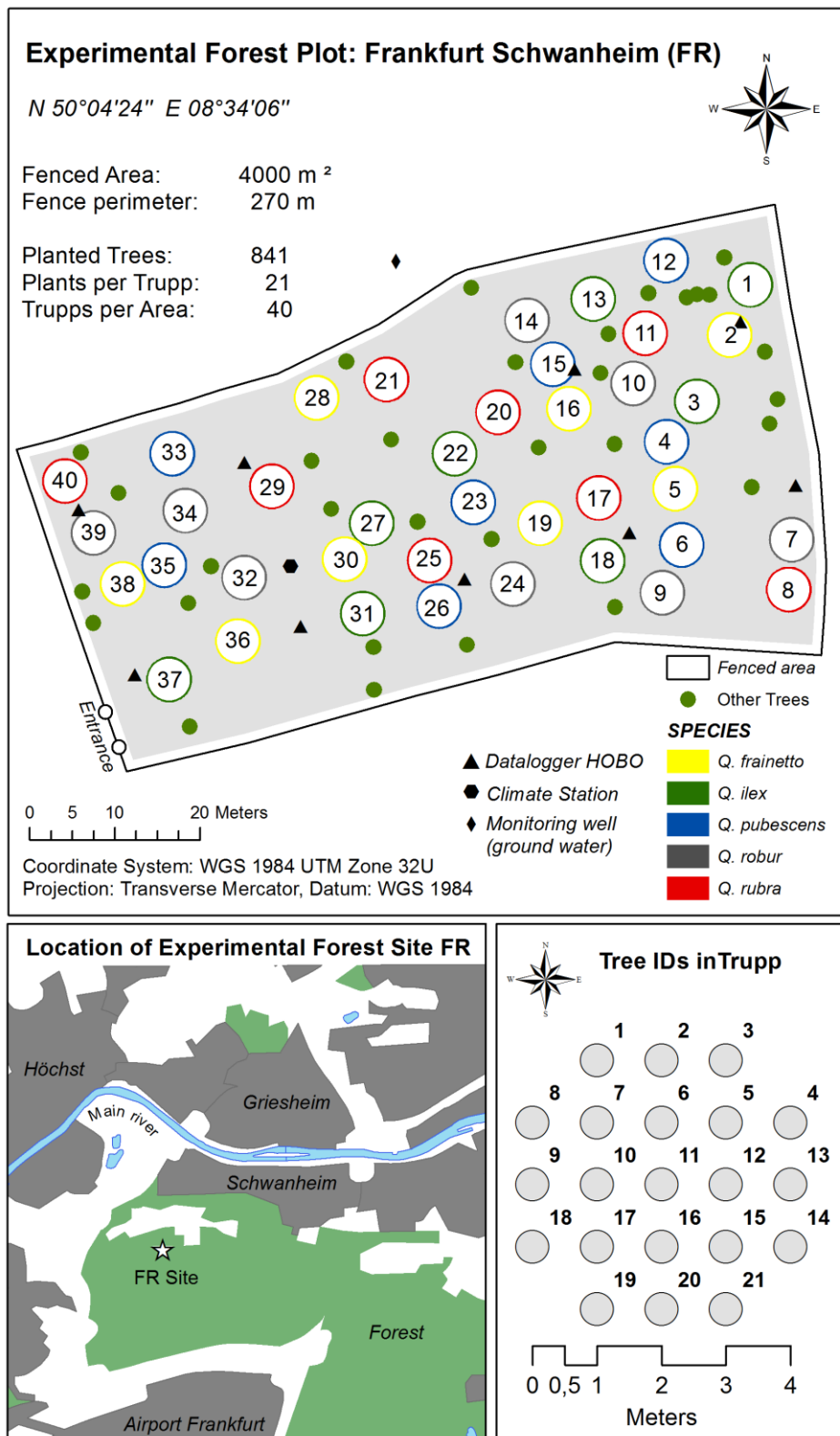


Figure 4: Experimental forest site in Frankfurt Schwanheim (FR). Map shows location of site, location of Trupps and measuring devices on site as well as information on tree identification. Tree IDs are four digit numbers composed of Trupp ID and tree ID as used in different assessments on the site. The forest road “Lange Schneise” runs north of the site (east-west, not shown). Map in the lower left corner was created from digital land model data: ©GeoBasis-DE BKG 2015, <http://www.bkg.bund.de>.

2.2. Monitoring of morphological and chemical leaf traits

In order to analyse the seasonal variability of morphological leaf traits, leaf pigment contents and leaf nitrogen content, and to further investigate the possibility of their estimation through non-invasive sensing by radiometric instruments (SPAD-502, Konica-Minolta, Osaka, JP), leaf samples of *Q. frainetto*, *Q. ilex* (current year and previous year leaves), *Q. pubescens*, *Q. robur* and *Q. rubra* were taken at Frankfurt Schwanheim (FR) from 17.05.2013 (doy 137) until 08.11.2013 (doy 312) at ~2 week intervals on the following days (doy): 137, 151, 169, 178, 193, 207, 227, 239, 253, 269, 281, 297 and 312. Leaves were sampled in early morning (between 06:00 and 08:00) randomly on the tree at one tree per plot (“Trupp”), resulting in 8 leaves per species (*Q. ilex*: 8 current year leaves and 8 previous year leaves) and 48 leaves in total per sampling date, spanning the whole spatial distribution of species within the forest site (~0,5 ha). The taxa *Q. cerris*, *Q. suber*, *Q. x hispanica* and *Q. x turneri* were sampled with $n = 30$ at 05.11.2013 (doy 309) from young trees of the Common Garden experimental site in the Botanical Garden, Frankfurt Riedberg. The sampled leaves were placed between moist paper towels and stored within air-tight Ziploc bags in a lightproof Styrofoam container for transportation. At the laboratory, leaves were stored for approx. one hour at 8°C in the dark (for rehydration purposes) before measurements were undertaken. Between sampling and measurement, not more than 3 hours passed.

After retrieving a leaf from the Ziploc bag, the surface was gently patted dry and the petiole was removed. The leaf was placed between 1,7 mm acrylic glass and a white sheet of plastic containing a fixed mm scale bar and scanned with a commercial hand scanner (Easypix Easy-scan, 300 dpi resolution, colour). After a leaf disc was punched out with a cork borer (Ø 21,6 mm or 15,5 mm depending on leaf size), the leaf left over leaf part was weighed on a precision scale (Mettler DeltaRange AE260, Giessen, DE) to determine the saturated fresh weight (Leaf_{FW} [g]), placed in a paper bag and dried for ~70 hours at 70°C in an oven (T6060, Heraeus, Hanau, DE) for the estimation of leaf dry weight (Leaf_{DW} [g]). Weight measurements were conducted on a piece of cardboard to counter distortions due to drying-induced static electrification. The leaf area corresponding to the weight measurements was later calculated from the total leaf area minus the punched out leaf disc, since a scan with already punched out leaf disc was found to lead to errors due to torsions. On the punched out leaf disc, 5 SPAD-

Materials & Methods

measurements were taken and leaf thickness (LT [mm]) was measured between leaf veins with a digital calliper (TCM 227 579; error $\pm 0,02$ mm). By means of a smaller leaf borer (\varnothing 15,5 mm or 10,5 mm), a subsample of the leaf disc was taken and both samples were scanned and weighed, to provide leaf area and leaf fresh weight as a base for later pigment content calculations. The two leaf samples were each placed in 2 ml Eppendorf cups, frozen in liquid nitrogen and stored at -80°C until further measurements. Leaf area and leaf subsample area were determined with ImageJ software 1.46r (Rasband W.S., ImageJ, NIH, Bethesda, Maryland, USA). The pixel to distance ratio was determined by the scale bar present on each scan, as mentioned above, and set in the software. The leaf area was then calculated by ImageJ software from the pixel count of the binary transformed scan.

2.2.1. Calculation of morphological leaf traits

From the measurements of saturated leaf fresh weight ($Leaf_{FW}$), leaf dry weight ($Leaf_{DW}$) and leaf area ($Leaf_A$), the morphological leaf traits were calculated as followed. Parameter abbreviation is given in curly brackets and units in square brackets. Subscript of the parameters abbreviation indicates their base of reference.

$$\text{Leaf Area } \{Leaf_A\} [mm^2] = Leaf\ area_{total} [mm^2] - \pi \left(\frac{\emptyset_{cork\ borer} [mm]}{2} \right)^2$$

$$\text{Leaf Dry Matter Content } \{LDMC\} [mg_{DW}g_{FW}^{-1}] = \frac{Leaf_{DW} [g]}{Leaf_{FW} [g]} * 1.000$$

$$\text{Specific Leaf Area } \{SLA_{DW}\} [m^2kg^{-1}] = \frac{Leaf_A [mm^2]}{Leaf_{DW} [g]} / 1.000$$

$$\{SLA_{FW}\} [m^2kg^{-1}] = \frac{Leaf_A [mm^2]}{Leaf_{FW} [g]} / 1.000$$

$$\text{Leaf Mass per Area } \{LMA_{DW}\} [g\ m^{-2}] = \frac{Leaf_{DW} [g]}{Leaf_A [mm^2]} * 1.000.000$$

$$\{LMA_{FW}\} [g\ m^{-2}] = \frac{Leaf_{FW} [g]}{Leaf_A [mm^2]} * 1.000.000$$

$$\text{Leaf Water Content } \{LWC_{FW}\} [mg\ g_{FW}^{-1}] = 1.000 - LDMC [mg_{DW}g_{FW}^{-1}]$$

$$\{LWC_A\} [g\ m^{-2}] = \frac{LWC_{FW} [mg\ g_{FW}^{-1}]}{1.000} * LMA_{FW} [g\ m^{-2}]$$

2.2.2. Determination of leaf pigment concentrations

The extraction and determination of leaf pigments was conducted in a dark laboratory ($< 0,5 \mu\text{mol quanta m}^{-2} \text{s}^{-1}$) and extracts were kept cool to avoid pigment degradation. The Eppendorf cups containing the leaf subsamples for pigment determination were transferred from -80°C storage to liquid nitrogen after a pre-cooled steel ball was inserted in each cup. Frozen samples were ground in a ball mill (MM400, Retsch GmbH, Haan, DE) for 30 seconds with a frequency of 30 s^{-1} . After grinding was completed, 1 ml of cold acetone ($\geq 99,5\%$) plus 0,05% (w/v) CaCO_3 as a pH buffer were added to the cups. Samples were placed in the ball mill for another 30 seconds at a lower frequency (10 s^{-1}) to transfer all leaf powder to the acetone solution. The contents of the Eppendorf cups were each transferred to a 10 ml falcon tube with the help of a glass funnel. The cups were thoroughly flushed with acetone (+ CaCO_3) to ensure that the pulverized leaf subsamples were completely transferred into the falcon tube. After flushing the funnel as well, the pigment extracts were filled up to 8 ml, mixed and placed horizontally in a cooled and lightproof container. The container was placed on a sample shaker (Heidolph Duomax 1030, Schwabach, DE) with a speed setting of 20 rpm for one hour to allow full pigment extraction of the ground leaf tissue. 2 ml of distilled water were added to the acetone extract, resulting in an 80% acetone pigment solution. After mixing the pigment extract thoroughly, 3 Eppendorf cups were filled with 1,5 ml of extract solution each (3 aliquots per leaf subsample). Extracts were centrifuged for 1 minute at 10 rpm before spectrophotometric measurement.

Pigment determination from extracts was conducted with a double beam spectrophotometer (Hitachi U2900, Krefeld, DE), using precision glass cuvettes (Hellma 104-OS, Müllheim, DE) against an 80% acetone solution at the reference beam. Absorption was measured at 470 nm, 663,2 nm, 646,8 nm and 750 nm to calculate the pigment concentration of the extract in $\mu\text{g ml}^{-1}$ modified from LICHTENTHALER (1987) as followed (modification consisted of inclusion of a reference wavelength at 750 nm).

Equations for the determinations of concentrations of chlorophyll a (Chl a), chlorophyll b (Chl b), total chlorophylls (Chl a+b) and total carotenoids (Car x+c) in leaf pigment extracts for 80% (v/v) acetone modified after LICHTENTHALER (1987).

$$\mathbf{Chl}_a [\mu g ml^{-1}] = 12,25 * A_{(663,2-750)} - 2,79 * A_{(646,8-750)}$$

$$\mathbf{Chl}_b [\mu g ml^{-1}] = 21,50 * A_{(646,8-750)} - 5,10 * A_{(663,2-750)}$$

$$\mathbf{Chl}_{a+b} [\mu g ml^{-1}] = 7,15 * A_{(663,2-750)} + 18,71 * A_{(646,8-750)}$$

$$\mathbf{Car}_{x+c} [\mu g ml^{-1}] = \frac{1000 * A_{(470-750)} - 1,82 * C_a - 85,02 * C_b}{198}$$

For the calculation of the Chl content per leaf area, Chl a [$\mu g ml^{-1}$] was multiplied by the volume of extract and divided by the used leaf area

$$\mathbf{Chl}_a [\mu g mm^2] = Chl_a [\mu g ml^{-1}] * Volume_{extract} [ml] / Area_{subsample} [mm^2]$$

2.2.3. Determination of leaf nitrogen concentrations

For the determination of leaf nitrogen concentrations, a subset of 30 samples of each of the species *Q. frainetto*, *Q. ilex* (current year leaves), *Q. pubescens*, *Q. robur* and *Q. rubra* was selected according to a wide span of values and seasonal representation. The leaf subsamples were dried at 40°C for 7 days in a drying oven (T6060, Heraeus, Hanau, DE). The dried leaf samples were pulverized in a mixer mill with steel balls (MM400, Retsch GmbH, Haan, DE) at a frequency of 30 s⁻¹ for 1 minute and 3 rounds, inverting the Eppendorf 2 ml cups in between. The pulverized leaf samples (2,5 – 6 mg) were transferred to tin boats (Elementar: 4 x 4 x 11 mm), weighed on a precision scale (Mettler Toledo XP6, Giessen, DE) and measured against a standard (Acetanilide, Merck; cas-no. 103-84-4) in an elemental analyser (vario PYRO Cube, Elementar Analysensysteme GmbH, Hanau, DE). Total leaf nitrogen (N) concentrations were given as percent of dry weight. Measurements were conducted at Senckenberg Görlitz, Department of Soil Zoology.

2.3. Non-invasive sensing of chemical leaf traits

The analysis of the absolute/optical Chl relationship and the analysis of the correlations between SPAD-meter values and total leaf nitrogen were conducted with the data derived from section 2.2. The mean of the 3 photometrically measured aliquots was correlated against the mean of 5 SPAD- measurements per leaf disc in the case of the absolute/optical Chl relationship. For the total leaf nitrogen concentrations, the amount of dried leaf tissue did not allow for multiple aliquots. Data import and management was conducted with Microsoft Excel (version 2010, Redmond, Washington, US). Models were fit to the data with GraphPad Prism's (version 5.04, La Jolla California, US) linear and non-linear regression equations. The homographic model was added manually to the software. Coefficients of correlation (Pearson's r), and determination (R^2), model comparisons and best fit parameter estimations were calculated by the statistical software as well, whereas the root mean square error (RMSE) calculations were conducted with Microsoft Excel with \hat{Y} as the predicted and Y as the measured value:

$$\text{Root Mean Square Error (RMSE)} = \sqrt{\frac{1}{n} \sum_{i=1}^n (\hat{Y}_i - Y_i)^2}$$

2.3.1. Assessment of SPAD-reading variability concerning application

In order to assess possible influences on the application of the SPAD-meter under field conditions several aspects were additionally monitored: (1) The spatial variability of SPAD-readings on a uniformly coloured leaf (2) a possible diurnal influence on readings due to changes in light and high air temperature influencing leaf water status and/or chloroplast movement, (3) the variability at the site level, per tree and per species.

Leaf scale variability of SPAD-readings

SPAD-reading variability on the leaf level was measured for *Q. frainetto*, *Q. ilex* (current year leaves), *Q. pubescens*, *Q. robur* and *Q. rubra* on mature leaves at 22.07.2013 (doy 203) at the Frankfurt Schwanheim site in full daylight. On each visually uniformly coloured leaf, 20 SPAD-measurements were taken. Data was recorded for 9 leaves per species. The standard deviation of SPAD-values for each leaf was calculated.

Diurnal variability of SPAD-readings

The diurnal variability of SPAD-readings and a possible species specific difference, due to contrasting leaf traits was monitored at 22.07.2013 (doy 203) at the Frankfurt Schwanheim site for the planted 5 *Quercus* species. Measurements were conducted on 8 leaves of different individuals per species at 3 hour intervals from 04:00 a.m. until 10:00 p.m. The same leaves were sampled on each interval to avoid the influence of different leaf chlorophyll contents. The chosen leaves were the same as the ones used in seasonal monitoring 2013 (cf. 2.4) and the subset of trees chosen, were all in close proximity to the climate station on site (cf. Figure 4). Dusk was at 05:39 a.m. and dawn at 21:23 p.m., therefore measurements spanned the diurnal cycle.

Temperature dependent variability

To further investigate a possible temperature dependency of SPAD-readings, data from *Q. ilex* leaves grown at the experimental forest site Frankfurt (FR) were collected between 20.08.2012 and 03.05.2013, including a large span of temperatures at the time of SPAD-measurement (for measurement protocol see 2.4 & 2.5.3). SPAD-measurements before August were not considered to avoid the influence of leaf development on linear regressions. Measurement interval was ~2 weeks with 18 dates of measurement for the given period over a span of ~8 month. SPAD-values at the different dates were plotted for each leaf separately and fitted by linear regression. Residuals and their root mean square error (RMSE cf. 2.3 for calculation) were calculated for each date of measurement (n = 18-21 leaves per date). Temperature at the time of measurement was obtained from the on-field climate station.

Interspecific variability

To quantify species specific representative SPAD-values and their variability as well as the variability of measured values per tree, measurements were performed from 22.08.2013 (doy 234) until 28.08.2013 (doy 240) on all trees at the Frankfurt Schwanheim site. 10 randomly chosen leaves per tree were measured resulting in ~155 trees per species and 7810 measurements in total.

Spatial distribution of SPAD-values at site level

In order to visualize the spatial variability of leaf greenness at the site level, a normalized chlorophyll content index [$NCCI = (SPAD_{tree}) (SPAD_{m_species})^{-1}$] was derived from SPAD values of single trees and the mean SPAD value of the species at the site. The NCCI followed a Gaussian distribution ($R^2 = 0,98$) with a range of 0,56 to 1,32 (n = 780). Break values for visualization were set for $SPAD_{tree} = SPAD_{m_species} \pm 0,5$ as well as below and above this range (cf. Figure 26) . The map was created with ArcGIS 10.

2.4. Seasonal monitoring of chlorophyll content and PS II functionality

The seasonal time course of chlorophyll content and PSII functionality was assessed by monitoring individual leaves of *Q. frainetto*, *Q. ilex*, *Q. pubescens*, *Q. robur* and *Q. rubra* with the SPAD-meter (SPAD-502, Konica-Minolta, Osaka, JP) and records of the fast Chl a fluorescence induction transient, measured with the “Plant Efficiency Analyser” (Pocket PEA, Hansatech, King’s Lynn, UK) in two consecutive years at Frankfurt Schwanheim forest experimental site (FR, cf. Figure 4) in 2012 and 2013. Leaves were labelled at the petiole with a piece of woollen yarn prior to the measurement campaign, shortly after bud break. Sun exposed leaves of 3 trees (visually healthy) per Trupp were chosen, resulting in 24 leaves per species distributed over the plantation site. Since very cold air temperatures in the winter 2011/2012 led to leaf shedding in *Q. ilex*, all monitored leaves in 2012 were leaves developed during that spring. In 2012, monitoring started at 06.06.2012 (doy 158) and measurements were performed in ~2 week intervals (depending on weather conditions) until 08.11.2012 (doy 313), resulting in 12 measuring days during the vegetation period 2012. The monitoring of the *Q. ilex* leaves was continued in ~2 week intervals during the winter period 2012/2013 until the start of the 2013 campaign (see 3.5.3). In 2013, monitoring started at 17.05.2013 (doy 137) and ended at 08.11.2013 (doy 312), resulting in 13 measuring days in ~2 week intervals during the vegetation period 2013. For the monitoring campaign 2013, the same trees as in 2012 were monitored again. In *Q. ilex*, additionally to the leaves monitored in 2012, current year leaves of 2013 were added to the monitoring program. To ensure comparability of Chl a fluorescence data, all PEA measurements were performed at night between midnight and day break. SPAD measurements were usually performed at early morning after sunrise but in some cases also at night. To cover possible spatial variability, 3 trees per Trupp were selected, resulting in 24 trees per species and 120 leaves per measuring day in 2012 (144 in 2013). One fast Chl a fluorescence transient was recorded per leaf, whereas for the SPAD values the mean of 5 measurements per leaf was documented.

Materials & Methods

The time course of individual leaf SPAD readings showed an increase in spring, followed by a period with minimal change and a decline at autumn. The equations of 3 linear regressions, individually fitted to the data points of each leaf (Figure 5), were used to derive the rate of increase at the phase of spring development and the rate of decline at autumnal senescence from the slopes of the regressions. The intersections of the linear regressions were used to quantify the end of development and the beginning of senescence, as well as to calculate the “core vegetation time”. The mean, the maximum and standard deviation of all SPAD-values within the core vegetation time were also calculated for each individual leaf. The parameter estimations were carried out in Microsoft Excel (version 2010) for leaves with complete traces.

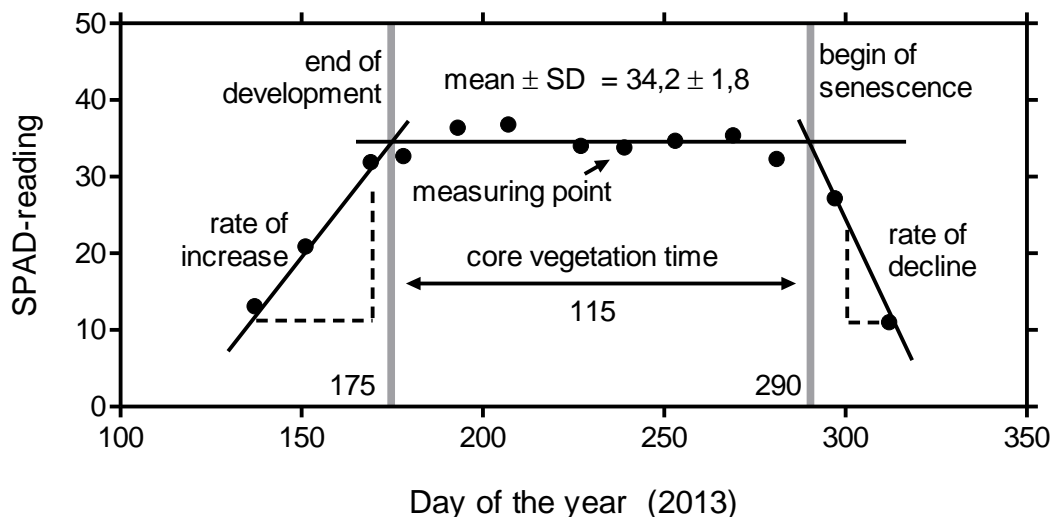


Figure 5: Estimation of plant developmental parameters through SPAD seasonal variability. Solid points show SPAD-readings of *Q. rubra* (ID 0914) on different days of the year (doy). Three linear regressions are fitted through the measuring points individually. The first interception marks the end of chlorophyll increase and defines the end of pigmental development (doy 175). The second interception marks the beginning of pigmental decrease and defining the beginning of senescence (doy 290). The core vegetation time is defined as the time between the end of development and the beginning of senescence (115 days). Rate of SPAD increase and decrease were estimated with the slope of the linear regression. Mean and standard deviation (SD) of SPAD values within the core vegetation time was calculated. This procedure has been carried out for five species with 18-24 trees per species at Frankfurt Schwanheim.

For the analysis of the fast Chl a fluorescence transient, parameters were calculated with the provided PEA Plus software (Hansatech, version 1.02) with the F_0 level set to 50 μs and the BioLyzer software (version 3.0, Ronald M. Rodriguez, Bioenergetics Lab Geneva, CH). Parameters were calculated according to STRASSER & STRASSER (1995) and STRASSER *et al.* (2000, 2004). For the seasonal time course analysis, the maximum quantum yield of primary photochemistry: $F_v/F_m [= (F_m - F_0) F_m^{-1} = \phi_{P0}]$ and the logarithmised Performance Index on absorption base ($\ln PI_{\text{abs}}$, STRASSER *et al.* 2000) were calculated (see Appendix II for parameter calculations with Chl a transient data). Integrals of individual leaf time courses of JIP-test parameters were calculated with the “area under curve” analysis function in GraphPad Prism (version 5.5) and summarized in Microsoft Excel. To assess possible differences in the shape of the Chl a transients at different days of the year, original Chl a transient data was additionally normalised to $F_0 (=F_{50\mu\text{s}})$ for equal starting points, double normalised to F_0 and $F_m (V_{\text{OP}})$ to rank all fluorescence values between zero and 1 or further calculated as differential V_{OP} curves (ΔV_{OP}) as depicted in Table 1.

Table 1: OJIP transient normalisations

Name	Abbreviation	Calculation
Normalised transient $F_0 (=F_{50\mu\text{s}})$	$F_{50\mu\text{s}}$ norm	$(F_t) (F_{50\mu\text{s}})^{-1}$
Double normalised transient F_0 & F_m	V_{OP}	$(F_t - F_{50\mu\text{s}})(F_m - F_{50\mu\text{s}})^{-1}$
Differential V_{OP} curve	ΔV_{OP} <i>(sample A – sample B)</i>	$(F_t^A - F_{50\mu\text{s}}^A)(F_m^A - F_{50\mu\text{s}}^A)^{-1} -$ $(F_t^B - F_{50\mu\text{s}}^B)(F_m^B - F_{50\mu\text{s}}^B)^{-1}$

2.5. Stress response analyses

2.5.1. Drought stress

Morphological leaf traits regarding the water status of the leaf were calculated along with other leaf traits mentioned above (2.2) for 9 *Quercus* taxa, but included in this section due to their thematic relation. Independent experiments concerning drought stress related leaf traits and responses to water shortage were conducted in 2011 and 2013 under greenhouse and climate chamber conditions. In the chronologically latest experiment “drought stress experiment A”, 3 *Quercus* species (*Q. ilex*, *Q. pubescens*, *Q. robur*) were grown under identical conditions in a climatic chamber one year prior to the measurements and all leaves used for analysis, have been developed under the same hydrologic and climatic conditions. These studies complement an earlier experiment termed “drought stress experiment B”, in which *Q. ilex*, *Q. robur* and their semi-evergreen hybrid *Q. x turneri* were exposed to decreasing water contents in the greenhouse under a semi-controlled environment. In this study, the focus was set on electron transport and gas exchange under severe drought stress.

Drought stress experiment A

Plant material

Plant material for the monitoring of drought stress responses and the measurement of certain drought related traits in 2013 was obtained from a tree nursery (Darmstädter Forstbaumschulen GmbH) in April of 2012 (20 trees per species). Trees

Table 2: Plant material used in the drought stress and heat stress experiment 2013. Age of trees at the time of purchase in April 2012. Provenance identification shown as labelled by the nursery.

Species	Age [years]	Provenance label
<i>Q. robur</i> L.	2	Upper Rhine valley, Germany
<i>Q. pubescens</i> WILLD.	1	QPU 360 Sud-Oust, France
<i>Q. ilex</i> L. ssp. <i>ilex</i> .	2	QIL 701 Languedoc, France

were planted in tall rose pots (diameter: 20 cm, height: 25,7 cm) after rinsing roots clean from soil (*Q. robur* was delivered with bare roots). At the bottom of the pot, 250 ml vermiculite (Deutsche Vermiculite Dämmstoffe GmbH, Sprockhöfel, DE) for uniform water uptake were topped with 3,5 L of soil (75 vol%) perligran (25 vol%) mixture (Perligran 0-6 mm, Knauf Aquapanel GmbH, Dortmund, DE). Soil was taken from Frankfurt Schwanheim and sieved (3 mm width) to remove organic residues (Soil texture: sand/silt/clay [%] 63/20/17). Perligran was mixed in the sandy soil to improve water holding capacity while simultaneously avoiding anoxia during water saturation of pots. Plants were placed in a climate chamber at the Goethe University (Biologicum, Frankfurt Riedberg) with a day/night period of 14/10 hours, 25/20 °C, 50% relative humidity and a light intensity at plant height of ~500-700 $\mu\text{mol quanta m}^{-2} \text{s}^{-1}$. Plants were fertilized as needed (NPK [%]: 7/5/6) and grown inside the climate chambers for one year to allow sufficient root growth before water was withheld at the onset of the drought stress experiment in 2013.

Pressure-Volume Analysis

In order to derive parameters of tissue water relations, pressure-volume (PV) curves were constructed in July 2013 for three unstressed individuals of the species *Q. ilex*, *Q. pubescens* and *Q. robur* (plant material: see above). Twigs were harvested in late afternoon, recut under distilled water and placed in water-filled Eppendorf cups to allow for the rehydration of tissue. Twigs were kept cool and dark within a sealed container until the next morning. The “bench dry method” (SACK *et al.* 2011) was used to obtain pairs of mass and water potential measurements from the same twigs over a range of water contents. The twigs were allowed to dehydrate on a laboratory bench at 16–17°C and a light intensity of 5–8 $\mu\text{mol quanta m}^{-2} \text{s}^{-1}$. Mass loss and water potential were measured until a pressure of 4 MPa did not suffice to re-wet the cutting surface of the twig. Weight measurements were conducted on a precision scale (Mettler DeltaRange AE260, Giessen, DE) before and after water potential measurements respectively, and the mean was used for the calculation of the relative water content

$$\text{RWC} = (\text{fresh weight} - \text{dry weight}) (\text{turgid weight} - \text{dry weight})^{-1}$$

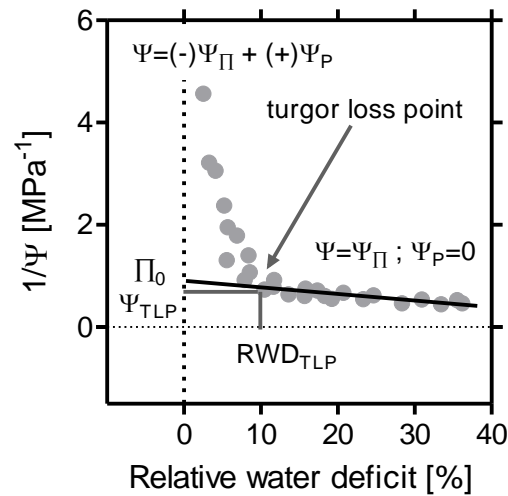


Figure 6: Pressure-volume curve constructed from subsequent measurements of leaf water content and water potential on a dehydrating twig. The reciprocal of water potential was plotted against the relative water deficit (RWD = 100 - relative water content) to visualize the influential components to total water potential and the derivation of pressure volume parameters. Above the turgor loss point (TLP), total water potential is the sum of osmotic and pressure potential. Below the TLP, the pressure potential is zero and the total water potential = osmotic potential (gravitational component and matrix potential can be neglected and are not shown). Π_0 : osmotic potential at saturation; Ψ_{TLP} : turgor loss point; RWD_{TLP} : relative water deficit at turgor loss point.

Water potential was measured in a pressure chamber (SKPM 1400, SKYE Instruments, Powys, Wales, UK) with compressed air and low pressurisation rates ($0,25 \text{ MPa min}^{-1}$). After the PV measurements were completed, the twigs were oven dried at 70°C (Heraeus T6060) to obtain the dry weight, necessary for RWC calculation. Results of PV analysis were obtained following SACK *et al.* (2011) and an Excel sheet provided by this resource. The reciprocal of the water potential was plotted against the RWD (Figure 6) and fitted for each individual twig. Data was controlled for oversaturation prior to analysis (SACK *et al.* 2011). Parameters were calculated from Figure 6 as following: saturated water content (SWC) as the intercept of water potential and water mass [data points above turgor loss point (TLP)] based on the twig dry weight; osmotic potential at saturation (Π_0 , the inverse of the y intercept) in the straight line region of the PV curve; the turgor loss point (Ψ_{TLP}); the relative water content at turgor loss point (RWC_{TLP}) as the first point in the straight line region of the PV curve and the modulus of elasticity (ϵ), determined by the slope of the pressure potential between full turgor and TLP.

Responses to water deficit

In order to comparatively investigate the responses of *Q. ilex*, *Q. pubescens* and *Q. robur* to decreasing soil water content and to monitor possible changes in the absolute/relative chlorophyll relationship and PSII functionality, 6 trees per species were subjected to drying by transpiration under controlled climatic conditions in September 2013 (day/night: 14/10 hours, 70/70 % rel. humidity, 20/20 °C, light intensity $\sim 500\text{-}700 \mu\text{mol quanta m}^{-2} \text{ s}^{-1}$). Prior to onset of the experiment it was assured that all leaves on the plants were fully developed to rule out possible differences in the amount of transpiration of unmaturing leaves. Additionally the soil in the pots was covered (not sealed) with aluminium foil to minimise water loss by evaporation. Pots were randomized daily in location within the climate chamber as well as in the sequence of measurement. After ceasing plant watering, soil water content, transpiration rate, leaf water content, predawn water potential, relative chlorophyll content, leaf pigment ratios and Chl fluorescence were assessed frequently until predawn water potential was below -4 MPa (limit of SKPM 1400 pressure chamber, SKYE Instruments, Powys, Wales, UK). Plant damage and survival were assessed by resprouting, after all leaves had been removed at the end of the experiment. Volumetric soil water content was quantified daily by a standing wave measurement device (ThetaProbe ML2x, Delta-T Devices, Cambridge, UK). The ThetaProbe was calibrated for the used soil/perligran mixture by a two point gravimetric calibration prior to the experiment to ensure full accuracy of 1% (as declared by manufacturer). 5 measurements with the ThetaProbe were conducted on each pot, to account for possible spatial differences in soil water acquisition. For the measurement of transpiration rates, pots were weighed daily (Mettler-Toledo SB12001, Giessen, DE) To ensure that water loss measured by weighing of the pots could be calculated as water loss on a leaf area basis, all leaves sampled in the course of the experiment (for RWC and water potential determinations) were weighed and scanned (Easy-scan, 300 dpi resolution, Easypix GmbH, Köln, DE) for the determination of leaf area. At the end of the experiment, all leaves of the trees were sampled, dried (70°C , until constant weight was reached, T6060, Heraeus, Hanau, DE) and leaf area was estimated through dry weight and specific leaf area (SLA) determined in 2.2.1 for the different species.

The rate of transpiration was calculated as:

$$\text{Transp. [g m}^{-2}\text{h}^{-1}] = \frac{\text{weight}_{\text{pot},d}[\text{g}] - (\text{weight}_{\text{pot},d+1}[\text{g}] + \text{weight}_{\text{sample}}[\text{g}])}{\Delta t [\text{h}] \times (\text{leaf area}_{\text{total}}[\text{m}^2] + \text{leaf area}_{\text{sample}}[\text{m}^2])}$$

Leaf water status was assessed infrequently with the intention to cover the whole range of drought perception without inducing additional stress due to large leaf area losses. Relative water content (RWC) and water potential measurements were conducted on leaves of the same twig. For the determination of RWC, leaves were sampled predawn and handled as described in 2.2. Water potential was measured predawn, when plant to soil water equilibrium was expected (LARCHER 2003) with a pressure chamber (SKPM 1400). One leaf of the measured twig was frozen in liquid nitrogen and stored at -80°C for subsequent pigment analysis (for method of pigment determination see 2.2.2). Relative chlorophyll content was assessed predawn with a SPAD-meter (SPAD-502, Konica-Minolta, Osaka, JP) with n = 3 measurements at the same leaf over the course of the whole experiment. PSII functionality was assessed predawn by recording of the fast Chl a fluorescence induction transient (Pocket PEA, Hansatech, King's Lynn, UK) on the same leaf at which the SPAD measurements were taken.

Drought stress experiment B

Plant material

For the drought stress experiment in the summer of 2011, 6 trees of *Q. robur* L. (5 years old, 2 m high, provenance: D-81705), *Q. ilex* L. ssp. *ilex* (5 years old, 1,5 – 2 m high, provenance: QIL 702) and their semi-evergreen hybrid *Q. x turneri* WILLD. var. *pseudoturneri* (5 years old, 2,5-3 m high) were grown in pots of 45L (*Q. ilex*, *Q. robur*) and 60 L (*Q. x turneri*), respectively. Pots were filled with loamy soil (sand + silt: 86-89%, clay: 11-14%) and sufficiently watered until the onset of the experiment. The plants were grown in a foliar greenhouse (Nitsch & Sohn GmbH, Kreuztal-Eichen, DE) since spring 2011 at the Botanical Garden in Frankfurt, Campus Bockenheim. Light intensity and temperature at 2 m height were constantly monitored with an iMetos sm SMT280 climate station (Pessl Instruments, Weiz, AT) inside the greenhouse. Plants

were randomly assigned to a control and a stress group to account for the semi-controlled environment of the greenhouse. The experiment was conducted between June 09th and August 30th 2011 with leaves fully matured and before the visual onset of leaf senescence.

Responses to water deficit

Water was withheld from the trees assigned to the stress group for a period of 18 to 22 days, after which the plants were rewatered and further monitored to ensure that the treatment was not fatal. The trees of the control group were watered any other day. Pots were weighed frequently to monitor the rate of water loss. Additionally the volumetric soil water content was quantified with a ThetaProbe (ML2x, Delta-T Devices, Cambridge, UK). Leaf water status was assessed by determination of predawn water potential. At the beginning of the experiment and at a state of drought stress (defined by a predawn water potential below -2MPa) gas exchange was measured under ambient and elevated CO₂ concentration. In order to monitor responses of photosynthesis, stomatal conductance and PSII functionality to decreasing soil water availability, gas exchange with the GFS-3000 and fast Chl a fluorescence transients were measured during the whole period of drought development to cover a range of different stress levels.

Water potential was measured predawn (completed before 5:00 a.m.) with a Scholander-Hamel pressure chamber (SKPM 1400) with a low rate of pressurisation on one twig per tree. Each twig was excised with the help of a razor blade, stored in an air tight and dark container and separately transported to the laboratory as fast as possible to ensure that no additional water was lost through transpiration.

Gas exchange was measured on randomly selected, south-exposed, mature and attached leaves in the morning (09:00 to 12:00) with the GFS 3000 gas exchange system (Walz, Effeltrich, DE). Measurements were performed at 400 mg kg⁻¹ CO₂ at 25 C cuvette temperature and 50% relative humidity. Light was provided by the GFS 3040L light source with an intensity of 900 μmol quanta m⁻² s⁻¹. The net rate of photosynthesis (P_N) and stomatal conductance (G_{H2O}) were calculated by the internal

GFS software according to the equation system of VON CAEMMERER & FARQUHAR (1981). The cuvette size was 8 cm². For leaves with a smaller leaf area than 8 cm², values were recalculated to actual leaf area. The maximum photosynthetic capacity (P_{Max}) was additionally assessed under elevated CO₂ (4,5%) and decreased O₂ (2%), in order to exclude stomatal and photorespiratory effects. During measurements, the partial pressure of CO₂ was kept constant by including 1 ml of 0,95M NaHCO₃, 0,05M Na₂CO₃ in a sponge inside the cuvette (BRÜGGEMANN 1992). P_{Max} was measured on detached leaves (leaf discs excised with a cork borer) with a Clark oxygen electrode in an LD 2/3 setup (Hansatech, King's Lynn, UK) at 25°C and 900 $\mu\text{mol quanta m}^{-2} \text{s}^{-1}$ (emitted by a LH36/2R light source). The electrode signal was amplified and directed to a strip chart recorder (SE120, Asea Brown Boveri, Zürich, CH). A calibration was carried out before each measurement, recording the signal of ambient O₂ concentration and 2% O₂ in the measuring gas (Length of segment: S_{Cal} [mm]). The interpolations of the rates of O₂ evolution in light and O₂ depletion in the dark (ΔS_{Ms} [mm] after 10 min) were used to calculate the maximal net photosynthetic capacity P_{Max} as followed:

$$P_{Max} [\mu\text{mol m}^{-2} \text{s}^{-1}] = \frac{\Delta S_{Ms} [\text{mm}] \times \text{voltage} [\text{mV}] \times \text{conc}_{O_2} [\mu\text{mol ml}^{-1}] \times \text{vol} [\text{ml}]}{S_{Cal} [\text{mm}] \times \text{voltage} [\text{mV}] \times \text{area}_{Leaf} [\text{m}^2] \times \text{time} [600\text{s}]}$$

With *voltage* [mV] being the electrical voltage, at which the signals of calibration and measurement were recorded. *Conc O₂* [$\mu\text{mol ml}^{-1}$] is temperature dependent and calculated as

$$(O_{2amb} - O_{2gas}) \times V_{mgas} [l \text{ mol}^{-1}] \times \frac{273,15^\circ\text{C}}{273,15^\circ\text{C} - T [^\circ\text{C}]} \times 1000$$

With $V_m = 22,414 \text{ l mol}^{-1}$. The cuvette's volume (*vol* [ml]) was empirically estimated under measuring conditions, including the carbonate buffer and sponges to be 5,80 ml.

Fast Chl a induction transients were measured predawn with the Pocket PEA (Hansatech, King's Lynn, UK) on five south exposed leaves per tree with $F_0 = F_{50\mu\text{s}}$ and analysed as described for Drought stress experiment A.

2.5.2. Heat stress

Experiments related to increased temperature were conducted with the species *Q. ilex*, *Q. pubescens* and *Q. robur* to monitor possible differences in heat acclimation and thermostability of the species and to identify a fluorescence signature that can be related to heat imposed damage of the photosystem. Besides diurnal monitoring of leaf temperatures at the forest tree plantation, laboratory experiments were conducted on trees, grown at controlled climatic conditions and subjected to increasing temperatures in a climate cabinet.

On a hot summers day in 2013 (22.07.2013), the air and adaxial leaf temperatures were monitored over the course of one day at the experimental forest site in Frankfurt Schwanheim. Air temperatures were recorded with the on-site climate station (cf. 2.1). Leaf temperature was measured in *Q. ilex*, *Q. pubescens* and *Q. robur* with an infrared thermometer (Voltcraft IR260-85, Conrad Electronic AG, Wollerau, CH) at the adaxial leaf surface at a distance of 5 to 10 cm. Measurements were performed from 04:00 a.m. until 10:00 p.m. in 3 hour intervals on the same leaves, in which diurnal SPAD-value variations were investigated (cf. 2.3.1). To prevent interference of reflected solar radiation, leaves were shaded during temperature measurements and values were noted after reaching equilibrium (approx. 3-5 s).

Plant material for the laboratory experiments was identical to the material described in 2.5.1. All leaves of the investigated trees developed while grown inside the climate chamber and had not experienced temperatures above 25 °C. 3 plants of each species were relocated to a climate cabinet (SGC120 Fitotron, Loughborough, UK) with day/night settings of 12/12 hours, 20/20 °C, 70/70% relative humidity and a daytime light intensity of 300-500 $\mu\text{mol quanta m}^{-2} \text{s}^{-1}$ two weeks before the onset of the experiment, to allow for sufficient acclimation. Temperature, relative humidity and day/night rhythm were automatically regulated by the control unit of the climate cabinet. Strips of air bubble film were placed inside the pots to prohibit excessive heating of the soil, while ensuring adequate gas exchange. To reduce soil temperature, the black pots were wrapped with fleece material and placed inside a tray filled with 2-3 cm of water, which allowed moisture wicking and cooling due to evaporation and sufficient water supply to the roots over the course of the experiment. Soil temperature

was frequently controlled with an immersion sensor thermometer (Voltcraft DT300, sensor length: 144 mm, Conrad Electronic AG, Wollerau, CH). Daytime temperatures were increased in steps of 5°C from 20 °C to 35 °C, whereas night-time temperatures were kept constant at 20 °C. Measurements were performed on the third and fourth day, respectively, allowing for a minimum of two days for acclimation at the target temperature (Figure 7). The plants were finally kept at 35°C day temperature for a total of 9 days.

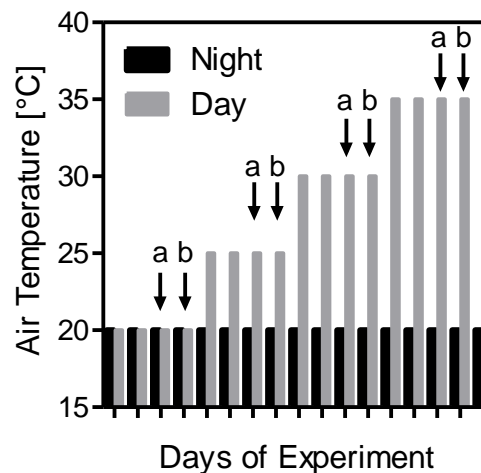


Figure 7: Schematic illustration of temperature increases during the heat stress experiment 2012. Night-time temperatures were kept constant at 20°C whereas daytime temperatures were increased after 4 days at target temperature at intervals of 5°C. Each column represents a time interval of 12 hours. At columns marked with the letter a, relative chlorophyll content was measured with the SPAD-502 and samples for pigment analysis were taken. At columns marked with the letter b, the critical temperature for PSII thermostability was assessed by measuring the response of ground fluorescence to increasing leaf temperature in the dark.

Thermal stability of PSII

On the fourth day at the target temperature, thermal stability of PSII was assessed according to HAVEAUX (1993) by constantly measuring the ground fluorescence (F_0) of a leaf disc subjected to gradually increasing temperature in the dark ($\sim 1,5 \text{ }^\circ\text{C min}^{-1}$). The leaf disc was placed in a custom built cuvette (also used for steady state fluorescence measurements, see below) after dark adaptation for 30 min at 20°C in measuring gas (2% O_2 , 4,5% CO_2 in N_2). A NiCr-Ni type K thermocouple (B+B Thermotechnik GmbH, Donaueschingen, DE) with a response time of 0,3 s was inserted

from the bottom of the cuvette, touching the abaxial leaf surface. Ground fluorescence was induced by the measuring light ($\sim 0,5 \mu\text{mol quanta m}^{-2} \text{s}^{-1}$) of the PAM 101 (Heinz Walz GmbH, Effeltrich, DE) and measured by the same device. The signal was recorded by a chart recorder (Servogor 220, BBC Goertz, AU). Leaf temperature was continuously increased indirectly through the thermoregulation of the cuvette by a water bath (Haake K20, Thermo Haake GmbH, Karlsruhe, DE). Figure 8 shows a typical recording from which the critical temperature (T_{crit} : break point of F_0 rise), T_{50} (where F_0 reaches 50% of peak value) and F_p (peak value of temperature dependent F_0 rise), were calculated for each single leaf disc. Measurements were performed on $n = 3$ leaves per species and target daytime temperature.

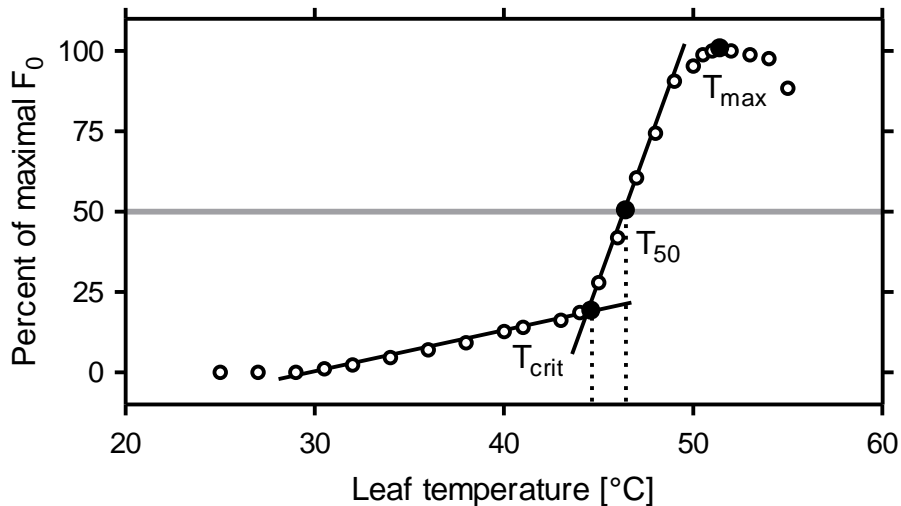


Figure 8: Temperature dependent rise of F_0 and derived parameters of PSII thermostability (example curve). Critical leaf temperature T_{crit} at the intersection of linear regressions of the slow and the fast rise of the F_0 -T relationship. T_{50} : leaf temperature when the 50% of T_{max} are reached. Trace recorded from single leaf in PAM setup (2% O_2 , 4,5% CO_2 , $\sim 0,03 \mu\text{mol quanta m}^{-2} \text{s}^{-1}$ at 1,6 kHz). Leaf temperature measured at abaxial side with Ni-Cr thermocouple.

In order to assess the status and functionality of PSII in the critical temperature range observed in the temperature dependent rise of F_0 (see above), OJIP transients were recorded from leaves at the following temperatures: 20, 30, 35, 40, 45 and 50 °C. Five leaves per species from acclimated plants (35°C for 9 days) were used for the experiment. To ensure that transients were not affected by closed reaction centres, the experiment was carried out in darkness with only a weak green light source. Leaves

were excised after a full daytime period and immersed in distilled water inside glass tubes. A custom built grate was used to submerge the randomly placed glass tubes inside a temperature controlled water bath (mgw Lauda RM, Lauda-Königshofen, DE). Temperature inside the glass tubes was monitored by a NiCr-Ni type K thermocouple (B+B Thermotechnik GmbH, Donaueschingen, DE). Temperature was increased from 20°C with a rate of $\sim 2 \text{ }^\circ\text{C min}^{-1}$ until the target temperature was reached, at which the leaves were kept for 10 min. To account for equal submersion times, the time interval at 20 °C was elongated for leaves at lower target temperatures, so that all leaves measured in course of the experiment were submerged for the same time period (25 min) until the fluorescence transient was recorded. Leaves were placed in a leaf clip heated to the same temperature and measured with the Pocket PEA.

An additional experiment was performed to investigate the temperature dependent alteration of the effective quantum yield of photochemistry (ϕ_{PSII}) at $\sim 350 \text{ } \mu\text{mol quanta m}^{-2} \text{ s}^{-1}$ in the temperature range between 30 and 50 °C. The PAM 101 setup was used as described above, with a NiCr-Ni type K thermocouple (B+B Thermotechnik GmbH, Donaueschingen, DE) controlling the abaxial leaf temperature in the cuvette. Since for the determination of ϕ_{PSII} the quantification of F_0 and F_m is unnecessary (see calculation below) the leaf discs were not dark adapted. The leaf temperature was increased indirectly through the warming of a water bath (Haake K20, Thermo Haake GmbH, Karlsruhe, DE). The temperature was kept constant for 5 min at the target temperatures of 30, 35, 40, 45 and 50 °C. A saturating flash (2 s, $\sim 5000 \text{ } \mu\text{mol quanta m}^{-2} \text{ s}^{-1}$) allowed the determination of F_m' . With the steady state fluorescence intensity F_s , noted immediately before the flash, ϕ_{PSII} was calculated with $(F_m' - F_s)(F_m')^{-1}$. The temperature dependent alteration of ϕ_{PSII} was measured for $n = 3$ leaves per species.

2.5.3. Cold stress in *Q. ilex*

In order to assess possible acclimation responses of the photosynthetic apparatus of the evergreen *Q. ilex* to Central European winter conditions and the possible influences of these conditions on the non-invasive sensing techniques established for the growing season, a monitoring program for *Q. ilex* was carried out over a period of 6 months. In the course of this program, changes in growth, structural damage, chlorophyll sensing by the SPAD-meter, pigment content, PSII functionality, electron transport and maximal photosynthetic capacity were assessed. To control for possible drought stress effects due to frozen soil, xylem sap flow was continuously monitored.

Trees from two different sites were chosen for the monitoring program and the intervals as well as the choice of measurements differed between these two sites (Table 3). At the experimental forest plot in Frankfurt Schwanheim (FR), the monitoring of the chlorophyll content by means of SPAD-readings (n=5 per leaf; one leaf per tree) and the measurements of the fast Chl a fluorescence transient (n=1 per leaf; one leaf per tree) was continued from the seasonal monitoring program (cf. 2.4) on the same leaves in two week intervals. Fluorescence measurements were performed predawn with the Pocket PEA. SPAD-measurements (n = 5 per leaf) were taken subsequent to the fluorescence measurements but not mandatorily before dawn. Height measurements and visual inspections of all *Q. ilex* trees at the forest site (n = 168) were carried out in fall 2012 and in spring 2013 to assess winter growth, terminal bud injury and tree mortality.

At the Botanical Garden Frankfurt (Campus Riedberg) measurements were performed on five 7 year old and 1,5-2 m tall *Q. ilex* L. ssp. *ilex* trees (provenance: QIL 702), planted in spring 2012 on a slope with southerly aspect. On each tree, 5 leaves were tagged prior to the monitoring program on which the fast Chl a fluorescence transient (n = 1 per leaf) and the relative chlorophyll content (n = 3 per leaf) were measured predawn, once a month (cf. Table 3). Another set of leaves was enclosed in aluminium foil before dawn to ensure dark adaptation for the later use in the analysis of steady state fluorescence and maximal photosynthetic capacity. Steady state fluorescence measurements were performed with a PAM 101 setup (described above) on both leaf surfaces of one leaf per tree (5 trees). A measurement protocol was used to additionally derive the Chl fluorescence decrease ratio (R_{Fd}), introduced according to

LICHTENTHALER *et al.* (2005) as a sensitive vitality index. Leaf discs were dark adapted inside the cuvette under measuring gas (2% O₂, 4,5% CO₂ in N₂) at 20°C for 10 min. After determination of F₀ and F_m, continuous saturating light (~2000 μmol quanta m⁻² s⁻¹) was applied for 20 min to determine the fluorescence in the steady state under saturating light (F_s), followed by a 2 s flash of light (~5000 μmol quanta m⁻² s⁻¹) to record F_m'. Non-photochemical quenching (NPQ) was calculated with (F_m-F_m')(F_m')⁻¹ and φ_{PSII} was calculated as in 2.5.2. R_{Fd} was calculated as (F_m-F_s)(F_s)⁻¹. After the fluorescence decays were recorded, leaf discs were frozen in liquid nitrogen and stored at -80°C for subsequent pigment determination as described above (cf. 2.2.2). Maximal photosynthetic capacity P_{Max} was measured as describe in 2.5.1 for one leaf per tree (n = 5 trees) at 20 °C and 900 μmol quanta m⁻² s⁻¹.

Table 3: Dates of measurements performed on *Q. ilex* trees at the Botanical Garden at Frankfurt, Riedberg and the experimental forest site in Frankfurt Schwanheim (FR) in the course of the winter monitoring program.

Date	DOY	Botanical Garden	Forest (FR)
06.11.2012	311	X	
23.11.2012	328		X
06.12.2012	341	X	
07.12.2012	342		X
20.12.2012	355		X
04.01.2013	4	X	X
14.01.2013	14		X
06.02.2013	37		X
12.02.2013	43	X	
21.02.2013	52		X
06.03.2013	65	X	X
19.03.2013	78		X
02.04.2013	92	X	
03.04.2013	93		X
18.04.2013	108		X
02.05.2013	122	X	
03.05.2013	123		X

Xylem sap flow velocities were continuously recorded on 3 of the 5 trees on which the above describe measurements were performed. Sap flow meters following the “heat ratio method” (ICT International, Armidale, AU) were installed by inserting 3 probes per tree into the xylem. Measurements were performed automatically every hour. Data was converted by the “Sap Flow Tool” software (version 1.2, ICT International, Armidale, AU/ Phyto IT, Mariakerke, BE). The sap flow velocities [cm h^{-1}] were correlated against the vapour pressure deficit of the air (VPD) over the course of the monitoring program to visualize possible deviation of the relationship due to drought stress. VPD was calculated after ALLEN *et al.* (1998) from the difference of the mean saturated vapour pressure (e_s) and the actual water vapour pressure (e_a) ($\text{VPD} = e_s - e_a$):

$$e_s = \frac{e^0(T_{max}) + e^0(T_{min})}{2} \quad ; \quad e^0(T) = 0,6108 \times \exp^{(17,27 \times T)(T+237,3)^{-1}}$$

Data of T_{max} , T_{min} and e_a were taken from the on-site iMetos climate station

3. Results

3.1. Investigation area

3.1.1. Climate at Frankfurt Schwanheim in 2012 and 2013

The climate conditions of 2012 and 2013 at FR site are outlined at daily resolution (Figure 9). Samples for the analysis of chemical and morphological leaf traits (see 3.2) were obtained, and SPAD and OJIP monitoring (see 3.3) was performed at high frequency during this interval (Figure 9). A significant temperature drop at the end of January marks the beginning of 2012 with minimum air temperature of $-17,1^{\circ}\text{C}$. The lowest temperature measured in that region (Frankfurt airport since 1949) was $-21,6^{\circ}\text{C}$ in 1968. Temperatures equal to $-17,1^{\circ}\text{C}$ or lower have been measured 10 times, since

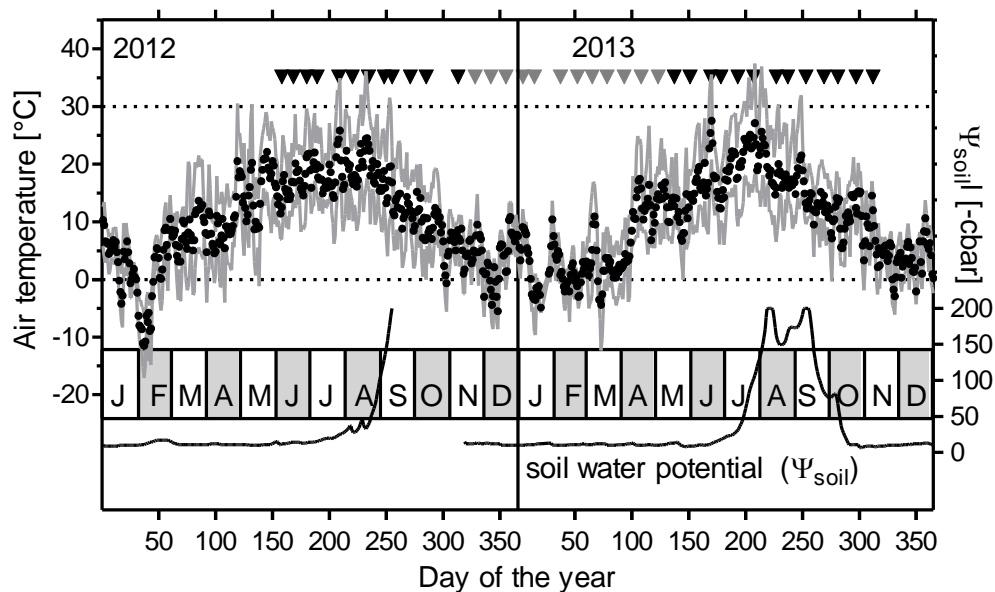
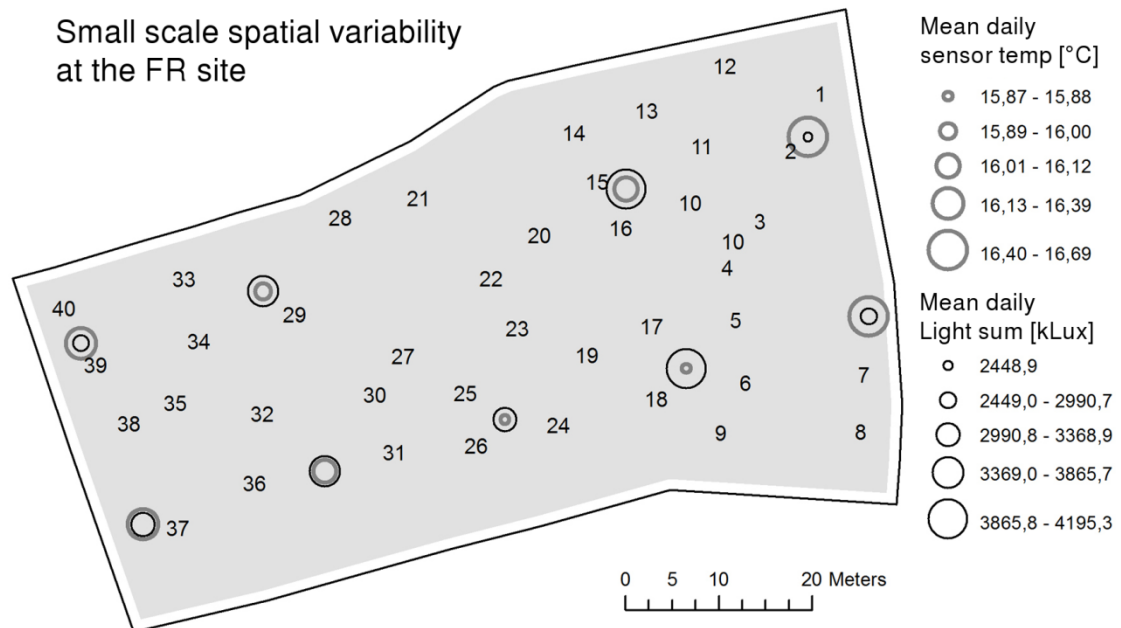


Figure 9: Temperature and soil water deficit at Frankfurt Schwanheim in 2012 and 2013. Daily minimum and maximum temperatures are indicated in greyscale above and below mean daily temperature (black dots) measured at Frankfurt Schwanheim experimental forest plot at 2 m height. Horizontal broken lines indicate 0° and 30°C . Soil water potential in (-) cbar (0-200) measured at 1 m depth on right y-axis. Values from September to November 2012 are missing. Months are indicated by alternate grey and white boxes in the bottom third of the graph. Triangles symbolize days of SPAD and predawn OJIP measurement of *Q. frainetto*, *Q. robur*, *Q. pubescens*, *Q. rubra* and *Q. ilex*. Winter measurements symbolized by grey triangles only for *Q. ilex*.

1949. This period of low temperature in early 2012 led to total leaf shedding in *Q. ilex*. Frost events were frequent until the end of April 2012, with a following sharp increase in air temperature to over 30°C at the end of April. Late frost occurred in the mid of May. The highest temperature recorded in 2012 was 36,1°C at the end of August, when (in combination with a period of low precipitation) a soil water deficit developed, which peaked in September (Figure 9). The duration of soil water potentials below -200 cbar (limit of watermark sensor) cannot be given, since the functionality of the sensor was lost due to the dry conditions (the sensor needed to be dug out and re-watered to ensure further function). After a warm December, temperatures plummeted in January 2013 with icy rain, leading to ice crusts on leaves. The beginning of the year 2013 was colder compared to 2012 with mean daily temperatures around zero to 5°C until the mid of April. The lowest temperature was recorded in March with -12,3°C. A late frost occurred at the end of May. In the end of July a period of hot days occurred with a maximum temperature of 37,4°C. Simultaneously a soil water deficit developed from the beginning of June and reached -200 cbar in 1 m depth at the beginning of August, declining in September.

3.1.2. Spatial distribution of abiotic growth factors at FR

Small scale spatial variability of abiotic growth factors was investigated at the FR site. 10 self-contained temperature/ light data loggers were installed on a 20 x 20 m grid at 1 m height at the site (HOBO pendant UA-002, Onset; Bourne, MA, USA) to monitor spatial variation in irradiance and temperature, due to inhomogeneous shading of the present vegetation. Mean daily temperatures varied up to 1,68 °C between sensors (values with direct sun exposure to sensor excluded [>25 kLux, empirically estimated]) with a mean range of 0,93°C in a 62 days interval between June and September (day 170-251, no data for 207-226). During this interval, the maximum difference between the temperature daily means of all sensor was 0,82°C. The mean daily light sum varied up to 1746,42 kLux between sensors during the same interval. A clear spatial trend in the variability of light and temperature was not found with the installed raster of 20 x 20 m at the site and sensors with a high mean daily light sum not mandatorily showed high mean daily temperatures (Figure 10). Soil nitrogen contents taken at 30 cm depth at



Trupp	Species	N _{soil} [%]	C _{soil} [%]	C/N	Trupp	Species	N _{soil} [%]	C _{soil} [%]	C/N
1	Q. ilex	0,15	2,90	19,25	21	Q. rubra	0,08	1,29	15,17
2	Q. frainetto	0,18	3,69	20,91	22	Q. ilex	0,07	1,09	15,70
3	Q. ilex	0,26	5,27	20,65	23	Q. pubescens	0,30	5,88	19,73
4	Q. pubescens	0,35	7,81	22,23	24	Q. robur	0,21	3,42	16,28
5	Q. frainetto	0,30	6,52	21,48	25	Q. rubra	0,20	3,26	16,49
6	Q. pubescens	0,16	2,85	17,29	26	Q. pubescens	0,21	4,30	20,14
7	Q. robur	0,11	2,07	18,09	27	Q. ilex	0,15	2,53	16,44
8	Q. rubra	0,17	3,58	21,14	28	Q. frainetto	0,14	2,15	15,63
9	Q. robur	0,25	6,07	23,99	29	Q. rubra	0,68*	14,36*	21,07
10	Q. robur	0,16	4,34	26,58	30	Q. frainetto	0,21	3,24	15,72
11	Q. rubra	0,06	0,91	15,24	31	Q. ilex	0,15	2,38	15,69
12	Q. pubescens	0,06	0,82	14,47	32	Q. robur	0,13	1,97	14,86
13	Q. ilex	0,16	3,23	20,81	33	Q. pubescens	0,18	2,78	15,40
14	Q. robur	0,10	1,79	17,08	34	Q. robur	0,21	3,43	16,02
15	Q. pubescens	0,15	2,72	17,93	35	Q. pubescens	0,19	2,95	15,15
16	Q. frainetto	0,10	1,67	17,22	36	Q. frainetto	0,19	2,90	15,34
17	Q. rubra	0,12	2,08	17,08	37	Q. ilex	0,13	2,03	16,19
18	Q. ilex	0,39	8,11	21,05	38	Q. frainetto	0,25	3,61	14,42
19	Q. frainetto	0,26	5,99	23,39	39	Q. robur	0,22	3,51	15,78
20	Q. rubra	0,21	3,62	17,34	40	Q. rubra	0,18	3,00	17,06

Figure 10: Spatial variability of selected abiotic growth factors at the FR site. Map shows FR site with depicted Trupp numbers. Information on soil nitrogen and carbon content at the Trupp locations (sampling depth: 30 cm, 2 aliquots of n=1 soil sample per Trupp) can be retrieved from the table below the map. Soil nitrogen and carbon contents for Trupp nr. 29 are strikingly high and probably influenced by an animal burrow (marked with asterisk). Mean daily temperature and light sums for period between June and September 2012 (no data for doy 207-226), recorded by data loggers in 10 min intervals are shown with graduated symbology in the map as well (data for sensor nr. 3 not shown due to technical defect).

Results

each Trupp varied to a great extent (min: 0,06%, max: 0,39%), mean: 0,18%) despite of the small area of the site (~0,5 ha). Likewise a spatial variability in soil carbon content was found, which was highly correlated to the soil nitrogen content ($R^2 = 0,95$). A clear spatial pattern (i.e. east-west decrease) in soil N and C contents was not observed. A vertical profile of the soil, taken at one position at the site, showed the fast decrease in N and C contents with increasing depth (Figure 11). The top soil layer below the organic humus layer was very thin, followed by a wind-borne sand substrate to a depth of ~75 cm. Lower layers than 75 cm were assigned to river sediment substrates. With increasing depth, the proportional shares of silt and clay decrease. At -95 cm the soil type was found to be pure sand (cf. Appendix VI).

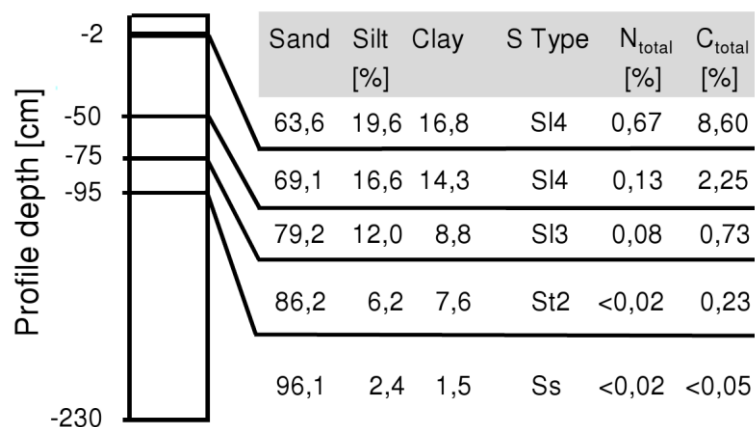


Figure 11: Soil profile of experimental forest site Frankfurt Schwanheim (FR). Samples taken and analysed by the Hessian Agency for Environment and Geology (HLUG) at 10.05.2012, n=1 per profile. Sl: sandy loam; St: loamy fine sand. Ss: Sand. Nitrogen (N) and carbon contents (C) are given in percent of dry weight.

3.2. Monitoring of morphological and chemical leaf traits

Morphological leaf traits derived from saturated fresh weight, dry weight and leaf area and chemical leaf traits derived from compound extractions of the same leaf samples were monitored for one growing season in 5 different *Quercus* species at FR.

3.2.1. Monitoring of morphological leaf traits

During the observation period of 175 days from 17st May (doy 137) until the 08th November 2013 (doy 312), seasonal variation of morphological leaf traits could be detected in all *Quercus* species of the experimental forest plot FR. From an initial value of the first observation date, the parameter values approached a constant level in a timeframe of approx. 4 to 8 weeks, which showed no further tendency of increase or decrease until the end of the observation period (Figure 12). The parameter value at constant level is about 50% smaller in specific leaf area on dry weight basis (SLA_{DW}) and 50% higher in leaf dry matter content (LDMC) when measured in May (Figure 12). For the time point, when the constant level was reached in the deciduous species *Q. frainetto*, *Q. pubescens*, *Q. robur* and *Q. rubra*, no significant interspecific difference was noted. The parameter values at constant level however varied significantly between species (Figure 13). In the deciduous species the constant level for SLA_{DW} and LDMC was reached in mid-June (doy 164) and leaf mass per area on fresh weight base (LMA_{FW}) two weeks earlier at doy 151. The current year leaves of the evergreen *Q. ilex* emerged later and reached the constant level of SLA_{DW} and LDMC at a later point in time at end of July (doy 207) and doy 178 for LMA_{FW} . The completion of leaf development ended 40 days later in *Q. ilex* compared to the deciduous *Quercus* species on the site. Previous year leaves of *Q. ilex* showed no increasing or decreasing tendency of parameter values throughout the season. The LDMC is higher in previous year *Q. ilex* leaves at the beginning of the observation period as compared to LDMC of current year leaves of *Q. ilex* at the end of the observation period.

Results

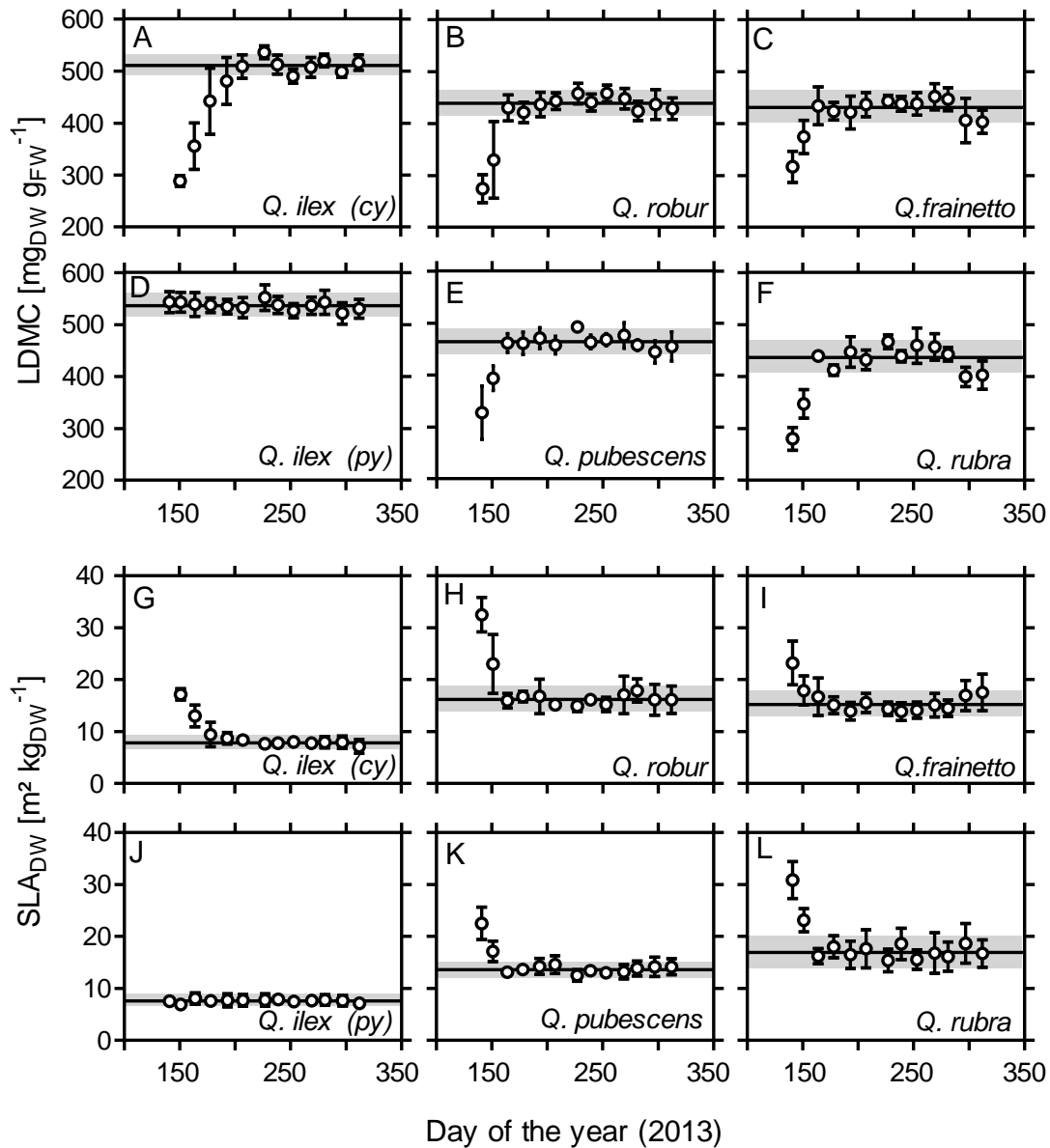


Figure 12: Seasonal variability of leaf dry matter content (LDMC) and specific leaf area (SLA_{DW}). LDMC (A-F) is the ratio of leaf dry weight (DW) to leaf fresh weight (FW) in $mg_{DW} g_{FW}^{-1}$. SLA_{DW} (G-L) is the ratio of leaf area to leaf dry weight in $m^2 kg_{DW}^{-1}$ (= inverse of LMA_{DW}). Leaves were randomly sampled at Frankfurt Schwanheim experimental forest site (FR) from 17th May (doy 137) until 08th November 2013 (doy 312). Means and standard deviations ($n=8$) are symbolized by white circles with error bars. Horizontal line and shaded area marks the mean and standard deviation of parameter with no seasonal influence. For *Q. ilex*, parameters of current year (cy) and previous year (py) leaves are shown.

The studied morphological leaf traits were derived from leaf fresh- and dry weight as well as leaf area. The data showed significant, up to twofold, interspecific differences once leaf development had finished. Four additional *Quercus* taxa were taken into account for the analysis of interspecific variance of morphological leaf traits. These taxa are the evergreen *Q. suber* L., the deciduous *Q. cerris* L., their hybrid *Q. x hispanica* LAM. (var. *Lucombeana*) and the hybrid of *Q. ilex* and *Q. robur*: *Q. x turneri* WILLD. (var. *Pseudoturneri*). The largest interspecific variability was found in the relation of leaf area to dry weight (SLA_{DW}) and in fresh weight to leaf area (LMA_{FW}). The order from the highest to the lowest value for a given parameter resembles the leaf life trait of the species. Where the evergreen species *Q. ilex* and *Q. suber* showed the highest values of a given parameter (i.e. SLA_{DW}), the deciduous species *Q. robur* and *Q. rubra* showed the lowest values and vice versa. The latter two species had similar morphological leaf traits and displayed no significant difference in any of the studied parameters (Appendix V). *Q. robur* and *Q. rubra* showed low investments of dry mass per leaf area, resulting in high leaf water contents per dry weight (=1000-LDMC), low ratios of dry to fresh weight and thinner leaves (see Appendix V). On the other hand, the evergreen species showed the opposite pattern with high investments of dry weight per leaf area and thicker leaves, having a higher ratio of dry weight to fresh weight. The hybrids of evergreen and deciduous parentals and the Mediterranean deciduous *Quercus* species showed intermediate leaf traits to a differing degree. Whereas *Q. x turneri* displayed intermediary leaf traits in comparison to its parental species *Q. ilex* and *Q. robur*, *Q. x hispanica* revealed more of a heterogeneous mixture, having a very low SLA_{DW} and greater leaf thickness such as its evergreen parent *Q. suber* but a lower LDMC. Likewise, the Mediterranean deciduous species *Q. frainetto*, *Q. pubescens* and *Q. cerris* showed intermediate leaf traits to a differing degree between the Mediterranean evergreens and *Q. robur*/*Q. rubra*. In the order *Q. frainetto*, *Q. pubescens*, *Q. cerris*, leaf traits moved in the direction of the evergreens, with *Q. cerris* displaying parameter values in the middle of the highest and lowest parameter values (Figure 13).

Results

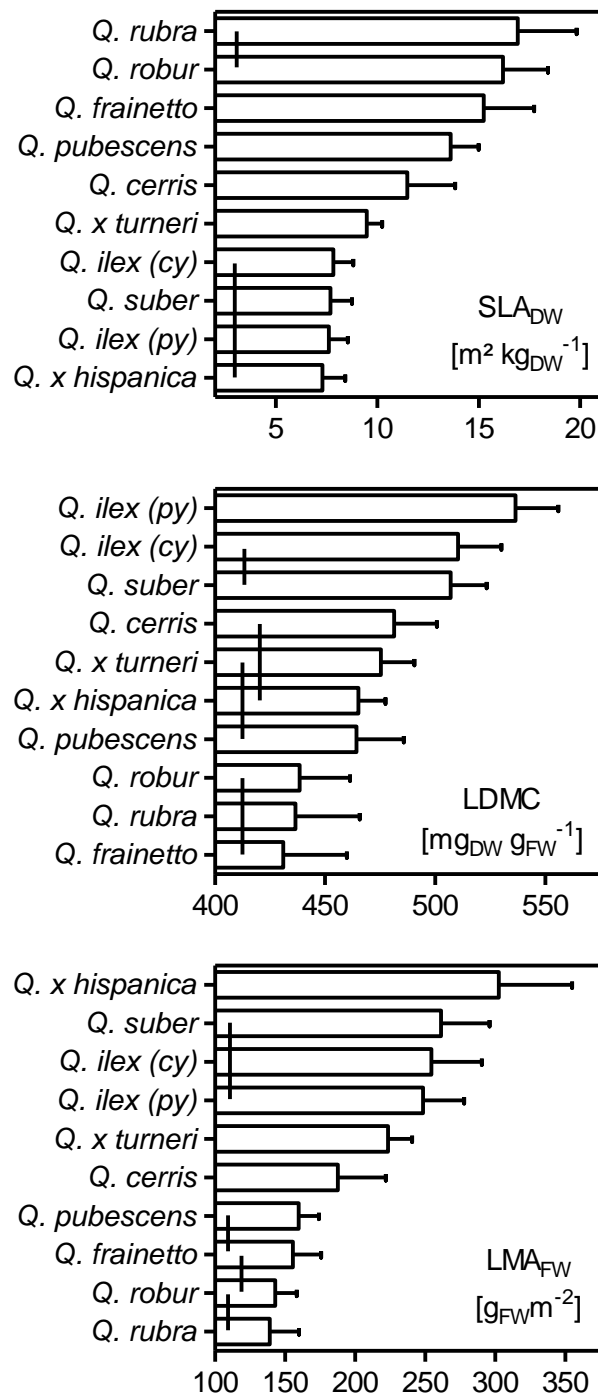


Figure 13: Interspecific variation of morphological leaf traits. Horizontal columns represent means of given value. Error bars represent the standard deviation of the mean. If columns are connected by a vertical bar, means are not significantly different ($p > 0,05$, one-way ANOVA with Tukey's post-test for multiple comparison. cy: current year leaves; py: previous year leaves; DW: dry weight; FW: fresh weight. Number of samples taken at Frankfurt Schwanheim (FR) at day 164–312:(2013): *Q. frainetto*: 87; *Q. ilex cy*: 62; *Q. ilex py*: 101; *Q. pubescens*: 85; *Q. robur*: 88; *Q. rubra*: 86. Samples taken at Botanical Garden Riedberg at day 309 (2013): *Q. cerris*: 31; *Q. suber*: 31; *Q. x hispanica*: 30; *Q. x turneri*: 32.

The parameters LDMC, SLA_{DW} and leaf thickness (LT) are related to each other through leaf density ρF [$g\ cm^{-3}$] by the following equation (PEREZ-HARGUINDEGUY *et al.* 2013):

$$LDMC = (\rho F \times SLA_{DW} \times LT)^{-1}$$

Since $LDMC \times SLA_{DW} = SLA_{FW}$ and $SLA_{FW}^{-1} = LMA_{FW}$ follows

$$LT = LMA_{FW} \times \rho F^{-1}$$

The leaf density ρF of saturated leaves showed no interspecific variation (one-way ANOVA with Tukey's multiple comparison post-test), despite the large difference in morphological leaf traits. If leaf dehydration can be excluded, LMA_{FW} is proportional to LT and can be used as a proxy for LT across the whole leaf for different *Quercus* taxa.

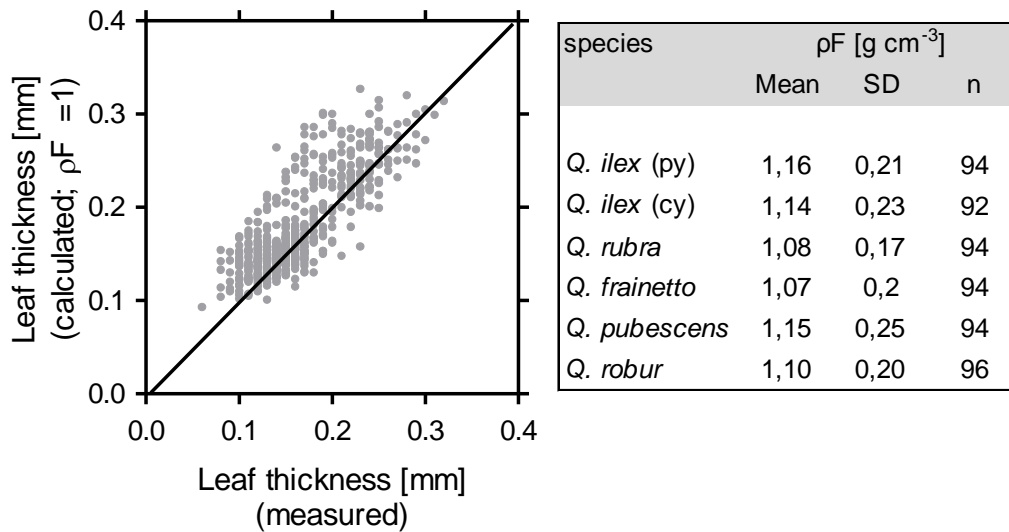


Figure 14: Estimation of leaf thickness with leaf density and LMA_{FW} . Leaf thickness was measured with a digital calliper on leaves of 5 different *Quercus* species throughout the vegetation period on the same leaf used for determining LMA_{FW} . Estimation of leaf thickness with the relation: $LT = LMA_{FW} \rho F^{-1}$. LT: Leaf thickness; LMA_{FW} : Leaf fresh mass per area; ρF : Leaf density [$g\ cm^{-3}$]. N = 564 data points. Calculation of ρF on species level with $\rho F = LMA_{FW}^{-1} \times LT^{-1}$. Statistical analysis show that means are not significantly different ($p > 0,05$, one-way ANOVA with Tukey's post-test.)

Results

3.2.2. Monitoring of chemical leaf traits

Leaf subsamples used for the monitoring of temporal variability of morphological leaf traits have been used to determine the concentrations of the photosynthetic pigments Chl a, Chl b and carotenoids (xanthophylls and carotenes) in the growing season 2013 (doy 137-312). The ratio of total Chl (a+b) to total Car (x+c) shows no significant interspecific difference. Above a total Chl concentration of approx. 100 mg m^{-2} the Chl/Car ratio was constant at $4,19 \pm 0,58$ ($m \pm \text{SD}$) ($n = 362$) irrespective of time of the year and species. Values of Chl below 100 mg m^{-2} occurred in the late season during autumnal senescence only and the corresponding Chl/Car ratio decreased strongly to values below one (Figure 15A). Developing leaves at the beginning of the growth period (doy 137) displayed no deviation from the constant ratio. If senescence was excluded by analysing the time interval from mid of May to mid-September only (doy 137- 253), a linear correlation ($R^2 = 0,906$) of Chl to Car across a wide range of concentrations was observed (Figure 15B).

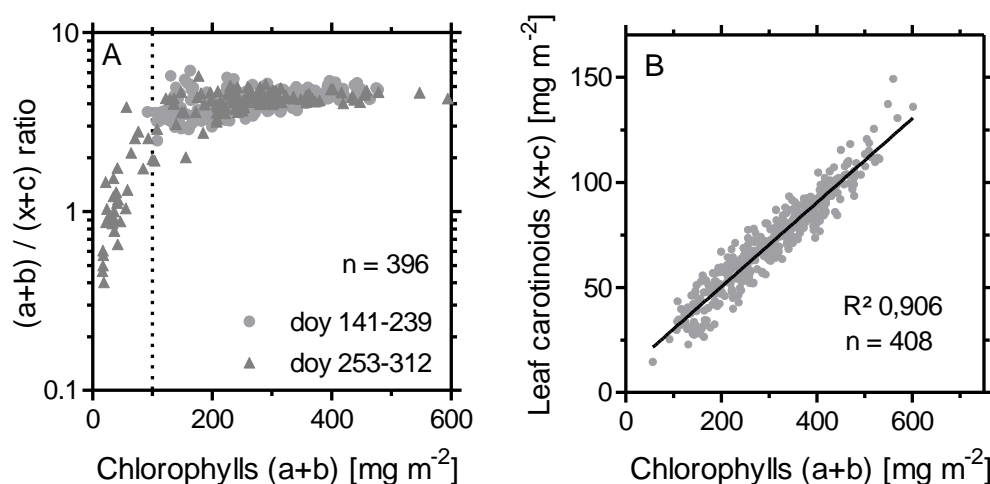


Figure 15: Relationship of leaf chlorophylls to leaf carotenoids. A: Chlorophyll / carotenoid ratio to total leaf chlorophyll of deciduous species (*Q. frainetto*, *Q. pubescens*, *Q. robur* and *Q. rubra*). Triangles and points symbolize different time periods: doy 137-239: 17.05.2013-27.08.2013; doy 253-312: 10.09.2013-08.11.2013. Vertical broken line indicates a leaf Chl concentration of 100 mg m^{-2} . Note logarithmic y axis. B: Total leaf carotenoids (xanthophylls + carotenes) [mg m^{-2}] to total leaf Chl (Chl a + Chl b) [mg m^{-2}] of *Q. frainetto*, *Q. ilex* (current and previous year leaves), *Q. pubescens*, *Q. robur* and *Q. rubra* combined, excluding senescent leaves ($n=408$; day of the year [doy] 137-253, 2013). Relation is linearly correlated with $R^2=0,906$; $y=0,20x+10,23$.

Similar to the ratio of total chlorophylls to total carotenoids, the ratio of chlorophyll a to chlorophyll b showed no interspecific variation. At very low total Chl concentrations ($\sim 50 \text{ mg m}^{-2}$) the ratio of Chl a to Chl b decreased. At higher Chl concentrations irrespective of developmental or senescent leaf stage, a constant a/b ratio of $3,28 \pm 0,44$ ($m \pm \text{SD}$) ($n = 396$) was observed. Over a wide range of values, Chl a and Chl b were linearly correlated ($R^2 = 0,891$).

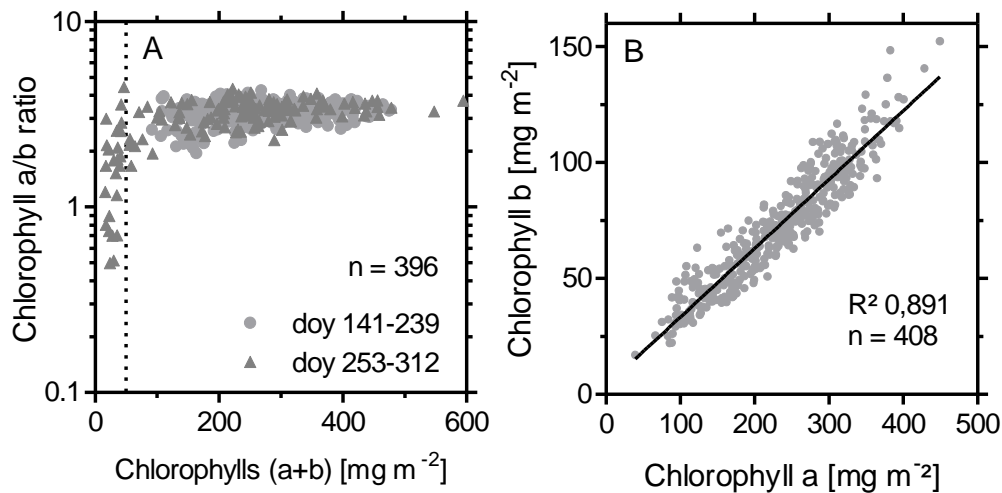


Figure 16: Relationship of chlorophyll a (Chl a) to chlorophyll b (Chl b). A: Chlorophyll a/b ratio to total leaf chlorophyll of deciduous species (*Q. frainetto*, *Q. pubescens*, *Q. robur* and *Q. rubra*). Triangles and points symbolize different time periods: doy 137-239: 17.05.2013-27.08.2013; doy 253-312: 10.09.2013-08.11.2013. Vertical dotted line indicates a leaf chlorophyll concentration of 50 mg m^{-2} . Note logarithmic y axis. B: Chl a [mg m^{-2}] to Chl b [mg m^{-2}] of *Q. frainetto*, *Q. ilex* (current and previous year leaves), *Q. pubescens*, *Q. robur* and *Q. rubra* combined, excluding senescent leaves ($n=408$; day of the year [doy] 137-253, 2013). Relation is linearly correlated with $R^2=0,891$; $y=0,297x+3,569$. Leaves were sampled in Frankfurt Schwanheim experimental forest site (FR).

For the analysis of leaf nitrogen content, 30 samples per species from a wide range of Chl contents and time of the growing season were selected. Plotting leaf nitrogen content in percent of sample dry weight [$\%_{\text{DW}}$] against Chl concentration [mg m^{-2}] revealed lower nitrogen content values at given Chl concentrations and two groups of data pairs below Chl concentrations of approx. 200 mg m^{-2} (Figure 17A). These two groups were not groupings of different species, since both groups contained values of all species, except for *Q. ilex*, where no values were contained in the lower grouping.

Results

Considering date of measurement, the group with high nitrogen content at low Chl concentrations contained only samples from the beginning of the growing season, whereas the group with low nitrogen content at low Chl concentration contained only samples from the end of the growing season. Converting the values of nitrogen content [%_{DW}] by SLA_{DW} to nitrogen content on area basis (Figure 17B), the interspecific difference in the relationship of nitrogen to Chl and the grouping of values from differing seasons vanished. Leaf nitrogen content on area basis and total leaf Chl on area basis were now linearly correlated ($R^2 = 0,763$), irrespective of species and time of the growing season.

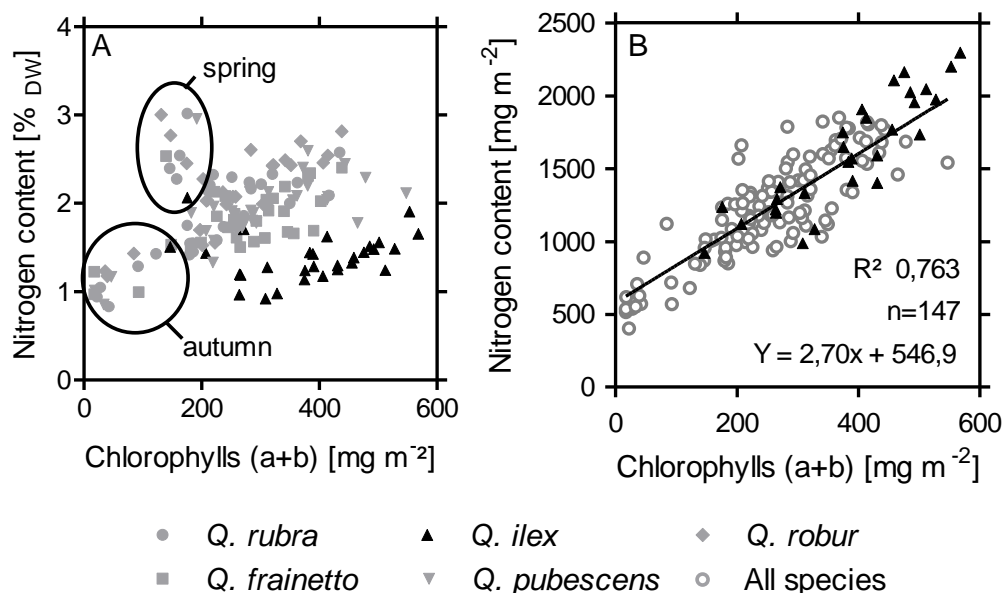


Figure 17: Relation of leaf chlorophyll to leaf nitrogen. A: Nitrogen content [% DW] to Chlorophylls relationship [mg m⁻²] for 5 *Quercus* taxa (*Q. rubra*, *Q. frainetto*, *Q. ilex*, *Q. robur*, *Q. pubescens*), differing in morphological leaf traits. B: Nitrogen content on area basis [mg m⁻²] to Chlorophylls [mg m⁻²] relation calculated with the use of specific leaf area (SLA_{DW}) for each single leaf ($n=147$). Linear correlation $R^2 = 0,763$, $y = 2,70x + 546,9$ for all species combined.

3.3. Non-invasive sensing of chemical leaf traits

On the subsamples used for the analysis of chemical leaf traits, measurements of light transmittance with the SPAD-meter have been performed, to determine the possibility for non-invasive sensing of chemical leaf compounds. The SPAD-meter is specifically constructed for in-vivo, non-invasive measurement of relative chlorophyll content by the use of LEDs with specific wavelengths. Therefore emphasis is placed on the relationship of SPAD-values to the chlorophyll content of the leaf. The additional relations of SPAD to carotenoids and total leaf nitrogen result from close correlation of these components with the chlorophyll content (see section 3.2.2).

In a first step, four additional *Quercus* taxa were included in the analysis of the correlation of total chlorophyll content to SPAD-readings to achieve general mathematical equations for the SPAD-Chl relationships. These taxa were the deciduous *Q. cerris*, the evergreen *Q. suber*, their hybrid *Q. x hispanica* and *Q. x turneri* (= *Q. robur* x *Q. ilex*). Samples from the beginning to the end of the growth period 2013 (doy 137 to 312) were used to control for possible seasonal variability and leaf age in the five field grown species (without the four taxa name listed above) at the experimental forest site FR. A large range of SPAD-values was obtained from 0,3 (*Q. frainetto*) to 53,8 (*Q. ilex*). SPAD-values below approx. 20 were solely derived from senescent leaves at the end of the growth period. The additional 4 taxa were sampled with n=30 at the beginning of November 2013 (doy 309). There were no senescent leaves for the evergreen *Q. suber* to harvest and senescence for the semi-evergreen hybrids and the deciduous *Q. cerris* had not yet begun on a larger scale. Four different denominators as a base for chlorophyll content were used to describe the amount of chlorophyll on the leaf level (Figure 18). Values of *Q. ilex* and *Q. rubra* were highlighted, because of their extremely contrasting morphological leaf traits (SLA_{DW} : *Q. ilex* 7,8 m² kg⁻¹; *Q. rubra* 16,9 m² kg⁻¹) to visualize value groupings in the relationship of SPAD-readings to Chl concentrations. If weight based or volume based Chl concentrations were related to SPAD-readings, an interspecific difference was observed in the relationship. Taxa with a higher leaf mass per area (=low SLA_{DW}) and thicker leaves tended to have lower amounts of leaf chlorophyll at the same SPAD-readings than taxa with lower leaf mass per area. Intra- and interspecific variability increased with increasing SPAD-values.

Results

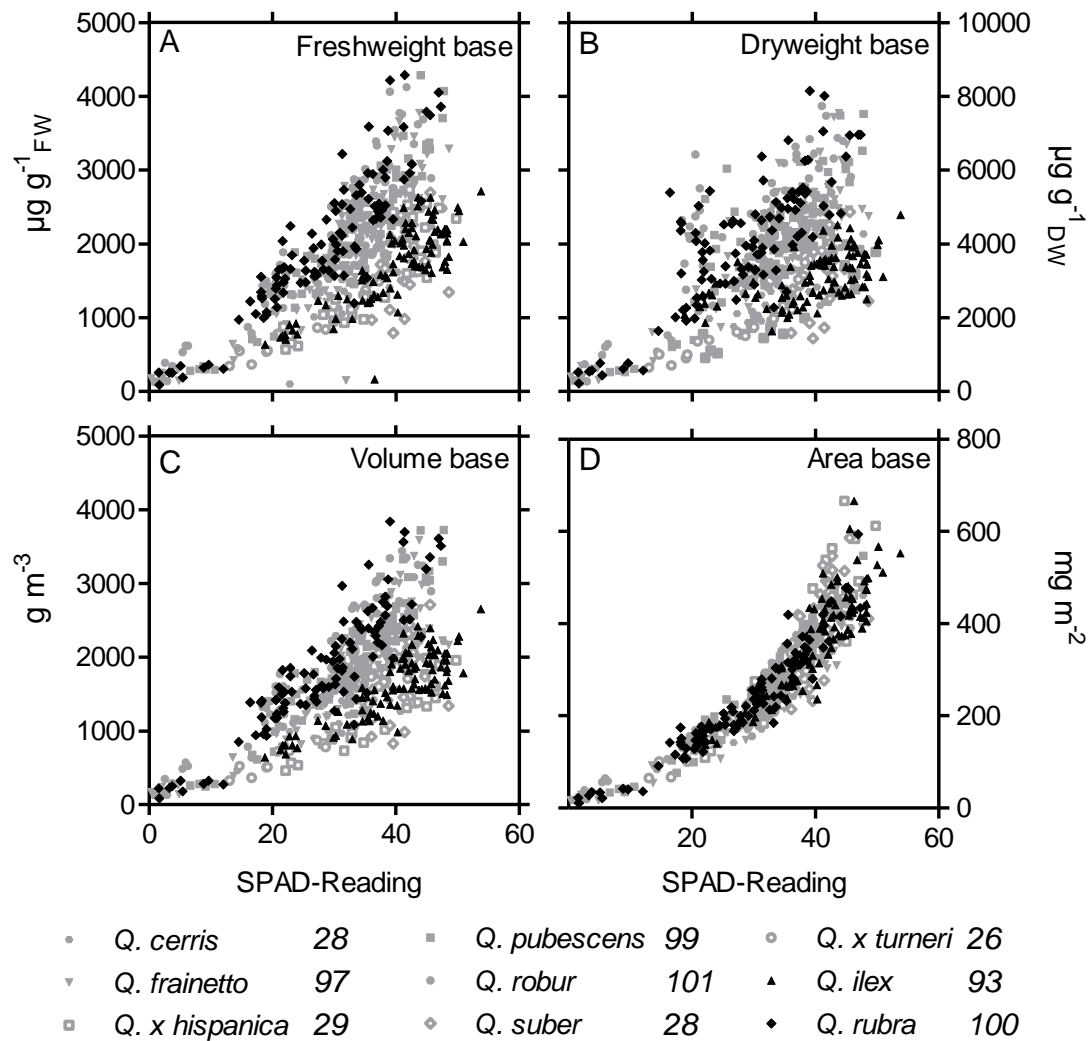


Figure 18: Correlation of SPAD-values to chlorophyll contents on different reference bases. A: Chl_{a+b} [$\mu\text{g g}^{-1}$ FW]; B: Chl_{a+b} [$\mu\text{g g}^{-1}$ DW]; C: Chl_{a+b} [g m^{-3}]; D: Chl_{a+b} [mg m^{-2}]. Chl: Chlorophyll a+b; FW: fresh weight; DW: dry weight. Coefficients of determination (R^2) in Table 4. Sample size in italics behind taxum name. *Q. ilex* and *Q. rubra* highlighted, because of their contrasting ratios of leaf area to leaf dry weight.

At low SPAD-values around 20, Chl concentrations on a dry weight basis showed an increased variability due to the lower dry weight/area ratio (LMA_{DW}) at the beginning of the growing season. The observed relationship between leaf chlorophyll content per leaf area and SPAD-reading (Figure 18D) was curvilinear, strongly correlated (Table 4) and showed no interspecific- and low intraspecific variation.

Table 4: species-specific correlation coefficients of SPAD-value and chlorophyll content with different reference bases. FW: fresh weight; DW: dry weight. Leaves sampled at 14 day intervals at multiple days in the year, when indicated. R² calculated through correlation coefficient Pearson's r. Highest coefficients of determination (R²) shaded.

Taxum	doy 2013	SPAD-range	n	Coefficient of determination (R ²)			
				[µg/g _{FW}]	[µg/g _{DW}]	[g/m ³]	[mg/m ²]
<i>Q. frainetto</i>	137 - 312	0,3 - 48,6	97	0,76	0,73	0,78	0,88
<i>Q. ilex</i>	151 - 312	18,8 - 53,8	93	0,68	0,34	0,69	0,79
<i>Q. pubescens</i>	137 - 312	1,0 - 47,8	99	0,84	0,70	0,83	0,89
<i>Q. robur</i>	137 - 312	2,6 - 45,7	101	0,80	0,59	0,81	0,87
<i>Q. rubra</i>	137 - 312	1,5 - 47,3	100	0,81	0,65	0,80	0,88
<i>Q. cerris</i>	309	22,8 - 47,7	28	0,72	0,66	0,69	0,94
<i>Q. suber</i>	309	35,0 - 48,6	28	0,14	0,12	0,13	0,38
<i>Q. x hispanica</i>	309	21,8 - 49,8	29	0,71	0,70	0,71	0,81
<i>Q. x turneri</i>	309	13,0 - 41,9	26	0,89	0,89	0,90	0,92

For prediction purposes, four different empirical models were calculated for the SPAD to area based Chl content relationship (for the single species and all species combined). The models were polynomial of first- (straight line; LINR) and second order (POLY), exponential (EXP), and a homographic model (HOMG). Best fit of models was quantified by R² and the root mean square error (RMSE) (Table 5). Chl content was non-linearly related to the SPAD-reading (Figure 19), hence the LINR model showed the lowest R² and the highest residual error. The best fits were obtained with the POLY and HOMG models that both show an R² of above 0,9 in 2/3 of the taxa. These two models were nearly identical in their output at SPAD-values between 5 and 45, with POLY having slightly higher R² and lower RMSE due to the additional parameter. A model comparison by Akaike Information Criterion (ΔAIC_c) for POLY and HOMG models favours HOMG for species specific models in 7 of 9 cases. The AIC balances the change in goodness of fit with the change in degrees of freedom (due to the number of parameters to fit). The probability ratios for one or the other model are however low, indicating that the differences were not very strong. For the combined data, the POLY model was favoured.

Results

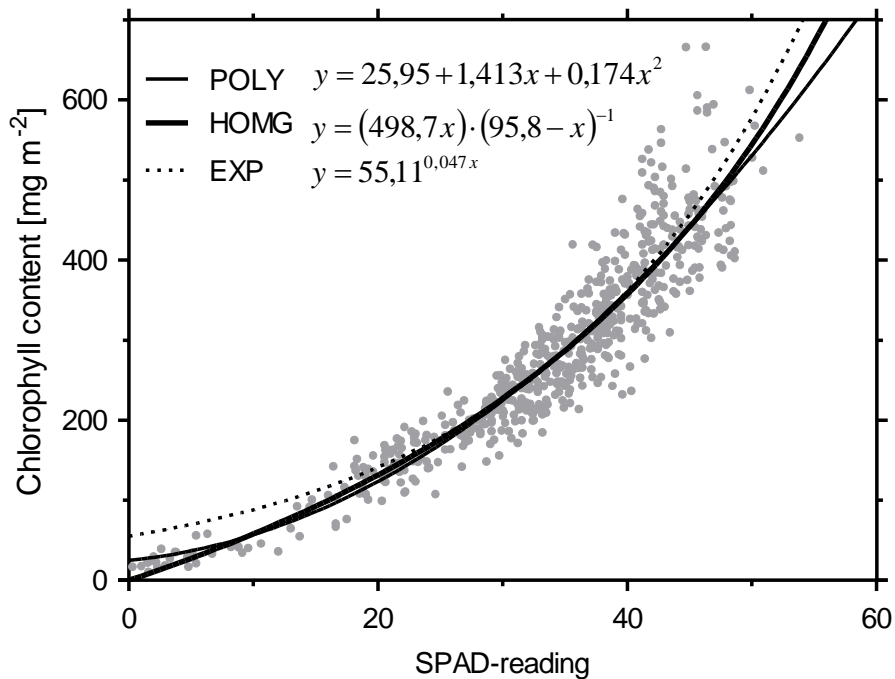


Figure 19: Empirical model fit for the total SPAD chlorophyll dataset. EXP: exponential model [$y = A^{B(SPAD)}$]; POLY: polynomial model, second order [$y = A + B(SPAD) + C(SPAD)^2$]; HOMG: homographic model [$y = A(SPAD) (B-SPAD)^{-1}$]. Sample size $n = 601$.

Table 5: Species-specific model fit for the correlation of area based chlorophyll content and SPAD-value. LINR: linear model [$y = A + B(SPAD)$]; EXP: exponential model [$y = A^{B(SPAD)}$]; POLY: polynomial model, second order [$y = A + B(SPAD) + C(SPAD)^2$]; HOMG: homographic model [$y = A(SPAD) (B-SPAD)^{-1}$].

Species	n	Coefficient of determination (R ²)				Root Mean Square Error (RMSE)			
		LINR	EXP	POLY	HOMG	LINR	EXP	POLY	HOMG
<i>Q. frainetto</i>	97	0,882	0,895	0,914	0,912	36,15	33,99	30,79	31,21
<i>Q. ilex</i>	93	0,792	0,787	0,798	0,794	54,35	54,94	53,51	54,06
<i>Q. pubescens</i>	99	0,890	0,915	0,925	0,926	36,55	32,01	30,07	29,99
<i>Q. robur</i>	101	0,873	0,906	0,914	0,911	34,98	30,10	28,77	29,27
<i>Q. rubra</i>	100	0,885	0,919	0,923	0,926	38,42	32,28	31,40	30,73
<i>Q. cerris</i>	28	0,938	0,938	0,945	0,940	21,40	21,36	20,13	20,96
<i>Q. suber</i>	28	0,378	0,347	0,427	0,351	75,44	77,32	72,39	77,06
<i>Q. x hispanica</i>	29	0,812	0,817	0,825	0,815	72,38	71,41	69,70	71,79
<i>Q. x turneri</i>	26	0,924	0,959	0,956	0,958	28,67	21,07	21,79	21,20
All species	601	0,830	0,862	0,870	0,869	51,31	46,15	44,70	45,00

The difference between the single species models and the global model (Figure 20) was more pronounced in *Q. cerris*, *Q. suber*, *Q. x hispanica* and *Q. x turneri* with comparable low samples sizes. The most obvious discrepancies occurred in *Q. suber* with its small range of values and at high SPAD-readings and Chl contents. Previous year leaves of *Q. ilex* showed no deviation from current year leaves in the Chl-SPAD relation. Best-fit values with 95% confidence intervals for single species and global model POLY and HOMG are given in Appendix III.

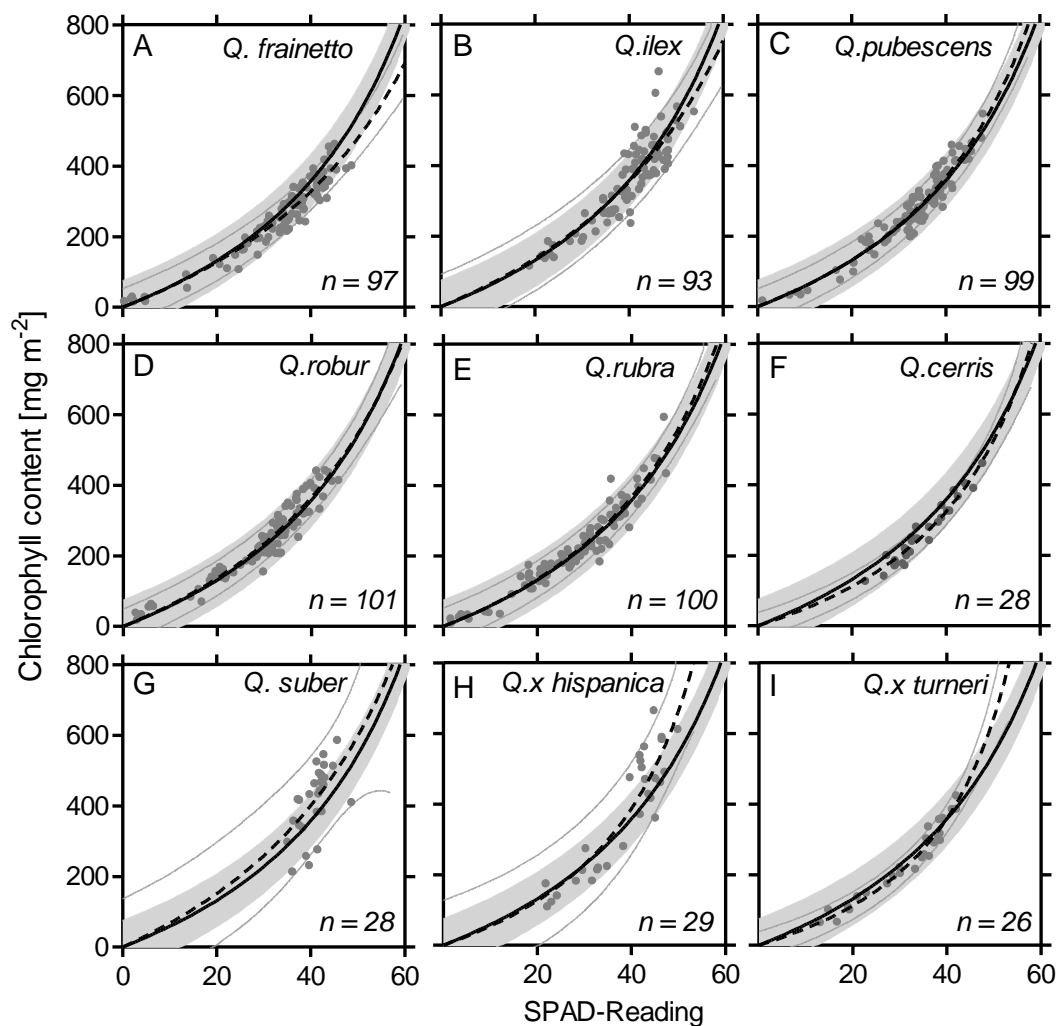


Figure 20: Species-specific fit of homographic model with 90% prediction bands of area based chlorophyll content to SPAD correlation. Black solid line symbolizes the all species model. Broken black line indicates species-specific model. Grey shaded area marks the 90% prediction intervals of the all species model. Grey solid lines give 90% prediction interval of species-specific model. Data points symbolized in dark grey. For coefficients of correlation and best-fit parameters consult Table 5 and Appendix III. All species model: $\text{Chl} [\text{mg m}^{-2}] = (498,7 \text{ SPAD})(95,8 - \text{SPAD})^{-1}$.

Results

Chl a and Chl b concentrations were non-linearly correlated to SPAD-readings (Figure 21 A) with high R^2 (Chl a: 0,903; Chl b: 0,832; n: 490). The calculated Chl a/b ratio (Figure 21 C) derived from the best-fit parameters of both second order polynomic regressions (Figure 21 A) visualizes the change of the ratio at low chlorophyll concentrations (cf. Figure 16). The same applies to the relation to total Car and the Chl / Car ratio (Figure 21 B,D). In contrast to leaf Chl, Car concentrations did not converge to zero, but to a value of approx. 30 mg m^{-2} at SPAD-readings below 20.

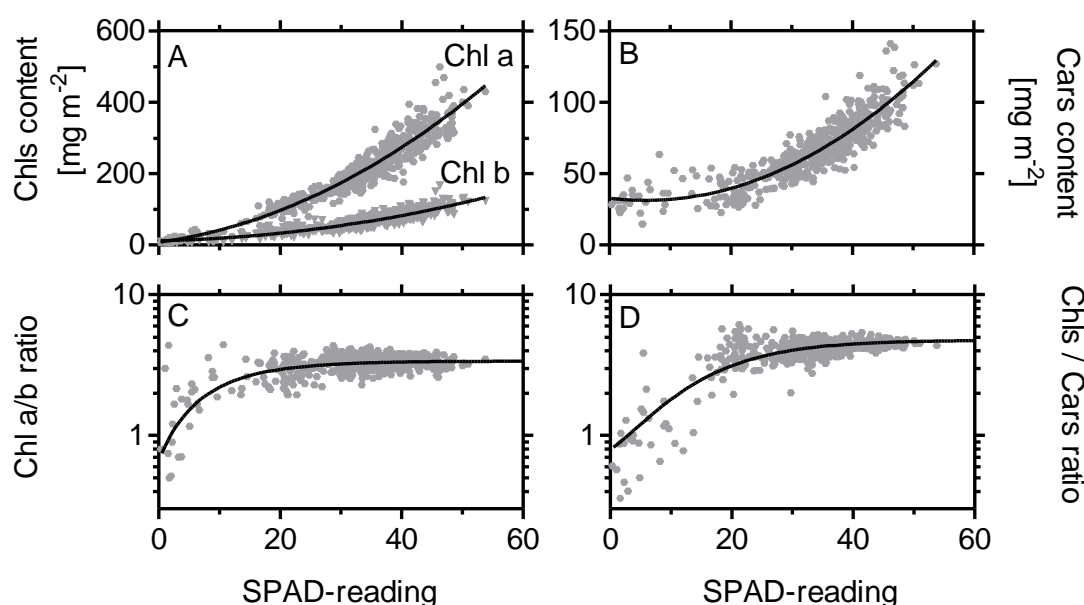


Figure 21: Relationships of chlorophyll a and b and carotenoid concentrations and their ratios to SPAD-measurements. Data combined from *Q. frainetto*, *Q. ilex*, *Q. pubescens*, *Q. robur* and *Q. rubra* (n=490) containing leaves from the whole growing season 2013. A,B: Chlorophyll and Carotenoid contents, fitted by polynomial 2. order regression. C,D: Pigment ratios. Black solid line calculated from equations given at table. Table: Best fit parameters of non-linear regressions for $y = A + Bx + Cx^2$.

Table 6: Best-fit parameter values for calculation of Chl a, Chl b, Cars and their ratios from SPAD measurements. A,B,C: Best fit values for polynomial regression 2. order: $y = A + Bx + Cx^2$.

Y	Unit	A	B	C	R^2
Chl a	$[\text{mg m}^{-2}]$	7,765	2,255	0,110	0,903
Chl b	$[\text{mg m}^{-2}]$	11,780	0,346	0,035	0,832
$\text{Chl}_{(a+b)}$	$[\text{mg m}^{-2}]$	25,950	1,141	0,174	0,870
$\text{Car}_{(x+c)}$	$[\text{mg m}^{-2}]$	32,610	-0,503	0,043	0,813

Total leaf Chl and total leaf nitrogen concentrations were linearly correlated on a leaf area basis (see section 3.2.2). Therefore SPAD-readings showed a non-linear relationship to nitrogen content, comparable to the non-linear relationship of leaf Chl to SPAD-readings (Figure 19). The data points were best fit by a polynomial second order regression with R^2 above 0,7 (Table 7). Fitting the HOMG model to the data led to ambiguous best-fit parameter values, therefore the POLY model was favoured. The low number of single species data points, (compared to the Chl samples), resulted in single species regressions with better fit to the data than a global regression approach (Table 7), comparable to the Chl/SPAD model fit in *Q. x hispanica* and *Q. x turneri* (Figure 20). Nitrogen concentrations were overestimated by the global model compared to the species model in *Q. frainetto* (Figure 22) at SPAD-values around 40. On the other hand, nitrogen concentrations at high SPAD-values seemed to be underestimated in *Q. ilex*, however, there are no data points for SPAD-values below 20, leading to a steeper slope at high readings (Figure 22C). The 90% prediction bands of the global model are narrow, given the high range of nitrogen concentrations. At the mean, prediction intervals were $327,9 \text{ mg m}^{-2}$ for a SPAD-range of 0-60 with the lowest interval between SPAD-values of 20 to 40. The largest 90% prediction interval with a value of $355,4 \text{ mg m}^{-2}$ was calculated at a SPAD-reading of 60.

Table 7: Best-fit species-specific parameters of 2. order polynomial regression for estimating leaf nitrogen with SPAD-readings. Single-species and global model parameters. Equation: Nitrogen content [mg m^{-2}] = $A+B(\text{SPAD})+C(\text{SPAD})^2$. N: sample size, A,B,C: Best fit parameters of polynomial regression. R^2 : coefficient of determination. RMSE: Root mean square error.

Species	n	A	B	C	R^2	RMSE
<i>Q. frainetto</i>	29	509,3	6,882	0,339	0,705	178,9
<i>Q. ilex</i>	29	1350	-38,33	1,052	0,764	188,2
<i>Q. pubescens</i>	30	508,8	23,60	0,050	0,776	153,0
<i>Q. robur</i>	29	677,6	7,157	0,416	0,785	145,3
<i>Q. rubra</i>	30	443,6	16,85	0,221	0,798	153,7
All species	147	562,6	9,28	0,3602	0,746	192,7

Results

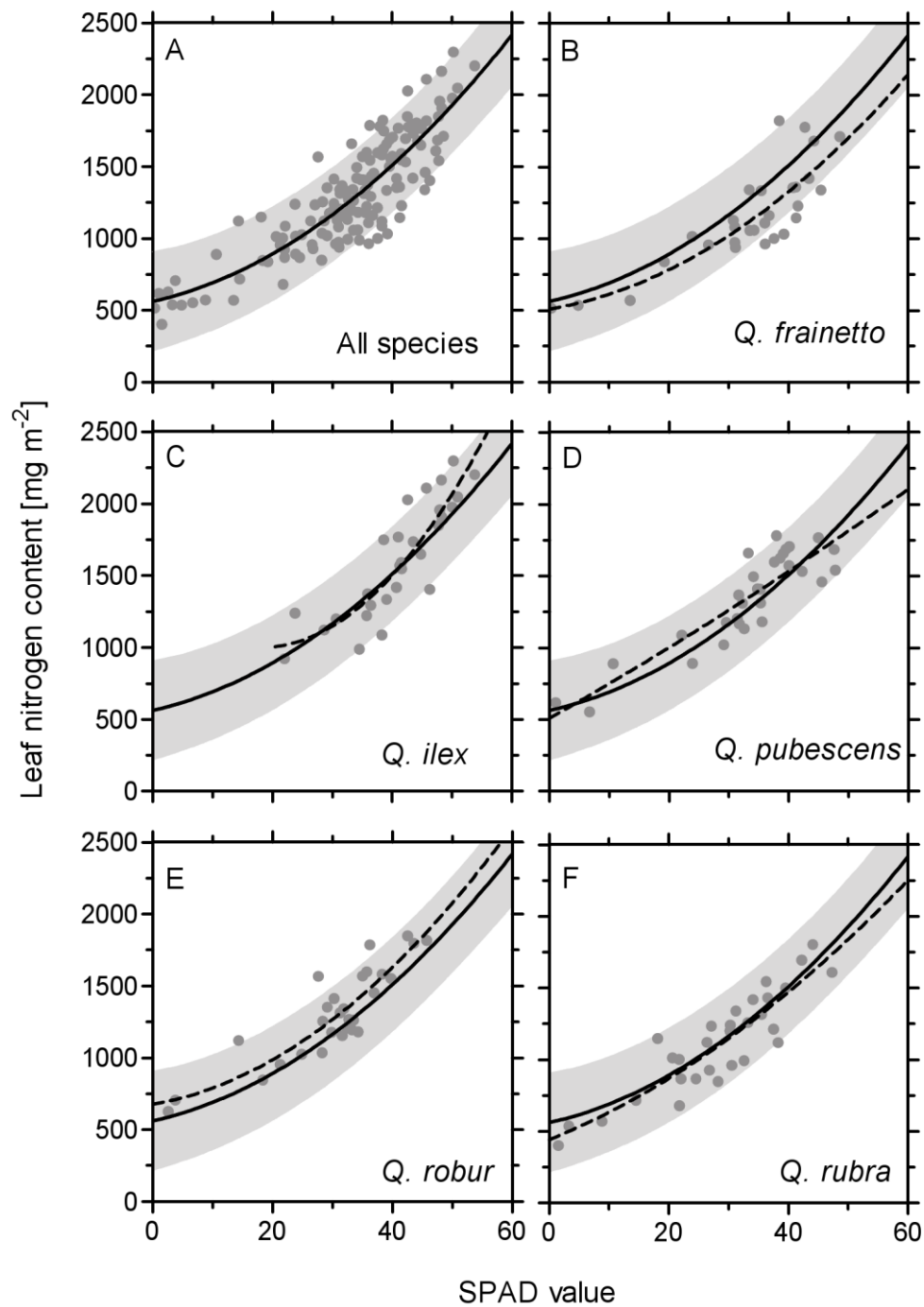


Figure 22: Species-specific fit of polynomial model with 90% prediction bands of area based leaf nitrogen content to SPAD correlation. Black solid line symbolizes the global all species model. Broken black line indicates species-specific model. Grey shaded area marks the 90% prediction intervals of the global model. Data points symbolized in dark grey. For sample size, coefficients of correlation, Root mean square error and best-fit parameters consult Table 7.

3.3.1. Assessment of SPAD-reading variability concerning application

To evaluate the applicability of SPAD readings in field monitoring of oaks, possible sources of variability between readings were analysed. First, the repeatability of the SPAD-readings on *Quercus* leaves was assessed in order to evaluate the precision of multiple SPAD measurements on the same leaf and to detect possible changes in the precision due to differences in leaf morphology. Possible diurnal fluctuations of SPAD values due to reasons other than chlorophyll content differences (chloroplast movement, change of leaf water status etc.) during the day were assessed in the field, to test if measurements may be taken throughout the day or need to be constrained to a specific condition. At last, representative species-specific SPAD-values and within species variations at the site level (0,5 ha) and the statistical distribution of these values were obtained through sampling of a large population of leaves.

Leaf scale variability of SPAD-readings

If SPAD measurements are not taken at the exact same position on the leaf, the variance of values on the leaf scale needs to be determined for a sense of repeatability and precision. The precision of the SPAD-meter in the range from zero to 50 is given with ± 1 SPAD unit by the producer and values greater than 50 may be less accurate (SPAD-502 Manual, Konica Minolta, Osaka, JP). The variance of SPAD-values measured on uniformly coloured leaves was similar in *Quercus* species with contrasting morphological leaf traits (Table 8). Standard deviations of the mean were in a range of about 1 to 3 SPAD - units with a mean of approx. 1,5 SPAD units in all species (except *Q. rubra* with a mean of 1,9).

Table 8: SPAD reading variability on leaf level in 5 different *Quercus* taxa. Standard deviations of SPAD-measurements (n=20) per leaf on 9 leaves per species. Measured at FR at doy203; 22.07.2013.

species	<i>Q. frainetto</i>	<i>Q. ilex</i>	<i>Q. pubescens</i>	<i>Q. robur</i>	<i>Q. rubra</i>
mean	1,5	1,5	1,5	1,4	1,9
min	0,8	0,9	0,7	0,9	1,0
max	2,2	2,5	3,0	2,5	3,0

Results

Diurnal variability of SPAD-readings

On mature leaves of *Q. frainetto*, *Q. ilex*, *Q. pubescens*, *Q. robur* and *Q. rubra*, no diurnal pattern, that could reveal dependencies of SPAD measurements to the time of the day (with the associated changes named above) was observed (Figure 23). With the consideration of SPAD-measurement repeatability on single *Quercus* leaves (cf. Table 8), the large majority of deviations observed during the day were within the mean standard deviation of repeated measures (1,5 SPAD values) or within the range of observed standard deviations (3 SPAD values).

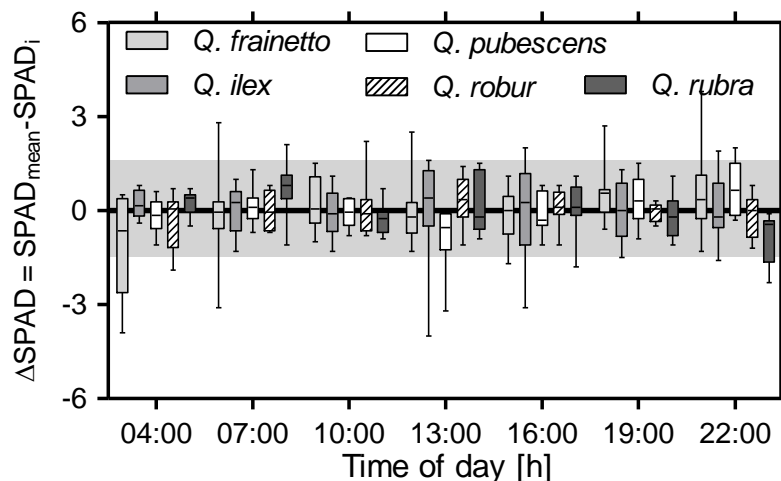


Figure 23: Diurnal variability of SPAD-readings of 5 different *Quercus* taxa on a hot summer day. Boxplots with min, 25% percentile, median, 75% percentile and max (n=8). Measured on same leaves. ΔSPAD calculated for every leaf at time i .; $\text{SPAD}_{\text{mean}}$: mean value of all measurements for a specific leaf. Grey shading shows $\pm 1,5$ SPAD values, the standard deviation of repeated measurements on a single oak leaf. Measured at (FR) at doy203; 22.07.2013. Dusk: 05:39, dawn: 21:23.

Temperature dependent variability during the season

A SPAD-reading deviation was estimated with the root mean square errors (RMSE), calculated from the linear regression residuals of SPAD values at different times during an 8 month period. Deviations of ~1 to 1,5 SPAD-units were noted independent of the temperature at the time of measurement. The deviations were within the range of SPAD-units, estimated as the precision for multiple repeated measurements across a uniformly coloured leaf (Table 8). Leaves were frozen at the time of SPAD-measurement several times, but only at minimum temperatures below -4°C ($-4,1$ and $-4,7^{\circ}\text{C}$) SPAD-readings showed an up to twofold SPAD-reading deviation, with a value increase compared to values measured at higher temperatures.

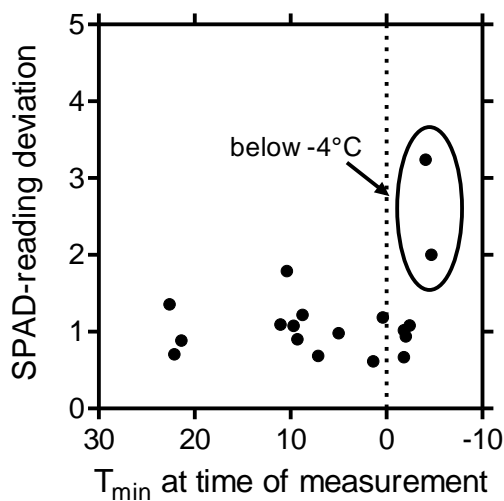


Figure 24: Temperature dependency of SPAD-readings in *Q. ilex*. At 18 different dates between August 8th 2012 and May 3rd 2013, SPAD values (mean of n=5 per leaf) of 18-21 leaves of different trees at the experimental forest site in Frankfurt Schwanheim (FR) were measured. Data points were fitted by linear regression and SPAD-reading deviation was calculated from the root mean square errors. SPAD-reading deviations were plotted against the minimum temperature at the time of measurement, obtained from the on-site climate station.

Results

Interspecific variability

Mean SPAD-readings showed species specific variability at the FR-site. All means except for *Q. robur* and *Q. rubra* were significantly different from each other ($p > 0,05$; one-way ANOVA & Tukey's post-test). *Q. robur* and *Q. rubra* showed the lowest mean values with ~ 34 and *Q. ilex* showed the highest mean with ~ 43 , followed by *Q. frainetto* (~ 39) and *Q. pubescens* (~ 37). The lowest mean values were below 20 (*Q. robur*: 19,1; *Q. rubra*: 19,9) and the highest above 50 (*Q. ilex*: 53).

Table 9: Intrinsic variability of SPAD-values on species- and individual tree level at Frankfurt Schwanheim (FR). Measurements performed in August 2013. N = 10 random SPAD measurements per tree. Number of trees sampled: *Q. frainetto*: 148; *Q. ilex*: 158; *Q. pubescens*: 168; *Q. robur*: 150; *Q. rubra*: 157. Different letters indicate that means are significantly different ($p < 0,05$; One-way ANOVA with Tukey's post-test for multiple comparison). CI: confidence interval.

	<i>Q. frainetto</i>	<i>Q. ilex</i>	<i>Q. pubescens</i>	<i>Q. robur</i>	<i>Q. rubra</i>
Species-Level					
Mean value	38,9	42,96	36,87	33,81	33,87
	a	b	c	d	d
Std. Deviation	3,88	4,08	3,01	4,33	4,70
Minimum	29,30	26,30	28,50	19,10	19,90
25% Percentile	36,10	40,18	34,93	31,28	31,35
Median	39,20	42,90	36,70	33,55	33,60
75% Percentile	41,80	45,50	39,00	37,13	37,40
Maximum	47,50	53,00	45,10	44,60	43,90
Range	18,2	26,7	16,6	25,5	24,0
Tree-Level					
Mean of SD	2,74	2,69	2,27	3,20	3,02
	a	a	b	c	c
90% CI	$\pm 0,29$	$\pm 0,26$	$\pm 0,21$	$\pm 0,39$	$\pm 0,29$

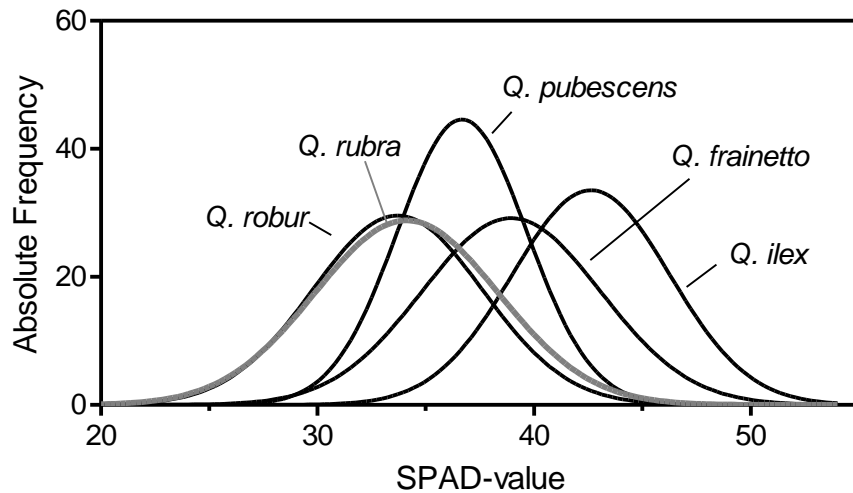


Figure 25: Gaussian fit of frequency distribution for species level in Frankfurt Schwanheim experimental forest site (FR). Measured in August 2013. N = 10 random SPAD measurements per tree. Number of trees sampled: *Q. frainetto*: 148; *Q. ilex*: 158; *Q. pubescens*: 168; *Q. robur*: 150; *Q. rubra*: 157. R^2 of Gaussian fit: *Q. frainetto*: 0,9152; *Q. ilex*: 0,9571; *Q. pubescens*: 0,9521; *Q. robur*: 0,9096; *Q. rubra* (grey line): 0,9102.

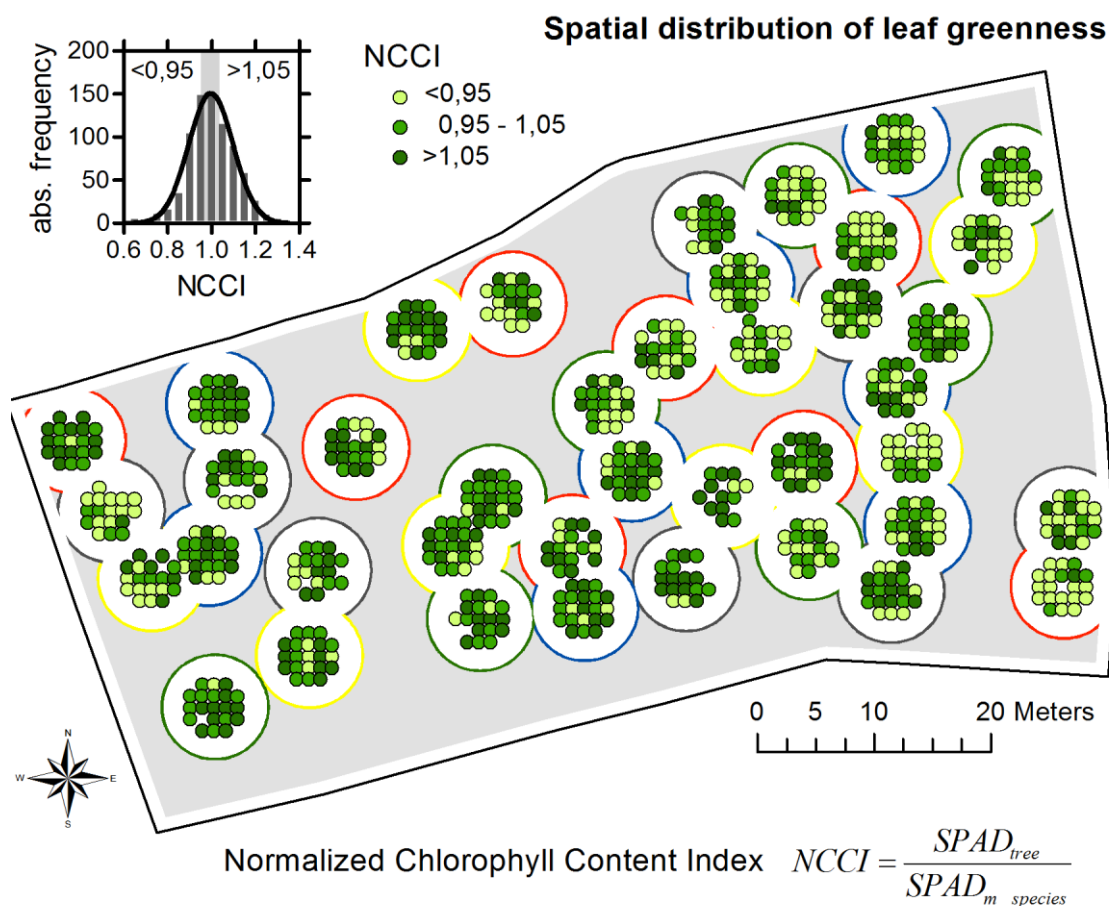
The total range of SPAD-means in different trees was approx. 20 SPAD-units, independently of species. The standard deviation of the mean was within the range of 3 to 5 SPAD-units with *Q. pubescens* showing the least variation and *Q. robur* having the highest. 50% of all measured values were within a range of 4 to 6 SPAD-units independent of the chosen species (range 25% to 75% percentile, Table 9). On the individual tree level the standard deviation of 10 measurements per tree for all trees per species, were in the mean at a range of 2 to 3,5 SPAD-units.

The SPAD-values measured at a population of trees of *Quercus* species with varying leaf traits at one point in time, followed a normal distribution (Figure 25), which allowed the use and comparison of mean SPAD values and their standard deviations. At the time of measurement (August 2013), frequency distribution showed no signs of skewing to higher or lower values. The widths of the curves were similar, with exception of *Q. pubescens*, where lower variability was observed. Mean values are significantly different, with the exception of *Q. robur* and *Q. rubra*, but all species shared a range of overlapping values. This range starts at approx. 30 and ends at 45 SPAD-units with the greatest overlap at approx. 38.

Results

Spatial distribution of SPAD-values at site level

In order to visualize the spatial variability of leaf greenness at the FR site, SPAD values measured for every single tree were normalized to the species mean, due to the interspecific variability of SPAD values. All Trupps (excluding ID 5, *Q. frainetto*) contain trees with all 3 NCCI classes. Nevertheless the proportion of trees with decreased NCCI was higher in the north-eastern and south-eastern part as well as at the western edge of the site. In the central part of the FR site, trees with higher NCCI were found to be proportionally increased. No correlation was found between the Trupps mean NCCI and the soil nitrogen contents.



	<i>Q. frainetto</i>	<i>Q. ilex</i>	<i>Q. pubescens</i>	<i>Q. robur</i>	<i>Q. rubra</i>
SPAD _{m_species}	38,9	42,96	36,87	33,81	33,87
n	148	158	168	150	157

Figure 26: Spatial distribution of leaf greenness at the FR site. Leaf greenness was quantified with a normalized chlorophyll content index (NCCI) calculated from SPAD-measurements of single trees (n = 10 per tree) and the species mean SPAD value at the site (measurements performed: 22-28.08 2013). NCCI and species are colour coded. N = 21 trees per Trupp. For abiotic factors at the site see Figure 10.

3.4. Seasonal monitoring of chlorophyll content and PS II functionality

The seasonal variability of leaf chlorophyll concentration and Chl a fluorescence was assessed by continuous monitoring of individually marked leaves throughout the vegetation period. In the first section, emphasis was placed on the seasonal variability of the chlorophyll content, measured by SPAD-meter, whereas in the second section the focus lay on PSII functionality derived from fast-transient Chl a fluorescence analysis. In the third section, the relationship between different JIP test parameters was investigated by correlation analysis. In the fourth section, chlorophyll content and parameters of Chl a fluorescence were related to each other.

3.4.1. Seasonal variability of chlorophyll content

From the time course of SPAD-values in the growth period, three distinct regions were identified (Figure 5). In the beginning of the growth period, SPAD values increased until a plateau was reached. Variations at the plateau were small and fall within the range of leaf scale variability (cf. 3.3.1). At a time point that marked the individual beginning of senescence, SPAD values dropped until the leaf was abscised. The rate of increase, the time when the plateau was reached, the beginning of senescence and the rate of decline were calculated for individual leaves via the intersections of linear regressions (cf. Figure 5). Full data sets for the whole vegetation period were available for 2013; in 2012 spring measurements started on day 158, so the initial leaf development phase was not covered.

In 2013, SPAD values increased at a rate of approx. 3 to 5 SPAD-units per week (see Appendix IV). *Q. rubra* showed the slowest rate of increase with $3,0 \pm 0,9 \text{ wk}^{-1}$, which differed significantly from the other *Quercus* species (*Q. frainetto*: $4,8 \pm 1,1$; *Q. ilex*: $5,5 \pm 1,4$; *Q. pubescens*: $4,1 \pm 1,4$; *Q. robur*: $4,1 \pm 1,0$). All deciduous species reached the plateau in the mid of June. No significant interspecific difference for this time point could be observed for the deciduous species. *Q. ilex* reached the plateau as the last species between the end of June and the beginning of July, but earlier than the end of structural leaf development (Figure 14). Since there was no significant difference in the time when the plateau was reached, the duration of the plateau phase correlated with the beginning of senescence ($R^2=0,841$) in 2013. *Q. frainetto* and *Q. robur* showed

Results

large intraspecific variation for the beginning of senescence (SD 26 to 30 days). In senescing leaves the slowest rate of decrease was observed in *Q. pubescens* resulting in 80% of leaves still being measurable at day 312 whereas in *Q. rubra* only one of initially 24 leaves was left at day 312 and 60% were already abscised two weeks prior.

In 2012, *Q. ilex* showed a significantly later end of development ($185,8 \pm 11,1$) as compared to 2013 ($177,3 \pm 11,0$) and a significantly lower rate of increase ($2,2 \pm 1,3$, compared to $5,5 \pm 1,4$). Inter-annual comparison of the beginning of senescence revealed a slightly earlier start in 2012, which was only significantly different in *Q. rubra*, coupled with a significantly slower rate of decline, which was only half of the velocity in *Q. rubra* and *Q. frainetto* compared to 2013 (Figure 27).

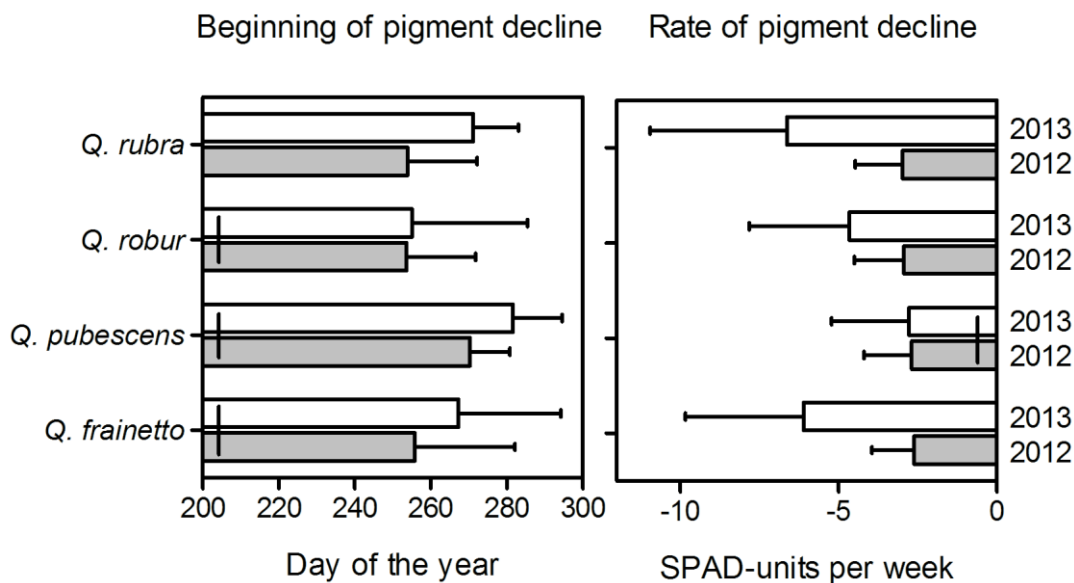


Figure 27: Inter-annual comparison of the beginning of senescence and the rate of SPAD-value decline at Frankfurt Schwanheim (FR). Beginning of senescence is defined as the beginning of chlorophyll decline, measured by SPAD-values on single leaves in 2 week intervals. Means and standard deviations are symbolized by horizontal columns with error bars. Connecting vertical lines indicate that means are not significantly different from each other ($p > 0,05$; unpaired t-test). Grey columns: 2012, white columns: 2013. Sample sizes 2012/2013: *Q. frainetto*: 22/22; *Q. pubescens*: 22/22; *Q. robur*: 21/18; *Q. rubra*: 22/17.

The species- and leaf specific time courses of seasonal variability are visualized in Figure 28. A relative SPAD-value was calculated with the mean SPAD value of the core vegetation time of each individual leaf. If the maximum value was used, unrepresentative values were weighed and intraspecific leaf comparisons at specific times were altered by larger errors. The SD of the mean SPAD value at the core vegetation time was generally low in a range from 1,6 (*Q. ilex*, *Q. pubescens*) to 2,4 (*Q. frainetto*) and within the range of standard deviations measured at the leaf scale (cf. 2.3.1). Alterations and fluctuations of SPAD values during the year were low and no trend of possible reaction to an abiotic factor were observed other than the development of the leaves and the beginning of senescence.

In *Q. ilex* autumnal senescence did not occur and a slight trend towards higher SPAD-values to the end of the year was observed. Additionally, a large intraspecific variance was noted in *Q. ilex* early in the growth period, when some leaves have reached plateau values, while others were still 25% below these values. Differences between the species were apparent later in the growth period. In *Q. pubescens*, senescence started late and the decline was rather low. Hence 19 of initially 24 leaves were still measurable at day 312 and the mean was not lower than 75% of the plateau phase value. *Q. pubescens* showed the longest core vegetation time of all studied deciduous species and was the only species (besides the *Q. ilex*) with all values of SPAD_{rel} above 50% at the beginning of November (Figure 28). In contrast to *Q. pubescens*, *Q. rubra* showed a rather collective beginning of senescence with a rapid decline, where in a period of 16 days 60% of all measured leaves were abscised or no data could be recorded. 15 days later not a single leaf was measurable. In *Q. frainetto* and *Q. robur* the intraspecific variability in the beginning of senescence was marked by high SDs. Single leaves showed declining values at the end of August, while other leaves showed no signs of chlorophyll decline until the beginning of October. No correlation was found between the mean SPAD value at core vegetation time and the beginning of senescence.

Results

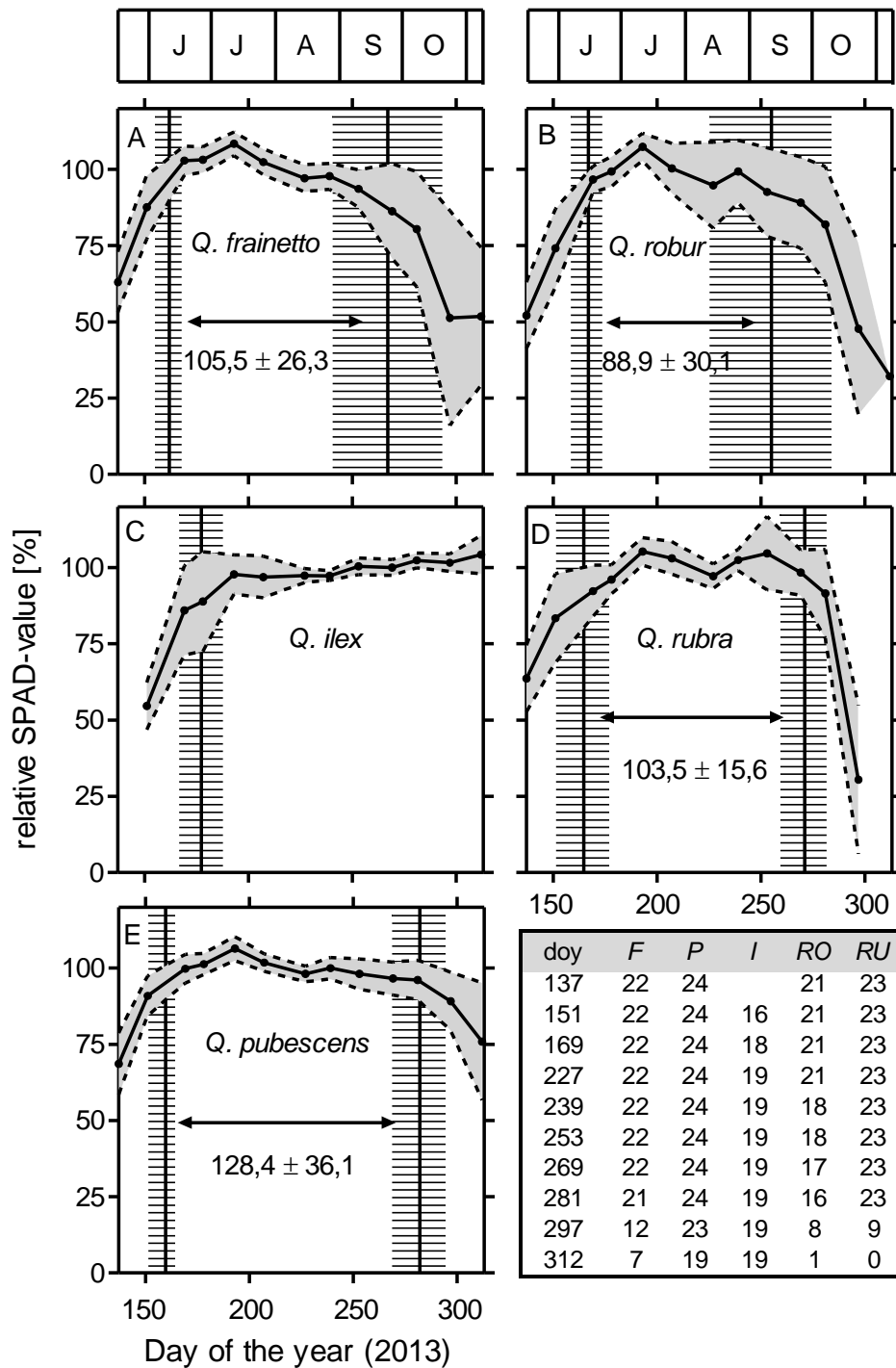


Figure 28: Seasonal variability of SPAD-readings and derived developmental parameters for 2013 at Frankfurt Schwanheim (FR). Rel. SPAD values of *Q. frainetto* (A), *Q. robur* (B), *Q. ilex* (C), *Q. rubra* (D) and *Q. pubescens* (E) in the growth period 2013. Sample sizes table on the bottom right (doy 178, 193 and 207 not shown). Rel SPAD values calculated for every individual leaf with $SPAD_{rel} = SPAD_i \times SPAD_{core}^{-1} \times 100$, where $SPAD_i$ is the individual SPAD value at the time i and $SPAD_{core}$ is the mean SPAD value in the period of core vegetation time. Broken line and the grey shading: Standard deviations. Vertical solid lines represent the end of development and beginning of senescence. SDs indicated by stacked horizontal lines. Mean and SD of the core vegetation time are displayed in the graph's centre. Since the evergreen *Q. ilex* shows no senescence, the core vegetation time cannot be calculated.

Mean SPAD-values at core vegetation time of individual plants, measured in 2012 and 2013, showed low interspecific and inter-annual variability (Figure 29). In all species, mean SPAD-values at core vegetation time of individual plants in consecutive years were significantly correlated (Pearson's r). To quantify the annual variability of SPAD-values per plant and species, prediction intervals of the correlations were calculated, which include 90% of data points. The 90% prediction intervals ranged from $\pm 5,1$ in *Q. frainetto* to $\pm 9,0$ in *Q. rubra*. For all species and data points combined, the coefficient of correlation was 0,67 and the 90% prediction interval was $\pm 7,2$ SPAD-units.

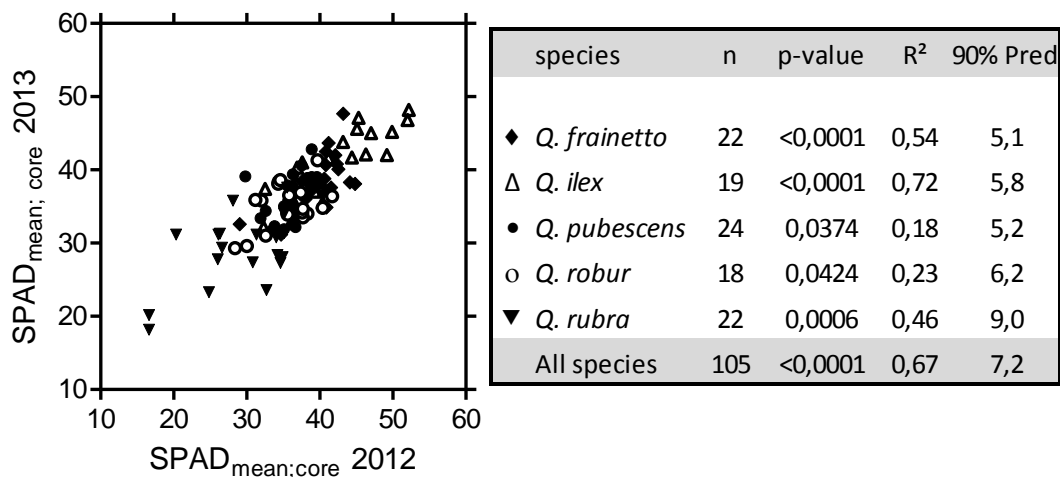


Figure 29: Correlation of mean SPAD-values in core vegetation time in two consecutive years. (2012 and 2013). $SPAD_{mean;core}$ is the mean SPAD value of an individual plant unaffected by periods of leaf development or leaf senescence. Correlation was tested for significance with Pearson's r . Correlations are significant with $p < 0,05$. "90% Pred" is the prediction interval of 90% of data points (in SPAD-units).

3.4.2. Seasonal variability of photosystem II functionality

PSII functionality was assessed by parameters derived from predawn fluorescence measurements of the fast OJIP fluorescence transient. Overall PSII functionality was estimated by the maximum quantum yield of PSII ($F_v/F_m = \phi_{p0}$) and the Performance Index (PI_{abs}). A seasonal trend, similar to the seasonal time course of chlorophyll content (see 3.4.1) was observed for F_v/F_m and PI_{abs} in 2012 and 2013 (Figure 30). A parameter rise at the time of leaf development led to a period with little change of parameter amplitude, followed by a substantial decrease at the end of the growing season (except for the evergreen *Q. ilex*). First measured F_v/F_m values at day 137 (17.05.2013), early after bud break were above 0,60 in all species. After the initial increase, F_v/F_m values showed little alteration and were in a range of 0,81 to 0,82 in 2012 (median for day 180-248) and 0,79 to 0,81 in 2013 (median for day 178-269). The time course of PI_{abs} (transformed by natural logarithm) resembled the time course of F_v/F_m in most parts and noticeable deviations in F_v/F_m were seen intensified in $\ln PI_{abs}$. In the autumnal decrease the values of F_v/F_m and $\ln PI_{abs}$ were unrepresentatively higher, since sample sizes decreased from the beginning of October (Figure 28) and data from leaves far progressed in senescence (not measurable) could not be obtained.

Early increase and development of the F_v/F_m and $\ln PI_{abs}$ showed little inter-annual variability, while the period of higher PSII functionality seemed to be longer in 2013 compared to 2012 in *Q. pubescens*, *Q. robur* and *Q. rubra*. In *Q. frainetto* the decrease of F_v/F_m and $\ln PI_{abs}$ did not vary between 2012 and 2013. In *Q. ilex* both parameters showed no tendency of decrease towards the end of the growing season and $\ln PI_{abs}$ seemed to further increase with time at 2013. Also in 2013, in all species a small depression after the initial increase was noted in F_v/F_m and $\ln PI_{abs}$ alike, at the fourth measurement in 2013 (day 178; 27.06.2013). A second local minimum in both parameters was observed during the summer at day 227 (15.08.2013) which is more pronounced in $\ln PI_{abs}$ than in F_v/F_m . In 2012 only one depression at the beginning of the growth period was observed at day 180 (28.06.2012) in $\ln PI_{abs}$ in *Q. robur* and *Q. rubra*.

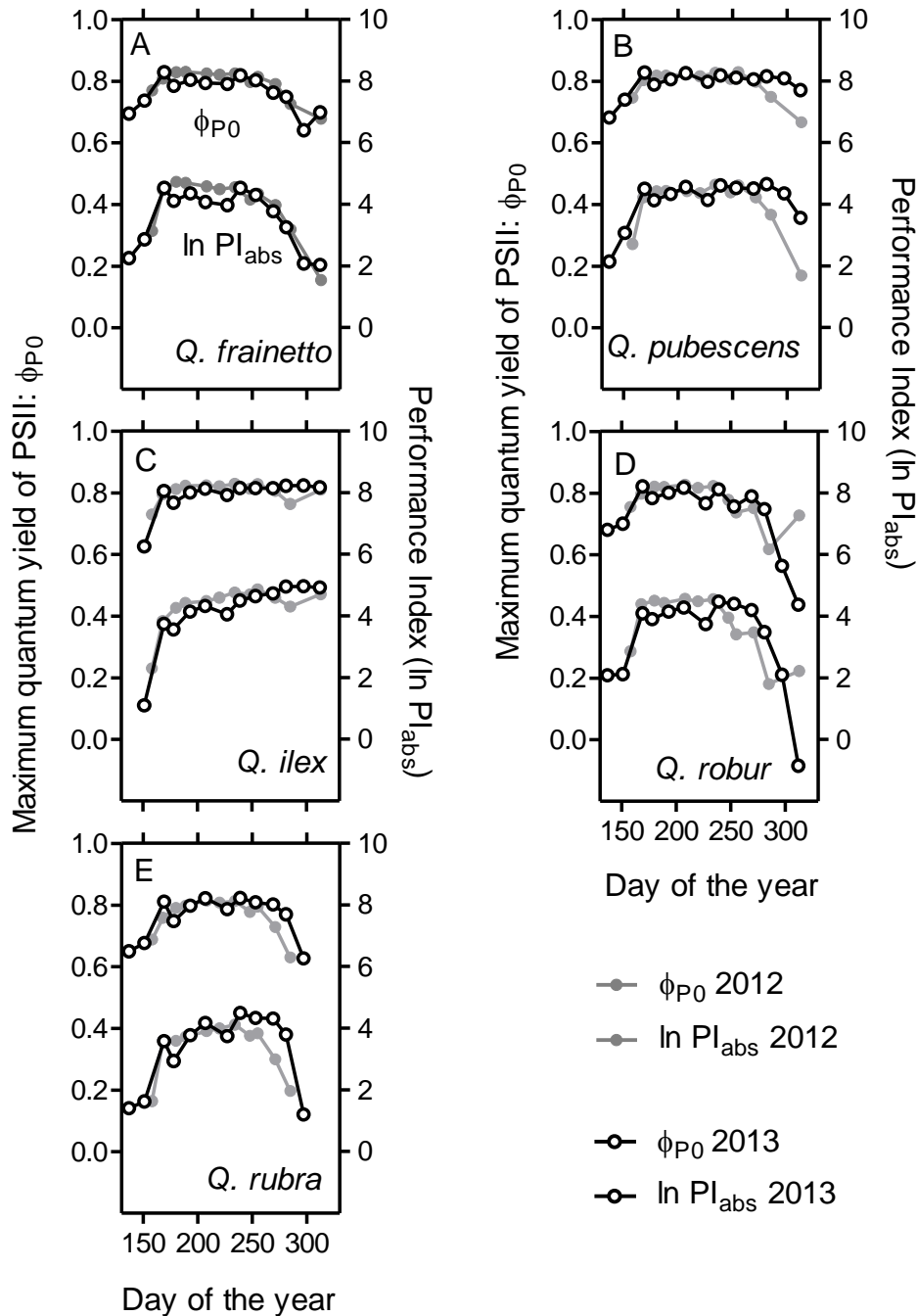


Figure 30: Seasonal variability of F_v/F_m and $\ln PI_{abs}$ in 2012 and 2013 at Frankfurt Schwanheim (FR). Parameter means of F_v/F_m and $\ln PI_{abs}$ of *Q. frainetto* (A), *Q. pubescens* (B), *Q. ilex* (C), *Q. robur* (D) and *Q. rubra* (E) in 2012 and 2013. F_v/F_m : Maximum quantum yield of PSII: $\phi_{P0} = F_v/F_m$ ($F_v = F_m - F_0$) with F_m = maximal fluorescence yield, F_0 = ground fluorescence at 50 μs . $\ln PI_{abs}$: The natural logarithm of the Performance Index on absorption base; an index for energy conservation from photons absorbed by PSII by the reduction of intersystem electron acceptors.

Results

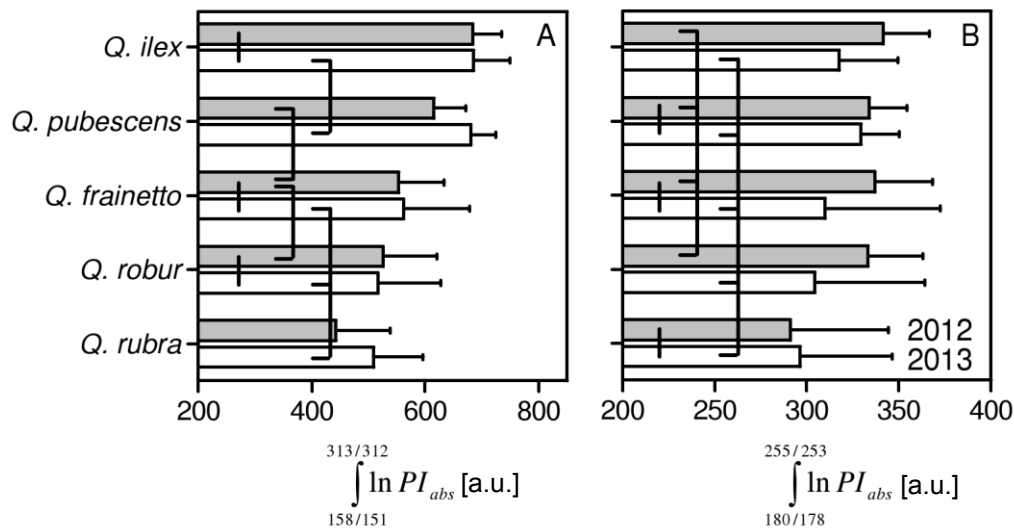


Figure 31: Integrals of individual leaf time courses of $\ln PI_{abs}$ in 2012 and 2013 in Frankfurt Schwanheim (FR). A: Integrals over the whole growth period (2012: doy 158-312, 155 days; 2013: doy 151-312, 161 days). B: Integrals over the core vegetation time (2012: doy 180-255, 75 days; 2013: doy 178-253, 75 days). Means and standard deviations are shown as columns. Upper column 2012, lower column 2013. Means values not connected by vertical bars are significantly different ($p < 0,05$; Between years: unpaired t-test, between species: one-way ANOVA with Tukey's post-test).

To quantify inter-annual and interspecific differences of PSII functionality for distinct periods of time, the area under the individual leaf time courses of $\ln PI_{abs}$ was calculated (Figure 31). For the whole growing season *Q. ilex* showed the highest values, despite of delayed development, since PSII functionality was not decreasing at the end of the year. Due to delayed senescence (especially in 2013), *Q. pubescens* showed high values as well. The lowest values for the integral of the whole growing season are observed in *Q. rubra*. Significant inter-annual differences were found in *Q. pubescens* and *Q. rubra*, for which higher values were observed in 2013. While the $\ln PI_{abs}$ integral for the whole growth period showed differences mainly due to the individual begin of senescence Figure 31B gives values calculated for a period in the growing season mostly unaffected by development and senescence (core vegetation time, see 3.4.1). The integral was calculated for a time span of 75 days from the end of June until early September. In *Q. ilex* and *Q. robur*, significant inter-annual differences were observed with higher values in 2012 (short vertical bars missing in Figure 31). Intraspecific variability in all species masked any interspecific effects, with the exception of *Q. rubra*, for which significantly lower values were observed, compared to all other

species in 2012. An analysis of the complete Chl a fluorescence transient was performed for the time intervals of leaf development and leaf senescence. Given that the deciduous species showed very similar fluorescence kinetics, Figure 32 displays the transients of *Q. pubescens* only, since this species retained the largest sample sizes for late measuring dates in the case of senescence. In *Q. ilex* the same results were observed for leaf development as in the deciduous species, even though delayed (Figure 30). During autumn, *Q. ilex* showed no signs of senescence, and fluorescence transients measured at November did not differ from transients measured in September.

When transients were normalized to F_0 (for equal starting intensities), F_J , F_I and F_m were decreased (less difference in F_J) at early measuring dates during leaf development compared to later measuring dates (Figure 32A). However, the fluorescence yield increase at different times was disproportional, resulting in an increased J-step at 2 ms at day 137 and day 151, when the transient was normalized to F_0 and F_m (Figure 32 B). This difference was further visualized by subtracting the transients to day 207 (completed leaf development), by which two local maxima became apparent close to the J-step. The largest peaks at the J-step occurred at the earliest measuring date (day 137). The signal was reduced two weeks later, but still clearly identifiable at day 151. At the I-step (30 ms), no differences were noted, neither in V_{OP} transients, nor in the differential curves, despite of lower F_I intensities (Figure 32 A). During autumnal senescence a reversed trend was observed and fluorescence intensities (again most noticeable at F_I and F_m) decreased as autumn progressed. The V_{OP} transients showed a deviation from the typical OJIP shape at day 285 with increased fluorescence at the J-step and a decreased I-step. At day 313, fluorescence at the J-step was strongly increased, showing a local maximum instead of the usual plateau. Further, the slope to the J-step was markedly intensified. At the differential curves, a large peak very close to the J-level was observed for day 313 and a minor peak at day 285. At the I-level, no increase compared to the earlier measuring dates was noted. Comparing the fluorescence kinetics of leaf development and leaf senescence,

Results

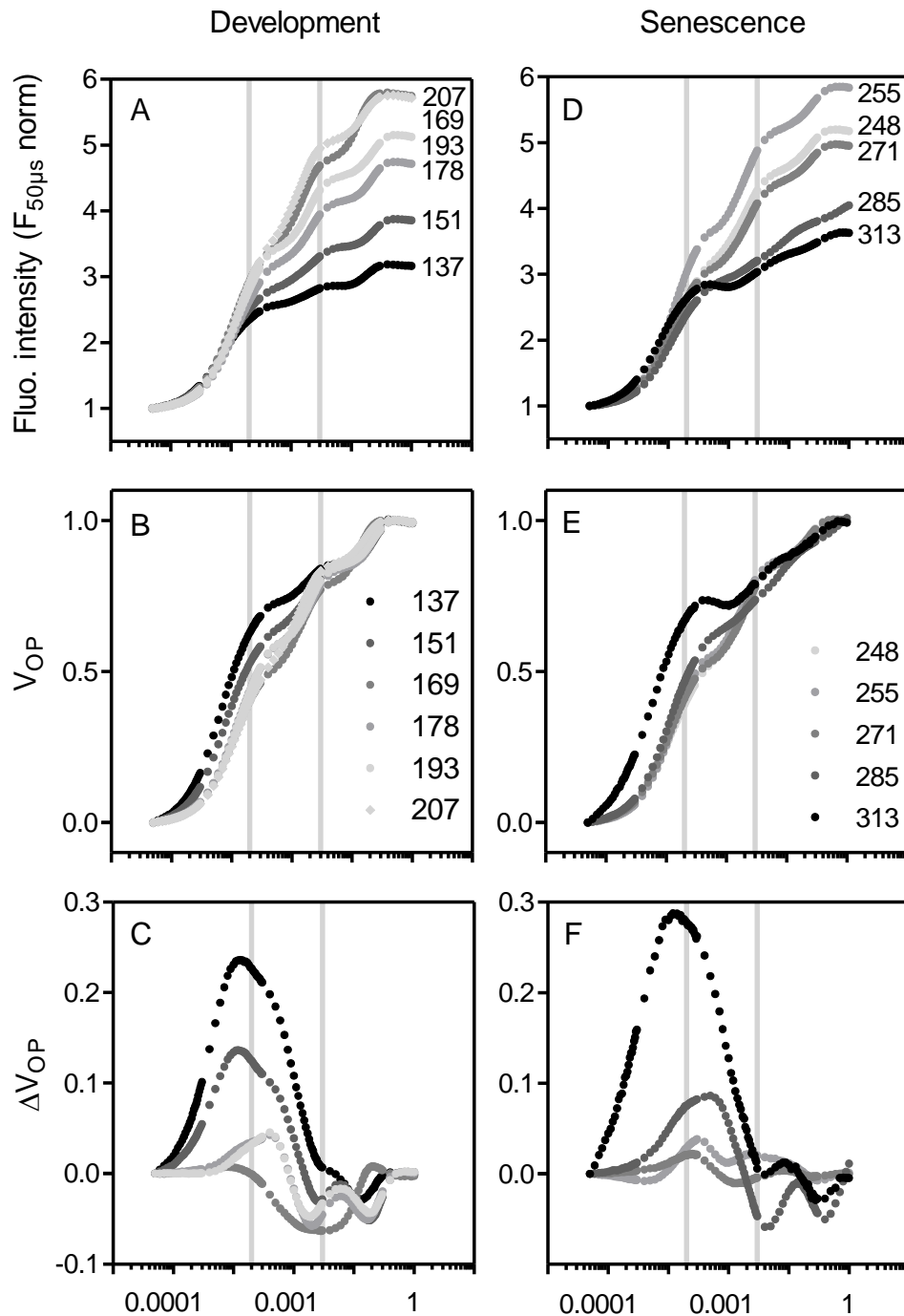


Figure 32: Fluorescence transient alterations during leaf development and senescence. Mean transients of *Q. pubescens* are shown (n = 19-24), measured predawn at given day of the year (Development: 2013; Senescence: 2012). A,E : Fluorescence intensity normalized to $F_{50\mu s} = F_0$. B,E: Double normalized transients (F_0 and F_m) $V_{OP} = (F_t - F_0) / (F_m - F_0)^{-1}$. C,E: Differential V_{OP} curves. Development: $\Delta V_{OP} = V_{OPdoyi} - V_{OPdoy207}$; Senescence: $\Delta V_{OP} = V_{OPdoyi} - V_{OPdoy248}$. Vertical grey lines indicate J- (2 ms) and I-step (30 ms) of the OJIP transient. Note logarithmical x-axis.

the similarities were apparent. In both cases the total fluorescence was decreased, yet disproportional, leading to relative increases around 2 ms. At the seasonal time course of PSII functionality (Figure 30), the comparably lower fluorescence intensities at F_m early and late in growing season led to the decreased maximum quantum yield of primary photochemistry ($F_v/F_m = \phi_{P0}$). The inclusion of the relative fluorescence intensity at the J-step in the equation of PI_{abs} , led to stronger increases at leaf development and greater decreases at leaf senescence compared to F_v/F_m (Figure 30).

3.4.3. Relationship between JIP-test parameters

In order to investigate the relationship between JIP-test parameters which represent important steps in the electron transport chain and the JIP-test vitality indices F_v/F_m and PI_{abs} , the parameters were correlated with each other. To include a wide range of possible interactions, all measurements performed during the seasonal monitoring protocol were included, independent of the time of year, the developmental status of the species or the species itself. Figure 33 shows that the selected parameters were significantly related, following distinct associations. The two parameters most often used to describe the functionality of primary photochemistry, $F_v/F_m (= \phi_{P0})$ and PI_{abs} , showed a very conservative relationship. Higher PI_{abs} values than 3 were only observed at ϕ_{P0} above 0,7. Leaves with ϕ_{P0} values below 0,7 were always correlated with very low values of PI_{abs} , but at ϕ_{P0} values above 0,7, the whole range of PI_{abs} values could be observed (Figure 33 A). The relationship of ϕ_{P0} to RC/ABS was similar to the relationship of ϕ_{P0} to PI_{abs} , with a linear decline of ϕ_{P0} at RC/ABS threshold of 0,5. PI_{abs} consists of three components (i.e. RC/ABS, $\psi_{E0}/(1-\psi_{E0})$ and $\phi_{P0}/(1-\phi_{P0})$, Figure 33 B,D,F, Appendix II), of which the one with the greatest range of values is $\phi_{P0}/(1-\phi_{P0})$. Whereas the relationship of PI_{abs} to and to RC/ABS appeared nonlinear, the relationship of PI_{abs} to $\psi_{E0}/(1-\psi_{E0})$ showed a linear development at increasing $\psi_{E0}/(1-\psi_{E0})$ values beyond 1, indicating a difference in the influence of component changes to PI_{abs} . $V_{OJ300\mu s}$, a parameter quantifying the K-step, indicative for limitations at the electron donor side of PSII, was found to only increase significantly at extremely low PI_{abs} values (Figure 33 E). In all parameter correlations, threshold values were observed, beyond which only very low values for the vitality indices could be detected.

Results

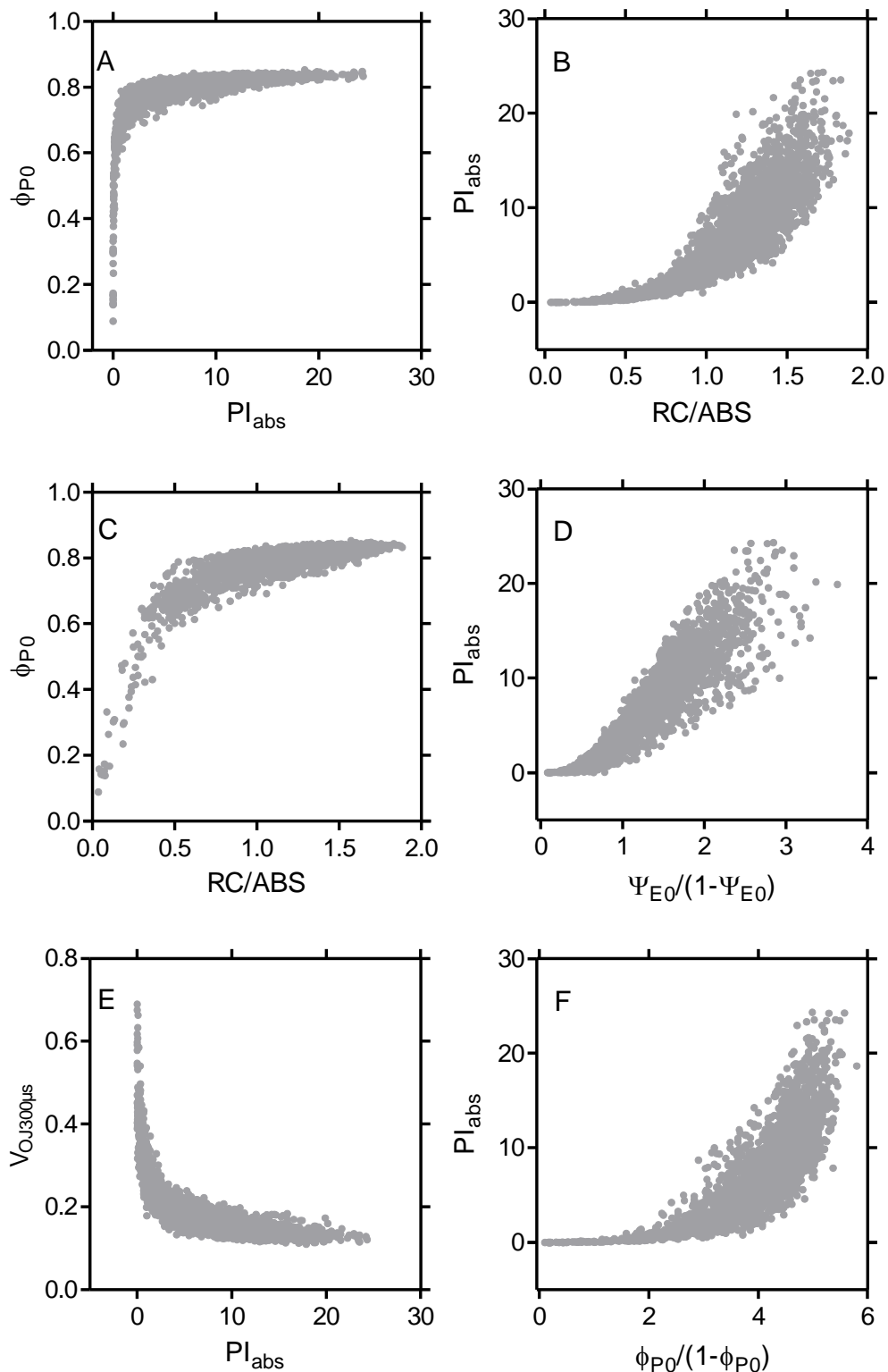


Figure 33: Relationship between JIP-test parameters during leaf development, senescence and steady state. Number of independent data points = 2527. Species: *Q. frainetto*, *Q. ilex* (current and previous year leaves), *Q. frainetto*, *Q. robur* and *Q. rubra* combined. Data from 2012 and 2013. Day of year range 137-313. All measurements were performed predawn (cf. 2.4).

3.4.4. Relationship between SPAD-readings and JIP-test parameters

The measurements of SPAD (cf. 3.4.1) and JIP-test values (cf. 3.4.2) were performed on the same leaf during the whole growing season, therefore it was possible to directly correlate the parameters with each other. Beside different ranges of SPAD values of different species (less values at lower SPAD regions and higher overall values in *Q. ilex*), no interspecific differences in the correlations were found. Figure 34 A and B show the positive correlations of SPAD-values with absolute fluorescence intensities. F_m is linearly correlated over the whole range with the SPAD-readings. For F_0 , after an initial increase at SPAD-values of approx. 20 to 25, a decreasing slope was noted. This led to a positive linear correlation of SPAD values with the variable fluorescence $F_v (= F_m - F_0)$ (not shown), which is the common normalization term in the majority of JIP-test parameters (cf. Appendix II). Figure 34 C and D show the correlations for the normalized fluorescence parameters of the J- (2 ms) and I- (30 ms) step: V_J and V_I [$V_t = (F_t - F_0)/(F_m - F_0)$]. For both parameters, negative linear relationships to the SPAD-values, with a difference in parameter range, and therefore a difference in slope were observed. RC/ABS, quantifying Q_A reducing RCs per PSII antenna Chl, which is calculated including the approximated initial slope of the fluorescence transient [$M_0 = 4(F_{300\mu s} - F_{50\mu s})/(F_m - F_{50\mu s})$ cf. Appendix II], V_J and $F_v/F_m (= \phi_{P0})$, is one of three terms, expressing partial potentials at steps of energy bifurcations [$PI_{abs} = RC/ABS \times \psi_{E0}/(1 - \psi_{E0}) \times \phi_{P0}/(1 - \phi_{P0})$, definition by STRASSER *et al.* 2010]. The correlation of PI_{abs} to SPAD-values was different to the correlations mentioned before. SPAD-values above 30 could be associated with high or low values of PI_{abs} , whereas at low SPAD-values no high values of PI_{abs} were observed.

Results

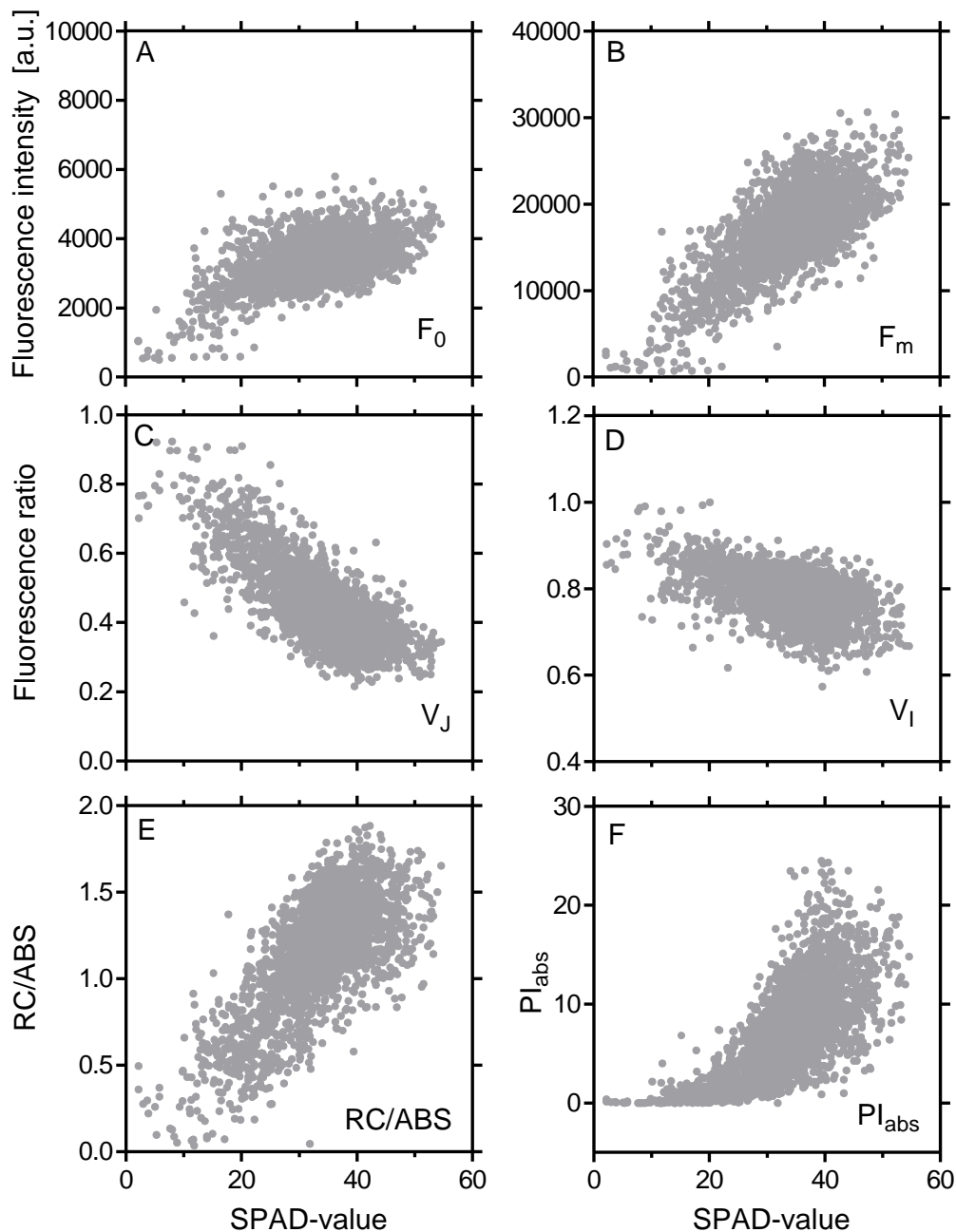


Figure 34: Correlations between SPAD-values and JIP-test parameters. A-F show independent data points of *Q. frainetto*, *Q. ilex* (current year leaves), *Q. pubescens*, *Q. robur* and *Q. rubra* from 2012 and 2013, including dates with leaf development and leaf senescence ($n = 2522$). A: Minimal (ground) fluorescence F_0 ($R^2 = 0,276$); B: Maximal fluorescence F_m ($R^2 = 0,553$); C: Relative variable fluorescence at J-step (2 ms) V_J ($R^2 = 0,588$); D: Relative variable fluorescence at I-step (30 ms) V_I ($R^2 = 0,272$); E: Q_A -reducing reaction centres per PSII antenna chlorophyll RC/ABS ($R^2 = 0,526$); F: Performance Index for energy conservation from photons absorbed by PSII to the reduction of intersystem electron acceptors PI_{abs} ($R^2 = 0,492$). All parameters are significantly correlated with SPAD-values (P-value $< 0,0001$; Pearson's r test for correlation)

3.5. Stress response analyses

In the first section, the drought stress response of *Quercus* taxa with varying leaf traits will be monitored in two different experimental setups. In the second section, responses to increasing temperature of *Q. robur*, *Q. pubescens* and *Q. ilex* will be examined, which had been cultivated under equal conditions in a climate chamber. The third section is concerned with the performance of *Q. ilex* under winter conditions.

3.5.1. Drought stress

In a first step, morphological leaf parameters related to the water content of the leaves as well as the relation of leaf water content to leaf water potential were analysed for their species-specific variability and their possible advantage in periods of drought. During drought stress treatment in two different experimental setups, the effect of decreasing soil water content on the response of the photosynthetic apparatus and on leaf gas exchange were examined.

The water content per leaf fresh weight of unstressed leaves was significantly different in *Q. ilex*, *Q. pubescens* and *Q. robur*, with *Q. ilex* showing the lowest values and *Q. robur* the highest. If the water content was based on leaf dry weight, this order was reversed (Appendix V). Per unit leaf area, leaf water content was increased by 30% in *Q. ilex* compared to *Q. pubescens* and *Q. robur* and no statistical difference was found in the latter two species (Figure 35). The highest leaf water content was found in current year leaves of *Q. ilex* (124,6 g m⁻²). The LWC_A of previous year leaves showed slightly lower values compared to current year leaves of the evergreen. *Q. frainetto* and *Q. pubescens* showed LWC_A values approx. 30% lower than *Q. ilex*, followed by the lowest values of 80,25 and 78,34 g m⁻² in *Q. robur* and *Q. rubra*, respectively. Leaf water content per area (LWC_A), as well as leaf thickness (LT) varied between species. Relating LWC_A to LT across leaf functional types (Figure 35) showed that increases in leaf water content per area were positively correlated to increases in LT across species and the trend found in the deciduous species was followed in the evergreen species.

Results

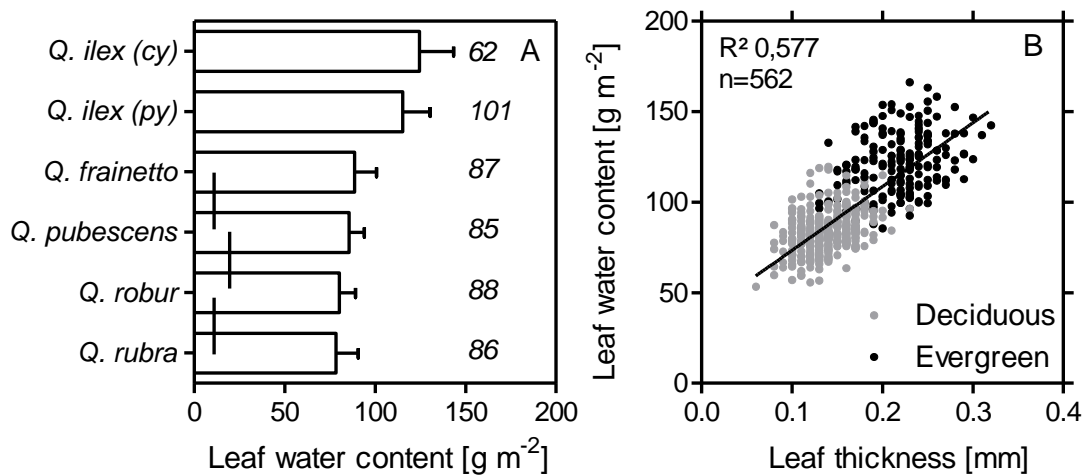


Figure 35: Relationship of leaf water content per area with leaf thickness. A: Species specific differences in Leaf water content per area (LWC_A) in g m⁻². Horizontal columns represent means with standard deviation. Means of connected columns are not significantly different ($p > 0,05$, one-way ANOVA with Tukey's post-test. cy: current year leaves; py: previous year leaves. Sample sizes in italics. B: Relationship of LWC_A to leaf thickness. Grey circles symbolize deciduous species (*Q. rubra*, n=94; *Q. frainetto*, n=94; *Q. pubescens*, n=93; *Q. robur*, n=96; total: 377) and black circles symbolize the evergreen *Q. ilex* (current year leaves, n=91; previous year leaves, n=94; total: 185). Leaves were sampled in early morning (May to November in 2 week intervals) and saturated between moist cloths prior to measurement. Leaf thickness was measured with a digital calliper. No species specific difference was found in the correlation of leaf thickness to leaf water content within the deciduous or the evergreen group. Linear regression: $R^2 = 0,577$; $y = 0,352x + 38,2$.

In pressure-volume (PV) analysis of detached twigs from well-watered plants, leaf water potential was measured subsequently in intervals of increasing leaf water deficit in the same leaf to derive the different components of total water potential and quantify points of interest in drought response. The inverse of leaf water potential was decreasing steeply in a non-linear fashion with increasing relative water deficit until a linear relationship was observed (Figure 36 A). The shape of the resulting PV-curve and the transition from the non-linear to the linear part of the curve were used to derive PV-parameters. The spider plot (Figure 36B) shows that values of *Q. robur* were relatively smaller compared to the other two species, especially compared to *Q. ilex* with the exception of saturated water content (SWC). SWC per dry weight was highest in *Q. robur* and lowest in *Q. ilex*, resembling the results of the morphological leaf traits above. The osmotic potential at full saturation (Π_0) was lowest in *Q. robur* (-1,25 MPa)

and significantly different from Π_0 of *Q. ilex* ($-1,64$ MPa) and *Q. pubescens* ($-1,87$ MPa). The turgor loss point (TLP) can be given in terms of water potential and water content of the leaf. Water potential at TLP was low in *Q. ilex* ($-2,11 \pm 0,24$ MPa) and *Q. pubescens* ($-2,3 \pm 0,23$ MPa). In *Q. robur* TLP was attained significantly earlier at $-1,55 \pm 0,13$ MPa. The relative water content (RWC), where TLP is reached was highest in *Q. ilex* (88,4%) and lowest in *Q. pubescens* (83,0%) (*Q. robur*: 83,8%). Variations in the PV curves of *Q. pubescens* and *Q. ilex* were in the range of 3 to 4,3% and therefore the interspecific differences in RWC_{TLP} were not significant. The modulus of elasticity (ϵ), a measure for the cell wall rigidity, was highest in *Q. ilex* with a value of 14,2 MPa. Lower values of ϵ were observed in *Q. pubescens* with 11,7 MPa and in *Q. robur* with 8,2 MPa (ϵ in *Q. ilex* significantly different from *Q. robur* and *Q. pubescens*, unpaired t-test).

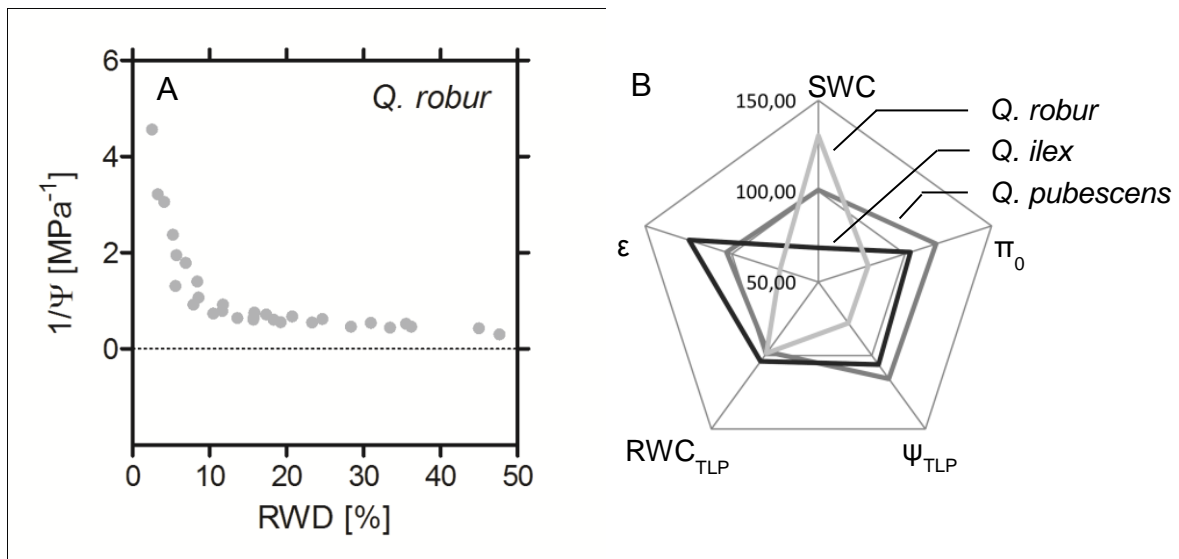


Figure 36: Pressure-volume curve and derived parameters. A: Data points of PV measurements for *Q. robur* ($n = 3$), Relative water deficit (=100 – relative water content) to the inverse of water potential ψ . B: Parameters derived from individual PV-curves visualized in a spider plot relative to the parameter mean of all measured PV-curves. SWC: saturated water content per drymass; Π_0 : osmotic potential at saturation; ψ_{TLP} : water potential at turgor loss point; RWC_{TLP} : Relative water content at turgor loss point; ϵ : modulus of elasticity.

Results

In another set of experiments, performed under controlled conditions in a climate chamber, soil water in the plant's pots was depleted by transpiration, led to a nonlinear decline in predawn water potential (ψ_{pd}) in all three species (Figure 37 A). Volumetric soil water contents above 12% yielded ψ_{pd} between $-0,15$ and $-0,85$ MPa. The decline in ψ_{pd} was steep and values of -4 MPa (limit of the measuring device) was reached at soil water contents of about 5 Vol%. The mean experimental duration per plant from saturated soil to ψ_{pd} of < -4 MPa was 14,5 days with a minimum of 7 days and a maximum of 28 days, due to intraspecific variability in leaf area and whole plant rate of transpiration. Between 10 Vol% and the end of the experiment (ψ_{pd} of ≤ -4 MP) 3,9 days passed, with no difference between the species.

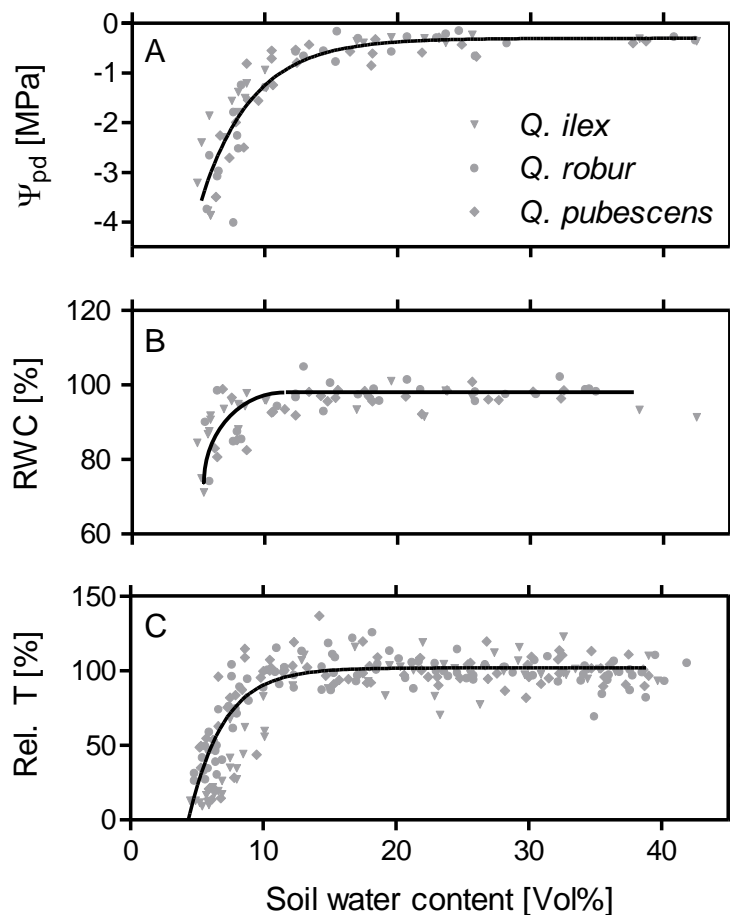


Figure 37: Responses of *Q. ilex*, *Q. pubescens* and *Q. robur* to soil water deficit. A: predawn water potential (ψ_{pd}) in MPa B: Relative water content RWC [%] $\{= (\text{fresh weight} - \text{turgid weight}) / (\text{fresh weight} - \text{dry weight})\}$ C: Rate of transpiration relative to mean rate of transpiration (Rel.T [%]), at soil water content >15 Vol%. Data points fitted by a one-phase decay. Calculation of transpiration rate at 2.5.1.

The mean relative water content (RWC) (93,4% in controls) decreased when soil water content fell below 10 Vol% (Figure 37 B). At ψ_{pd} of -2 MPa, RWC was approx. 80% and the lowest RWC measured was 71% at a soil water content of 5,4% and ψ_{pd} of below -4 MPa in *Q. ilex*. In a similar fashion to the development of RWC, transpiration did not decrease until soil water content reached values around 10 to 12 Vol% (Figure 37 C). The total sum of water loss from the beginning to the end of the experiment was 1161 ml per plant. At this point more than 80% of available soil water was depleted, before adjustments of transpiration rate were initiated. The change in relative transpiration was an adjustment rather than a total inhibition, since a large range of values was observed. The lowest measured values of relative transpiration at 5,4 Vol% was 9,2% of the mean transpiration above 15% soil water content. No interspecific difference was detected in the response of ψ_{pd} , RWC and transpiration to decreasing soil water content in potted plants of *Q. ilex*, *Q. pubescens* and *Q. robur* under climate chamber conditions.

Primary photochemistry responses to water deficit, after dark recovery, resemble the response of leaf RWC to decreasing soil water content (Figure 37 B). F_v/F_m decreases rapidly from a value of around 0,8 at soil water contents below 10 Vol% (Figure 38). $\ln PI_{abs}$ resembles the signal of ϕ_{p0} with no earlier decline being recognisable.

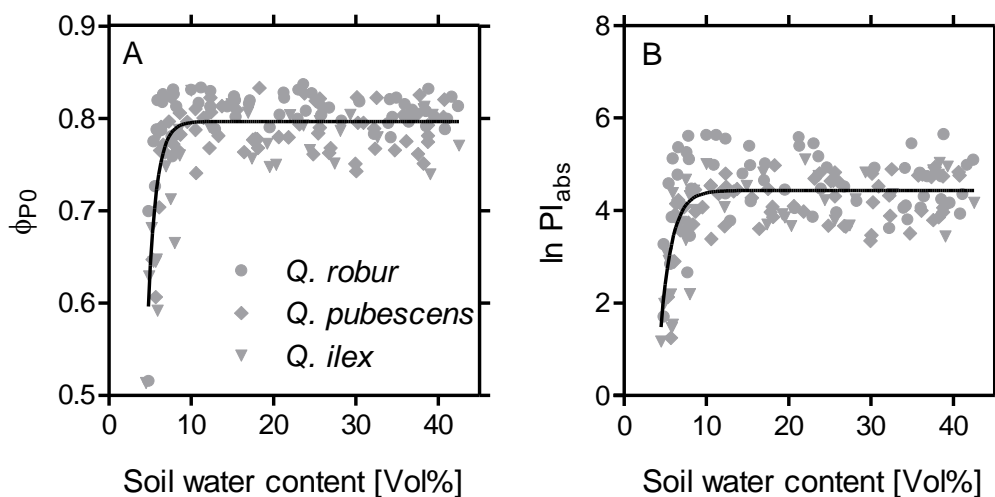


Figure 38: Fluorescence response of *Q. ilex*, *Q. pubescens* and *Q. robur* to decreasing soil water content. A: Maximum quantum yield of primary photochemistry (ϕ_{p0}). B: Ln of Performance Index (PI_{abs}). Data points of 5 plants of the species *Q. robur*, *Q. pubescens* and *Q. ilex*. Data points fitted by a one-phase decay.

Results

In a different experimental setup (cf. 2.5.1 Experiment B), the drought stress response of *Q. robur*, *Q. ilex* and their semi-evergreen hybrid *Q. x turneri* were analysed under greenhouse conditions. Gas exchange rates and Chl fluorescence induction curves were measured over a period of 18 to 22 days, during which the group of stressed plants was forced to replenish the residual water in their pots, while control plants were well watered. Over a wide range of photosynthetic rates (P_N), PI_{abs} remained unaffected (Figure 39 A), but at values of PI_{abs} below 3,5, only low values of P_N were observed. The drop in PI_{abs} in response to drought stress happened at levels of water deficit, at which also transpiration was adjusted (cf. Figure 37 & Figure 38). In Figure 39 B it is shown that P_N was reduced with decreasing stomatal conductance (G_{H2O}). The relationship of P_N and G_{H2O} showed strong association with low variability between species, especially at G_{H2O} below approx. $75 \text{ mmol m}^{-2}\text{s}^{-1}$. P_N reached saturation at G_{H2O} above 75 to $100 \text{ mmol m}^{-2}\text{s}^{-1}$ and did not further improve with increasing stomatal conductance. With increasing water stress, however, only low values of G_{H2O} were observed.

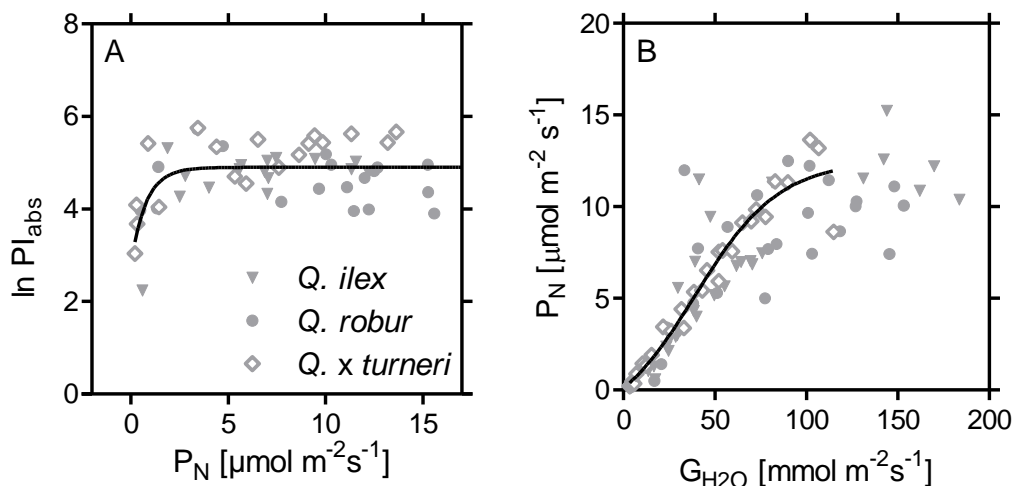


Figure 39: Relationship of PI_{abs} and gas-exchange in *Q. robur*, *Q. ilex* and *Q. x turneri* during water stress. A: \ln of Performance Index PI_{abs} to rate of photosynthesis P_N (at $900 \mu\text{mol quanta m}^{-2}\text{s}^{-1}$ and 400 ppm CO_2) B: P_N to stomatal conductance G_{H2O} . Data points of plants with a range of predawn water potentials from < -1 to $> -2 \text{ MPa}$.

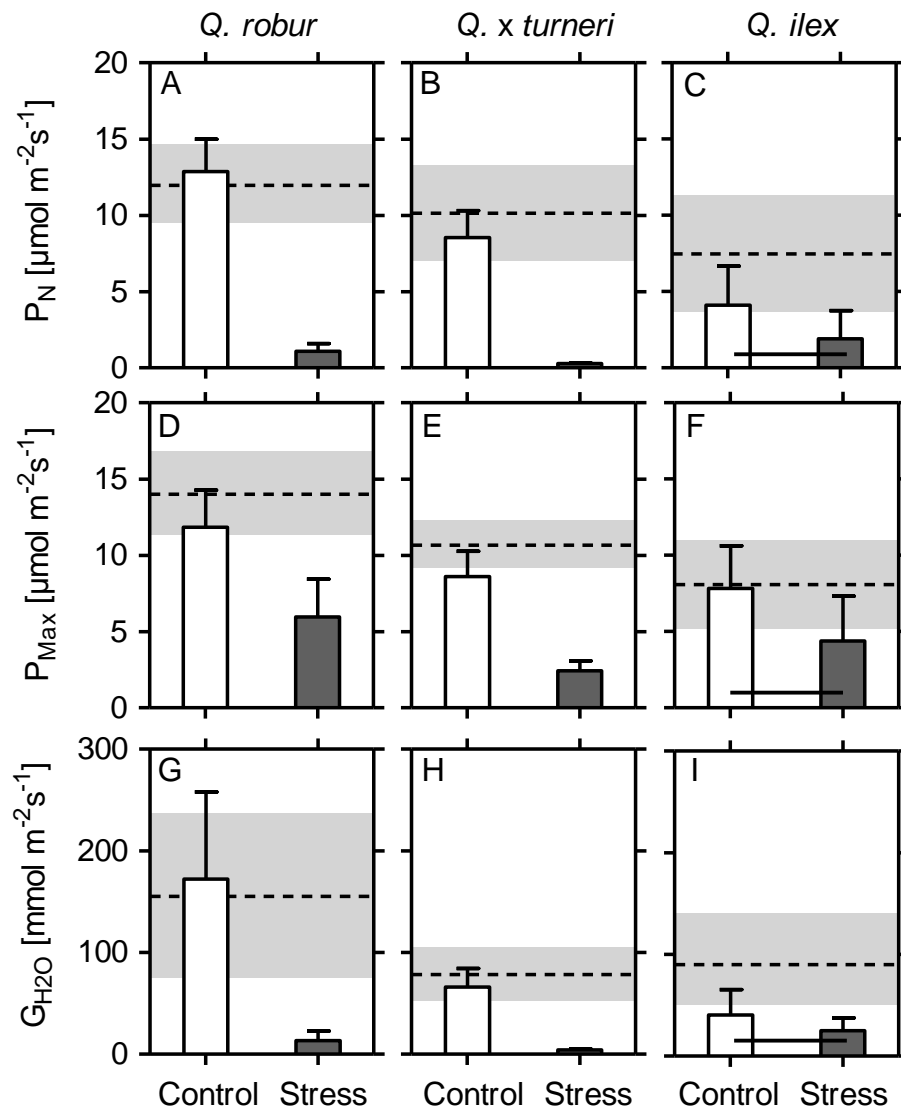


Figure 40. Gas-exchange data as affected by drought stress. Taxa: *Q. robur* (A,D,G), *Q. x turneri* (B,E,H) and *Q. illex* (C,F,I). Control group (n=3) consists of well watered plants, whereas in the stress group (n=3) water was withheld for 18 to 22 days until plants developed a predawn water potential below -2 MPa at the time of measurement. Horizontal broken line and shaded area symbolise mean and standard deviations of parameter value before the onset of the experiment (n = 6). Means of columns connected by horizontal line are not significantly different ($p > 0,05$; unpaired t-test). A,B,C: net photosynthetic rate P_N under ambient gas conditions and $900 \mu\text{mol}(\text{quanta})\text{m}^{-2}\text{s}^{-1}$. D,E,F: photosynthetic capacity (P_{Max}) under 2% O_2 , $4,5\%$ CO_2 and $900 \mu\text{mol}(\text{quanta})\text{m}^{-2}\text{s}^{-1}$. G,H,I: stomatal conductance ($G_{\text{H}_2\text{O}}$). Data from KOLLER *et al.* (2013).

Results

The withholding of water for 18 to 22 days in the stress group led to increased water deficit and decreasing ψ_{pd} (not shown). Besides measured parameter values at the beginning of the experiment, a control group was included to account for possible influences of light and temperatures. At $\psi_{pd} \leq -2$ MPa, P_N was severely decreased compared to the control group (Figure 40 A-C). In *Q. ilex* the difference between the control and the stress group was less pronounced, since control values were lower, compared to *Q. robur* and *Q. x turneri*, thus being not significantly different (Figure 40C). Corresponding to P_N , G_{H_2O} also decreased, as their association was already shown in Figure 39. To exclude potential influences of stomatal limitations and photorespiration, photosynthetic capacity (P_{Max}) under low O_2 (2%) and high CO_2 (4.5%) was assessed at equal light intensities to in situ gas-exchange measures. Values of P_{Max} were higher compared to values of P_N at species-level, however, values of the stress group were suppressed in comparison to the control (Figure 40 D-F).

3.5.2. Heat stress

To assess the response of *Quercus* species to heat and to determine the alteration of pigments and PSII functionality therein, saplings of *Q. robur*, *Q. pubescens* and *Q. ilex* were equally acclimated in a climate chamber and subsequently exposed to 5°C air temperature increases from 20° to 35°C in a climate cabinet. The meteorological data of the climate station at Frankfurt airport from 1949 until 2013 showed that 75% of the annual maximum temperatures are above 32°C, reaching 38,7°C in 2003.

A diurnal observation of leaf and air temperatures from predawn until after sunset showed the close connection of leaf temperature to ambient temperature (Figure 41). Ambient air temperature was maximal at 14:00 with 33,8°C. Leaf temperature exceeded air temperature in some cases. Highest leaf temperature measured were 42,2°C in *Q. ilex*, 38,5°C in *Q. pubescens* and 39,6°C in *Q. robur* at midday. No species-specific difference in the response of leaf temperature to ambient air conditions was found during the in situ measurements.

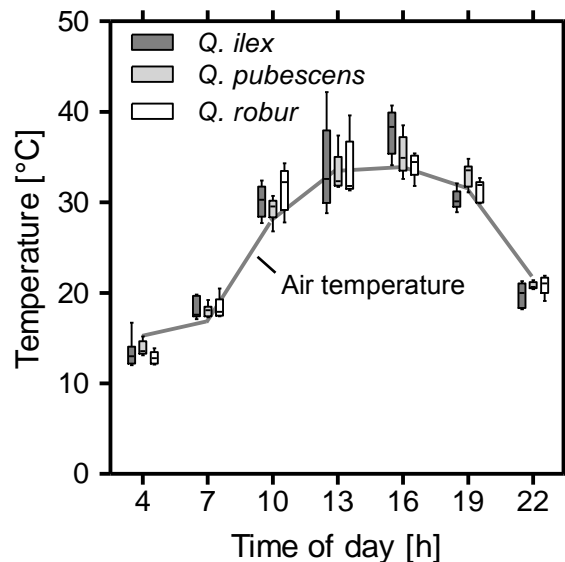


Figure 41: Diurnal fluctuations of leaf temperature. Columns show minimum, 25% quantile, medium, 75% quantile and maximum of leaf temperature (n = 8). Grey line indicates ambient air temperature in the shade (2 m height). Measurements were taken at 22.07.2013 at Frankfurt Schwanheim experimental forest site at clear skies with a handheld infrared thermometer. Ambient air temperature was measured at the site by means of an iMetos climate station.

Results

After acclimation to ambient temperatures of 35°C for 9 days, temperature thresholds of photosynthetic partial reactions were determined. Thermostability of PSII, quantified through the temperature dependent rise of ground fluorescence (F_0) (Figure 8), showed a shift towards higher values, as ambient air temperature was increased (Table 10). The critical temperature of PSII stability (T_{crit}), was approx. 20 °C higher ($T_{crit} \sim 44^\circ\text{C}$) than temperatures in cultivation (20°C). The increase in air temperature to 35°C resulted in an increase in T_{crit} of about 4°C. The temperature at which F_0 reaches 50% of its max values (T_{50}) was linearly correlated to T_{crit} ($R^2=0,856$) and on average 2,4°C higher. No species specific difference in the acclimation of thermostability of PSII to increasing ambient temperatures was observed.

Table 10: Acclimation of PSII thermostability to increasing temperatures. AdT: Ambient daytime temperature; T_{crit} [°C]: Critical temperature when ground fluorescence begins to rise rapidly and PSII starts to break down; T_{50} [°C]: Temperature at which F_0 reaches 50% of its maximum. Statistics: Two-Way ANOVA with Bonferroni multiple comparison post-test. AdT effected T_{crit} and T_{50} significantly.

	AdT [°C]	<i>Q. ilex</i>			<i>Q. pubescens</i>			<i>Q. robur</i>		
		mean	SD	<i>n</i>	mean	SD	<i>n</i>	mean	SD	<i>n</i>
T_{crit}	20	43,8	1,2	3	44,5	0,9	3	44,3	1,7	2
	25	44,6	0,6	3	45,7	0,9	3	45,3	0,4	3
	30	45,0	0,9	2	45,9	0,1	2	45,7	1,2	2
	35	47,1	0,9	3	46,4	2,3	3	48,3	0,8	3
T_{50}	20	47,3	0,4	3	46,8	0,8	3	47,4	2,1	2
	25	47,0	0,6	3	47,9	1,1	3	47,7	0,5	3
	30	47,4	0,5	2	48,1	0,7	2	48,2	0,5	2
	35	49,1	0,6	3	48,4	2,1	3	50,8	1,2	3

Leaf temperature (T_{leaf}) induced alterations in the fast Chl fluorescence induction transient were assessed by submerging leaves acclimated to 35°C air temperature in water, which was subsequently heated in 5° steps to 50°C. With increasing T_{leaf} , the shape of the OJIP transient and the values of the derived JIP-test parameters changed, yet interspecific differences between *Q. ilex*, *Q. pubescens* and *Q. robur* in the response to increased temperature were not detected. At T_{leaf} above 20°C, decreases at the I-step as well as decreases in the maximal fluorescence yield F_m were observed (Figure 42 A), leading to early declines in PI_{abs} (Figure 42 D) and relative increases in ΔV_{IP} (Figure 42 C) but not in the effective quantum yield of PSII (ϕ_{PSII}) (Figure 42D). At a T_{leaf} of 35°C a fluorescence increase at the K-step slowly developed, strongly increasing to 45°C as visible in the differential ΔV_{OJ} transient display (Figure 42 B). The local maxima of the K-steps at different T_{leaf} appear at 0,0005-0,001 s, later than the time used in the calculation of $V_{\text{OJ}300\mu\text{s}}$ (0,0003 s), a parameter quantifying this peak [$V_{\text{OJ}300\mu\text{s}}=(F_{300\mu\text{s}}-F_0)/(F_{2\text{ms}}-F_0)$] occurring between 200-300 μs under standardized conditions (SRIVASTAVA *et al.* 1997). PI_{abs} decreased before the development of the K-step (Figure 42 B). Further increase in leaf temperature to 50°C (higher than the measured critical temperature for PSII thermostability T_{crit} , cf. Table 10) led to a further increase in $V_{\text{OJ}300\mu\text{s}}$, whereas PI_{abs} and ϕ_{PSII} values declined towards zero.

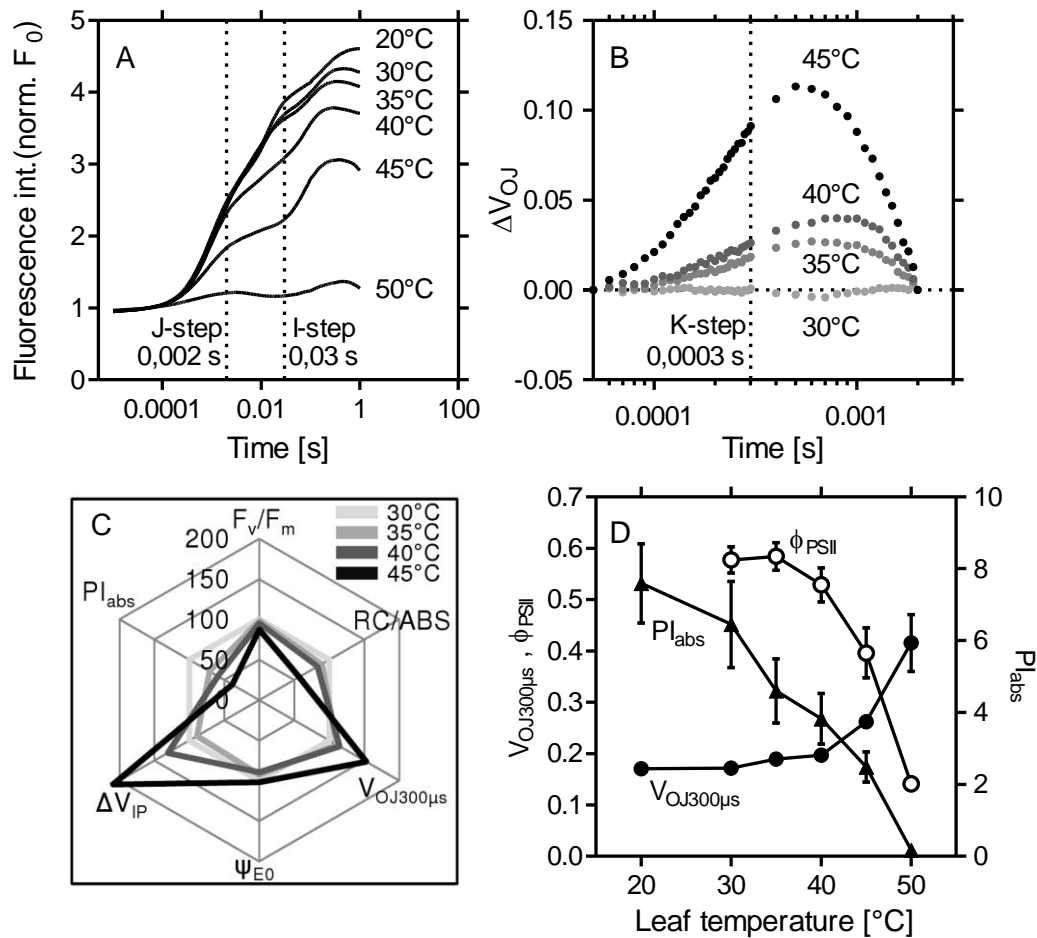


Figure 42: Temperatures induced alterations of Chl a fluorescence transients and JIP-test parameters in plants acclimated to 35°C. A: OJIP transients normalised to F_0 , measured in darkness. J- and I-step indicated by vertical broken line. B: K-step development in differential transient display $\Delta V_{OJ} = V_{OJ,i} - V_{OJ,20^\circ C}$. $V_{OJ} = (F_t - F_0)(F_{2ms} - F_0)^{-1}$; Means of 5 different leaves per species ($n=15$ combined, since no interspecific difference in K-step development was observed) Plants acclimated to 35°C (9 days). Position of K-step indicated by vertical, broken line. C: Spider plot, showing the relative change [%] of JIP-test parameters compared to T_{leaf} of 30°C for all species combined ($n=15$ per T_{leaf}) D: $V_{OJ300\mu s} [(F_{300\mu s} - F_0)/(F_{2ms} - F_0)]$ and the Performance Index (PI_{abs}) in relation to leaf temperature. $n=15$; \pm SEM; species combined. Decrease of the effective quantum yield (ϕ_{PSII}) in light ($\sim 300 \mu\text{mol quanta m}^{-2} \text{s}^{-1}$) with increasing leaf temperature. Means and SEM of ϕ_{PSII} ($n=9$), shown combined for *Q. ilex*, *Q. pubescens* and *Q. robur*, since no significant interspecific difference at each temperature was ($p > 0,01$; one-way ANOVA with Tukey's post-test).

3.5.3. Cold stress in *Q. ilex*

The responses of *Q. ilex* to winter conditions were observed in the period from November 2012 to May 2013 in the forest (Schwanheim experimental forest site FR) as well as in the Botanical Garden at Frankfurt Riedberg. The winter period was characterized by a slightly warmer November and December (mean air temperature) compared to the 30 year normperiod 1981 to 2010 (Table 11). Nevertheless air temperatures below zero degrees Celsius were observed from November until April with minimal winter temperatures in March 2013. March was exceptionally cold with a mean air temperature 3,6 °C below the norm and 23 frost days (norm: 9,5 days, 1981 to 2010). Another notable exception from the norm was the number of ice days in January 2013, which were twice as high. The coldest measured winter at Frankfurt in the period from 1949 until 2013 (1963) had minimum temperatures of –21,6 two meters above ground, 121 frost- and 56 ice days, which means that one third of the year temperatures below zero degrees Celsius were noted. The mean minimum temperature for this time period was –13,2 (\pm 3,7) with 78,71 (\pm 18,1) frost days and 15,2 (\pm 10,4) ice days. The historical data allows the comparison of the winter period 2012/2013 to values already measured at that location and allows estimates of winters that should be further expected in the future, despite of a warming climate.

Table 11: Climate parameters for the winter period 2012/2013. Data from station 1420, Airport Frankfurt am Main. Values for the normperiod 1981 to 2010 are shown in brackets. Height of all temperature measurements is 2 meters above ground, except for the minimum ground temperature (5 cm). Frost days are days with a minimum temperature (2 m) below zero degrees Celsius. Ice days are characterized with daily maximum temperatures below zero degrees Celsius. All data derived from the German meteorological service DWD (www.dwd.de).

		Air _{mean}	Air _{min}	Air _{ground}	Air _{max}	Frost days	Ice days
		[°C]	[°C]	[°C]	[°C]	[d]	[d]
November	2012	6,4 (5,6)	–4,1	–7,1	15,1	4 (7,4)	0 (0,8)
December	2012	3,8 (2,5)	–8,7	–12,4	13,6	11 (15,1)	1 (3,8)
January	2013	1,8 (1,6)	–8,7	–10,3	13,9	17 (16,7)	12 (5,9)
February	2013	1,1 (2,4)	–5,4	–9,9	8,1	18 (15,8)	2 (2,8)
March	2013	2,8 (6,4)	–10,5	–16,4	17,2	23 (9,5)	2 (0,1)
April	2013	10,3 (10,3)	–3,5	–7,0	25,6	4 (3,1)	0 (0,0)
May	2013	13,0 (13,0)	1,2	–0,4	23,6	0 (0,2)	0 (0,0)

Results

In about 50% of all winters in the last 65 years frost- and ice days are close to the observed values in 2012/2013. The minimum temperature of 2012/2013 is close to the 75% quantile of the historical data, which indicates that in approx. 75% of winters, the minimum temperature is lower than $-10,4\text{ }^{\circ}\text{C}$.

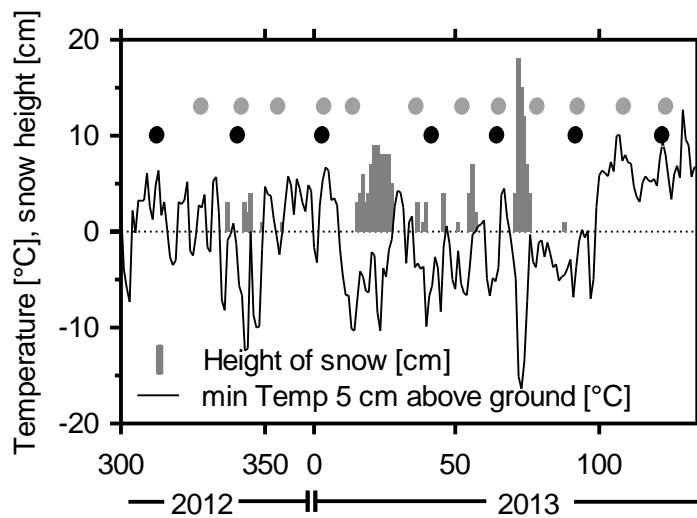


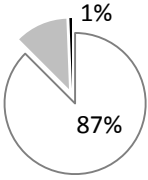
Figure 43: Daily trend of ground temperature and height of snow in the winter 2012/2013. Meteorological data from station 1420 airport Frankfurt am Main. Black and grey circles symbolize measurements performed at the Botanical Garden and Schwanheim Forest respectively. All data taken from the German meteorological service DWD (www.dwd.de).

The daily trend of the minimum temperature 5 cm above ground (Figure 43) indicates minor frost events in the beginning of the year with a local minimum in December reaching to $-12,4\text{ }^{\circ}\text{C}$ with snow coverage and one prior and one later event with -8 degrees and no snow cover. From mid of January on, a cold period with freezing rain and sleet in Frankfurt led to ice-coverage of leaves. A period of low temperatures only sparsely disconnected by few days with minimum temperatures above zero degrees Celsius continued until the beginning of April, when temperatures rose abruptly. At the time, when the minimal temperature of the whole winter period was measured in March 2013 ($-15,1\text{ }^{\circ}\text{C}$), a snow cover was present.

These conditions led to terminal bud injury in 12% of trees (Table 12). For one of the 168 assessed trees, winter conditions were fatal and no resprouting occurred in spring. Leaves were not abscised and no measureable difference in tree height or width was observed during the winter period.

Table 12: Winter injury of *Q. ilex* at Frankfurt Schwanheim. Data from 3,5 years old trees from Frankfurt Schwanheim experimental forest site (planted in 2011) in the winter 2012/2013. Control assessment was conducted in autumn 2012.

Assessment criteria	nr of trees
No Change	147
Terminal bud injury	20
Death	1
Sum	168



A pie chart illustrating the distribution of assessment criteria. The largest slice, representing 'No Change', is 87%. The next largest, 'Terminal bud injury', is 12%. The smallest slice, 'Death', is 1%.

When studying the influence of the winter conditions on leaf pigments, the ratio of Chl a to Chl b showed no significant deviations during the winter period 2012/2013 in *Q. ilex* (Figure 44). The ratio of total Chl to total Car (Chl/Car), however, slowly declined until a significant drop to 75% on day 92 (from 3,65 to 2,72) occurred. It recovered quickly to a value of 3,35 (92%) 30 days later, which was not significantly different to the ratio measured at the beginning of the winter period. The relative concentration of chlorophyll was monitored with the SPAD-meter in two week intervals at the Botanical Garden and at Frankfurt Schwanheim experimental forest site, where no drop at day 92 was observed. It can be concluded that the decline in the ratio of Chl/Car is due to an increase of carotenoids rather than to a decrease in chlorophylls. No sequential decline or increase of SPAD-values was noted at both sites. However, deviations from the mean SPAD-value were observed twice, with a difference to SPAD_{mean} of 3,1 and 1,8 SPAD units (values increased compared to the mean). These differences coincided with minimum temperatures below -4°C (cf. Figure 24), when leaves were frozen at the time of measurement (07.12.2012 and 06.03.2013) (cf. 2.3.1).

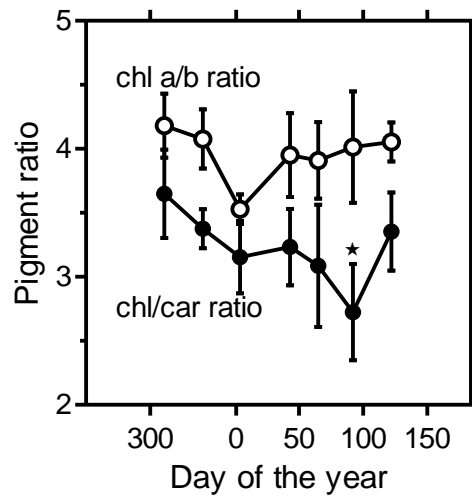


Figure 44: Variations of pigment ratios in *Q. ilex* during winter conditions. Means and standard deviations of relative chlorophyll a to b ratio (white circles) and chlorophylls (a+b) to carotenoids (xanthophylls + carotenes) (black circles) are shown ($n = 5$). Values are calculated relative to the mean of the first measurement at day 311, 2012. Chl/Car ratio at day 92 is significantly different to the first date of measurements ($p < 0,05$; one-way ANOVA with Tukey's post-test with absolute values).

In order to monitor possible alterations of the dark reactions of photosynthesis due to winter conditions, O_2 evolution under strongly elevated CO_2 and decreased O_2 was measured, avoiding stomatal influence and photorespiration. Possible changes in the light reactions and/or spatial differences of upper or lower leaf chloroplasts were quantified by measuring the steady state Chl fluorescence under continuous saturated light with a PAM setup. A response to winter conditions was observed in gas-exchange as well as in the steady-state fluorescence. The maximum assimilation rate (P_{max}) decreased after day 341 to values below $10 \mu\text{mol m}^{-2} \text{s}^{-1}$ at day 43 and recovered at the beginning of May 2013. A similar trend was observed in the effective quantum yield of photochemistry (ϕ_{PSII}), for which the first parameter decrease was noted on day 43 in 2013, but no differences in values of the adaxial and abaxial leaf surface were found. On the contrary, in the fluorescence decrease ratio (R_{Fd}) and non-photochemical quenching (NPQ), higher values for the adaxial leaf surface were observed in comparison to the abaxial leaf surface. This difference vanished after a sharp decline between day 4 and 43 (values of NPQ are not shown beyond day 4, because of simultaneous decline of F_v/F_m). The time course of R_{Fd} is primarily due to a response of the maximal fluorescence (F_m), whereas the steady state fluorescence in light (F_t)

showed no significant alteration. A local minimum was reached on day 92, when R_{Fd} was only $\sim 20\%$ of initial values. Values were recovering and almost reached autumnal values only 30 days later. At that last date of measurement at the beginning of May 2013, R_{Fd} values were again different on the upper and the lower leaf surface, like in autumn.

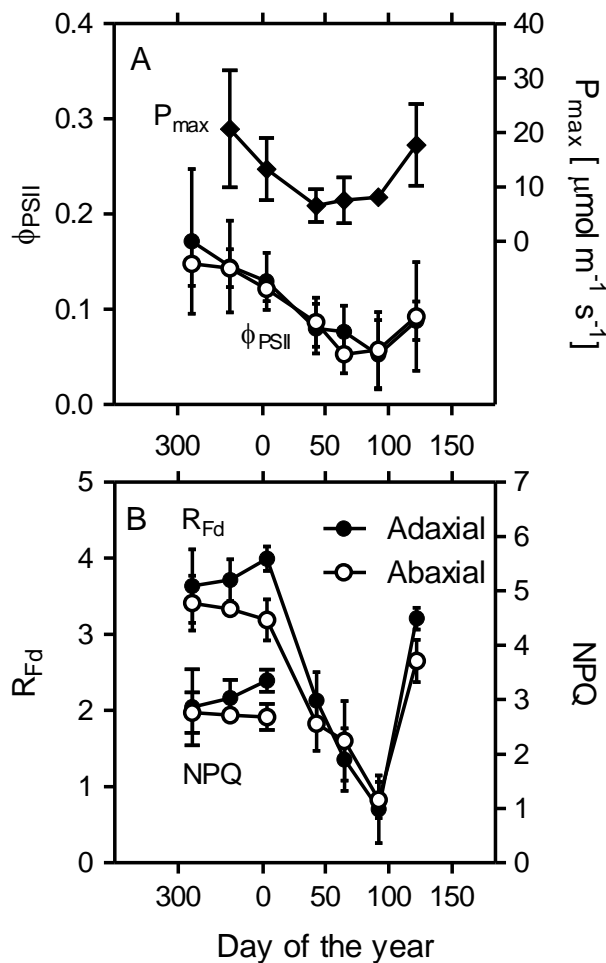


Figure 45: Winter response of photosynthetic leaf traits in *Q. ilex*. A: Effective quantum yield of photochemistry ϕ_{PSII} and maximal assimilation rate P_{max} under 4,5% CO_2 , 2% O_2 , 20°C and $\sim 2000 \mu\text{mol quanta m}^{-2} \text{s}^{-1}$. B: Fluorescence decrease ratio R_{Fd} and non-photochemical quenching NPQ (shown only for dates without a significant decrease in F_v/F_m). Sample size: $n=5$ per date of measurement. Solid black circles show values measured on the upper (adaxial) leaf surface and white circles show values measured on the lower (abaxial) leaf surface.

Results

Measurements of the fast OJIP transient were performed predawn at two week intervals for 6 months at two different sites. The maximum quantum yield of primary photochemistry ($F_v/F_m = \phi_{p0}$) rapidly decreased after day 4 in 2013 at the Botanical Garden (Figure 46 A). At the forest site (FR), the decrease was delayed by about 30 days and began after day 37 in 2013. After this decrease values at both sites showed no significant differences anymore. The lowest ϕ_{p0} values at both sites were measured at day 92 with $0,346 \pm 0,092$ for *Q. ilex* at the Botanical Garden and $0,380 \pm 0,085$ at the forest site. Two weeks later ϕ_{p0} recovered to values not significantly different from the beginning of the winter period. Analyses of the full OJIP transients at the time of the decline (Figure 46B), showed that F_0 was only affected at a late point in time resulting in a minor decrease. The decrease of ϕ_{p0} during the winter period 2012/2013 in *Q. ilex* was therefore solely an effect of declining maximum fluorescence. Fluorescence intensities at the J- (2 ms) and I-step (30 ms) of the transient also declined, leading to increases in V_J and V_I , when normalized and consequently to decreasing RC/ABS, ψ_0 and PI_{abs} values.

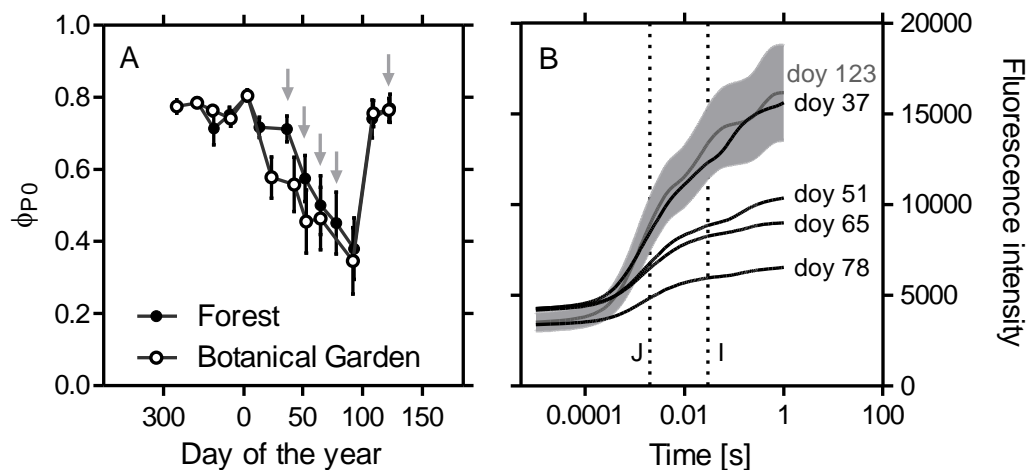


Figure 46: Development of maximum quantum yield (ϕ_{p0}) of *Q. ilex* during the winter 2012/2013. A: Means and standard deviations are shown as black solid circles for plants growing at Frankfurt Schwanheim experimental forest site (FR) and white circles for plants growing at the Botanical Garden at Frankfurt Riedberg on a south exposed slope without cover. Measurements were performed predawn on the same leaves for all points in time. Sample size $n = 21$ (forest); $n = 25$ (Botanical Garden). Grey arrows point to data of the forest site, shown as full transients in B. B: Mean OJIP transients ($n=21$) of 5 points in time during the F_v/F_m decline and recovery at Frankfurt Schwanheim. For day 123, mean and SD are shown in grey to visualize intraspecific variation in recovery. J- and I-steps at 2 ms and 30 ms are represented by vertical broken lines. Note logarithmic x-axis.

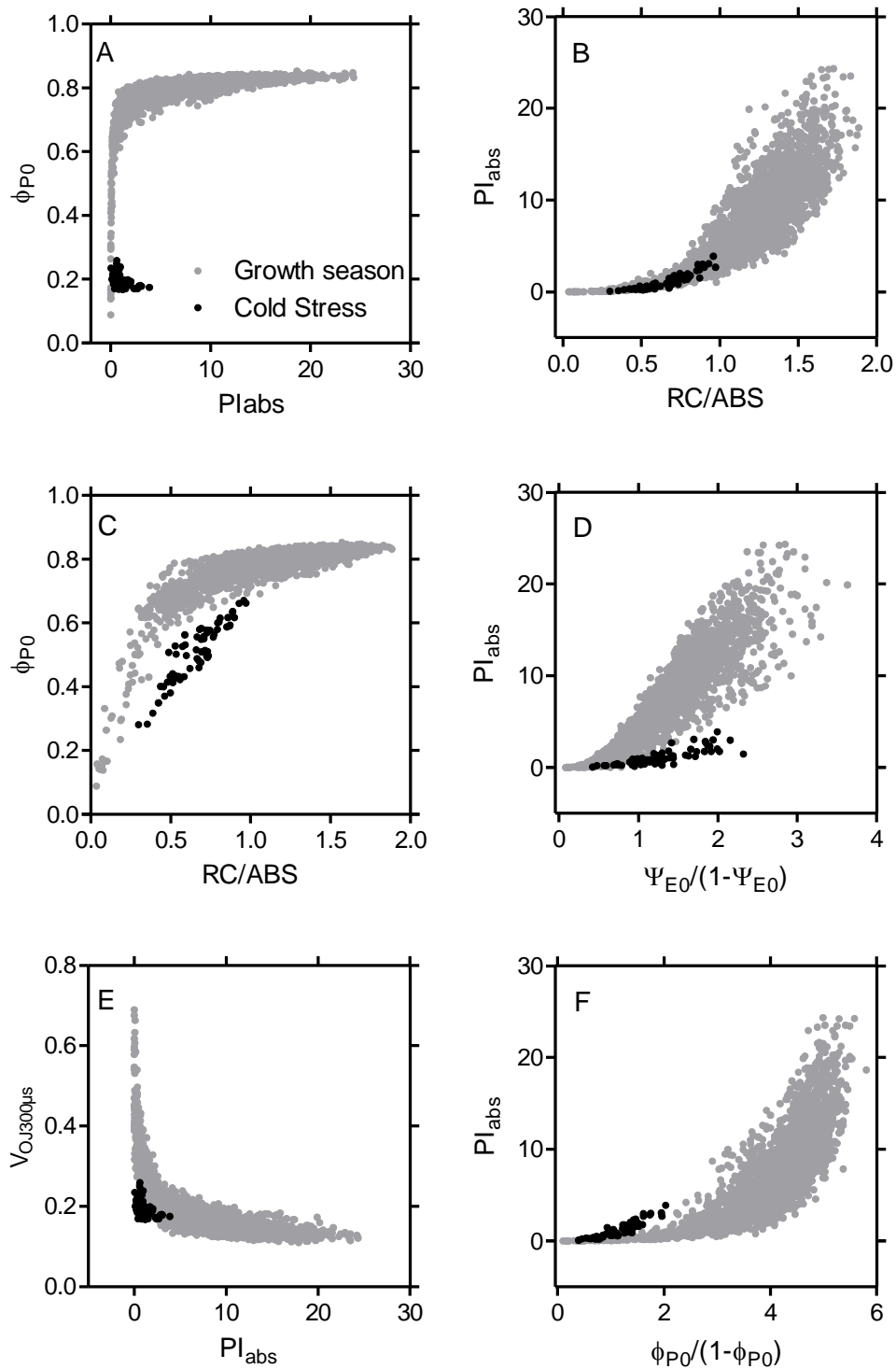


Figure 47: Relationships between JIP-test parameters during the natural annual time-course and under cold stress conditions. Measurement of OJIP transients during the growing seasons 2012 & 2013 cf. 2.4 & Figure 33). Data points representing cold stressed leaf samples are from day 51, 65 & 78 cf. Figure 46) Species: seasonal: *Q. frainetto*, *Q. ilex* (current and previous year leaves), *Q. frainetto*, *Q. robur* and *Q. rubra* combined; cold stress: *Q. ilex*. Number of independent data points: seasonal = 2527; cold stress = 63. All measurements performed predawn.

Results

In Figure 46, the original OJIP transients of the measurement days 51, 65 and 78 (doy 2013) are depicted with the significantly suppressed J,I steps and F_m . However, the relationship between the selected JIP-test parameters, derived from the original transients, to each other differed compared to the relationships observed during the natural time-course (Figure 47) observed from spring to autumn in 2012 and 2013. PI_{abs} was already strongly declined, but the influence of the components $\phi_{P0}/(1 - \phi_{P0})$ and $\psi_{E0}/(1 - \psi_{E0})$ was changed. At the same levels of $\phi_{P0}/(1 - \phi_{P0})$ and $\psi_{E0}/(1 - \psi_{E0})$, PI_{abs} was relatively increased in the former and decreased in the latter during cold stress, whereas the relationship between RC/ABS and PI_{abs} remained unchanged (Figure 47 B,D,F). Also at the same RC/ABS values, ϕ_{P0} was notably lower in the cold stressed plants (Figure 47 C)

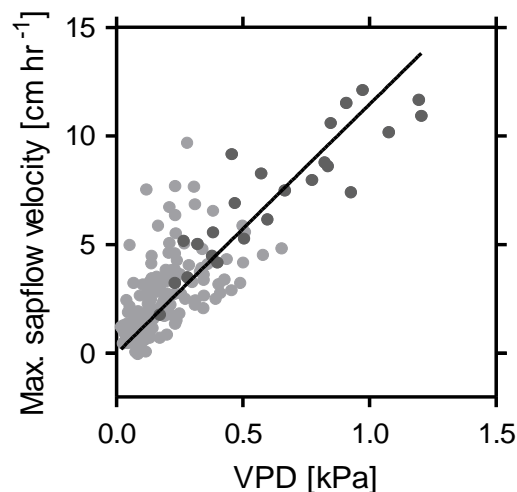


Figure 48: Daily maximal sap flow velocities of *Q. ilex* during winter 2012/2013. Each point represents the mean daily maximal sap flow velocity of 3 HRM sap flow meters installed on different trees of *Q. ilex* at Botanical Garden Frankfurt, Riedberg against the vapour pressure deficit (VPD) of the air for the period 01.11.2012 until 01.05.2013. Dark grey symbols represent data from doys 99 (09.04.2013) on, when minimum temperature at 5 cm above ground was always above 0°C (cf. Figure 43).

To ensure that that the observed fluorescence responses of PSII were not due to drought stress developed through frozen soil or xylem embolism by xylem freezing, the sap flow velocity was monitored over the whole winter period. Sap flow velocities at winter were low (75% quantile below 5 cm hr⁻¹) and significantly correlated with the vapour pressure deficit (VPD) of the air ($p < 0,0001$; $R^2: 0,676$). No deviations of this relation, like low sap flow velocity at high VPD, indicating insufficient water supply, were observed.

4. Discussion

4.1. Investigation areas

The experimental forest site in Frankfurt Schwanheim (FR) is located in the Main river basin in Southern Hesse. The greater region is characterized by a comparatively warm and dry climate in an area extending from Baden-Württemberg and Rhineland-Palatinate through the Upper Rhine Valley to the Main River basin (Figure 49). In summer the region is characterized by high temperatures and a high number of summer- and hot days (max T >25°C and >35°C) coupled with low precipitation, leading to increased loss of soil water to the atmosphere. The warmer temperatures in spring lead to an earlier beginning of the growth period compared to other regions in Germany (DWD 2015) but the temporal variability was found to be large. For example, in 2012 the growth period started 8-10 days earlier and in 2013 16-20 days later than usual [compared to norm period 1961-1990 for that region (DWD 2015)]. Due to further increases in temperatures and decreases in precipitation, models predict soil water contents to decrease by 20% in this region in the next 30 years, with the highest

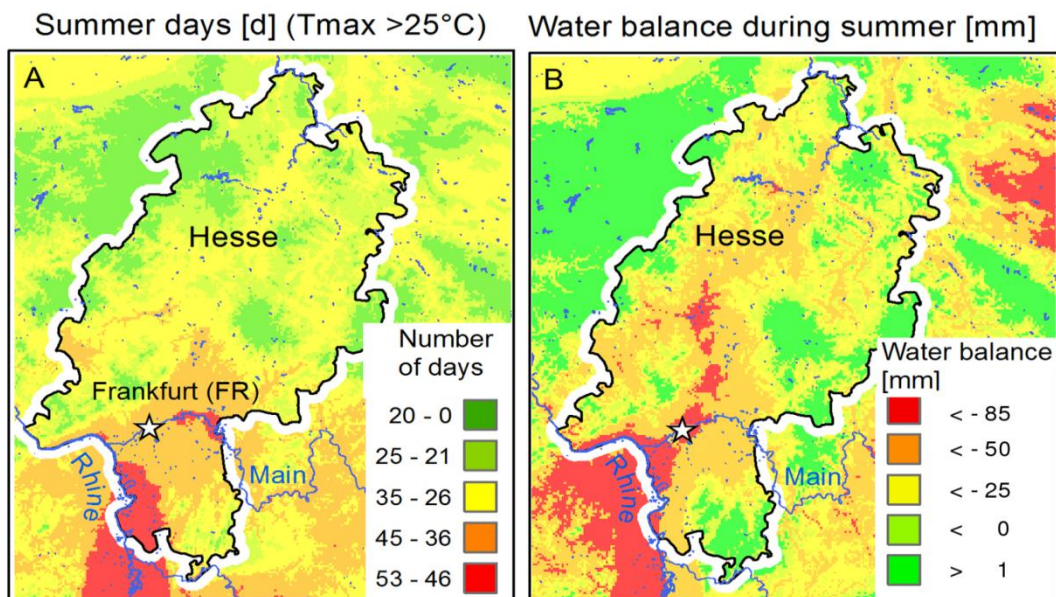


Figure 49: Map of summer days and water balance in Hesse (norm period 1961-1990). Climate data from DWD (<http://dwd.de>). State boundaries and water bodies from digital landscape model (DLM) ©GeoBasis-DE BKG 2015, (<http://www.bkg.bund.de>). Experimental forest site Frankfurt (FR) marked by white star. Summer days: days with maximal temperatures above 25°C. Water balance: balance between precipitation and potential evaporation over grassland. Projection: UTM 32U.

impact on sandy soils (RENNENBERG *et al.* 2004). Especially in the proximity of past basins of the Rhine and Main rivers, sandy soils are predominant, of either fluvial or windblown origin (HLUG 2015), with low water holding capacity and nutritional status. The soil profile at the FR site is well characterized by its river influence, with very high proportions of sand (>50%) in all layers, increasing further with depth. The organic topsoil and the topmost layer, containing higher N and C contents are very thin, but have shown great spatial variety in thickness up to 10 cm due to dents and former forestry lanes (cf. Figure 10, Appendix VI). The planted trees may however only benefit indirectly from this higher N-content by runoff and/or displacements, since (according to common planting practice) the topsoil was cut and flipped prior to planting to avoid early competition. Thus, trees root in soil with N-content of 0,18% on average with an observed range of 0,06% to 0,39% (cf. Figure 10). N-deficient soils may shift carbon investments towards root growth (MÜLLER-STOLL 1947), leading to enhanced water supply and a possible advantage during drought. On the other hand, higher N-contents support general growth (LARCHER 2003), posing a competitive advantage for other species in close proximity of the planting hole. While site preparation by shelterwood cutting leaves a light canopy, reducing temperature extremes and soil water loss through evaporation, the spatial and temporal differences in light exposure on the site increase (JOHNSON *et al.* 2009). The photon flux density (measured with LI-250A, Licor, Bad Homburg, DE) was found to decrease up to 90% depending on Pine crown density and direct shading by stems. On dry and N-deficient stand, small spatial differences in temperature and sun exposure may result in possible advantages or disadvantages affecting the growth and vitality of the planted trees as well as of competition by annual and perennial species. In order to uncover spatial trends, data collection within a 20 x 20 m raster was performed at the stand (cf. 2.1). The spatial variability in light exposure and temperature as well as the variability of soil N-content did not represent the variability visually distinguishable by differences in ground cover and plant height at the site. The spatial scale of influencing abiotic factors is presumably very small, due to the irregular distribution of shelter trees, undergrowth, natural rejuvenation and topsoil thickness as to provide a representative spatial interpolation. Thus only the direct measurement of plant traits related to photosynthetic performance may provide an adequate mean of integrating multiple abiotic and biotic factors influencing the plants vigour on irregularly structured stands with high spatial variability.

4.2. Monitoring of morphological and chemical leaf traits

Oak leaves from different species are different in shape, size and composition, yet they all are essentially organs utilized for the same function: photosynthesis. They constitute the most important interface between the whole organism and the atmosphere. Having to effectively conduct light capture, CO₂ uptake and transpiration, while simultaneously providing a defence against herbivory and other hazards, adaptations to different environments and climates led to a high diversification (cf. ABRAMS *et al.* 1990, CORCUERA *et al.* 2002). With more than 250.000 different vascular plant species, a handful of key traits (BUSSOTTI & POLLASTRINI 2015) are sufficient to describe the leaves' economics on a global scale (REICH *et al.* 1997, WRIGHT *et al.* 2004). There are major trade-offs in the amount of invested carbon per area of light capture, leaf longevity, resource allocation and maximal photosynthetic rate in environments with different water supply and climatic seasons (REICH *et al.* 1997, LARCHER 2003, WRIGHT *et al.* 2004). The *Quercus* taxa, studied in the context of this thesis vary in their natural species distribution, having adapted to a Mediterranean and temperate climate, leading to diverse leaf morphologies as well as to differences in leaf life strategies and nutrient/biomass allocations. Monitoring the establishment of these possible future forest trees in Central Europe for the first time, knowledge is needed on the interspecific differences of key leaf traits, their seasonal variability and their possible effect on the radiometric estimation of pigment- and nitrogen contents, as well as on the functionality of primary photochemistry.

The investment of carbon per surface of light capture is quantified by the ratio of (oven dried) leaf mass to projected leaf area (Leaf mass per area, LMA_{DW}) or its inverse (specific leaf area, SLA_{DW}) (PÉREZ-HARGUINDEGUY *et al.* 2013). The ratio is a key trait in leaf economics (REICH *et al.* 1997, WRIGHT *et al.* 2004) and in combination with the leaf dry matter content (LDMC) was found to be the best trait for plant functional screening (ROCHE *et al.* 2004, POSSEN *et al.* 2014). A high LMA_{DW} [synonym for specific leaf mass SLM (HUNT & COOPER 1967) and leaf specific mass LSM, that was described as “sclerophyllous character” by Stocker 1931 (LARCHER 2003) or termed “degree of sclerophylly”(MÜLLER-STOLL 1947)] is associated with a higher allocation of biomass to structural components of the leaf rather than metabolites (REICH *et al.* 1998), increased leaf longevity (WRIGHT *et al.* 2004), increased leaf toughness

Discussion

(STEINBAUER 2001), increased drought tolerance (BUSSOTTI *et al.* 2015), increased thermotolerance (ZHANG *et al.* 2012) and decreased photosynthetic capacity per unit leaf nitrogen (REICH *et al.* 1998, WRIGHT *et al.* 2004). SLA_{DW} was found to decrease in all species during leaf development and maturation until reaching a constant value (cf. Figure 12). In the developmental phase, the leaf is a carbon sink (THOMAS & OUGHAM 2014) and decreasing SLA_{DW} values are due to the subsequent build-up of leaf structural tissue (increasing LDMC). At mid-June (doy 164), the structural leaf development was completed in the deciduous species, while the completion of structural development in *Q. ilex* was still underway. The synchronous leaf development of the deciduous species surprises, since it has been shown that bud break and leaf development vary between species and within provenances of the same species (BUSSOTTI *et al.* 2015). The seasonal development in 2013 does not have to be representative, since temperatures in spring were unusually cold that year (Figure 9), so that bud break was delayed for all species. Earlier bud break and development could lengthen the growth period (cf. 4.4), but on the other side immature leaves are prone to damage by late frost events (BUSSOTTI *et al.* 2015). In this matter, the evergreen *Q. ilex* has an advantage over the deciduous species, since previous year leaves can be photosynthetically active in spring without being susceptible to late frost damage.

In the comparison of morphological leaf traits, evergreen and semi-evergreen *Quercus* taxa are characterized by a low SLA_{DW} and group together (Figure 13). Leaf longevity however is not the only factor contributing to the ratio of leaf area to dry weight, otherwise SLA_{DW} would be resembled by two groups only: long-lived and winter-deciduous. *Q. robur* and *Q. rubra* with the highest latitudinal natural distributions show the highest values of SLA_{DW} but the transition to the evergreens is stepwise along the Mediterranean deciduous species and significantly different between taxa. The variability in SLA_{DW} quantified by the standard deviations of the mean for all matured leaves was small, despite of the random sampling from a pool of 168 trees per species. This shows the highly specified adaptations in morphological leaf traits inherited by the species, despite being exposed to the same climatic and edaphic conditions. However, the mass to area ratios were also found vary greatly within the same species grown at different environments, indicating a certain amount of phenotypic plasticity, despite their strong genetic basis (CASTRO-DIEZ *et al.* 2000).

RAMIREZ-VALIENTE *et al.* (2010) found a 2,8% difference of SLA_{DW} and 28% for total leaf size in response to annual climate in *Q. suber* seedlings. BUSSOTTI *et al.* (2002) observed up to 24% difference in LMA_{DW} between *Q. ilex* at sites with different water availability. Phenotypic plasticity is an important trait for the selection of future forest species, by being able to respond to a changing climate in its range of genetic possibilities (BUSSOTTI *et al.* 2015). A comparison of values obtained from different studies is however challenging, since protocols of measurement vary (GARNIER *et al.* 2001, RYSER *et al.* 2008, PEREZ-HARGUINDEGUY *et al.* 2013). The water status of leaves can vary diurnally, especially on warm summer days, affecting obviously fresh weight measures, but also measures of leaf area (GARNIER *et al.* 2001). GARNIER *et al.* (2001) therefore recommends the use of saturated fresh weight for taxa with $SLA_{DW} > 10$ [$m^2 kg^{-1}$] when species are compared (includes all deciduous *Quercus* taxa), but oversaturation in the rehydrating progress, where water enters i.e. intercellular air spaces, may also lead to errors (RYSER *et al.* 2008). Hence, the measurement protocol used for the determination of morphological leaf traits (cf. 2.2), utilizing the rehydrated fresh weight, may be most beneficial in the interspecific comparison of *Quercus* leaves at different points of time in the growth period.

Two factors controlling SLA_{DW} are LDMC and leaf thickness, which can each contribute to a different degree (WITKOWSKI & LAMONT 1991). LDMC is increasingly used as an indicator of plant species' resource use strategy, because of its position in the trade-off between assimilation and growth on one side, and conservation of resources within tissues at the other (VAIERETTI *et al.* 2007). With leaf thickness (LT) on the other hand, being an important leaf trait in terms of i.e. optical leaf properties and physical leaf strength (PEREZ-HARGUINDEGUY *et al.* 2013), measurement is not straight forward. The small dimension, hairs and veins make LT difficult and time consuming to measure accurately. A promising estimate of LT was found in LMA_{FW} (VILE *et al.* 2005) with a global dataset and was confirmed herein for the studied *Quercus* taxa (Figure 14). LMA_{FW} might prove to be a good reflection of the actual average thickness over the whole leaf blade (WHITE & MONTES 2005), since it was found to be proportional to leaf thickness with no interspecific differences in pF, which is commonly assumed to be ~ 1 (PEREZ-HARGUINDEGUY *et al.* 2013). A lower SLA_{DW} will be accompanied by greater LT but similar LDMC when extra cells have similar proportions, however, LDMC and

Discussion

LT will be greater when cells are more numerous in the densest tissues (CASTRO-DIEZ *et al.* 2000). LT and LDMC actually contribute to SLA_{DW} to different degrees in the studied *Quercus* taxa, which was apparent in the different order when sorted by value (Figure 13). A demonstrative example poses the hybrid *Q. x hispanica*. Not significantly different in SLA_{DW} to its evergreen parental species *Q. suber*, the hybrid showed the highest LT (estimated by LMA_{FW}), but a medium value of LDMC, comparable to its deciduous parental species *Q. cerris* (cf. Figure 13). The confirmation of the strong correlation between LT and LMA_{FW} in *Quercus*, offers an additional information insight to leaf strategy, with no change in the leaf trait measuring protocol as developed in this study. Knowledge of the seasonal variability of morphological leaf traits, due to the subsequent build-up of dry weight in the sink phase of the leaves is important, when other traits, like pigment- or nitrogen contents, are to be calculated on a leaf mass base.

Chlorophylls and carotenoids are the most abundant pigments in leaves and their breakdown can be an early indicator of environmental stress (HENDRY & PRICE 1993, HÖRTENSTEINER & KRÄUTLER 2011). The total concentration of leaf Chl alone has been used as an estimation of tree vitality (PERCIVAL *et al.* 2008). Cars are vital for the photochemical apparatus and are associated with light harvesting, photoprotection via the quenching of Chl triplet states, singlet oxygen scavenging, excess energy dissipation and structure stabilization (DEMMIG-ADAMS *et al.* 1996, FRANK & COGDELL 1996). Changes of environmental conditions can change carotenoid composition, their total content and its ratio to the total amount of Chl (PEÑUELAS & FILELLA 1998, DEMMIG-ADAMS *et al.* 2012). Likewise, the ratio of Chl a to Chl b (a/b) can be altered in the response to shading and may also function as an early indicator of senescence (BROWN *et al.* 1991). Therefore, one of the most frequently used techniques to measure the degree of abiotic stresses and to follow the time course of senescence is the quantification of chloroplast pigment contents and their ratios (PINTÓ-MARIJUAN & MUNNÉ-BOSCHE 2014). The pigment contents and their ratios were determined for *Quercus* species with contrasting leaf life strategy and morpho-anatomy over the course of the whole leaf life span to identify possible species-specific alterations or adjustments to environmental or developmental phases, which could influence the use of non-invasive optical pigment estimations.

While autumnal senescence is the most often perceived event of pigment degradation through leaf yellowing and colour change at the end of the temperate zones' growing season, several abiotic stresses may lead to a loss of photosynthetic pigments, without being an initiator of senescence (PINTÓ-MARIJUAN & MUNNÉ-BOSCHE 2014). In this context, the ratio of Chl/Car was previously used to distinguish between senescence and abiotic stresses since the kinetics of Chl and carotenoids loss can be strongly altered depending on the stressor (HENDRY & PRICE 1993). Apart from senescence and stress, the total pigment contents, the Chl a/b and Chl/Car ratio can be modified by developmental and environmental factors such as local light environment and nutrient availability (LICHTENTHALER 1987, TERASHIMA & HIKOSAKA 1995, LICHTENTHALER *et al.* 2001, KITAJIMA & HOGAN 2003). KITAJIMA & HOGAN (2003) observed differences in Chl content and Chl a/b ratio in seedlings grown under high ($\sim 1100 \mu\text{mol m}^{-2} \text{s}^{-1}$) and low ($\sim 100 \mu\text{mol m}^{-2} \text{s}^{-1}$) light conditions. Additionally, the light intensity had an effect on the relationship of Chl to nitrogen and significant interspecific variability was noted in the relationships. The difference in light quality through shading of a dense canopy can also result in contrasting leaf types (sun and shade leaves) with different pigment composition and ratios (LICHTENTHALER 1987, TERASHIMA & HIKOSAKA 1995, LICHTENTHALER *et al.* 2001). The re-acclimation of sun leaves overgrown and subsequently shaded can again lead to changing Chl a/b and nitrogen contents (TERASHIMA & HIKOSAKA 1995). The constant value of $4,19 \pm 0,58$ ($m \pm \text{SD}$; $n=362$) for the Chl/Car ratio observed in non-senescent *Quercus* leaves (cf. Figure 15), resembles the values reported for sun leaves with sun chloroplast in *Fagus sylvatica* by LICHTENTHALER *et al.* (1987, 2001). The values for the Chl a/b ratio ($3,28 \pm 0,44$) corresponds to values of sun leaves as well. Shade leaves have been associated with lower values of Chl a/b and higher Chl/Car ratios compared to sun leaves (LICHTENTHALER 1987, LICHTENTHALER *et al.* 2001), resulting from biochemical acclimation to the differences in light quality. The light gradients by leaf shading could not have been as strong as to considerably change the light quality to such a degree that pigment alterations were induced, leading to the sun leaf characteristics in all leaves.

Discussion

Despite the spatial variability in light and soil nutrient status of the sampled plots (cf. Figure 10), the large seasonal time span of sampling and large interspecific differences in leaf life strategies mentioned above, the ratios of Chl a/b and of Chl/Car were highly linearly correlated in the monitored *Quercus* species over a large range of Chl values (cf. Figure 15 & Figure 16). No deviations of these strong correlations were found in the absence of autumnal leaf senescence that could be attributed to any abiotic stress, despite the occurring dry and hot periods during the season (cf. Figure 9).

All pigment ratio alterations observed at the monitoring campaign were attributed to autumnal senescence, which does on the other hand not exclude the fact that stressful conditions might have led to an earlier onset of this final leaf stage in individual trees. The Chl/Car ratio declined rapidly at Chl concentrations of approx. 100 mg m⁻². ADAMS *et al.* (1990) observed a similar threshold in *Platanus occidentalis* leaves during senescence (~150 mg m⁻²), which was accompanied by a marked decline of O₂ evolution on area basis preceded by a minor decline of Photosynthesis due to the total Chl loss. Changes in the Chl a/b ratio were observed in the *Quercus* taxa only at a late stage of senescence at very low Chl contents (~ 50 mg m⁻²). The same threshold was observed by ADAMS *et al.* (1990) in two subsequent years, indicating that the total Chl decline is a well regulated process with a parallel loss of PSII and PSI (ADAMS *et al.* 1990, MIERSCH *et al.* 2000) until the threshold is reached. In connection with the changing ratio of Chl a/b, impediments of the electron transfer beyond Q_A were observed by HOLLAND *et al.* (2014), which were assigned to changes in the ratio of PSII to PSI. BROWN *et al.* (1991) stated that the Chl a/b ratio could be used as an early indicator of senescence. This is obviously not the case for *Quercus* under the monitored conditions, where senescence was indicated by an earlier decline in total Chl content, and changes in the a/b ratio occurred at an advanced stage of senescence (cf. Figure 16).

Strongly associated to the chlorophyll content is leaf nitrogen (N) (cf. Figure 17). Nitrogen is an abundant element in living organisms (fourth after C, O and H) and a limiting factor for plant growth and development (LARCHER 2003, TAIZ & ZEIGER 2010, BALAZADEH *et al.* 2014). Leaf nitrogen was found to be (amongst others) correlated with mass based maximum photosynthetic rate, leaf life span and SLA_{DW} (EVANS 1989, HIKOSAKA & HIROSE 2000, PEREZ-HARGUINDEGUY *et al.* 2013). In photosynthetically active leaves, the major part of N (~80%) is bound in chloroplast proteins with Rubisco

representing the largest N storage (KANT *et al.* 2011). When N supply is limited, plants have to economize this valuable resource, with a negative consequence on Rubisco activity and light absorption through chlorophylls (LARCHER 1994, REICH *et al.* 1998, MORALES *et al.* 2006). N limitation has been associated with an earlier onset of leaf senescence (ADICOTT 1968, LARCHER 2003). The correlation of chlorophyll- and nitrogen contents has often been used to assess the leaf nutritional status through the much easier chlorophyll estimation (i.e. PINKARD *et al.* 2006, PERCIVAL *et al.* 2008, DJUMAEVA *et al.* 2012, UCHINO *et al.* 2013). The leaf nitrogen content is typically measured with samples of dried and pulverized leaf tissue and therefore displayed in mass units of dry weight or percent of dry leaf weight [%_{DW}] (PEREZ-HARGUINDEGUY *et al.* 2013). Typical ranges reach up to 3% in leaves of broadleaved trees and up to 2% in leaves of sclerophyllous species (LARCHER 1994). An impairment of leaf photosynthetic processes has been reported for leaves with foliar N contents below 1,5% of dry weight in *Q. robur*, *Acer pseudoplatanus* and *Fagus sylvatica* (PERCIVAL *et al.* 2008). Since leaf dry matter content (LDMC) varied seasonally and between species (cf. Figure 12 & Figure 13), this threshold based on leaf dry weight cannot be generalised. The difference becomes apparent when correlating leaf Chl (a+b) [mg m⁻²] and leaf N [%_{DW}] of the deciduous and evergreen oak species (cf. Figure 17). Over a wide concentration range, the N content is lower in the evergreen *Q. ilex* compared to the deciduous oak taxa (Figure 17 A). The seasonal development of dry weight influences the relationship at low Chl concentrations. By converting the leaf nitrogen content per dry weight with SLA_{DW} to an area basis, all interspecific differences in the N/Chl relationship vanished, resulting in a linear correlation, which was uninfluenced by morphological traits and seasonal development, showing their close relationship apart from interspecific differences in leaf structural, non-photosynthetic components.

The monitoring and determination of the temporal and interspecific variability of morphological leaf traits, leaf pigment contents with their correlations and alterations and the relationship of leaf nitrogen to total leaf chlorophylls in the different *Quercus* taxa grown under Central European conditions has set the basis to investigate the possibility of optical, non-destructive sensing of these compounds.

4.3. Non-invasive sensing of chemical leaf traits

The leaf chlorophyll content is most accurately measured by extracting the pigments from the tissue in a solvent, followed by in vitro measurement of the solution in a photospectrometer. However, accurate measures of pigment content are not always needed for many applications in agri- and silviculture and approximate contents may be sufficient (VAN DER BERG & PERKINS 2004). This is especially true, when time series measurements are needed in monitoring or when sampling material is scarce. The optical, non-destructive techniques, that have become commercially available in recent years, allow sufficiently accurate measurements and quantify subtle changes in pigment content before being visible (RICHARDSON *et al.* 2002). In this section, the absolute/optical chlorophyll relationships of the *Quercus* taxa in this study are reviewed and possible sources of variability are discussed.

Aside from the SPAD-502 chlorophyll meter, which has been used in this work and in the majority of studies published, four other chlorophyll meters (not considered in this study) are on the market using the same principle of measurement. These are the CCM-200 (Opti-Sciences Inc, Hudson, USA; measuring wavelengths (mw): 653 nm/931 nm), CL-01 (Hansatech Instruments Ltd, King's Lynn, UK; mw: 620 nm/940 nm), AtLEAF (FT Green LLC, Wilmington, USA; mw: 660 nm/940 nm) and Dualex (Force-A, Orsay, FR; mw: not specified). As mentioned above, the SPAD-502 is the market leader followed by the CCM-200, evaluated on the basis of published articles (cf. PARRY *et al.* 2014). The Force-A Dualex is a development of the French CNRS (Centre National de la Recherche Scientifique) and allows the additional measurement of leaf flavonoids by the measurement of light transmittance at 375 nm. The chlorophyll meters listed above use the absorption maxima of chlorophyll a and chlorophyll b in the red light spectrum, where the signal cannot be distorted by changes in carotenoid content, since carotenoids absorb light not further than 550 nm (LICHTENTHALER 1987). Therefore all estimations regarding the carotenoid content derived from chlorophyll meter readings depend on the strong correlation of chlorophylls to carotenoids (cf. Figure 15). To account for differences in leaf morphology like tissue thickness, a reference wavelength at NIR is measured by all chlorophyll meters, where no Chl absorption is expected. The calculations of the meter's output value vary from meter to meter and include confidential coefficients

(PARRY *et al.* 2014), leading to major differences in the output value. Despite of the reference wavelength at NIR, to account for differences in leaf morphology, variations of absolute/optical Chl values between different species have often been reported (i.e. YAMAMOTO *et al.* 2002, COSTE *et al.* 2010, SILLA *et al.* 2010, PARRY *et al.* 2014). These differences have, among other reasons, been associated with changing leaf optical properties due to differences in leaf morphology (i.e. MONJE & BUGBEE 1992). YAMAMOTO *et al.* (2002) ascribes the differences found in *Sorghum* and *Cajanus* to differing LT and LMA_{DW} and NIGAM & ARUNA (2008) found a negative correlation of SPAD values with SLA_{DW} in *Arachis hypogaea*. MARENCO *et al.* (2009) observed correlations of SLA_{DW}, LT, LWC_{FW} and LMA_{FW} with SPAD values in a comparison of 6 amazon tree species. Adding LMA_{FW} (proxy for LT; cf. Figure 14) to the correlation equation of an all species model, SILLA *et al.* (2010) were able to achieve better model fitting with different *Quercus* species, measured with the CCM-200. Leaf age was also reported to influence the absolute/optical Chl relationship in *Quercus* by SILLA *et al.* (2010), due to potential seasonal variations in morphological traits, changes in irradiance and chloroplast movement. Changes in leaf water status and diurnal variation in irradiance were found to affect SPAD-measurements in maize plants (MARTINEZ & GUIAMET 2004). NAUŠ *et al.* (2010) report up to 35% differences in SPAD values due to chloroplast movement, when *Nicotiana tabacum* plants were transferred from growth light (70 $\mu\text{mol m}^{-2} \text{s}^{-1}$) to higher blue light (340 $\mu\text{mol m}^{-2} \text{s}^{-1}$).

If the absolute/optical chlorophyll relationship was highly variable and correlation equations were needed to be constructed multiple times to cover a large number of influencing factors, the use of the surrogate measure would be rather impractical and the benefits of the method largely reduced. If additional, morphological information was essentially needed for every leaf that was sampled, the benefit of the non-destructiveness would also have vanished, placing the accurate chlorophyll determination by traditional extraction methods in favour. Relating the absolute Chl concentrations to the optical SPAD readings, the influence of the base of reference became apparent. When the absolute chlorophyll content was based on fresh weight, dry weight or volume, there was an interspecific difference in the relationship due to differences that were attributed to the morphological leaf traits (see Figure 18). Another discrepancy appeared in the relationship of SPAD readings with chlorophyll content

Discussion

based on sample dry weight. There are two time intervals in the growing season, when chlorophyll concentrations are low: At leaf development, when the chlorophyll content was slowly increasing and at autumnal senescence, when the chlorophyll content was decreasing. On the other side, if the seasonal variation in SLA and LDMC is considered, the leaf dry weight was low at leaf development and reached a plateau value at the end of development. The dry weight was not decreasing at leaf senescence. Therefore, two groups could be distinguished at low SPAD values, one with leaves from the beginning and one with leaves from the end of the growth period. In this case, the seasonal variability of the leaf dry weight had a pronounced effect on the absolute/optical Chl relationship. The same pattern was observed at the relationship of leaf nitrogen to leaf chlorophylls, when the nitrogen concentration was not corrected by SLA_{DW} (see Figure 17). PENG *et al.* (1995) noted, that variations in N[%] in different growth stages and varieties of rice resulted mostly from differences in LT and SLA_{DW} . Also PENG *et al.* (1993) and UCHINO *et al.* (2013) stated that the addition of LMA_{DW} or SLA_{DW} , respectively, improved the correlation of the SPAD-value with N [%] obtained in different seasons and growth stages. These confounding effects could be eliminated when foliar concentrations were expressed on a leaf area basis (BALASUBRAMANIAN *et al.* 2000). Thus, the influence of leaf morphological traits on the relationship of SPAD-values to Chl and N was not due to changes in the optical properties of the sample, but due to the reference base of the measured component. The reference wavelength in the near infrared (NIR) spectrum is a feature of all the different chlorophyll meters on the market, which make use of the principle of light transmittance through the leaf sample. The transmission of NIR is not influenced by chlorophyll and is therefore primarily determined by non-chlorophyll compounds (PARRY *et al.* 2014). These non-chlorophyll compounds (primarily cell-walls) absorb red and NIR radiation similarly. With the relation of emitted and absorbed amounts of the red and NIR radiation in the intrinsic calculation of the SPAD-value, light absorbed by compounds other than Chl are excluded (MONJE & BUGBEE 1992, PARRY *et al.* 2014). This leads to a relationship between the optically sensed- and destructively quantified (absolute/optical) compound concentrations without interspecific or seasonal variability as observed with an area base reference (Figure 18 D).

When the chlorophyll content was based on leaf area, the relationship was curvilinear, as proposed by MARKWELL *et al.* (1995) and RICHARDSON *et al.* (2002). According to the Beer-Lambert law, the relationship between the *in vivo* and the *in vitro* measurements would be linear, if the absorbance was solely dependent on the pigment concentration (MONJE & BUGBEE 1992). A linear absolute/optical Chl relationship has been observed in some cases even when leaf area was used as the base of reference (i.e. DWYER *et al.* 1991, MADEIRA *et al.* 2003, RUIZ-ESPINOZA *et al.* 2010). This observed linearity can be an effect of a small range of values, missing SPAD-values of the lower range or of a small sample size. PARRY *et al.* (2014) argue that the SPAD-values are linearly correlated to chlorophyll concentrations only if the uniform distribution of chlorophyll is assumed. But chlorophyll is not uniformly distributed in the leaf (FUKSHANSKY *et al.* 1993). Spatial variability is found in cells within tissue layers, chloroplasts within cells and in the structural organization of grana within chloroplasts (FUKSHANSKY *et al.* 1993). Thus the transmission of light through a leaf is not only affected by the concentration of chlorophyll but also by its spatial distribution, which leads to deviations from linearity (UDDLING *et al.* 2007). The non-uniform distribution of Chl increases with increasing Chl content, leading to higher relative amounts of transmitted radiation compared to a uniform Chl distribution, because the efficiency of red light absorbance increases with uniformity (PARRY *et al.* 2014). With this so called “sieve effect” (RABINOWITCH 1951), optical measurements are relatively lower (Chl concentrations [mg m^{-2}] would be underestimated), leading to the curvilinear rise (with SPAD-values on the x-axis; cf. Figure 19) in the absolute/optical Chl relationship at SPAD values higher than approx. 20 (MONJE & BUGBEE 1992; MARKWELL *et al.* 1995, RICHARDSON *et al.* 2002; UDDLING *et al.* 2007; MARENCO *et al.* 2009; PARRY *et al.* 2014). If transposed (SPAD-values on the y-axis), the curves would resemble the Lambert-Beer curves at high concentrations (deviation from linearity); the effect of underestimation is however, stronger due to the “sieve effect”. This effect may also influence the higher variability at higher Chl concentrations, which can be observed in the data, since there is an increase in chlorophyll density in chloroplasts rather than an increase in the number of chloroplasts (TERASHIMA & SAEKI 1983). RICHARDSON *et al.* (2002) indicate that at high Chl concentrations, the total amount of transmitted red light is markedly decreased, resulting in greater error. In this regard, Konica Minolta states that with SPAD-values above 50 less accuracy has to be expected (User-Manual SPAD-

Discussion

502, Konica Minolta, Osaka, JP). With the CCM-200, this effect in combination with the larger sampling window may have led to the differences in the best-fit model parameters of different *Quercus* species and leaf ages noted by SILLA *et al.* (2010), since deviations at high Chl contents are markedly higher at the CCM-200 compared to the SPAD-meter (CEROVIC *et al.* 2012). The spatial distribution of Chl is however not static, and can be affected by chloroplast movement, (NAUŠ *et al.* 2010), which may lead to substantial reading differences. However, the amount of Chl movement seems to be correlated with the cell diameter, resulting in greater restriction on Chl movement in narrow, more columnar cells of sun leaves in comparison to shade leaves (DAVIS *et al.* 2011). In *Quercus*, no diurnal variability in SPAD-values was observed (cf. Figure 23). Another source of potential heterogeneity in Chl distribution are leaf veins (MONJE & BUGBEE 1992, UDDLING *et al.* 2007). Concerning veins, the smaller sampling size window of the SPAD-502 compared with the CCM-200 is an advantage, but the inclusion of veins in the measurement cannot be avoided, especially with small leaves as in *Q. ilex* and *Q. suber*.

At SPAD-values lower than approx. 20 the “detour effect” may lead to a lower transmission due to light scattering by cell wall components, artificially increasing the optical readings at low chlorophyll contents (UDDLING *et al.* 2007; PARRY *et al.* 2014). This can result in y-axis intercepts of the absolute/optical Chl relationships higher than zero (cf. Figure 19). Different Chl distribution patterns and therefore differing “sieve” and “detour” effects (and not differences in leaf morphology), are accounted responsible for the observed interspecific differences found in the literature (UDDLING *et al.* 2007, PARRY *et al.* 2014). For prediction purposes, a mathematical model has to be fit to the data points in order to derive unknown absolute Chl values from known Chl meter readings. As indicated above linear and non-linear regressions have been used for this purpose by various authors with partly large variability among absolute/optical Chl relationships even with similar species. Apart from the differences in non-uniform distribution of Chl and the resulting “sieve” and “detour” effects, sources of variability can include variability among chlorophyll-meters of the same type, and differences in the determination of the absolute Chl concentrations. PARRY *et al.* (2014) found low variability between 5 different SPAD-meters (mean coefficient of variation: 1,10% for SPAD-meters developed between 1992 and 2008) and higher variability between 25

CCM-200 (2,6% for CCM-200 meters manufactured between 2007 and 2013), especially at high readings. The use of different extraction methods, extraction solvents, Chl concentration equations and varying resolution of spectrometers are seen as the main source of variability among absolute/optical Chl relationships and their correlation equation coefficients in the literature (PARRY *et al.* 2014). This has to be kept in mind, when the correlations equations are used for prediction purposes.

Two mathematical models for the empirical fit of the curvilinear SPAD/Chl relationship are generally used, namely an exponential and a second order polynomial regression. DEMAREZ *et al.* (1999) and COSTE *et al.* (2010) proposed a model supposedly superior to the exponential (EXP) and polynomial (POLY) model named “homographic model” (HOMG). MARKWELL *et al.* (1995) justified the use of the exponential model for limited data sets, since it forces a more appropriate fit than the polynomial model. The absolute/optical Chl relationship of the *Quercus* taxa in this study was not fitted well by the exponential model due to pronounced deviations at low chlorophyll contents. The POLY and HOMG model fitted the data points over the whole range and coefficients of determination of up to 0,958 were attained. Figure 19 shows how similar these two models fit the data, especially in the SPAD range from 10 to 50. The HOMG model underestimates the SPAD-values below 5 in contrast to the trend in the data, which is better represented by the POLY model in that region. The models deviate from each other at SPAD-values above 50, outside the range of observed values. Nevertheless, the HOMG model’s slope increases more, following the trend of the data in that region. A statistical model comparison, taking into account the goodness of fit and the model’s complexity (Akaike Information Criterion, GraphPad PRISM 5.04), favours the HOMG model since it is simpler, but Table 5 shows how close the R² as well as the root mean square errors are. Comparing the single species versus the global model favoured the species-specific models. Figure 20 displays the deviations of the models and their 90% prediction intervals. In some cases the low range of measured values (i.e. for *Q. suber*; Figure 20 G), high variability at high chlorophyll contents (i.e. *Q. x hispanica*; Figure 20 H) and low number of data points in a specific range (*Q. x turneri*; Figure 20 I) result in different equation coefficients, leading to deviations of the curves from the all-species curve (or global model) at SPAD-ranges that are not well represented by data (see MARKWELL *et al.* 1995). Hence, the global all-species

Discussion

model is preferred over the species-specific for prediction purposes of absolute Chl contents in *Quercus*. The same applies to the relationship of SPAD-values to leaf nitrogen content (on leaf area basis, Figure 22), where the single-species models are usually nested within the 90% prediction intervals of the all-species model (since the correlation of SPAD/N is not as strong as SPAD/Chl). The strong correlations of leaf nitrogen to leaf Chl, carotenoids to Chl and Chl a to Chl b across the diverse taxa of *Quercus* observed during the growing season (Table 6 & Table 7), in combination with the exclusion of non-chlorophyll compounds by the use of red and NIR wavelength of the optical Chl-meter, with the knowledge about possible sources of variation, allow reliable estimates of area-based concentrations and interpretations of relative value alterations under field conditions for further monitoring purposes. Since all leaf samples showed characteristic pigment compositions of sun leaves, the transferability to leaves shaded by a dense canopy cannot be given without further research. When possible, south-faced, unshaded leaf samples should be taken, when major differences in light quality are expected to influence the pigment composition of the leaves and thus the relationship between SPAD- meter readings and indirect measures.

The investigation of the absolute/optical Chl relationship in *Quercus* was supplemented with observational measurements on the spatial and temporal variability, concerning the applicability of the method in the field. The spatial variability of SPAD readings on a single leaf blade was found to be low (1-3 units, mean ~1,5 units), confirming the findings of LICHTENTHALER *et al.* (2002) on the low spatial variability of Chl and Cars per leaf area (<3%). This range needs to be considered, when repeated measures on the same leaves are made to monitor seasonal or stress dependent alteration of the pigment content. The Chl content of different leaves of the same tree was found to be surprisingly low (SD in a range of 2-4 SPAD units), calculated from 10 measurements per tree on 781 trees, important for repeated measurements on trees, when measurements cannot be performed on the same leaf, due to experimental circumstances. This may change however, when self-shading develops with age and leaves develop sun and shade characteristics (LICHTENTHALER *et al.* 2001, DAVIS *et al.* 2011). Between the species, the Chl content per leaf area was found to be significantly different, independent on tree location at the site. Thus, the dimension of a Chl reading has to be placed in the context of values observed for the species. If a SPAD value of 40

was found to be rather exceptionally high in *Q. rubra*, the same value would be considered exceptionally low for *Q. ilex* (e.g. Figure 25). Spatial investigations of leaf greenness (Figure 26) including different species, therefore demand normalisation procedures. The normalisation of mean tree SPAD values may be calculated through the species mean SPAD value of the sampled population, to visualize deviations in leaf greenness in response to abiotic site factors like light exposure or soil N content (normalised chlorophyll content index NCCI, 2.3.1 & Figure 26). Diurnal fluctuations of SPAD-readings as observed by NAUŠ *et al.* (2010) were not found (Figure 23), despite of strong irradiance and high temperatures at the day of measurement. Variations observed were in the range of repeated measures on the same leaf blade, as described above. Deviations from this range in the context of temperature were found only at low, sub-zero temperatures. SPAD-readings were observed to be increased at air temperatures below -4°C (Figure 24). Variations in SPAD-readings at these temperatures may be artificial, due to changes in infrared transmission, changes in the ratio of transmission to reflectance, changes in the spatial distribution of chlorophyll (increased sieve effect), or a relative increase of Chl per area due cell dehydration by ice formation (BALL *et al.* 2002). LARCHER (2000) noted that leaves of *Q. ilex* started to freeze at -4 to -5°C , accompanied by ice formation in intercellular spaces with dehydration occurring as a result of the intercellular water migration towards the ice formed in the apoplast and the extracellular spaces.

The optical measurement of Chl content by means of the SPAD meter was found to be very applicable under field conditions, with no influence of time of day, irradiance, unstressed water status, leaf morphology or leaf temperature (except on frozen leaves) and a high repeatability in the studied *Quercus* taxa. The method is therefore suitable for the comparative, non-invasive determination of Chl and nitrogen contents in the field, tracking developmental or stress induced alterations of light harvesting capacity (i.e. nutrient limitation, timelier or accelerated senescence) of native and introduced *Quercus* taxa with contrasting morphological leaf traits under Central European conditions.

4.4. Seasonal monitoring of chlorophyll content and PS II functionality

The monitoring of the temporal variability of chlorophyll content and PSII functionality at the leaf level allows the comparative assessment of possible advantages of one species as compared with other species at a given site and provides reference data for the distinction between developmental and stress induced alterations. In a discussion about possible species-specific advantages or beneficial traits, it is important to not only consider plant fitness at a single point in time, but also to have information on the seasonal dynamics of parameters that estimate plant fitness. The chlorophyll content, as an estimator of the plant's light harvesting capacity and the fluorescence parameters F_v/F_m and PI_{abs} used for the estimation of the quantum yield of primary photochemistry and energy conservation to the reduction of the intersystem electron acceptors, followed three distinct stages during the growth period in all investigated species: a rise in spring during leaf development, a steady state phase with little change in parameter value and a subsequent decline in late summer and autumn (Figure 28 & Figure 30, except in the evergreen *Q. ilex*, for which no decline was observed). It has to be considered that the seasonal monitoring of chlorophyll contents and Chl fluorescence discussed below refer to the first flush only. Since leaf growth in *Quercus* is episodic, a second flush (or even a third) may occur during the season, from which the described phases and rates may differ

A significant surplus of carbon for above- and belowground growth and storage can only be produced in green leaf tissue, thus the time interval for carbon gain is restricted to the time between budbreak and leaf abscission in deciduous species. Higher leaf chlorophyll contents facilitate higher potential energy uptakes per time and thus higher potential performances. But not all of the light energy harvested by Chl, can be used for photosynthesis. The efficiency of electron trapping and electron transport regulate the effective use of absorbed light and the amount of energy dissipated by non-photochemical pathways. F_v/F_m and the Performance Index PI_{abs} , quantify the maximal possible uptake and use of absorbed energy by the chlorophylls. With the maximal possible light harvesting and energy conversion capacity in mind, plants in competition for resources at a site may benefit from early budbreak, fast photosynthetic leaf maturation, a late begin of senescence and/or a slow rate of decline of chlorophyll content and PSII functionality on the leaf level.

The time of budbreak of the first flush is sensitive to the non-variable photoperiod (KÖRNER & BASLER 2010). On the one hand it is genetically controlled and differs between *Quercus* provenances planted on the same site (BUSSOTTI *et al.* 2015), but on the other hand it shows a certain amount of plasticity, influenced by variable factors like temperature in winter and spring (BUSSOTTI *et al.* 2015). Trees of provenances with climates, in which phenological tracking of temperatures bears a smaller risk of injury might be less sensitive to the photoperiod and thus more likely to track temperature changes in spring (KÖRNER & BASLER 2010). *Q. robur* is considered a late leafing species (SPARKS & CAREY 1995) but the other investigated *Quercus* species did not significantly differ in the timing of budbreak from *Q. robur* at the FR site (except for *Q. ilex*). At Oxfordshire in South England, MORECROFT *et al.* (2003) reported budbreak for *Q. robur* between mid-April and the beginning of May (doy 102-121; 1996, 1999 and 2000). In southern Hesse, BOTH & BRÜGGEMANN (2009) observed budbreak in solitary and mature *Q. robur* at doy 110 and 123 (2006 and 2007). A warming climate with increased springtime temperatures could promote earlier budbreak (KOVATS *et al.* 2014, KÖRNER & BASLER 2010). Phenological records since 1950 indeed show a tendency for increasingly earlier leaf development in *Q. robur* (0,12 days per year for record from 1951-1996; MENZEL 2003), especially during the last two decades (SCHLEIP *et al.* 2011). As stated above, earlier budbreak may provide a competitive advantage,

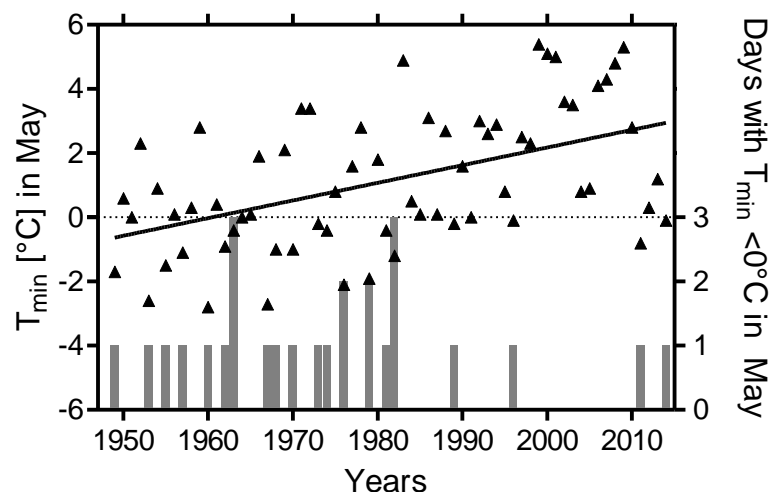


Figure 50: Historical record of late frost events at Frankfurt. Minimal temperature (T_{\min}) in the month of May as black triangles, fitted by linear regression. Days with T_{\min} lower than 0°C in May symbolized by grey columns. Record from DWD station 1420 Frankfurt airport for the years 1949 until 2014.

Discussion

primarily because light intensity and day length peak at late June (summer solstice at June 21st) and decrease subsequently leading to similarly decreasing daily potential photosynthetic carbon uptakes (MORECROFT *et al.* 2003). On the other hand, late frost events in May pose a serious threat to the developing tissue and can lead to damage or even total loss of the flush. Despite of a tendency to rising minimal temperatures and a decrease in the frequency of late frost events in early spring at Frankfurt (Figure 50), late frost events still occur and can have a devastating effect. The late frost event in May 2011 after leaf development (locally to -10°C) caused massive leaf damage in German forest trees and reset spring development by leaf greening by 7-9 weeks (KREYLING *et al.* 2012). *Q. ilex* can make use of favourable conditions in early spring with its previous year leaves, (if they were not damaged by extremely low temperatures <-20°C) which are not susceptible to late frost. Budbreak may occur later than in the deciduous species as observed at the FR site in 2013 and by BOTH & BRÜGGEMANN in 2007 (delayed 20 days compared to *Q. robur*) and thus avoiding late frost damage on immature leaf tissue. On the same trees, however, BOTH & BRÜGGEMANN (2009) observed a difference in budbreak between *Q. robur* and *Q. ilex* of only 3 days in spring 2006. Therefore, an evergreen leaf life strategy is not by itself a warrant for late frost resilience.

Leaf development after budbreak in spring as well as the previously occurring stem growth (~10 days before budbreak; BARBAROUX & BRÉDA 2002), rely entirely on surplus reserves, stored during the previous year growing season (LACOINTE *et al.* 1993, BARBAROUX & BRÉDA 2002) until a positive carbon balance is reached in the developing leaves (~11 days in *Q. robur*; MORECROFT *et al.* 2003). Leaf expansion is relatively fast (~15 days from budbreak to maximal leaf area in *Q. petraea*; BARBAROUX & BRÉDA 2002) and less variable than the speed of leaf maturation (MIYAZAWA *et al.* 1998). The period of leaf maturation is marked by simultaneous increases in leaf dry mass per leaf area, leading to decreasing SLA_{DW}, increasing LDMC and increasing leaf chlorophyll- and nitrogen contents (cf. Figure 12 & Figure 28). The rate of photosynthesis at saturating light intensity increases as well during leaf development and it has been found to reach full capacity with the completion of the structural development (MIYAZAWA *et al.* 1998), which was attained in the mid of June in all deciduous species. Despite of the differences in morphological leaf traits in the Mediterranean *Quercus* species compared to *Q. robur* and *Q. rubra* structural

development was completed at similar points in time (cf. Figure 12). MORECROFT *et al.* (2003) reported a period of up to 70 days for photosynthetic maturation in *Q. robur* in 3 years with different climate, whereas a period of only 30 days was reported under Mediterranean climate conditions by GRASSI & MAGNANI (2005). In *Q. ilex*, the period of dry mass allocation was elongated compared to the deciduous species (Figure 12). MIYAZAWA *et al.* (1998) found that species with a large LMA_{DW} (low SLA_{DW}), which characterizes *Q. ilex* against the deciduous species, also have longer periods of photosynthetic maturation. In the evergreen, the slower rate of maturation is at least in part compensated by the photosynthetically active leaves of the previous year. BOTH & BRÜGGEMANN (2009) report that despite of the slow attainment of full photosynthetic capacity, the light harvesting capacity and electron supply to the Calvin cycle were fully sufficient 7 days after budbreak, with F_v/F_m values $>0,7$. Nevertheless, energy supply exceeded the capacity of energy use by photosynthesis and their capacity for energy dissipation during the day, leading to photoinhibition and decreased midday F_v/F_m values of $<0,4$ one week after budbreak. The slow development of full photosynthetic capacity despite of already sufficient light harvesting capacity was assumed to be related to a low carbon sink strength at spring (BOTH & BRÜGGEMANN 2009), which on the other hand can be influenced by climate (BAUERLE *et al.* 2012). At the FR site F_v/F_m did not increase significantly faster than the morphological leaf traits or chlorophyll contents in the deciduous species, but lowest F_v/F_m values were already above 0,6 in all species at the first time date of measurement in 2013 (doy 137). This difference to the observations of BOTH & BRÜGGEMANN (2009) may be due the fact that measurements were performed predawn on juvenile individuals under a *Pinus* canopy in contrast to mature and solitary standing specimens at midday. In *Q. ilex*, F_v/F_m values reached optimal levels (“excellent” = 0,76-0,83; MOHAMMED *et al.* 2003) earlier than structural maturation and the “end of development” (definition: Figure 5). Even though the steady state level of chlorophyll content had not been reached yet, SPAD values of *Q. robur* and *Q. rubra* at this point in time were already as high as the steady state levels, indicating that photosynthesis was probably not limited by light harvesting. As stated above, an earlier budbreak and faster photosynthetic leaf maturation have a more pronounced effect on the daily potential photosynthetic carbon gain due to increased day length and light intensity than delayed senescence begin in autumn. The potential maximum light harvesting capacity can be sensed and quantified by the chlorophyll

Discussion

content and the recording of the fast Chl a fluorescence transient, but light harvesting and PSII integrity are not the only limiting factors for photosynthetic productivity in spring as BOTH & BRÜGGEMANN (2009) have pointed out.

Analysis of the fast Chl a induction curves reveal a similar fluorescence O-J rise with steadily increasing intensity of maximal fluorescence yield in developing leaves (Figure 32) of all species alike. The photochemical phase (O-J rise), related mainly to the reduction of the primary electron acceptor Q_A and strongly dependent on the number of absorbed photons (STIRBET & GOVINDJEE 2012), was less effected by leaf age than the thermal phase (J-I-P rise, STIRBET & GOVINDJEE 2012). This led to differences in the time resolved double normalized fluorescence yields. The differential V_{OP} curves (ΔV_{OP}) showed a peak at around 1 ms at the first date of measurement (Figure 32 C), which steadily declined and transitioned to a smaller shoulder at ~9 ms as leaves got older. The shapes of the OJIP transients and their change of shape with time during leaf development were very similar to the transients recorded during autumnal leaf senescence (Figure 32 F). HOLLAND *et al.* (2014) observed similar changes in OJIP transients during natural autumnal senescence of different deciduous *Quercus* taxa. The peak at the J-level (~2 ms) is associated with a decrease of Q_A^- re-oxidation, since the disablement of Q_A^- re-oxidation results in maximal fluorescence yield (F_m) at the J-step without influencing the O-J rise (KALAJI *et al.* 2014). A decrease in the rate of Q_A^- re-oxidation can be due to a decreased PQ pool size and/or a reduction of electron transport acceptors in and around PSI (KALAJI *et al.* 2014, SCHANSKER *et al.* 2005). Thus trapped energy is disposed effectively at an early step in the electron transport chain, decreasing the risk of a high electron pressure at times of low photosynthetic capacity. It seems as if not energy absorption, but energy trapping and electron transport are the limiting factors during both photosynthetic leaf maturation and senescence. A difference in the rate of development of the potential light harvesting capacity by increased rate of chlorophyll accumulation does not by itself seem to translate into a competitive advantage of trees or species. Since PI_{abs} is calculated as a function of 3 components (RC/ABS , ψ_{E0} , ϕ_{P0} cf. Appendix II), which represent important steps of energy bifurcations, limitations in energy trapping and electron transport translate into decreased PI_{abs} values (even when the maximum quantum yield is quite stable over a wide range of PI_{abs} : Figure 33 A) and may thus be preferred to quantify the performance

capacity of PSII. Based on the range of possible approachable values of the 3 components of PI_{abs} , alteration at different steps of the OJIP transient influence PI_{abs} to a different degree (cf. Figure 33 B,D,F). It must be noted, however, that (at least under natural conditions) changes in PI_{abs} are the result of alterations in all components at the same time (to different degrees). Additional to the fluorescence intensities at O- and the P-step [F_0 and F_m ; $(F_m - F_0) F_m^{-1} = F_v / F_m = \phi_{P0}$] changes at the K- ($F_{300\mu s}$) and the J-step (F_{2ms}) have an impact on PI_{abs} . $F_{300\mu s}$ is used in the calculation of RC/ABS only, whereas F_{2ms} is used in the calculation of RC/ABS and ψ_{E0} . Changes in ϕ_{P0} showed the largest influence on PI_{abs} , since the parameter is an element in the calculation of all three components. In the relationship of the JIP-test parameters to each other, certain threshold values were apparent, beyond which PSII functionality appeared to be severely suppressed. At RC/ABS values below 1, only very low PI_{abs} values were observed, whereas gradual decreases of ϕ_{P0} were noted at RC/ABS values below 0,5. In leaf samples with very low PI_{abs} values (recorded primarily during leaf senescence), $V_{OJ300\mu s}$ revealed a strong increase (Figure 33 E). $V_{OJ300\mu s}$ quantifies the K-step in the altered OJIP transient (to OKJIP, GUISSÉ *et al.* 1995), associated with the impairment of electron donation by the oxygen evolving complex (SRIVASTAVA *et al.* 1997, STRASSER 1997, OUKARROUM *et al.* 2007).

The steady state phase, defined as the time interval in the vegetation period when the influence of leaf development and leaf senescence were insignificant (termed “core vegetation time” cf. Figure 5), was characterized by more or less constant values with low variability. In the steady state phase, the fluorescence parameters showed no interspecific variability. The maximum quantum yield of primary photochemistry (ϕ_{P0}) was in a range of values described for healthy samples (BJÖRKMAN & DEMMIG, 1987, MOHAMMED *et al.* 2003), indicating daytime conditions did not lead to prolonged photoinhibition. In contrast to the fluorescence parameters ϕ_{P0} and $\ln PI_{abs}$, chlorophyll contents, measured as SPAD values, varied between species in the steady state phase (Table 9). The chlorophyll contents variability during this stage was low for individual leaves (1,6-2,4 SD). Trees with lower chlorophyll contents in 2012 also showed lower values in 2013 and vice versa (Figure 29), indicating that factors influence the leaf greenness on small spatial scales (Figure 26). Additionally, SPAD values of different leaves on a single tree did not vary to a large extent (Table 9). The length of the core

Discussion

vegetation time was correlated to the begin of senescence at the FR site in 2013 (not shown), due to similar time points for the end of development (Appendix IV), which may have been influenced by very low springtime temperatures in this particular year, synchronizing budbreak of the different species. On a larger time scale (1951-1996) the growing season for *Q. robur* in Germany showed an increasing trend of 0,22 days per year due to earlier budbreak and later begin of senescence (MENZEL 2003), and expected further changes in phenology are highly confident in climate change scenarios (KOVATS *et al.* 2014). Photosynthesis is primarily influenced by the absorbed irradiance, the biochemical capacity for photosynthesis (rate of carboxylation & rate of electron transport), temperature and the CO₂ concentration at the carboxylation site (DE PURY & FARQUHAR 1997). An increased amount of chlorophyll per unit area, which has been shown to correlate with an increased amount of nitrogen per unit area (Figure 17 B), would lead to a higher amount of absorbed irradiance per growing season (DE PURY & FARQUHAR 1997). HARLEY & BALDOCCHI (1995) have shown a positive correlation of leaf nitrogen content with the maximal carboxylation rate (V_{cmax}) and maximal electron transport rate (J_{max}). In this context, trees displaying high SPAD values during the growing season with interannual continuity, would benefit from a higher annual carbon acquisition, which could lead to an additional flush, further increasing leaf area and height, increasing root growth or increasing non-structural carbon reserves, resulting in a an advantage over its competitors. Annual time courses of photosynthetic capacities of *Q. robur*, *Q. ilex* and *Q. x turneri* controlled for temperature and CO₂ concentration at the carboxylation site do not correspond to the steady state time courses of chlorophyll content and leaf nitrogen (BOTH & BRÜGGEMANN 2009). BAUERLE *et al.* (2012) observed similar time courses of SPAD values in *Q. alba* and other deciduous tree species, but deviating time courses of V_{cmax} and J_{max} . The annual time course of biochemical capacity for photosynthesis might be influenced to a larger part by the photoperiod, than by the nitrogen content or temperature (BAUERLE *et al.* 2012), which could result in further decreased daily potential photosynthetic capacities as estimated from chlorophyll contents and predawn fluorescence parameters. However, the photoperiod does not change from year to year or with climate, thus trees with leaves, displaying a longer core vegetation period and higher SPAD values are expected to have an increased carbon gain integrated over the season, than trees with lower light harvesting capacities and shorter core vegetation period.

Despite of unfavourable conditions for photosynthesis and carbon gain in the late growing season (MORECROFT *et al.* 2003) a delay or deceleration of the senescence process may provide a competitive advantage. While shoot and leaf growth is episodic in *Quercus* (JOHNSON *et al.* 2009), root growth is continuous and ceases mainly due to greater carbon sinks in the developing flushes (LARCHER 1994). A prolonged period of leaf greenness with a positive carbon balance may therefore increase the root to shoot ratio, beneficial for water and nutrient allocation in the next growing season. The senescence process is generally assumed to be comprised of several phases. In a first phase, total chlorophyll, nitrogen and protein contents decrease in a balanced matter (MUNNÉ-BOSCH & ALEGRE 2004), not affecting the quantum yield efficiency of primary photochemistry (MIERSCH *et al.* 2000). A further advancement of the senescence process is accompanied by further decrease in chlorophyll content with impairments of the photosynthetic electron transport and changing Chl a/b ratios, (HOLLAND *et al.* 2014). Several factors like decreased water availability, high temperatures or nitrogen deficiency can lead to an earlier beginning of leaf senescence, whereas other factors like increased nitrogen may result in a delay (ADDICOTT 1968, LARCHER 2003, MUNNÉ-BOSCH & ALEGRE 2004, BALAZADEH *et al.* 2014). However, low leaf nitrogen contents during the core vegetation time were not found to correlate with an earlier beginning of senescence at the FR site in 2012 and/or 2013 (not shown). For *Q. robur*, the photoperiod has been identified to be the main driver for the beginning of senescence (DELPIERRE *et al.* 2009). Nevertheless, temperature influences this timing on different levels. ESTRELLA & MENZEL (2006) found that a mean daily temperature below 8°C triggers senescence in autumn and warmer temperatures delay senescence, whereas high spring and early summer temperatures advance leaf yellowing (MENZEL 2003). Combining these influences, phenological models forecast a trend of delayed senescence until 2099 for *Q. robur* in Central Europe (DELPIERRE *et al.* 2009). *Q. robur* and *Q. frainetto* showed a higher variability amongst individual trees for the onset of leaf yellowing on the site compared to *Q. rubra* and *Q. pubescens* (Figure 28), with some individuals of *Q. robur* showing a decline as soon as August. Since a large spatial variability of photoperiod or air temperatures is rather unlikely and the plant material stems from the same batch and same provenance, the differences in the begin of senescence (cf. Figure 28 & Appendix IV) may result from an individual susceptibility to unfavourable conditions. A good correlation was found between the beginning of

Discussion

senescence and the duration of the core vegetation time (2013) (not shown), since leaf development was very similar in all deciduous trees and species in this particular year. A soil water deficit was developed in both years, apparent by decreasing values of soil water potential, but at different times of the year. In 2012, soil water deficit developed in the beginning of August and reached the 200 cbar mark at mid-September, leading to an earlier (but not significant) beginning of senescence, as compared to 2013. In 2013, water deficit developed in July and reached the 200 cbar mark at the beginning of August, which presumably resulted in a later begin of senescence, however, the rate of Chl decrease was faster. *Q. rubra* seemed to be most affected by the decreased soil water potential. Abrams (1990) reported that *Q. rubra* was more restricted to mesic sites, representing an exception of North American oaks, which normally have an advantage among co-occurring species of other genera during drought events. Contrary to the senescence behaviour of the other deciduous species, *Q. pubescens* showed no alteration in the beginning of senescence or in the rate of decrease between both years, so that only a very small number of leaves were abscised and the chlorophyll content of remaining leaves was still high at the last day of measurement in November 2013. The increased period of leaf greenness and the sustained high values of maximal quantum yield resulted in an increased period of light harvesting and potential carbon gain compared to the other deciduous species (cf. Figure 31). Since *Q. pubescens* trees did not show a higher number of leaf flushes per year as compared to *Q. robur* and similar aboveground height at the FR site, the carbon surplus assimilated during the prolonged vegetation period may provide increased root growth, favourable for stands with low soil moisture and nutrient contents. On the other hand, trunk starch reserves influence crown density and vitality in the next growing season. BRÉDA *et al.* (2006) observed that the amount of dead branches and twigs in 2004 was correlated to the amount of starch reserves in 2003, when early senescence in oaks was induced by drought. *Q. ilex* with a true evergreen leaf life strategy can benefit from warm autumnal and early winter temperatures. The seasonal integral of the Performance Index as a marker of the seasonal capacity for light trapping and electron transport was therefore higher in *Q. ilex* and *Q. pubescens* compared to the other species due to no or late senescence.

The information about the annual time course of leaf chlorophyll content and quantum yield efficiency is of great importance when representative values for a comparative analysis between different species in the same developmental stage or different years have to be estimated. Otherwise developmental stages may mask or blur the observed effect of a stressor. Since the developmental phase and the beginning of senescence may vary between species, the time period of the core vegetation time seems most appropriate for this task. During this phase, changes in SPAD values were small (mean SD = 1,9). Based on the observations in 2012 and 2013 at the FR site, the period from mid of July to mid of August would yield values of SPAD and PEA measurements with no developmental constraints for all *Quercus* species. Calculating the integral of the Performance Index for this period, no significant differences between the species were found in 2013, suggesting that environmental conditions or other factors were not negatively influencing or favouring one species over the other at the FR site. In 2012, only *Q. rubra* showed significantly lower values compared to the other species at the site. In fact the integral of the Performance Index was not significantly lower in 2012 compared to 2013 in *Q. rubra*, but all other species showed similar low values like *Q. rubra* in 2013. In this year a strong soil water deficit developed in early July. If species at different sites were assessed, to quantify if any factors have led to an earlier onset of leaf senescence and thus to a comparatively shorter core vegetation time and seasonal potential carbon gain, measurements should be taken at the edge of the core vegetation time at the end of August to the beginning of September (cf. Figure 28 & Figure 30).

Since Chl a fluorescence is the light emitted by Chl a molecules upon excitation, it could be argued that the chlorophyll concentration has a major influence on the fluorescence yield of a sample. It has been shown that the measured fluorescence intensity for dilute solutions of Chl molecules is proportional to the quantum yield of fluorescence, multiplied by the number of absorbed photons and the Chl concentration (LAKOWICZ 2007). SPAD measurements and OJIP transients were recorded from the same leaves within a short time span, enabling correlations across multiple species, seasons and years to observe, if indeed the chlorophyll content of the leaf has an influence on the calculated JIP-test parameters. Figure 34 shows the relationships between fluorescence parameters and SPAD-values. For all parameters significant

Discussion

correlations were observed. Similar results have been obtained in different genotypes of *Litchi chinensis* SONN. (FU *et al.* 2013), *Carica papaya* L. (CASTRO *et al.* 2011) and *Coffea canephora* PIERRE (TORRES-NETTO *et al.* 2005). On the contrary, DINÇ *et al.* (2012) found only marginal effects of Chl deficiency by magnesium and sulphate starvation on the fluorescence rise kinetics and virtually unchanged F_0 and F_m values in leaves of hydroponically grown sugar beet plants. They concluded that the activity of the remaining electron transport chain remained largely unaffected with no overall changes in the antenna size. In the JIP test, to quantify the absorption flux per cross section, the cross section is approximated by F_0 and/or F_m ($ABS/CS_0 = F_0$; $ABS/CS_m = F_m$, STRASSER & STRASSER 1995, STIRBET & GOVINDJEE 2011), indicating a correlation of chlorophyll content with the fluorescence intensity as a basic assumption. Since data points from the period of leaf development and leaf senescence are present in the correlation analysis of Figure 34, one could argue that low JIP-test values at low Chl concentrations are not causally dependent, but the product of low photosynthetic capacity during leaf developmental processes. Removing data pairs from dates before July 27th and after September 10th ($n = 1497$) to include to the largest part values from the core vegetation time (cf. Figure 31) and only to a minor part data pairs from leaves with an accelerated begin of senescence (cf. Figure 28) still yielded significant correlations in the above named parameters.

The highest correlation coefficient (R^2 0,526 with $n = 2522$ and R^2 0,441 with $n = 1497$) in both cases was found in the parameter RC/ABS, a measure of the apparent antenna size [$RC/ABS \sim Chl_{RC}/Chl_{antenna} = Chl_{RC}/(Chl_{tot}-Chl_{RC})$] referring to Chl of PSII only, (STIRBET & GOVINDJEE 2011). RC/ABS quantifies the relative amount of fully active (Q_A reducing) RCs per absorbing antenna chlorophylls (STRASSER & STRASSER 1995, STIRBET & GOVINDJEE 2011). Since a change in the ratio of PSII to PSI was not assumed due to unaltered ratios of Chl a to Chl b (CEPPI *et al.* 2012), RC/ABS (as well as F_0 and F_m) may provide a proportional approximation of the total chlorophyll content and correlate with the SPAD value. The correlation was observed, but the coefficients of determination (R^2) were low, due to the large variability of Chl fluorescence parameter values at a given SPAD value, indicating that dependencies are not very strong. DINÇ *et al.* (2012) and KALAJI *et al.* (2014) suggest that changes in F_0 and F_m can be buffered at decreasing Chl content due to a deeper penetration of the light beam and thus a

relatively higher fluorescence contribution by chlorophyll molecules situated in lower leaf layers. Stronger changes in fluorescence parameters have to be expected at changing Chl a/b ratios (DINÇ *et al.* 2012), which have only been observed in the advanced phase of senescence. In contrast to F_0 , F_m , V_J , V_I and RC/ABS, the JIP-test parameter PI_{abs} showed a non-linear relationship to the chlorophyll content due to normalisation operations (cf. Figure 34). For PI_{abs} , high and low values can be expected at high chlorophyll contents whereas at SPAD-values below ~25 only low values of PI_{abs} were observed. This threshold has also been reported by PERCIVAL *et al.* (2008) who observed photosynthetic impairments in leaves of *Q. robur* at SPAD values below 25. Under the natural conditions observed in 2012 and 2013 at the FR site, the selected JIP-test parameters were correlated to the leaf chlorophyll content. Different stresses might however alter these relationships significantly.

4.5. Stress response analyses

4.5.1. Drought stress

A high variability in morphological leaf traits was found among the different studied *Quercus* taxa (cf. 3.2.1), of which LMA_{DW} (also termed “degree of sclerophylly” i.e. MÜLLER-STOLL 1947) had been correlated with the mean annual rainfall at their area of distribution (WRIGHT *et al.* 2004). At regions with low annual rainfall, like in the Mediterranean, the proportion of plants with higher LMA_{DW} is increased compared to Central Europe, thus it can be concluded that plants with a higher LMA_{DW} are better adapted to dry conditions (POORTER *et al.* 2009). Sclerophyllous leaves, distinguished from malacophyllous leaves by higher LMA_{DW} values (NARDINI 2001, FLEXAS *et al.* 2014) have been attributed a higher resistance to transpirational water loss (ZHOU *et al.* 2013). Next to a high LMA_{DW} , the leaf water content per leaf area (LWC_A) was found to be higher in *Q. ilex* compared to the deciduous taxa. LWC_A has been termed “degree of succulence” (MÜLLER-STOLL 1947), but the correlation of LWC_A with leaf thickness across all *Quercus* taxa showed that the relationship was linear across all taxa and that higher LWC_A values in *Q. ilex* are rather due to increased leaf thickness than to a specific water storage function. In a study by NARDINI (2001), sclerophyllous and malacophyllous tree species (amongst others *Q. ilex* and *Q. robur*) showed no difference in leaf hydraulic conductance and thus no higher resistance to water loss. Loss of leaf hydraulic conductance and stomatal conductance are both closely correlated to leaf water potential (BRODRIBB & HOLBROOK 2003) and seem not to be predetermined by the ratio of leaf mass to leaf area. SALLEO & LO GULLO (1990) conclude in a comparison of *Q. suber*, *Q. ilex* and *Q. pubescens* that sclerophylly cannot be considered as significantly related to a drought avoiding strategy. However, LMA_{DW} has been found to correlate with the cell wall rigidity (ϵ : modulus of elasticity) (SALLEO & LO GULLO 1990, BURGHARDT & RIEDERER 2003), even if their association cannot be regarded as a functional relationship (CORCUERA *et al.* 2002). ϵ is derived by pressure volume analysis, relating leaf water content to leaf water potential. The modulus of elasticity (ϵ) was found to be almost twofold higher in *Q. ilex* in comparison to *Q. robur* (cf. Figure 36), despite of equal growth conditions and adequate water supply in the

climate chamber. ABRAMS (1990) summarized values of ϵ of 14 North American *Quercus* species, ranging from 2,75 to 38 MPa and showing the large variability despite of close relatedness. A cell wall with a higher rigidity (higher ϵ) enables a greater decrease in water potential with minimal water loss (LARCHER 2003) and has been used to quantify the plants adaptation (and their performance capacity) to water limited environments (NIINEMETS 2001, CORCUERA *et al.* 2002). More negative water potentials were needed in *Q. ilex* and *Q. pubescens* to reach the turgor loss point compared to *Q. robur*. Since the plant cell most probably can only sense changes in turgor and volume and not changes in the associated water potential (JONES 2007), *Q. ilex* may endure a greater intensity of stress and recover from water loss faster than *Q. robur* (SALLEO & LO GULLA 1990). The relative water content at the turgor loss point however, was not significantly different between the species (> 80%), which could point to a higher physiological tolerance to decreased soil water potential in *Q. ilex* during drought development (ZHOU *et al.* 2013). A water deficit of only 20% in relation to turgid weight leads to turgor loss and associated malfunction like reduced cell elongation and growth, stomatal closure and decreased photosynthesis (LARCHER 2003, JALEEL *et al.* 2009). Comparing the values of water potential of several species, at which P_N was still positive, FLEXAS *et al.* (2014) summarised that *Q. ilex* was better adapted to water deficit than *Q. pubescens* and *Q. pubescens* was better adapted than *Q. robur*. This ranking resembles the results from the pressure volume analyses. AREND *et al.* (2011) reported a shoot-height and stem-diameter decrease by drought in *Q. pubescens* of 27,8% and 31,2% compared to 40,6% and 41,2% in *Q. robur*, respectively, substantiating species-specific differences in the response to soil water deficit.

At night, when stomata are closed and transpiration is minimal, plants water status approximates soil water status and equilibrium is restored (LARCHER 2003). The measurement of predawn plant water potential is therefore unaffected by the daily disparity between the velocity of water loss and water uptake and thus a comparable standard for the measurement of increasing water deficit. At FR, soil water deficits developed during each summer, measured as a change in soil water potential in 50 cm depth. In both years, the maximum range of the watermark sensor installed in the iMetos climate station was reached (200 cbar or 0,2 MPa). In the experimental setup,

Discussion

predawn soil water potential decreased only at low volumetric soil water content (~12%), but the decrease was very fast, compared to the soil water deficit development under field conditions (cf. Figure 9). Even though differences in ϵ were observed and a later response to soil water deficit was expected in *Q. ilex*, no difference in was noted between the species. This may be due to the high speed of the water deficit development in the pots. The very low water potential of below -4 MPa were reached in a time span of only ~4 days after soil water content had dropped below 10% in all species, not allowing for slower adjustments like changes in chlorophyll content. BRÉDA *et al.* (2006) showed that the decrease of xylem hydraulic conductivity is closely linked to the water potential and that species of Mediterranean type ecosystems can endure lower water potentials than species from temperate ecosystems. However, the difference between *Q. ilex*, *robur* and *Q. petraea* was not very high and 50% of loss in xylem hydraulic conductivity was shown to occur at water potentials between -2,5 to -3,5 MPa (BRÉDA *et al.* 2006). None of the species adjusted its transpiration rate prior to the decrease of water potential despite the significant loss of soil water. For the deciduous oak *Q. robur* and *Q. petraea*, BRÉDA *et al.* (2006) report a missing “safety margin”, defined as the difference between a 10% loss of stomatal conductivity and a 10% loss of xylem hydraulic conductivity, suggesting that stomatal response occurs quite late. Responses may be different in the field, where the decrease of soil water potential is slower and plants have more time to adjust and acclimate to drying conditions.

The fast decrease of predawn water potential at a soil moisture content below 10% was accompanied by a decrease in transpiration rate (Figure 37) and changes in the fluorescence parameters ϕ_{P0} and PI_{abs} (Figure 38). Whereas AREND *et al.* (2012) found no difference in the response of stomatal conductance to decreasing Ψ_{pd} in *Q. robur* and *Q. pubescens*, $F_v/F_m (= \phi_{P0})$ significantly decreased in *Q. robur*. ϕ_{P0} however, is known to respond quite late to water deficit (i.e. EPRON & DREYER 1992, EPRON *et al.* 1993), but several authors have found PI_{abs} to respond earlier (i.e. TACH *et al.* 2007, ŽIVČÁK *et al.* 2008, JEDMOWSKI *et al.* 2013). Only very low values of PI_{abs} (< 3) corresponded to low values of net photosynthesis (P_N), and the influence of stomatal limitations was much greater at moderate water deficits between ψ_{pd} -1 to -2 MPa than limitations in primary photochemistry (cf. Figure 39 B). Independently of species, P_N decreased strongly in a linear fashion with G_{H_2O} below a threshold of approx. $60 \text{ mmol m}^{-2} \text{ s}^{-1}$ as a

consequence of the limitation of CO₂ supply. EPRON & DREYER (1992) observed similar declines in P_N and G_{H₂O} in *Q. rubra*, *Q. petraea* (Matt.), and *Q. cerris* upon drought stress. An initial decrease of P_N, due to stomatal limitation at moderate drought stress can therefore not be sensed by predawn measured fluorescence parameters (Figure 39 A). Steady state fluorescence measurements in daylight respond earlier to moderate water deficit. Non-photochemical energy quenching increases due to a pH mediated high de-epoxidation state of the xanthophyll pool, dependent on light intensity and stress intensity (HALDIMANN et al. 2008). This, in turn, leads to a decrease of the effective quantum yield in the light-adapted state (Φ_{PSII}) (HALDIMANN *et al.* 2008, KOLLER *et al.* 2014). On the other hand, as drought stress decreases to levels requiring additional adjustments, like sustained alterations in electron transport that manifest in retained changes in RCs per absorption or electron acceptor capacities beyond Q_A overnight, a decrease in PI_{abs} could be associated with a low P_N. Non-stomatal limitations occurred as water deficit developed further, visible by changes in P_{Max} at high CO₂ and low O₂ concentrations, excluding effects of CO₂ limitations or photorespiration (cf. Figure 40 D-F). Adjustments in pigment composition as a response to water deficit were not observed in *Q. robur*, *Q. ilex* or *Q. pubescens* under experimentally induced drought. However, HALDIMANN *et al.* (2008) detected decreases in total leaf chlorophyll in *Q. pubescens* at a natural stand in the Swiss Alps upon drought stress. In their study, the Chl/Cars ratio was also decreased, resulting from a net increase of carotenoids and xanthophylls, presumably as a key factor in the protection of the photosynthetic apparatus against photo-oxidative damage (DEMMIG-ADAMS *et al.* 1996, ADAMS *et al.* 2004). Decreased Chl content and a decreased Chl/Cars ratio in combination with chronic photoinhibition was also reported for *Q. ilex* in response to drought stress (BAQUEDANO & CASTILLO 2006, 2007) and for various other species (JALEEL *et al.* 2009). The contrary results are presumably due to the shorter exposure to drought in the climate chamber experiment with the limited amount of soil water in the pots. Decreases in pigment content upon drought stress can therefore not be excluded under field conditions and could be monitored by the SPAD-meter. The adjustment of total chlorophyll content and the alterations in pigment composition are likely to be modifications, following the quicker responses like stomatal adjustments and increased energy dissipation by PSII, since biochemical adjustments occur as part of a long-term response (ARVE *et al.* 2011). The pigmental adjustments observed by HALDIMANN *et al.*

Discussion

(2008) were reversed as conditions became more favourable and Ψ_{pd} increased in late summer, thus the drought stress experienced by the trees did not lead to senescence (despite min Ψ_{pd} values of -2,50 MPa). BRÉDA *et al.* (2006) on the other hand, report earlier beginnings of senescence in drought stressed deciduous oaks during the exceptionally hot and dry summer of 2003 in France at the border to Germany. Whether drought stress leads to senescence or not, may not only depend on the intensity of stress, defined by the plants water status but also by the duration of stress, rate of stress development and other accompanying factors.

In conclusion, the stomatal and non-stomatal responses to decreasing water availability seem to occur in sequence first, than parallel, depending on stress intensity and speed of deficit development and most likely influenced by additional factor as temperature and light intensity. Stomatal limitations of photosynthesis are to be expected before changes in fluorescence yields measured predawn occur. Concerning the fast Chl a fluorescence transient, changes in PI_{abs} could be detectable earlier than significant changes in F_v/F_m , if the rate of drought stress development is not too fast. While experiments under controlled climatic conditions on potted plants allowed for the determination of daily whole plant water loss and control for the uncertainty of differential root architecture among individuals and species, the rate of developing water deficit was found to be very fast, impeding the observation of species-specific response differences and slower adjustments. Responses to drought stress, requiring the degradation or synthesis of pigments to reduce the amount of absorbed light or increase the dissipation of absorbed energy, can be temporary and reversible or the beginning of senescence leading to nutrient reallocation and subsequent leaf loss. Thus, levels of drought stress, affecting the plant beyond decreases in P_N through stomatal limitations and leading to alterations in light harvesting and electron transport, may well be sensed by changes in SPAD values and alterations of the fast Chl a transient.

4.5.2. Heat stress

The response of photosynthesis to temperature follows the form of an optimum curve with three distinct phases: cold limit, optimal temperature range and heat limit (DREYER *et al.* 2001, LARCHER 2003). The experimentally determined optimal temperature range for Mediterranean plants lies between 15-30°C; 25-30°C for most species (FLEXAS *et al.* 2014). Above the optimal temperature range at the heat limit, the photosynthetic yield declines severely as primary processes of photosynthesis are inhibited (SCHREIBER & BERRY 1977, HAVAUX 1992, MOHANTY *et al.* 2012). The decline is associated with a reversible heat-dependent reduction of the Rubisco activation state (HALDIMANN & FELLER 2004), increased membrane fluidity and protein denaturation (BERRY & BJÖRKMAN 1980, YORDANOV *et al.* 1986). Because of the sensitivity of thylakoid membranes to heat (MOHANTY *et al.* 2012), disturbances of photosynthesis are among the first indicators of plant heat stress (LARCHER 2003). Among the thylakoid protein complexes, PSII is much more susceptible to heat stress than PSI (HAVAUX *et al.* 1991), therefore changes in the fluorescence emission of PSII, as recorded by the PEA and PAM devices, can be used for the determination of temperature induced impairments of photosynthesis (SCHREIBER & BERRY 1977). Under field conditions, photosynthesis is sometimes found to be depressed already above 20°C, since contrary to experimentally controlled conditions, increases in leaf temperature are most often accompanied with high irradiance and decreased water availability (GULIAS *et al.* 2009, FLEXAS *et al.* 2014). Since PSII is also affected by high light stress, the combination of these two stressors has an additive effect (LARCHER 2003).

The temperature record of the Frankfurt airport climate station (station ID 1420, DWD) showed that since 1949 the maximal air temperatures recorded were above 32°C in 75% of all years until 2013. The highest recorded air temperature at this station was recorded in 2003 with 38,7°C in the shade. During the observation period, air temperature reached 37,4°C by the end of July 2013. An equally high or higher temperature was only observed 3 times since 1949 at Frankfurt airport (1957, 2002 and 2003). Leaf temperature tracks air temperature and exceeds it (cf. Figure 41), especially when soil water deficit leads to stomatal closure and to the loss of heat exchange through transpiration. For the future climate, mean temperature increases, increases in

Discussion

the frequency of extreme temperature events (heat waves) and increased risk for droughts are predicted by the IPCC (KOVATS *et al.* 2014), requiring a comparable assessment of interspecific differences in the response to heat stress for the introduced tree species. Additionally, the knowledge on the changes in the fluorescence signal possibly allows the detection of heat stress in a spatial context, allowing managerial interventions to mitigate climate change dependent disadvantages.

The critical temperature of PSII thermostability was found to increase by 2-4°C with increasing growth temperature from 20°C to 35°C, with no significant differences between the Mediterranean species *Q. ilex* and *Q. pubescens* to *Q. robur*. Similar rates of T_{crit} acclimation have been observed by GHOUIL *et al.* (2003) in seedlings of *Q. suber*. T_{crit} was found to be significantly higher, when the heat stress is associated with drought (HAVAUX 1992, GHOUIL *et al.* 2003). The margin for maximal T_{crit} acclimation is presumably small, since DREYER *et al.* (2001) did not find significant differences in T_{crit} for seven temperate and deciduous tree species. LARCHER (2003) summarized T_{50} values (temperature at 50% damage) of several authors, reporting threshold temperatures of deciduous trees of ~50°C and up to 55°C in evergreen species, proposing a possible slight advantage of *Q. ilex* under field conditions. However, alterations of the fluorescence transient occur at lower temperatures (Figure 42). As DREYER *et al.* (2001) reported, F_m usually declines at lower temperatures than the increase of F_0 , which was attributed to conformational changes in PSII associated with energy dissipation (DEMMIG-ADAMS *et al.* 1998, DREYER *et al.* 2001). This decline of F_m was observed in all species (Figure 42). As a result, PI_{abs} was found to decrease at temperatures about 20°C, steadily at each increment of T_{leaf} , whereas most of the observed JIP-test parameters changed at 40°C (cf. Figure 42 C). Visualizing relative JIP-test parameter changes in a spider plot (Figure 42 C), increases in ΔV_{IP} and $V_{OJ300\mu s}$ stand out in addition to the PI_{abs} decline. Increasing fluorescence intensities at the I-step are commonly associated with reduced activity of the PSI acceptor side (SCHANSKER *et al.* 2005) or decreases in PSI content (OUKARROUM *et al.* 2009, CEPPI *et al.* 2012). Since increasing fluorescence at the I-step would however lead to a decrease in ΔV_{IP} ($=1-V_I$), instead of the increase observed, the situation must be reversed. An aggregation of additional PSI units in the short time frame of the conducted measurements (25 min) is rather unlikely, thus a temperature induced increase of PSI activity or the effect of

changing ratios of active PSII to PSI due to the different heat susceptibilities of the two systems are proposed as explanations. This unproportioned increase in relation to the other JIP-test parameters has not been observed during drought stress, cold stress, leaf development or leaf senescence and could thus be used for the short-term distinction of heat stress effects. However, if this increase in ΔV_{IP} was dependent on temperature, the alteration would not be conserved to measure at a later point in time, when temperatures have decreased (i.e. predawn). $V_{OJ300\mu s}$ quantifies the formation of a so-called K-step (GUISSE *et al.* 1995) at 300 μs . The K-step is associated with an impairment of electron donation by the oxygen evolving complex (SRIVASTAVA *et al.* 1997, STRASSER 1997, OUKARROUM *et al.* 2007) and is usually observed in response to heat stress (STRASSER 1997, MATHUR *et al.* 2011, TOTH *et al.* 2007). Figure 42 B showed that the K-step was underestimated by $V_{OJ300\mu s}$, since the local maxima in the differential curves developed approx. 200-700 μs later. However, the underestimation of the K-step by $V_{OJ300\mu s}$ does not omit stress identification and the K-step develops not until PI_{abs} has already severely declined (cf. Figure 33 E). It must be noted that the determination of T_{crit} , through the rapid rise of F_0 as well as the measurement of the OJIP transient require dark adapted samples. However the temperatures to which the leaves have been exposed to are very improbable to occur naturally in darkness. TSIMILLI-MICHAEL *et al.* (1999) reported that increased water temperature had only a minor effect on the OJIP transients measured on light adapted foraminifer symbionts compared to organisms that were exposed to 32°C in darkness. The plants may use additional pathways to reduce the electron pressure, built up through heat induced limitations of photosynthesis, like the pH regulated energy dissipation by xanthophylls in light (DEMMIG-ADAMS *et al.* 1996, ADAMS *et al.* 2004). This is reflected in the later response of ϕ_{PSII} to heat, measured at 300 μmol quanta $m^{-2} s^{-1}$, which decreased at 35°C, at higher temperatures than PI_{abs} in darkness.

4.5.3. Cold stress in *Q. ilex*

Increasing mean annual temperatures and increased risk for drought in Central Europe (KOVATS *et al.* 2014) may favour tree species from southern distributions, better adapted to these conditions. However, despite of an overall warming it is likely that cold winters remain a feature of the temperate climate for the next decades (CHRISTENSEN *et al.* 2013) and limit the establishment of these species. Moreover, introduced species, which are well adapted to climatic conditions of the next century, need to simultaneously survive conditions of the current climate. For juvenile *Q. ilex* trees (Lake Garda district), LARCHER (2000) identified a threshold temperature of -15°C for leaf tissue, (LT_{50} : 50% of tissue was irreversibly damaged) for trees with a maximal frost tolerance in January. In the winter period 2012/2013 the lowest temperatures ($-16,4^{\circ}\text{C}$ at 5 cm above ground) were recorded as late as March, when frost resistance in *Q. ilex* was not maximal and de-hardening had probably occurred due to increased day length (LARCHER 2000). However, no irreversible damages were noted during the observation period and all leaves were retained on the trees. For terminal buds, LT_{50} was identified to be only 2°C lower at $\sim -17^{\circ}\text{C}$ and winter conditions in 2012/2013 led to

Table 13: Compiled meteorological data from Frankfurt airport for the period 1949 until 2013. Min T depicts the minimum temperature of the year. Frost days and ice days are days with minimum temperature below zero degrees and maximum temperature below zero degrees, respectively. Data analysed by means of column statistics. Data provided by DWD, station 1420, daily resolution.

	min T [°C]	Frost days [d]	Ice days [d]
Minimum	-21,6	42	1
25% Percentile	-15,9	68	8
Median	-12,9	79	13
75% Percentile	-10,4	93	20
Maximum	-4,3	121	56
Mean	-13,2	79	15
Std. Deviation	3,7	18	10
Number of values	65	65	65

terminal bud injury in 12% of trees at the FR site. One year earlier, the air temperature 5 cm above ground reached $-20,1^{\circ}\text{C}$, which led to a total loss of all leaves at the plantation sites. Terminal bud injury was high in all species between planting in spring 2011 and the assessment in spring 2012, but has also to be assigned to the exceptionally dry spring at planting in 2011 as well. Compared to the last 65 years, the winter period 2012/2013 was around average, concerning the number of ice and frost days and slightly warmer concerning the minimal temperature. The lowest temperature recorded at the Frankfurt airport climate station since 1949 was $-21,6$ at 2 m height and $-26,2$ at 5 cm above ground. The adult *Q. ilex* individuals investigated by BRÜGGEMANN *et al.* (2009) in Frankfurt city survived these winters (1963 and 1968). Even though winter temperatures are projected to increase in the future, harsh frost periods have to be expected due to intermediate continental climate. In contrast to the deciduous *Quercus* species, which endure the winter periods in a dormant and leafless state, the evergreen taxa are enabled to photosynthesize during favourable conditions all year round. The competitive advantage of an evergreen leaf life strategy is however concomitant with a risk of over-excitation by excess light at low temperatures as well as of freezing injury. Compared to other Mediterranean species, LARCHER (2000) identified *Q. ilex* (ssp. *ilex*) as the one with the highest stability of the photosynthetic apparatus to cold. Under Mediterranean conditions, evergreen *Quercus* taxa were found to acclimate to low temperature and high irradiance with decreases in maximum quantum yield of PSII and permanent accumulation of de-epoxidated xanthophylls (MARTINEZ-FERRI *et al.* 2004, ARANDA *et al.* 2005, CORCUERA *et al.* 2005). Further, it has been found that the susceptibility to photoinhibition may vary with the provenance of the seed material (CAMARERO *et al.* 2012), an important detail for the selection of provenances chosen for introduction to Central European stands. The study repeated here, on the response of *Q. ilex* to Central European winter conditions complements earlier studies of evergreen and semi-evergreen *Quercus* taxa in the Rhine-Main region by BRÜGGEMANN *et al.* (2009), HOLLAND & BRÜGGEMANN (2011), PFLUG & BRÜGGEMANN (2012) and BOTH & BRÜGGEMANN (2009), who found similar responses.

Discussion

On the pigment level, the risk of over-excitation can be reduced either by a decrease of the fraction of absorbed radiation (by a decrease of total chlorophyll) or by dissipating absorbed energy through carotenoids. Not only the increase of total carotenoids to chlorophyll but especially the conversion of the xanthophyll Violaxanthin (V) to Zeaxanthin (Z) via Antheraxanthin (A) by de-epoxidation and the subsequent association of Z to PSII in the presence of a trans-thylakoid pH gradient are efficient means of energy dissipation in the form of heat (DEMMIG-ADAMS *et al.* 1996, ADAMS *et al.* 2004). Z accumulation and its overnight retaining have been found to be a major response in evergreen *Quercus* taxa to sub-zero temperatures (BRÜGGEMANN *et al.* 2009, HOLLAND & BRÜGGEMANN 2011, PFLUG & BRÜGGEMANN 2012). In the present study, the chlorophyll to carotenoid ratio decreased steadily with the lowest value at the beginning of April at the end of the prolonged frost period (Figure 44). Since SPAD values showed no tendency for a decline, the decrease in the Chl/Cars ratio was presumably due to an increase of the total amount of carotenoids. In photoprotection, carotenoids are especially potent to scavenge electrons from excited Chl, triplet Chl and excited oxygen (DEMMIG-ADAMS *et al.* 1996). The increase of the de-epoxidation state of the xanthophylls [$DES = (A+Z)(V+A+Z)^{-1}$] has been observed in evergreen and semi-evergreen *Quercus* taxa predawn (in a state of “chronic photoinhibition”) and additionally in the course of the day (as “dynamic photoinhibition”) (BRÜGGEMANN *et al.* 2009, PFLUG & BRÜGGEMANN 2012). A decrease in predawn F_v/F_m has been found to correlate with a DES increase (HOLLAND & BRÜGGEMANN 2011), but they are not necessarily causally related and may also represent two different mechanisms to reduce over-excitation of the photosynthetic apparatus (MARTINEZ-FERRI *et al.* 2004). Especially under low temperature and high light conditions, absorbed energy can exceed its possible use by photosynthesis (e.g. temperature dependent enzyme activity) and the probability of electron transfer to oxygen species increases [formation of reactive oxygen species (ROS)], which subsequently damage components of the photosynthetic apparatus like D1 protein. A shift of the equilibrium between D1 protein degradation during dynamic photoinhibition and synthesis towards degradation results in a decrease of F_v/F_m (DEMMIG-ADAMS *et al.* 2006). The result is a decreased maximum quantum yield, which can be interpreted either as damage to the photosystem (in susceptible species) but also as a protection against further over-excitation (in species making use of this process for reversible down regulation of PSII). Chronic photoinhibition in

combination with a decreased Chl/Cars ratio (and decreases in Chl content) has been identified as a response of *Q. ilex* also to drought stress (BAQUEDANO & CASTILLO 2006, 2007) with similar demands for over-excitation avoidance. PFLUG & BRÜGGEMANN (2012) reported changes in the OJIP transient other than the decline of F_v/F_m , which have also been observed in *Q. ilex* in the winter period 2012/2013. The JIP-test parameter ABS/RC increases, which was interpreted as a reduction in the Q_A reducing RCs per PSII antenna Chl (STRASSER *et al.* 2010), by so called “silenced RCs” (STRASSER *et al.* 2004). However, the relationship between ABS/RC (the inverse of RC/ABS) and F_v/F_m was found to be altered in cold stressed leaves compared to the relationship observed during the growth period from spring to autumn (Figure 47). In contrast to the changes observed in the correlation of RC/ABS to F_v/F_m ($F_v/F_m = \phi_{P0}$), the relationship between RC/ABS and PI_{abs} (of which RC/ABS is one of 3 components) was not found to be altered under cold stress, suggesting an influence of F_v/F_m . Indeed, at equal levels of Q_A reducing RCs per PSII antenna Chl (RC/ABS), the relationship between the trapped excitation energy per absorption (F_v/F_m , ϕ_{P0}) and the dissipated excitation energy per absorption ($1-F_v/F_m$, $1-\phi_{P0}$) was changed with increases in dissipation. This led to overestimations of PI_{abs} in cold stressed leaves (Figure 47 A) and notable deviations of the influence of electron transport beyond Q_A^- (ψ_{E0}) on PI_{abs} (Figure 47 D). Presumably, the changes in the relationship between energy absorption, trapping and dissipation observed in the JIP-test parameters are due the status of chronic photoinhibition with the predawn elevated DES levels, leading to relative increases in energy dissipation by the xanthophylls. Thus PI_{abs} values may be overestimated in the state of chronic photoinhibition and ϕ_{P0} may be better suited to quantify the decline of PSII functionality during winter conditions.

Concerning the correlation of ϕ_{P0} to DES, MARTINEZ-FERRI *et al.* (2004) observed a further decrease of ϕ_{P0} with no further change in predawn DES towards the end of winter. The energy scavenging capacity of DES was probably exceeded and over-excitation led to a cumulative damage to the photosystem, comparable to the steady decline in January. ϕ_{P0} did however decrease not before January, even though minimal temperatures had reached -10°C in December. Similar observations were reported by HOLLAND & BRÜGGEMANN (2011) in *Q. suber* and *Q. x hispanica*, where frost periods in December under cloudy conditions did not lead to a ϕ_{P0} decrease. Only

Discussion

when low temperatures were combined with high light, ϕ_{P0} declined. Predawn DES on the other hand was already increased at low temperatures in December. At the winter period 2012/2013 irradiances were very low in November and December as well (mean daily hours of sunshine 0,99 and 0,85). In January and February however, low temperatures resulted in ϕ_{P0} declines, despite of equally low irradiances (0,61 and 0,99 h/d). The decrease of ϕ_{P0} was mainly due to a decrease of the maximum fluorescence yield F_m and delayed for 2 weeks in plants at the forest site under shelterwood compared to unshaded plants at the Botanical Garden site (Figure 46). It is suspected that the shade provided by the evergreen *Pinus* cover provided more protection from excess light but may have also buffered low temperatures. Photoinhibition was not rapidly reversible, thus acclimation to 20°C for 30 min still yielded decreases in photosynthetic capacities and effective quantum efficiencies under light conditions as the winter progressed and ϕ_{P0} steadily declined. Decreased photosynthetic capacity was found to be an inherent acclimation of sclerophyllous evergreens to winter conditions (ADAMS *et al.* 2004). The fluorescence decrease ratio, a vitality index describing the relationship between F_m and the steady-state fluorescence in the light-adapted state (LICHTENTHALER *et al.* 2005) was more closely linked to ϕ_{P0} than to ϕ_{PSII} which describes the quantum yield of PSII electron transport in the light-adapted state. This can be attributed to the fact that changes in ϕ_{P0} were mainly due to decreases in F_m , which translate directly to R_{FD} [$R_{FD} = (F_m - F_s) F_s^{-1}$] whereas ϕ_{PSII} is normalised to the maximal fluorescence yield in light F_m' ($\phi_{PSII} = (F_m' - F_s) F_m'^{-1}$). LICHTENTHALER *et al.* (2005) reported that high light led to damage and inactivation of photosynthetic systems in the upper leaf half, whereas photosystems of chloroplasts located in the middle and lower part of the leaf were unaffected and thus protected from over-excitation. In *Q. ilex*, differences between fluorescence yields of the adaxial and abaxial side were only marginal at first and completely lost, when ϕ_{P0} decreased in January. Decreases in ϕ_{P0} and increases in predawn DES have also been reported as a photoprotective mechanism under summer drought conditions (PEGUERO-PINA *et al.* 2009). Measurement of sap flow velocities were performed during the winter period to reveal possible drought stress due to frozen soil or root damage. Sap flow velocity was positively correlated to vapour pressure deficit (VPD) (Figure 48). Despite the low values recorded for sap flow velocities during winter, no change in the relationship was visible (e.g. to low sap flow at high VPD) which could indicate that water availability was not altered by low temperatures.

5. Conclusion and Outlook

The seasonal dynamics and species specific variability of key functional leaf traits for the estimation of plant vitality in Oak species of differing natural distributions and adaptations have been monitored under Central European conditions in a common garden type forest experimental plantation in Southern Hesse. Alterations in morphological and pigmental leaf traits, changes in the fast Chl fluorescence induction transient and phenological alterations are responses of plants to their environment which occur at different time scales, intensities and taxa specificity, affecting the potential carbon acquisition capacity of a leaf to different degrees. During leaf development, the leaf is a carbon sink and the structure for light capturing is built with species specific differences in the amount of invested biomass per area of potential light harvest. The concomitant increase in pigments per chloroplast and chloroplasts per cell determine the maximal light harvesting capacity per time and area. On the larger time scale, the potential annual carbon acquisition is furthermore determined by the time of budbreak, the end of leaf development, the length of the core vegetation time, the beginning of senescence and the rate of decline during senescence. At the level of the chloroplast, the probability that an absorbed photon leads to the reduction of the primary electron acceptor Q_A can be determined through the ratio of the maximal variable fluorescence to the maximal fluorescence yield (F_v/F_m , Φ_{P0}). Further, with the analysis of the OJIP transient and the application of the JIP-test, potential energy losses in the electron transport chain behind PSII can be quantified. Decreases in any of the above named, non-invasively measurable photosynthetic leaf traits are indications for losses in the potential carbon acquisition capacity, and the subsequent steps towards CO_2 fixation involve even more steps of energy loss. Thus, alone or in combination, a monitoring of morphological, pigmental and photosynthetic traits will provide important supplemental information for the assessment of individual tree vitality at a given time and place. The data and dependencies presented within this thesis provide a reference and enable for the first time an application for a comparative assessment of these key functional leaf traits in a number of Oak species of different functional groups (deciduous, semi-deciduous, evergreen) with a predicted potential range in Central Europe in a changing climate.

Conclusion and Outlook

Concerning the morphological leaf traits, a significant species specific variability with low intraspecific variability has been observed under the Pine shelterwood at the FR site. Additional samples should be investigated in the steady state phase, when structural leaf development is completed, to test for interannual variability of the traits. Likewise, the key morphological leaf traits of the same genotypes could be investigated at sites with different managemental practice, onsite competition and soil nutritional status, possible at the other two experimental forest plantations in Rüsselsheim (higher density of Pine and natural rejuvenation shelterwood) and Lampertheim (no shelterwood). This would provide information on possible adjustments in the species' leaf economic strategies as a response to different site characteristics, enabling silvicultural interventions. The end of structural development was found to be not significantly different in the deciduous species and only in *Q. ilex* with the highest ratio of leaf dry mass to leaf area, a delay was noted in 2013. It was mentioned above that the exceptionally cold spring in 2013 may have led to a delay of budbreak, possibly resulting in apparently synchronised starting points of leaf development, which might not have been representative. A monitoring of the structural leaf development, ideally coupled with a monitoring of leaf chlorophyll content and functionality of primary photochemistry could reveal a species specific difference in leaf development as observed for leaf senescence. In this case the strong correlation between the beginning of senescence and the length of the core vegetation time observed in 2013, may be altered. The non-destructive, optical monitoring of chlorophyll concentrations in single leaves over the course of the whole growth period allowed to distinguish the different occurring developmental phases and information on inter- and intraspecific variability. For single comparative measurements of morphological, pigmental or photosynthetic traits, the time interval herein termed "core vegetation time" should be considered, when no influence of leaf development or leaf senescence on the measurements have to be expected. For Central European conditions, the interval between mid of July to the end of August provides such a timeframe. Periods with increasing soil water deficit may however lead to an earlier begin of the leaf senescence process, shortening the timeframe to mid of August. Measurements concerning a species specific response to environmental conditions which lead to earlier onsets of senescence should be taken in the timeframe of end of August, to the mid of September. The focus of this thesis lay in measurements on the

leaf level, however, concerning the assessment of tree vitality, the total sum of leaves per canopy is of great importance. Within this study, the variability of leaf greenness in different leaves of one canopy was found to be low during the core vegetation time, thus representative values can be collected with a low number of samples per tree. Another important focal point for further research is the correlation of parameters quantifying annual photochemical capacity with the actual carbon use and allocation within the tree. The interspecific difference in carbon allocation to roots and shoots, the development of deep penetrating taproots and the response in growth to low water availability and/or nutrient supply are further important points to consider, when tree species are comparatively assessed for the use in stands, prone to potential climate hazards.

It has been shown in this thesis that values obtained by SPAD-meter measurements from light transmission in the red and near infrared (NIR) portion of the electromagnetic spectrum (ES) are strongly and non-linearly correlated with area based leaf chlorophyll and concentrations in all *Quercus* taxa. These absolute/optical Chl relationships showed no significant interspecific variability despite of large differences in key morphological leaf traits. The observed strong linear relationship of leaf nitrogen content and leaf chlorophyll (both on area base) thus also enables an estimation of foliar nutrient status through the non-destructive sensing of chlorophyll. Additional tests have shown that the Chl-meter was very well applicable under field conditions, since the meter-readings were not influenced by the time of day, changes in water content, leaf structure or air temperature (deviations at frozen leaves have to be assumed). Thus a non-destructive estimation of chlorophyll content as a proxy for light harvesting capacity and foliar nutrient status has been established for the use in different *Quercus* species with a wide range of morphological leaf traits. The Chl-meter measurements therefore allow an unbiased quantification of pigment content and may thus be used as a supplemental tool in small scale vitality assessments of single trees, especially in highly structured stands under shelterwood with a large spatial variability of abiotic, influential factors. The established calibration equations allow for the conversion of Chl-meter readings to pigment and nitrogen contents during all phases of seasonal development. For evergreen species, alterations in the pigment ratio Chl/Car have to be accounted for. Similar alterations may be observed during severe and prolonged drought stress, a situation which did not occur in the years of analysis. The relationship between the

Conclusion and Outlook

used transmission based Chl estimations and reflectance based estimations should be further investigated. The recording of the whole reflectance spectrum from the visible to the far infrared may provide further information useful for species distinction, pigments other than chlorophyll and water status. Further it may allow closing the gap to remote sensing which enables the monitoring of larger spatial areas through the use of aerial or satellite spectral data. However aerial or satellite derived spectral data introduces greater variability in the transition from the leaf to the canopy level, is limited in resolution and may not be used for plantations under shelterwood. The use of Chl fluorescence data derived from the fast fluorescence induction curve was found to be well applicable across different species, thus enabling a comparative assessment of energy trapping and transport, providing an additional tool in the assessment of plant fitness at a single point in time or integrated over periods of time. Correlations of several JIP-test parameters derived from Chl fluorescence induction transients to SPAD values were observed during the seasonal monitoring in 2012 and 2013, with and without the inclusion of signals measured in developing and senescent leaves. During these consecutive years high temperatures as well as soil water deficits were recorded, which did not result in significantly altered OJIP transients after night-time recovery. It has been shown in this thesis, however, that heat, cold as well as drought stress may result in transient alterations and thus in JIP-test parameter changes without concomitant decreases of Chl content. Lower chlorophyll contents in developing and senescing leaves were associated with certain lower or higher JIP-test parameter values (i.e. RC/ABS, V_J) under unstressed conditions, however, JIP-test parameters may decrease or increase even further under stress conditions.

The data provided in this thesis allows for the first time the classification and ranking of otherwise referenceless SPAD-meter and PEA readings, in a continuum of measureable values, observable under naturally occurring seasonal and pronounced stress conditions in *Quercus* species under Central European conditions and the quantification of the buffer range to threshold values, at which severe impediments ought to be expected. The causes for detected decreases in vitality, sensed by the monitoring of functional leaf traits need to be further identified to provide sufficient silvicultural management tools in the restructuring of prone stands by species mixture and species introduction in a proactive climate change mitigation strategy.

References

- ABRAMS M. D. (1990): *Adaptations and responses to drought in Quercus species of North America*. Tree physiology, 7(1-2-3-4), 227-238.
- ADAMS W. W., WINTER K., SCHREIBER U., SCHRAMMEL P. (1990): *Photosynthesis and chlorophyll fluorescence characteristics in relationship to changes in pigment and element composition of leaves of Platanus occidentalis L. during autumnal leaf senescence*. Plant Physiology, 92(4), 1184-1190.
- ADAMS W. W., ZARTER C. R., EBBERT V., DEMMIG-ADAMS B. (2004): *Photoprotective strategies of overwintering evergreens*. Bioscience, 54(1), 41-49.
- ADDICOTT F. T. (1968): *Environmental factors in the physiology of abscission*. Plant physiology, 43(9), 1471.
- ALLEN R. G., PEREIRA L. S., RAES D., SMITH M. (1998): *Crop evapotranspiration-Guidelines for computing crop water requirements-FAO Irrigation and drainage paper 56*. FAO, Rome, 300, 6541.
- ARANDA I., CASTRO L., ALÍA R., PARDOS J. A., GIL L. (2005): *Low temperature during winter elicits differential responses among populations of the Mediterranean evergreen cork oak (Quercus suber)*. Tree Physiology, 25(8), 1085-1090.
- AREND M., KUSTER T., GÜNTHARDT-GOERG M. S., DOBBERTIN M. (2011): *Provenance-specific growth responses to drought and air warming in three European oak species (Quercus robur, Q. petraea and Q. pubescens)*. Tree Physiology, 31(3), 287-297.
- AREND M., BREM A., KUSTER T. M., GÜNTHARDT-GOERG M. S. (2012): *Seasonal photosynthetic responses of European oaks to drought and elevated daytime temperature*. Plant Biology, 15(s1), 169-176.
- ARVE LE, TORRE S, OLSEN JE AND TANINO KK (2011). *Stomatal Responses to Drought Stress and Air Humidity*. In: Abiotic Stress in Plants - Mechanisms and Adaptations, Shanker A.(Ed.), Intech Europe, 267-280.
- BAKER N. R. (2008): *Chlorophyll fluorescence: a probe of photosynthesis in vivo*. Annu. Rev. Plant Biol., 59, 89-113.
- BALASUBRAMANIAN V., MORALES A. C., CRUZ R. T., THIYAGARAJAN T. M., NAGARAJAN R., BABU M; ABDULRACHMAN S., HAI L. H. (2000): *Adaptation of the chlorophyll meter (SPAD) technology for real-time N management in rice: a review*. International Rice Research Notes, 25(1), 4-8.
- BALAZADEH S., SCHILDHAUER J., ARAÚJO W. L., MUNNÉ-BOSCH S., FERNIE A. R., PROOST S., ..., MUELLER-ROEBER B. (2014): *Reversal of senescence by N resupply to N-starved Arabidopsis thaliana: transcriptomic and metabolomic consequences*. Journal of Experimental Botany, 65(14) 3975-3992.
- BALL M. C., WOLFE J., CANNY M., HOFMANN M., NICOTRA A. B., HUGHES D. (2002): *Space and time dependence of temperature and freezing in evergreen leaves*. Functional Plant Biology, 29(11), 1259-1272.
- BAQUEDANO F. J., CASTILLO F. J. (2006): *Comparative ecophysiological effects of drought on seedlings of the Mediterranean water-saver Pinus halepensis and water-spenders Quercus coccifera and Quercus ilex*. Trees, 20(6), 689-700.
- BAQUEDANO F. J., CASTILLO F. J. (2007): *Drought tolerance in the Mediterranean species Quercus coccifera, Quercus ilex, Pinus halepensis, and Juniperus phoenicea*. Photosynthetica, 45(2), 229-238.

References

- BARBAROUX C., BRÉDA N. (2002): *Contrasting distribution and seasonal dynamics of carbohydrate reserves in stem wood of adult ring-porous sessile oak and diffuse-porous beech trees*. *Tree Physiology*, 22(17), 1201-1210.
- BAUERLE W. L., OREN R., WAY D. A., QIAN S. S., STOY P. C., THORNTON P. E., ... REYNOLDS R. F. (2012): *Photoperiodic regulation of the seasonal pattern of photosynthetic capacity and the implications for carbon cycling*. *Proceedings of the National Academy of Sciences*, 109(22), 8612-8617.
- BERRY J., BJORKMAN O. (1980): *Photosynthetic response and adaptation to temperature in higher plants*. *Annual Review of Plant Physiology*, 31(1), 491-543.
- BJÖRKMAN O., DEMMIG B. (1987): *Photon yield of O₂ evolution and chlorophyll fluorescence characteristics at 77 K among vascular plants of diverse origins*. *Planta*, 170(4), 489-504.
- BLACKBURN G. A. (2007). *Hyperspectral remote sensing of plant pigments*. *Journal of experimental botany*, 58(4), 855-867.
- BMUB (2008): *Deutsche Anpassungsstrategie an den Klimawandel*. Bundesministerium für Umwelt, Naturschutz, Bau und Reaktorsicherheit. Vom Bundeskabinett beschlossen: 17.12.2008. <http://www.bmub.bund.de>.
- BOLTE A., EISENHAUER D. R., EHRHART H. P., GROß J., HANEWINKEL M., KÖLLING C., ... AMERELLER K. (2009): *Klimawandel und Forstwirtschaft–Übereinstimmungen und Unterschiede bei der Einschätzung der Anpassungsnotwendigkeiten und Anpassungsstrategien der Bundesländer*. *vTI Agriculture and Forestry Research* 4(59), 269-278
- BOTH H., BRÜGGEMANN W. (2009): *Photosynthesis studies on European evergreen and deciduous oaks grown under Central European climate conditions. I: a case study of leaf development and seasonal variation of photosynthetic capacity in Quercus robur (L.), Q. ilex (L.) and their semideciduous hybrid, Q. × turneri (Willd.)*. *Trees*, 23(5), 1081-1090.
- BRÉDA N., HUC R., GRANIER A., DREYER E. (2006): *Temperate forest trees and stands under severe drought: a review of ecophysiological responses, adaptation processes and long-term consequences*. *Annals of Forest Science*, 63(6), 625-644.
- BRESTIČ M., ŽIVČÁK M. (2013): *PSII fluorescence techniques for measurement of drought and high temperature stress signal in crop plants: protocols and applications*. In *Molecular Stress Physiology of Plants* (87-131). Springer India.
- BRODRIBB T. J., HOLBROOK N. M. (2003): *Stomatal closure during leaf dehydration, correlation with other leaf physiological traits*. *Plant Physiology*, 132(4), 2166-2173.
- BROWN S.B., HOUGHTON J.D., HENRY G.A.F. (1991): *Chlorophyll breakdown*. In: *Chlorophylls*. CRC Press, Boca Raton, FL, USA. 465-489.
- BRÜGGEMANN, W. (1992): *Low-temperature limitations of photosynthesis in three tropical Vigna species: a chlorophyll fluorescence study*. *Photosynthesis research*, 34(2), 301-310.
- BRÜGGEMANN W., BERGMANN M., NIERBAUER K. U., PFLUG E., SCHMIDT C., WEBER D. (2009): *Photosynthesis studies on European evergreen and deciduous oaks grown under Central European climate conditions: II. Photoinhibitory and light-independent violaxanthin deepoxidation and downregulation of photosystem II in evergreen, winter-acclimated European Quercus taxa*. *Trees*, 23(5), 1091-1100.
- BURGHARDT M., RIEDERER M. (2003): *Ecophysiological relevance of cuticular transpiration of deciduous and evergreen plants in relation to stomatal closure and leaf water potential**. *Journal of Experimental Botany*, 54(389), 1941-1949.
-

-
- BUSSOTTI F., BETTINI D., GROSSONI P., MANSUINO S., NIBBI R., SODA C., TANI C. (2002): *Structural and functional traits of Quercus ilex in response to water availability*. Environmental and Experimental Botany, 47(1), 11-23.
- BUSSOTTI F., POLLASTRINI M., HOLLAND V., BRÜGGEMANN W. (2015): *Functional traits and adaptive capacity of European forests to climate change*. Environmental and Experimental Botany, 111, 91-113.
- BUSSOTTI F. (2004): *Assessment of stress conditions in Quercus ilex L. leaves by OJIP chlorophyll a fluorescence analysis*. Plant Biosystems, 138(2), 101-109.
- BUTLER W. L. (1978): *Energy distribution in the photochemical apparatus of photosynthesis*. Annual Review of Plant Physiology, 29(1), 345-378.
- CAPE J. N., PERCY K. E. (1996): *The interpretation of leaf-drying curves*. Plant, Cell & Environment, 19(3), 356-361.
- CAMARERO J. J., OLANO J. M., ALFARO S. J. A., FERNÁNDEZ-MARÍN B., BECERRIL J. M., GARCÍA-PLAZAOLA J. I. (2012): *Photoprotection mechanisms in Quercus ilex under contrasting climatic conditions*. Flora-Morphology, Distribution, Functional Ecology of Plants, 207(8), 557-564.
- CARTER G. A., KNAPP A. K. (2001): *Leaf optical properties in higher plants: linking spectral characteristics to stress and chlorophyll concentration*. American Journal of Botany, 88(4), 677-684.
- CASTRO-DÍEZ P., PUYRAVAUD J. P., CORNELISSEN J. H. C. (2000): *Leaf structure and anatomy as related to leaf mass per area variation in seedlings of a wide range of woody plant species and types*. Oecologia, 124(4), 476-486.
- CEPPI M. G., OUKARROUM A., ÇIÇEK N., STRASSER R. J., SCHANSKER G. (2012): *The IP amplitude of the fluorescence rise OJIP is sensitive to changes in the photosystem I content of leaves: a study on plants exposed to magnesium and sulfate deficiencies, drought stress and salt stress*. Physiologia plantarum, 144(3), 277-288.
- CEROVIC Z. G., MASDOUMIER G., GHOZLEN N. B., LATOUCHE G. (2012): *A new optical leaf-clip meter for simultaneous non-destructive assessment of leaf chlorophyll and epidermal flavonoids*. Physiologia plantarum, 146(3), 251-260.
- CHRISTENSEN J. H., KANIKICHARLA K. K., MARSHALL G., TURNER J. (2013): *Climate phenomena and their relevance for future regional climate change*. In: *Climate Change 2013: The Physical Science Basis*. Contribution of Working Group I to the Fifth Assessment Report of the Intergovernmental Panel on Climate Change. Cambridge University Press, Cambridge, United Kingdom and New York, NY, USA, 1217-1308.
- CORCUERA L., CAMARERO J. J., GIL-PELEGRÍN E. (2002): *Functional groups in Quercus species derived from the analysis of pressure–volume curves*. Trees, 16(7), 465-472.
- CORCUERA L., MORALES F., ABADIA A., GIL-PELEGRÍN E. (2005): *Seasonal changes in photosynthesis and photoprotection in a Quercus ilex subsp. ballota woodland located in its upper altitudinal extreme in the Iberian Peninsula*. Tree Physiology, 25(5), 599-608.
- COSTE S., BARALOTO C., LEROY C., MARCON É., RENAUD A., RICHARDSON A. D., ROGGY J.C., SCHIMANN H., UDDLING J., HÉRAULT B. (2010): *Assessing foliar chlorophyll contents with the SPAD-502 chlorophyll meter: a calibration test with thirteen tree species of tropical rainforest in French Guiana*. Annals of Forest Science, 67(6), 607.
- DAVIS P. A., CAYLOR S., WHIPPO C. W., HANGARTER R. P. (2011): *Changes in leaf optical properties associated with light-dependent chloroplast movements*. Plant, cell & environment, 34(12), 2047-2059.
-

References

- DELPERRIERE N., DUFRÉNE E., SOUDANI K., ULRICH E., CECCHINI S., BOÉ J., FRANÇOIS C. (2009): *Modelling interannual and spatial variability of leaf senescence for three deciduous tree species in France*. *Agricultural and forest meteorology*, 149(6), 938-948.
- DEMAREZ V. (1999): *Seasonal variation of leaf chlorophyll content of a temperate forest. Inversion of the PROSPECT model*. *International Journal of Remote Sensing*, 20(5), 879-894.
- DEMMIG-ADAMS B., GILMORE A. M., ADAMS W. (1996): *In vivo function of carotenoids in higher plants. Carotenoids 3*. *The FASEB Journal*, 10(4), 403-412.
- DEMMIG-ADAMS B., MOELLER D. L., LOGAN B. A., ADAMS III W. W. (1998): *Positive correlation between levels of retained zeaxanthin+ antheraxanthin and degree of photoinhibition in shade leaves of Schefflera arboricola (Hayata) Merrill*. *Planta*, 205(3), 367-374.
- DEMMIG-ADAMS B., ADAMS W. W., MATTOO A. (2006): *Photoprotection, photoinhibition, gene regulation, and environment* (Vol. 21). Springer Science & Business Media.
- DEMMIG-ADAMS B., COHU C. M., MULLER O., ADAMS III W. W. (2012): *Modulation of photosynthetic energy conversion efficiency in nature: from seconds to seasons*. *Photosynthesis research*, 113(1-3), 75-88.
- DE PURY D., FARQUHAR G. D. (1997): *Simple scaling of photosynthesis from leaves to canopies without the errors of big-leaf models*. *Plant, Cell & Environment*, 20(5), 537-557.
- DINÇ E., CEPPI M. G., TÓTH S. Z., BOTTKA S., SCHANSKER G. (2012): *The chl a fluorescence intensity is remarkably insensitive to changes in the chlorophyll content of the leaf as long as the chl a/b ratio remains unaffected*. *Biochimica et Biophysica Acta (BBA)-Bioenergetics*, 1817(5), 770-779.
- DJUMAIEVA D., LAMERS J. P. A., MARTIUS C., VLEK P. L. G. (2012): *Chlorophyll meters for monitoring foliar nitrogen in three tree species from arid Central Asia*. *Journal of Arid Environments*, 85, 41-45.
- DREYER E., LE ROUX X., MONTPIED P., DAUDET F. A., MASSON F. (2001): *Temperature response of leaf photosynthetic capacity in seedlings from seven temperate tree species*. *Tree Physiology*, 21(4), 223-232.
- DUYSENS L. N. M., SWEERS H. E. (1963): *Mechanism of two photochemical reactions in algae as studied by means of fluorescence*. *Studies on microalgae and photosynthetic bacteria*, 353-372.
- DWD (2015): *Deutscher Klimaatlas, Deutscher Wetter Dienst (German Climate Atlas, German Meteorological Service)*. Access: 23.02.2015. http://www.dwd.de/bvbw/appmanager/bvbw/dwdwww/Desktop?_nfpb=true&_pageLabel=P28800190621308654463391&switchLang=de&seCh=1.
- DWYER L. M., TOLLENAAR M., HOUWING L. (1991): *A nondestructive method to monitor leaf greenness in corn*. *Canadian Journal of Plant Science*, 71(2), 505-509.
- ELLENBERG H. (1996): *Vegetation mitteleuropas mit den Alpen*. Ulmer, Stuttgart.
- EPRON D., DREYER E. (1992): *Effects of severe dehydration on leaf photosynthesis in Quercus petraea (Matt.) Liebl.: photosystem II efficiency, photochemical and nonphotochemical fluorescence quenching and electrolyte leakage*. *Tree Physiology*, 10(3), 273-284.
- EPRON D., DREYER E., AUSSENAC G. (1993): *A comparison of photosynthetic responses to water stress in seedlings from 3 oak species: Quercus petraea (Matt) Liebl, Q rubra L and Q cerris L*. In *Annales des sciences forestières* (Vol. 50, No. Supplement, 48-60). EDP Sciences.
- ESTRELLA N., MENZEL A. (2006): *Responses of leaf colouring in four deciduous tree species to climate and weather in Germany*. *Climate Research*, 32(3), 253.
-

-
- EVANS J. R. (1989): *Photosynthesis and nitrogen relationships in leaves of C3 plants*. *Oecologia*, 78(1), 9-19.
- FIELD C. B., RANDERSON J. T., MALMSTRÖM C. M. (1995): *Global net primary production: combining ecology and remote sensing*. *Remote sensing of Environment*, 51(1), 74-88.
- FISCHER R., LORENZ M., KÖHL M., MUES V., GRANKE O., IOST S., ... DE VRIES W. (2010): *The condition of forests in Europe*. 2010. Executive Report. ICP Forests and European Commission, Hamburg and Brussels, 21.
- FLEXAS J., DIAZ-ESPEJO A., GAGO J., GALLÉ A., GALMÉS J., GULÍAS J., MEDRANO H. (2014): *Photosynthetic limitations in Mediterranean plants: a review*. *Environmental and Experimental Botany*, 103, 12-23.
- FREDLUND, D. G., & RAHARDJO, H. (1993): *Soil mechanics for unsaturated soils*. John Wiley & Sons.
- FU X., ZHOU L., HUANG J., MO W., ZHANG J., L, J., ... HUANG X. (2013): *Relating photosynthetic performance to leaf greenness in litchi: A comparison among genotypes*. *Scientia Horticulturae*, 152, 16-25.
- FUKSHANSKY L., MARTINEZ V. REMISOWSKY A., MCCLENDON J., RITTERBUSCH A., RICHTER T., MOHR H. (1993): *Absorption spectra of leaves corrected for scattering and distributional error: a radiative transfer and absorption statistics treatment*. *Photochemistry and Photobiology*, 57 (3), 538-555.
- FRANK H. A., COGDELL R. J. (1996): *Carotenoids in photosynthesis*. *Photochemistry and photobiology*, 63(3), 257-264.
- GARNIER E., SHIPLEY B., ROUMET C., LAURENT G. (2001): *A standardized protocol for the determination of specific leaf area and leaf dry matter content*. *Functional Ecology*, 15(5), 688-695.
- GHOUIL H., MONTPIED P., EPRON D., KSONTINI M., HANCHI B., DREYER E. (2003): *Thermal optima of photosynthetic functions and thermostability of photochemistry in cork oak seedlings*. *Tree Physiology*, 23(15), 1031-1039.
- GLATZER K., SCHRAMM E. (2010): *Klimabezogener Umbau der Eichenwälder mit mediterranen Eichen—Eine vorläufige Wirkungs-und Folgenabschätzung*. BiK-F Knowledge Flow Paper, (5).
- GRASSI G., MAGNANI F. (2005): *Stomatal, mesophyll conductance and biochemical limitations to photosynthesis as affected by drought and leaf ontogeny in ash and oak trees*. *Plant, Cell & Environment*, 28(7), 834-849.
- GUISSÉ B., SRIVASTAVA A., STRASSER R. J. (1995): *The polyphasic rise of the chlorophyll a fluorescence (OKJIP) in heat stressed leaves*. *Arch Sci Geneve*, 48, 147-160.
- GULÍAS J., CIFRE J., JONASSON S., MEDRANO H., FLEXAS J. (2009): *Seasonal and inter-annual variations of gas exchange in thirteen woody species along a climatic gradient in the Mediterranean island of Mallorca*. *Flora-Morphology, Distribution, Functional Ecology of Plants*, 204(3), 169-181.
- HALDIMANN P., GALLÉ A., FELLER U. (2008): *Impact of an exceptionally hot dry summer on photosynthetic traits in oak (Quercus pubescens) leaves*. *Tree physiology*, 28(5), 785-795.
- HALDIMANN P., FELLER U. (2004): *Inhibition of photosynthesis by high temperature in oak (Quercus pubescens L.) leaves grown under natural conditions closely correlates with a reversible heat-dependent reduction of the activation state of ribulose-1, 5-bisphosphate carboxylase/oxygenase*. *Plant, Cell & Environment*, 27(9), 1169-1183.
- HANEWINKEL M., CULLMANN D. A., SCHELHAAS M. J., NABUURS G. J., ZIMMERMANN N. E. (2013): *Climate change may cause severe loss in the economic value of European forest land*. *Nature Climate Change*, 3(3), 203-207.
-

References

- HARBINSON J., ROSENQVIST E. (2003): *An introduction to chlorophyll fluorescence*. In: *Practical Applications of Chlorophyll Fluorescence in Plant Biology*. Springer US, 1-29.
- HARLEY P. C., BALDOCCHI, D. D. (1995): *Scaling carbon dioxide and water vapour exchange from leaf to canopy in a deciduous forest. I. Leaf model parametrization*. Plant, Cell & Environment, 18(10), 1146-1156.
- HAVAUX M., GREPPIN H., STRASSER R. J. (1991): *Functioning of photosystems I and II in pea leaves exposed to heat stress in the presence or absence of light*. Planta, 186(1), 88-98.
- HAVAUX M. (1992): *Stress tolerance of photosystem II in vivo antagonistic effects of water, heat, and photoinhibition stresses*. Plant Physiology, 100(1), 424-432.
- HAVAUX M. (1993): *Rapid photosynthetic adaptation to heat stress triggered in potato leaves by moderately elevated temperatures*. Plant, Cell & Environment, 16(4), 461-467.
- HAWKINS T. S., GARDINER E. S., COMER G. S. (2009): *Modeling the relationship between extractable chlorophyll and SPAD-502 readings for endangered plant species research*. Journal for Nature Conservation, 17(2), 123-127.
- HENDRY G.A.F., GRIME J.P. (1993): *Methods in comparative plant ecology*. Chapman & Hall, London, UK.
- HENDRY G.A.F., PRICE A.H. (1993): *Stress indicators: chlorophylls and carotenoids*. In: *Methods in comparative plant ecology*. Chapman & Hall, London, UK.
- HJMANS R. J., CAMERON S. E., PARRA J. L., JONES P. G., JARVIS A. (2005): *Very high resolution interpolated climate surfaces for global land areas*. International journal of climatology, 25(15), 1965-1978.
- HIKOSAKA K., HIROSE T. (2000): *Photosynthetic nitrogen-use efficiency in evergreen broad-leaved woody species coexisting in a warm-temperate forest*. Tree Physiology, 20(18), 1249-1254.
- HLUG (2015): *Bodenviewer*, Hessisches Landesamt für Umwelt und Geologie (soilviewer, Hessian Agency for the Environment and Geology) Access: 23.02.2015. <http://bodenviewer.hessen.de/viewer.htm>.
- HMUELV (2014): *Waldzustandsbericht 2014*. Hessisches Ministerium für Umwelt, Klimaschutz, Landwirtschaft und Verbraucherschutz & Nordwestdeutsche Forstliche Versuchsanstalt. PAAR U., DAMMANN I., WEYMAR J., SPIELMANN M., EICHHORN, J. (Eds).
- HOLLAND V., BRÜGGEMANN W. (2011): *Photosynthetic properties of Quercus × hispanica Lam. and Q. suber L. under harsh Central European winter conditions*. Photosynthetica, 49(3), 459-465.
- HOLLAND V., KOLLER S., BRÜGGEMANN W. (2014): *Insight into the photosynthetic apparatus in evergreen and deciduous European oaks during autumn senescence using OJIP fluorescence transient analysis*. Plant Biology, 16, 801-808.
- HÖRTENSTEINER S., KRÄUTLER B. (2011): *Chlorophyll breakdown in higher plants*. Biochimica et Biophysica Acta (BBA)-Bioenergetics, 1807(8), 977-988.
- HUNT L. A., COOPER J. P. (1967): *Productivity and canopy structure in seven temperate forage grasses*. Journal of applied Ecology 4: 437-458.
- JALEEL C. A., MANIVANNAN P., WAHID A., FAROOQ M., AL-JUBURI H. J., SOMASUNDARAM R., PANNEERSELVAM R. (2009): *Drought stress in plants: a review on morphological characteristics and pigments composition*. Int. J. Agric. Biol, 11(1), 100-105.
-

-
- JEDMOWSKI C., ASHOUB A., BRÜGGEMANN W. (2013): *Reactions of Egyptian landraces of *Hordeum vulgare* and *Sorghum bicolor* to drought stress, evaluated by the OJIP fluorescence transient analysis*. Acta Physiologiae Plantarum, 35(2), 345-354.
- JEDMOWSKI C., BAYRAMOV S., BRÜGGEMANN W. (2014): *Comparative analysis of drought stress effects on photosynthesis of Eurasian and North African genotypes of wild barley*. Photosynthetica, 52(4), 564-573.
- JOHNSON P. S., SHIFLEY S. R., ROGERS R. (2009): *The ecology and silviculture of oaks*. 2nd edition. CABI Wallingford, UK
- JONES H. G. (2007): *Monitoring plant and soil water status: established and novel methods revisited and their relevance to studies of drought tolerance*. Journal of experimental botany, 58(2), 119-130.
- KALAJI H. M., SCHANSKER G., LADLE R. J., GOLTSEV V., BOSA K., ALLAKHVERDIEV S. I., ... ŽIVČÁK M. (2014): *Frequently asked questions about in vivo chlorophyll fluorescence: practical issues*. Photosynthesis research, 122(2), 121-158.
- KANT S., BI Y. M., ROTHSTEIN S. J. (2011): *Understanding plant response to nitrogen limitation for the improvement of crop nitrogen use efficiency*. Journal of Experimental Botany, 62(4), 1499-1509.
- KAUTSKY H., HIRSCH A. (1931): *Neue versuche zur Kohlensäureassimilation*. Naturwissenschaften, 19(48), 964-964.
- KITAJIMA K., HOGAN K. P. (2003): *Increases of chlorophyll a/b ratios during acclimation of tropical woody seedlings to nitrogen limitation and high light*. Plant, cell & environment, 26(6), 857-865.
- KLESSINGER M., MICHL J. (1995): *Excited states and photochemistry of organic molecules*. VCH New York.
- KOLLER S., HOLLAND V., BRÜGGEMANN W. (2013): *Effects of drought stress on the evergreen *Quercus ilex* L., the deciduous *Q. robur* L. and their hybrid *Q. × turneri* Willd.* Photosynthetica, 51(4), 574-582.
- KOLLER S., JEDMOWSKI C., KAMM K., BRÜGGEMANN W. (2014): *The South Hesse Oak Project (SHOP): Species- and site-specific efficiency of the photosynthetic apparatus of Mediterranean and Central European Oaks*. Plant Biosystems-An International Journal Dealing with all Aspects of Plant Biology, 148(2), 237-248.
- KÖLLING C. (2007): *Bäume für die Zukunft*. LWF aktuell, Magazin für Wald, Wissenschaft und Praxis, H, 60, 35-37.
- KÖRNER C., BASLER D. (2010): *Phenology under global warming*. Science, 327(5972), 1461-1462.
- KOVATS R.S., VALENTINI R., BOUWER L.M., GEORGOPOULOU E., JACOB D., MARTIN E., ROUNSEVELL M., SOUSSANA J.-F. (2014): *Europe*. In: *Climate Change 2014: Impacts, Adaptation, and Vulnerability*. Part B: Regional Aspects. Contribution of Working Group II to the Fifth Assessment Report of the Intergovernmental Panel on Climate. Cambridge University Press, Cambridge, United Kingdom and New York, NY, USA, pp. 1267-1326.
- KRAUSE G. H., WEIS E. (1991): *Chlorophyll fluorescence and photosynthesis: the basics*. Annual review of plant biology, 42(1), 313-349.
- KREYLING J., STAHLMANN R., BEIERKUHNLEIN C. (2012): *Spatial variation in leaf damage of forest trees after the extreme spring frost event in May 2011*. Allg Forst- u. Jagd-Zeitung 183, 15-22.
- LACOINTE A., KAJI A., DAUDET F. A., ARCHER P., FROSSARD J. S., SAINT-JOANIS B., VANDAME M. (1993): *Mobilization of carbon reserves in young walnut trees*. Acta Botanica Gallica, 140(4), 435-441.
-

References

- LAKOWICZ J. R. (2007): *Principles of fluorescence spectroscopy*. Springer Science & Business Media.
- LANG M., LICHTENTHALER H. K. (1991): *Changes in the blue-green and red fluorescence-emission spectra of beech leaves during the autumnal chlorophyll breakdown*. *Journal of plant physiology*, 138(5), 550-553.
- LARCHER W. (1994): *Ökophysiologie der Pflanzen (Ecophysiology of plants)*. Stuttgart: Eugen Ulmer.
- LARCHER W. (2000): *Temperature stress and survival ability of Mediterranean sclerophyllous plants*. *Plant biosystems*, 134(3), 279-295.
- LARCHER W. (2003): *Physiological plant ecology: ecophysiology and stress physiology of functional groups*. Springer Science & Business Media.
- LICHTENTHALER H.K. (1987): *Chlorophylls and Carotenoids: Pigments of photosynthetic biomembranes*. In: *Methods in Enzymology* 148, 99. 350-382. Academic Press Inc, New York.
- LICHTENTHALER H. K. (1998): *The stress concept in plants: an introduction*. *Annals of the New York Academy of Sciences*, 851(1), 187-198.
- LICHTENTHALER H. K., BABANI F., LANGSDORF G., BUSCHMANN C. (2001): *Measurement of differences in red chlorophyll fluorescence and photosynthetic activity between sun and shade leaves by fluorescence imaging*. *Photosynthetica*, 38(4), 521-529.
- Lichtenthaler H. K., Buschmann C., Knapp M. (2005): *How to correctly determine the different chlorophyll fluorescence parameters and the chlorophyll fluorescence decrease ratio R_{Fd} of leaves with the PAM fluorometer*. *Photosynthetica*, 43(3), 379-393.
- MADEIRA A. C., FERREIRA A., DE VARENNES A., VIEIRA M. I. (2003): *SPAD meter versus tristimulus colorimeter to estimate chlorophyll content and leaf color in sweet pepper*. *Communications in soil science and plant analysis*, 34(17-18), 2461-2470.
- MARENCO R. A., ANTEZANA-VERA S. A., NASCIMENTO H. C. S. (2009): *Relationship between specific leaf area, leaf thickness, leaf water content and SPAD-502 readings in six Amazonian tree species*. *Photosynthetica*, 47(2), 184-190.
- MARKWELL J., OSTERMAN J. C., MITCHELL J. L. (1995): *Calibration of the Minolta SPAD-502 leaf chlorophyll meter*. *Photosynthesis Research*, 46(3), 467-472.
- MARTÍNEZ D. E., GUIAMET J. J. (2004): *Distortion of the SPAD 502 chlorophyll meter readings by changes in irradiance and leaf water status*. *Agronomie*, 24(1), 41-46.
- MARTÍNEZ-FERRI E., MANRIQUE E., VALLADARES F., BALAGUER L. (2004): *Winter photoinhibition in the field involves different processes in four co-occurring Mediterranean tree species*. *Tree physiology*, 24(9), 981-990.
- MATHUR S., JAJOO A., MEHTA P., BHARTI S. (2011): *Analysis of elevated temperature-induced inhibition of photosystem II using chlorophyll a fluorescence induction kinetics in wheat leaves (*Triticum aestivum*)*. *Plant Biology*, 13(1), 1-6.
- MENZEL A. (2003): *Plant phenological anomalies in Germany and their relation to air temperature and NAO*. *Climatic Change*, 57(3), 243-263.
- MIERSCH I., HEISE J., ZELMER I., HUMBECK K. (2000): *Differential degradation of the photosynthetic apparatus during leaf senescence in barley (*Hordeum vulgare* L.)*. *Plant Biology*, 2(6), 618-623.
- MIYAZAWA S. I., SATOMI S., TERASHIMA I. (1998): *Slow leaf development of evergreen broad-leaved tree species in Japanese warm temperate forests*. *Annals of Botany*, 82(6), 859-869.
-

-
- MOHAMMED G. H., ZARCO-TEJADA P., MILLER J. R. (2003): *Applications of chlorophyll fluorescence in forestry and ecophysiology*. In *Practical applications of chlorophyll fluorescence in plant biology*. Springer US, 79-124.
- MOHANTY P., KRESLAVSKI V. D., KLIMOV V. V., LOS D. A., MIMURO M., CARPENTIER R., ALLAKHVERDIEV S. I. (2012): *Heat stress: susceptibility, recovery and regulation*. In *Photosynthesis*. Springer Netherlands, pp. 251-274.
- MONJE O. A., BUGBEE B. (1992): *Inherent limitations of nondestructive chlorophyll meters: a comparison of two types of meters*. HortScience, 27(1), 69-71.
- MORALES F., ABADÍA A., ABADÍA J. (2006): *Photoinhibition and photoprotection under nutrient deficiencies, drought and salinity*. In *Photoprotection, photoinhibition, gene regulation, and environment*. Springer Netherlands, 65-85.
- MORE D., WHITE J. (2002): *The illustrated encyclopedia of trees*. Timber Press. Oregon.
- MORECROFT M. D., STOKES V. J., MORISON J. I. L. (2003): *Seasonal changes in the photosynthetic capacity of canopy oak (*Quercus robur*) leaves: the impact of slow development on annual carbon uptake*. International Journal of Biometeorology, 47(4), 221-226.
- MÜLLER-STOLL W. R. (1947): *Der Einfluss der Ernährung auf die Xeromorphie der Hochmoorpflanzen*. Planta, 35(1), 225-251.
- MUNNÉ-BOSCH S., ALEGRE L. (2004): *Die and let live: leaf senescence contributes to plant survival under drought stress*. Functional Plant Biology, 31(3), 203-216.
- NARDINI A. (2001): *Are sclerophylls and malacophylls hydraulically different?*. Biologia Plantarum, 44(2), 239-245.
- NAUŠ J., PROKOPOVÁ J., ŘEBÍČEK J., ŠPUNDOVÁ M. (2010): *SPAD chlorophyll meter reading can be pronouncedly affected by chloroplast movement*. Photosynthesis research, 105(3), 265-271.
- NIEMANN G. J., PUREVEEN J. B., EIJKEL G. B., POORTER H., BOON J. J. (1992): *Differences in relative growth rate in 11 grasses correlate with differences in chemical composition as determined by pyrolysis mass spectrometry*. Oecologia, 89(4), 567-573.
- NIGAM S. N., ARUNA R. (2008): *Stability of soil plant analytical development (SPAD) chlorophyll meter reading (SCMR) and specific leaf area (SLA) and their association across varying soil moisture stress conditions in groundnut (*Arachis hypogaea* L.)*. Euphytica, 160(1), 111-117.
- NIINEMETS Ü. (2001): *Global-scale climatic controls of leaf dry mass per area, density, and thickness in trees and shrubs*. Ecology, 82(2), 453-469.
- NW-FVA (2013). *Waldentwicklungsszenarien für das Hessische Ried: Entscheidungsunterstützung vor dem Hintergrund sich beschleunigt ändernder Wasserhaushalts- und Klimabedingungen und den Anforderungen aus dem europäischen Schutzgebietssystem Natura 2000*. SPELLMANN et al. (Eds) Beiträge aus der Nordwestdeutschen Forstlichen Versuchsanstalt (Vol. 10). Universitätsverlag Göttingen.
- OUKARROUM A., EL MADIDI S., SCHANSKER G., STRASSER R. J. (2007): *Probing the responses of barley cultivars (*Hordeum vulgare* L.) by chlorophyll a fluorescence OLKJIP under drought stress and re-watering*. Environmental and Experimental Botany, 60(3), 438-446.
- OUKARROUM A., SCHANSKER G., STRASSER R. J. (2009): *Drought stress effects on photosystem I content and photosystem II thermotolerance analyzed using Chl a fluorescence kinetics in barley varieties differing in their drought tolerance*. Physiologia Plantarum, 137(2), 188-199.
-

References

- PARRY C., BLONQUIST J.M., BUGBEE B. (2014): *In situ measurement of leaf chlorophyll concentration: analysis of the optical/absolute relationship*. Plant, Cell & Environment, 1-13.
- PEGUERO-PINA J. J., SANCHO-KNAPIK D., MORALES F., FLEXAS J., GIL-PELEGRÍN E. (2009): *Differential photosynthetic performance and photoprotection mechanisms of three Mediterranean evergreen oaks under severe drought stress*. Functional Plant Biology, 36(5), 453-462.
- PENG S., GARCÍA F. V., LAZA R. C., CASSMAN K. G. (1993): *Adjustment for specific leaf weight improves chlorophyll meter's estimate of rice leaf nitrogen concentration*. Agronomy Journal, 85(5), 987-990.
- PENG S., LAZA M. R. C., GARCIA F. V., CASSMAN K. G. (1995): *Chlorophyll meter estimates leaf area-based nitrogen concentration of rice*. Communications in Soil Science & Plant Analysis, 26(5-6), 927-935.
- PEÑUELAS J., FILELLA I. (1998): *Visible and near-infrared reflectance techniques for diagnosing plant physiological status*. Trends in plant science, 3(4), 151-156.
- PERCIVAL G. C., KEARY I. P., NOVISS K. (2008): *The potential of a chlorophyll content SPAD meter to quantify nutrient stress in foliar tissue of sycamore (Acer pseudoplatanus), English oak (Quercus robur), and european beech (Fagus sylvatica)*. Arboriculture & urban forestry, 34(2), 89-100.
- PÉREZ-HARGUINDEGUY N., DÍAZ S., GARNIER E., LAVOREL S., POORTER H., JAUREGUBERRY P., ..., CORNELISSEN J. H. C. (2013): *New handbook for standardised measurement of plant functional traits worldwide*. Australian Journal of Botany, 61(3), 167-234.
- PETERSEN R. (2007): *Eichen-Trupp-Pflanzung-erste Ergebnisse einer Versuchsfläche im NFA Neuhaus*. Forst und Holz, 62(3), 19.
- PFLUG E., BRÜGGEMANN W. (2012): *Frost-acclimation of photosynthesis in overwintering Mediterranean holm oak, grown in Central Europe*. International Journal of Plant Biology, 3(1), e1.
- PINKARD E. A., PATEL V., MOHAMMED C. (2006): *Chlorophyll and nitrogen determination for plantation-grown Eucalyptus nitens and E. globulus using a non-destructive meter*. Forest Ecology and Management, 223(1), 211-217.
- PINTÓ-MARIJUAN M., MUNNÉ-BOSCH S. (2014): *Photo-oxidative stress markers as a measure of abiotic stress-induced leaf senescence: advantages and limitations*. Journal of experimental botany, 65(14), 3845-3857.
- POLLEY H., KROIHER F. (2006): *Struktur und regionale Verteilung des Holzvorrates und des potenziellen Rohholzaufkommens in Deutschland im Rahmen der Clusterstudie Forst-und Holzwirtschaft*. Arbeitsbericht, Institut für Waldökologie und Waldinventuren.
- POORTER H., NIINEMETS Ü., POORTER L., WRIGHT I. J., VILLAR R. (2009): *Causes and consequences of variation in leaf mass per area (LMA): a meta-analysis*. New Phytologist, 182(3), 565-588.
- POSSEN B. J., ANTONONEN M. J., OKSANEN E., ROUSI M., HEINONEN J., KOSTIAINEN K., ... VAPAAVUORI E. M. (2014): *Variation in 13 leaf morphological and physiological traits within a silver birch (Betula pendula) stand and their relation to growth*. Canadian Journal of Forest Research, 44(6), 657-665.
- RABINOWITCH E. (1951): *Photosynthesis and Related Processes*. Interscience Publishers, Inc., New York
- RAMÍREZ-VALIENTE J. A., SÁNCHEZ-GÓMEZ D., ARANDA I., VALLADARES F. (2010): *Phenotypic plasticity and local adaptation in leaf ecophysiological traits of 13 contrasting cork oak populations under different water availabilities*. Tree physiology, 30(5), 618-627.
- REICH P. B., WALTERS M. B., ELLSWORTH D. S. (1997): *From tropics to tundra: global convergence in plant functioning*. Proceedings of the National Academy of Sciences, 94(25), 13730-13734.
-

-
- REICH P. B., ELLSWORTH D. S., WALTERS M. B. (1998): *Leaf structure (specific leaf area) modulates photosynthesis–nitrogen relations: evidence from within and across species and functional groups*. *Functional Ecology*, 12(6), 948-958.
- RENNENBERG H., SEILER W., MATYSSEK R., GESSLER A., KREUZWIESER J. (2004): *Die Buche (Fagus sylvatica L.)—ein Waldbaum ohne Zukunft im südlichen Mitteleuropa*. *Allgemeine Forst- und Jagdzeitung*, 175(10-11), 210-224.
- RICHARDSON A. D., DUIGAN S. P., BERLYN G. P. (2002): *An evaluation of noninvasive methods to estimate foliar chlorophyll content*. *New Phytologist*, 153(1), 185-194.
- ROCHE P., DÍAZ-BURLINSON N., GACHET S. (2004): *Congruency analysis of species ranking based on leaf traits: which traits are the more reliable?*. *Plant Ecology*, 174(1), 37-48.
- ROSENQVIST E., VAN KOOTEN O. (2003): *Chlorophyll fluorescence: a general description and nomenclature*. In: *Practical Applications of Chlorophyll Fluorescence in Plant Biology*. Springer US, 31-77.
- ROSSINI M., PANIGADA C., MERONI M., COLOMBO R. (2006): *Assessment of oak forest condition based on leaf biochemical variables and chlorophyll fluorescence*. *Tree physiology*, 26(11), 1487-1496.
- RUIZ-ESPINOZA F. H., MURILLO-AMADOR B., GARCIA-HERNANDEZ J. L., FENECH-LARIOS L., RUEDA-PUENTE E. O., TROYO-DIEGUEZ E., KAYA C., BELTRAN-MORALES A. (2010): *Field evaluation of the relationship between chlorophyll content in basil leaves and a portable chlorophyll meter (SPAD-502) readings*. *Journal of plant nutrition*, 33(3), 423-438.
- RYSER P., BERNARDI J., MERLA A. (2008): *Determination of leaf fresh mass after storage between moist paper towels: constraints and reliability of the method*. *Journal of experimental botany*, 59(9), 2461-2467.
- SACK L., COWAN P. D., JAIKUMAR N., HOLBROOK N. M. (2003): *The 'hydrology' of leaves: co-ordination of structure and function in temperate woody species*. *Plant, Cell & Environment*, 26(8), 1343-1356.
- SACK L., PASQUET-KOK J., PROMETHEUSWIKI CONTRIBUTORS (2011): *Leaf pressure-volume curve parameters*. In: *PrometheusWiki*. Access: July 2013. [http://www.publish.csiro.au/prometheuswiki/tiki-pagehistory.php?page=Leaf pressure-volume curve parameters&preview=16](http://www.publish.csiro.au/prometheuswiki/tiki-pagehistory.php?page=Leaf%20pressure-volume%20curve%20parameters&preview=16)
- SALLEO S., GULLO M. L. (1990): *Sclerophylly and plant water relations in three Mediterranean Quercus species*. *Annals of Botany*, 65(3), 259-270.
- SCHANSKER G., TÓTH S. Z., STRASSER R. J. (2005): *Methylviologen and dibromothymoquinone treatments of pea leaves reveal the role of photosystem I in the Chl a fluorescence rise OJIP*. *Biochimica et Biophysica Acta (BBA)-Bioenergetics*, 1706(3), 250-261.
- SCHLEIP C., CORNELIUS C., MENZEL A. (2011): *Wenn der Maitrieb zum Märztrieb wird*. *LWF Aktuell* 85, 15-18.
- SCHMIEDINGER A., BACHMANN M., KÖLLING C., SCHIRMER R. (2009): *How to select tree species for trials against the background of climate change?*. *Forstarchiv*, 80(1), 15-22.
- SCHREIBER U., BERRY J. A. (1977): *Heat-induced changes of chlorophyll fluorescence in intact leaves correlated with damage of the photosynthetic apparatus*. *Planta*, 136(3), 233-238.
- SCHREIBER U. (2003): *In Vivo Chlorophyll Fluorescence: Assessment and Analysis of Photosynthesis Function*. In: *Physiological plant ecology: ecophysiology and stress physiology of functional groups*. Larcher, W., Springer Science & Business Media., pp. 73-77.
-

References

- SILLA F., GONZÁLEZ-GIL A., GONZÁLEZ-MOLINA M. E., MEDIÁVILLA S., ESCUDERO A. (2010): *Estimation of chlorophyll in Quercus leaves using a portable chlorophyll meter: effects of species and leaf age*. Annals of forest science, 67(1), 108.
- SIMS D. A., GAMON J. A. (2002): *Relationships between leaf pigment content and spectral reflectance across a wide range of species, leaf structures and developmental stages*. Remote sensing of environment, 81(2), 337-354.
- SOLOMON S., QIN D., MANNING M., CHEN Z., MARQUIS M., AVERYT K. B., ... MILLER H. L. (2007): *IPCC, Climate change 2007: the physical science basis*. Contribution of working group I to the fourth assessment report of the intergovernmental panel on climate change. <http://www.ipcc.ch>.
- SPARKS T. H., CAREY P. D. (1995): *The responses of species to climate over two centuries: an analysis of the Marsham phenological record, 1736-1947*. Journal of Ecology, 321-329.
- SRIVASTAVA A., GUISSÉ B., GREPPIN H., STRASSER R. J. (1997). *Regulation of antenna structure and electron transport in photosystem II of Pisum sativum under elevated temperature probed by the fast polyphasic chlorophyll a fluorescence transient: OKJIP*. Biochimica et Biophysica Acta (BBA)-Bioenergetics, 1320(1), 95-106.
- STEINBAUER M. J. (2001): *Specific leaf weight as an indicator of juvenile leaf toughness in Tasmanian bluegum (Eucalyptus globulus ssp. globulus): implications for insect defoliation*. Australian Forestry, 64(1), 32-37.
- STIRBET A., GOVINDJEE (2011). *On the relation between the Kautsky effect (chlorophyll a fluorescence induction) and photosystem II: basics and applications of the OJIP fluorescence transient*. Journal of Photochemistry and Photobiology B: Biology, 104(1), 236-257.
- STIRBET A., GOVINDJEE (2012): *Chlorophyll a fluorescence induction: a personal perspective of the thermal phase, the J-I-P rise*. Photosynthesis research, 113(1-3), 15-61.
- STOCKER O. (1931): *Transpiration und Wasserhaushalt in verschiedenen Klimazonen. I. Untersuchungen an der arktischen Baumgrenze in Schwedisch-Lappland*. Jahrbücher für wissenschaftliche Botanik 75: 494-549.
- STRASSER B.J., STRASSER R.J. (1995): *Measuring fast fluorescence transients to address environmental questions: The JIP-test*. In: *Photosynthesis: from Light to Biosphere* EDS: MATHIS P., Kluwer Academic Publishers, Dordrecht, The Netherlands, 977-980
- STRASSER B. J. (1997): *Donor side capacity of photosystem II probed by chlorophyll a fluorescence transients*. Photosynthesis Research, 52(2), 147-155.
- STRASSER R. J., SRIVASTAVA A., TSIMILLI-MICHAEL M. (2000): *The fluorescence transient as a tool to characterize and screen photosynthetic samples*. In: *Probing photosynthesis: mechanisms, regulation and adaptation*. Eds: YUNUS M. *et al.*, Taylor & Francis, London, 445-483.
- STRASSER R. J., TSIMILLI-MICHAEL M., SRIVASTAVA A. (2004): *Analysis of the chlorophyll a fluorescence transient*. In: *Chlorophyll fluorescence: A signature of photosynthesis*. Advances in Photosynthesis and Respiration. Vol. 19. Eds: PAPAGEORGIU C., GOVINDJEE. Kluwer, Dordrecht, Netherlands. 321-362.
- STRASSER R. J., TSIMILLI-MICHAEL M., QIANG S., GOLTSEV V. (2010): *Simultaneous in vivo recording of prompt and delayed fluorescence and 820-nm reflection changes during drying and after rehydration of the resurrection plant Haberlea rhodopensis*. Biochimica et Biophysica Acta (BBA)-Bioenergetics, 1797(6), 1313-1326.
- TACH L.B., SHAPCOTT A., SCHMIDT S., CRITCHLEY C. (2007): *The OJIP fast fluorescence rise characterizes Graptophyllum species and their stress responses*. Photosynthesis Research, 94(2-3), 423-436.
-

-
- TAIZ L., ZEIGER E. (2010): *Plant physiology*. Sunderland, MA, USA.
- TERASHIMA I., SAEKI T. (1983): *Light environment within a leaf I. Optical properties of paradermal sections of Camellia leaves with special reference to differences in the optical properties of palisade and spongy tissues*. *Plant and Cell Physiology*, 24(8), 1493-1501.
- TERASHIMA I., HIKOSAKA K. (1995): *Comparative ecophysiology of leaf and canopy photosynthesis*. *Plant, Cell & Environment*, 18(10), 1111-1128.
- THOMAS H., OUGHAM H. (2014): *The stay-green trait*. *Journal of experimental botany*, 65(14), 3889-3900.
- TORRES-NETTO A., CAMPOSTRINI E., DE OLIVEIRA J. G., BRESSAN-SMITH R. E. (2005): *Photosynthetic pigments, nitrogen, chlorophyll a fluorescence and SPAD-502 readings in coffee leaves*. *Scientia Horticulturae*, 104(2), 199-209.
- TÓTH S. Z., SCHANSKER G., GARAB G., STRASSER R. J. (2007): *Photosynthetic electron transport activity in heat-treated barley leaves: the role of internal alternative electron donors to photosystem II*. *Biochimica et Biophysica Acta (BBA)-Bioenergetics*, 1767(4), 295-305.
- TSIMILLI-MICHAEL M., PÊCHEUX M., STRASSER R. J. (1999): *Light and heat stress adaptation of the symbionts of temperate and coral reef foraminifers probed in hospite by the chlorophyll a fluorescence kinetics*. *Zeitschrift für Naturforschung C*, 54(12), 671-680.
- UCHINO H., WATANABE T., RAMU K., SAHRAWAT K. L., MARIMUTHU S., WANI S. P., ITO O. (2013): *Calibrating chlorophyll meter (SPAD-502) reading by specific leaf area for estimating leaf nitrogen concentration in sweet sorghum*. *Journal of Plant Nutrition*, 36(10), 1640-1646.
- UDDLING J., GELANG-ALFREDSSON J., PIIKKI K., PLEIJEL H. (2007): *Evaluating the relationship between leaf chlorophyll concentration and SPAD-502 chlorophyll meter readings*. *Photosynthesis Research*, 91(1), 37-46.
- VAIERETTI M. V., DÍAZ S., VILE D., GARNIER E. (2007): *Two measurement methods of leaf dry matter content produce similar results in a broad range of species*. *Annals of botany*, 99(5), 955-958.
- VAN DEN BERG A. K., PERKINS T. D. (2004): *Evaluation of a portable chlorophyll meter to estimate chlorophyll and nitrogen contents in sugar maple (Acer saccharum Marsh.) leaves*. *Forest Ecology and Management*, 200(1), 113-117.
- VAN HEERDEN P. D. R., SWANEPOEL J. W., KRÜGER G. H. J. (2007): *Modulation of photosynthesis by drought in two desert scrub species exhibiting C 3-mode CO 2 assimilation*. *Environmental and experimental botany*, 61(2), 124-136.
- VILE D., GARNIER E., SHIPLEY B., LAURENT G., NAVAS M. L., ROUMET C., ..., WRIGHT I. J. (2005): *Specific leaf area and dry matter content estimate thickness in laminar leaves*. *Annals of botany*, 96(6), 1129-1136.
- VON CAEMMERER VON S. V., FARQUHAR G. D. (1981): *Some relationships between the biochemistry of photosynthesis and the gas exchange of leaves*. *Planta*, 153(4), 376-387.
- WELLBURN A. R. (1994): *The spectral determination of chlorophylls a and b, as well as total carotenoids, using various solvents with spectrophotometers of different resolution*. *Journal of plant physiology*, 144(3), 307-313.
- WHITE J. W., MONTES-R C. (2005): *Variation in parameters related to leaf thickness in common bean (Phaseolus vulgaris L.)*. *Field crops research*, 91(1), 7-21.
- WITKOWSKI E. T. F., LAMONT B. B. (1991): *Leaf specific mass confounds leaf density and thickness*. *Oecologia*, 88(4), 486-493.
-

References

- WRIGHT I. J., REICH P. B., WESTOBY M., ACKERLY D. D., BARUCH Z., BONGERS F., ... VILLAR R. (2004): *The worldwide leaf economics spectrum*. *Nature*, 428 (6985), 821-827.
- YAMAMOTO A., NAKAMURA T., ADU-GYAMFI J. J., SAIGUSA M. (2002): *Relationship between chlorophyll content in leaves of sorghum and pigeonpea determined by extraction method and by chlorophyll meter (SPAD-502)*. *Journal of Plant Nutrition*, 25(10), 2295-2301.
- YORDANOV I., DILOVA S., PETKOVA R., PANGELOVA T., GOLTSEV V., KUSS K. H. (1986): *Mechanisms of the temperature damage and acclimation of the photosynthetic apparatus*. *Photobiochemistry and photobiophysics* 12, 147-155.
- ZHANG J. L., POORTER L., HAO G. Y., CAO K. F. (2012): *Photosynthetic thermotolerance of woody savanna species in China is correlated with leaf life span*. *Annals of botany*, mcs172.
- ZHOU S., DUURSMA R. A., MEDLYN B. E., KELLY J. W., PRENTICE I. C. (2013): *How should we model plant responses to drought? An analysis of stomatal and non-stomatal responses to water stress*. *Agricultural and Forest Meteorology*, 182, 204-214.
- ZINGG A., BÜRGI A. (2008): *Trockenperioden seit 1900 und Waldwachstum: eine Analyse langfristiger Datenreihen (Drought periods since 1900 and growth of forest stands: an analysis of long-term data series)*. *Schweizerische Zeitschrift für Forstwesen*, 159(10), 352-361.
- ŽIVČÁK M., BRESTIČ M., OLŠOVSKÁ K., SLAMKA P. (2008): *Performance index as a sensitive indicator of water stress in *Triticum aestivum* L.* *Plant Soil Environ*, 54(4), 133-139.

List of Figures

Figure 1:	Shift of the potential range of major tree species in Germany.....	12
Figure 2:	Schematic representation of the light reaction and its principle organization within the thylacoid membrane.....	17
Figure 3:	Fast and slow chlorophyll fluorescence transients.....	19
Figure 4:	Experimental forest site in Frankfurt Schwanheim (FR).....	24
Figure 5:	Estimation of plant developmental parameters through SPAD seasonal variability.	34
Figure 6:	Pressure-volume curve constructed from subsequent measurements of leaf water content and water potential on a dehydrating twig.	38
Figure 7:	Schematic illustration of temperature increases during the heat stress experiment 2012.....	44
Figure 8:	Temperature dependent rise of F_0 and derived parameters of PSII thermostability (example curve).	45
Figure 9:	Temperature and soil water deficit at Frankfurt Schwanheim in 2012 and 2013.....	51
Figure 10:	Spatial variability of selected abiotic growth factors at the FR site.	53
Figure 11:	Soil profile of experimental forest site Frankfurt Schwanheim (FR).	54
Figure 12:	Seasonal variability of leaf dry matter content (LDMC) and specific leaf area (SLA_{DW}).	56
Figure 13:	Interspecific variation of morphological leaf traits.....	58
Figure 14:	Estimation of leaf thickness with leaf density and LMA_{FW}	59
Figure 15:	Relationship of leaf chlorophylls to leaf carotenoids.	60
Figure 16:	Relationship of chlorophyll a (Chl a) to chlorophyll b (Chl b).....	61
Figure 17:	Relation of leaf chlorophyll to leaf nitrogen.....	62
Figure 18:	Correlation of SPAD-values to chlorophyll contents on different reference bases.....	64
Figure 19:	Empirical model fit for the total SPAD chlorophyll dataset.	66
Figure 20:	Species-specific fit of homographic model with 90% prediction bands of area based chlorophyll content to SPAD correlation.	67
Figure 21:	Relationships of chlorophyll a and b and carotenoid concentrations and their ratios to SPAD-measurements.	68
Figure 22:	Species-specific fit of polynomial model with 90% prediction bands of area based leaf nitrogen content to SPAD correlation.	70
Figure 23:	Diurnal variability of SPAD-readings of 5 different <i>Quercus</i> taxa on a hot summer day.	72
Figure 24:	Temperature dependency of SPAD-readings in <i>Q. ilex</i>	73

List of Figures

Figure 25: Gaussian fit of frequency distribution for species level in Frankfurt Schwanheim experimental forest site (FR).	75
Figure 26: Spatial distribution of leaf greenness at the FR site.	76
Figure 27: Inter-annual comparison of the beginning of senescence and the rate of SPAD-value decline at Frankfurt Schwanheim (FR).	78
Figure 28: Seasonal variability of SPAD-readings and derived developmental parameters for 2013 at Frankfurt Schwanheim (FR).	80
Figure 29: Correlation of mean SPAD-values in core vegetation time in two consecutive years.	81
Figure 30: Seasonal variability of F_v/F_m and $\ln PI_{abs.}$ in 2012 and 2013 at Frankfurt Schwanheim (FR).	83
Figure 31: Integrals of individual leaf time courses of $\ln PI_{abs}$ in 2012 and 2013 in Frankfurt Schwanheim (FR).	84
Figure 32: Fluorescence transient alterations during leaf development and senescence.	86
Figure 33: Relationship between JIP-test parameters during leaf development, senescence and steady state.	88
Figure 34: Correlations between SPAD-values and JIP-test parameters.	90
Figure 35: Relationship of leaf water content per area with leaf thickness.	92
Figure 36: Pressure-volume curve and derived parameters.	93
Figure 37: Responses of <i>Q. ilex</i> , <i>Q. pubescens</i> and <i>Q. robur</i> to soil water deficit.	94
Figure 38: Fluorescence response of <i>Q. ilex</i> , <i>Q. pubescens</i> and <i>Q. ilex</i> to decreasing soil water content.	95
Figure 39: Relationship of PI_{abs} and gas-exchange in <i>Q. robur</i> , <i>Q. ilex</i> and <i>Q. x turneri</i> during water stress.	96
Figure 40: Gas-exchange data as affected by drought stress.	97
Figure 41: Diurnal fluctuations of leaf temperature.	99
Figure 42: Temperature induced alterations of Chl a fluorescence transients and JIP-test parameters in plants acclimated to 35°C.	102
Figure 43: Daily trend of ground temperature and height of snow in the winter 2012/2013.	104
Figure 44: Variations of pigment ratios in <i>Q. ilex</i> during winter conditions.	106
Figure 45: Winter response of photosynthetic leaf traits in <i>Q. ilex</i>	107
Figure 46: Development of maximum quantum yield (Φ_{P0}) of <i>Q. ilex</i> during the winter 2012/2013.	108
Figure 47: Relationships between JIP-test parameters during the natural annual time-course and under cold stress conditions.	109
Figure 48: Daily maximal sap flow velocities of <i>Q. ilex</i> during winter 2012/2013. ...	110
Figure 49: Map of summer days and water balance in Hesse.	111
Figure 50: Historical record of late frost events at Frankfurt.	129

List of Tables

Table 1:	OJIP transient normalisations.	35
Table 2:	Plant material used in the drought stress and heat stress experiment 2013.	36
Table 3:	Dates of measurements performed on <i>Q. ilex</i> trees at the Botanical Garden at Frankfurt, Riedberg and the experimental forest site in Frankfurt Schwanheim (FR) in the course of the winter monitoring program.	48
Table 4:	Species-specific correlation coefficients of SPAD-value and chlorophyll content with different reference bases..	65
Table 5:	Species-specific model fit for the correlation of area based chlorophyll content and SPAD-value..	66
Table 6:	Best-fit parameter values for calculation of Chl a, Chl b, Cars and their ratios from SPAD measurements..	68
Table 7:	Best-fit species-specific parameters of 2. order polynomial regression for estimating leaf nitrogen with SPAD-readings.....	69
Table 8:	SPAD reading variability on leaf level in 5 different <i>Quercus</i> taxa.....	71
Table 9:	Intrinsic variability of SPAD-values on species- and individual tree level at Frankfurt Schwanheim (FR).	74
Table 10:	Acclimation of PSII thermostability to increasing temperatures.	100
Table 11:	Climate parameters for the winter period 2012/2013.	103
Table 12:	Winter injury of <i>Q. ilex</i> at Frankfurt Schwanheim.	105
Table 13:	Compiled meteorological data from Frankfurt airport for the period 1949 until 2013..	148

List of abbreviations

A (lower case)	Leaf area
A (upper case)	Antheraxanthin
AdT	ambient daytime temperature
AIC	Akaike Information Criterion
AL	Actinic light
approx.	approximately
ATPase	ATP synthase/hydrolase complex
Car	Carotenoids
Chl	Chlorophyll
Chl a	Chlorophyll a
Chl b	Chlorophyll b
CI	confidence interval
cy	current year
DCMU	(3-(3',4' dichlorophenyl)-1,1' dimethylurea)
DES	De-epoxidation state
doy	day of the year
DW	dry weight
ES	Electromagnetic Spectrum
ETC	Electron Transport Chain
EXP	exponential regression
FNR	Ferredoxin NADP ⁺ - reductase
FR	Experimental Forest Site Frankfurt Schwanheim
FW	fresh weight
GPS	Global Positioning System
HOMG	homographic model
IPCC	The Intergovernmental Panel on Climate Change
LDMC	leaf dry matter content
LED	Light-emitting diode
LHC	Light Harvesting Complex
LINR	first order polynomial regression (linear)
LMA	Leaf mass per area
LT	leaf thickness
LWC	leaf water content
mw	measuring wavelenghts
N	Nitrogen

NCCI	normalised chlorophyll content index
NIR	near-infrared
NPQ	non-photochemical quenching
OEC	Oxygen-Evolving Complex
OJIP	Fast Chl a Fluorescence induction transient
PAM	Pulse amplitude modulated
PEA	Plant Efficiency Analyzer
Pheo	Phaeophytin
POLY	second order polynomial regression
PQ	Plastoquinone
PS	Photosystem
PV	pressure-volume
py	previous year
RC	Reaction Centre
rel. T	relative rate of transpiration
R _{Fd}	Fluorescence decrease ratio
RMSE	root mean square error
ROS	Reactive Oxygen Species
RWC	Relative Water Content
RWD	Relative Water Deficit (= 1-RWC)
SD	standard deviation
SLA	Specific Leaf Area
SP	saturating light pulse
SPAD	Name of Chlorophyll-meter by Konica Minolta (Special Products Analysis Division)
SWC	Saturated Water Content
T	Temperature
TLP	Turgor Loss Point
V	Violaxanthin
VPD	Vapour Pressure Deficit
x+c	xanthophylls and carotenes
Z	Zeaxanthin
φPSII	Effective quantum yield of photochemistry in the light- adapted state

For abbreviations concerning the JIP-test parameters, see Appendix II

Day of the year calendar

2012

	Jan	Feb	Mar	Apr	May	Jun	Jul	Aug	Sep	Oct	Nov	Dec
1	1	32	61	92	122	153	183	214	245	275	306	336
2	2	33	62	93	123	154	184	215	246	276	307	337
3	3	34	63	94	124	155	185	216	247	277	308	338
4	4	35	64	95	125	156	186	217	248	278	309	339
5	5	36	65	96	126	157	187	218	249	279	310	340
6	6	37	66	97	127	158	188	219	250	280	311	341
7	7	38	67	98	128	159	189	220	251	281	312	342
8	8	39	68	99	129	160	190	221	252	282	313	343
9	9	40	69	100	130	161	191	222	253	283	314	344
10	10	41	70	101	131	162	192	223	254	284	315	345
11	11	42	71	102	132	163	193	224	255	285	316	346
12	12	43	72	103	133	164	194	225	256	286	317	347
13	13	44	73	104	134	165	195	226	257	287	318	348
14	14	45	74	105	135	166	196	227	258	288	319	349
15	15	46	75	106	136	167	197	228	259	289	320	350
16	16	47	76	107	137	168	198	229	260	290	321	351
17	17	48	77	108	138	169	199	230	261	291	322	352
18	18	49	78	109	139	170	200	231	262	292	323	353
19	19	50	79	110	140	171	201	232	263	293	324	354
20	20	51	80	111	141	172	202	233	264	294	325	355
21	21	52	81	112	142	173	203	234	265	295	326	356
22	22	53	82	113	143	174	204	235	266	296	327	357
23	23	54	83	114	144	175	205	236	267	297	328	358
24	24	55	84	115	145	176	206	237	268	298	329	359
25	25	56	85	116	146	177	207	238	269	299	330	360
26	26	57	86	117	147	178	208	239	270	300	331	361
27	27	58	87	118	148	179	209	240	271	301	332	362
28	28	59	88	119	149	180	210	241	272	302	333	363
29	29	60	89	120	150	181	211	242	273	303	334	364
30	30		90	121	151	182	212	243	274	304	335	365
31	31		91		152		213	244		305		366

Appendix I

2013

	Jan	Feb	Mar	Apr	May	Jun	Jul	Aug	Sep	Oct	Nov	Dec
1	1	32	60	91	121	152	182	213	244	274	305	335
2	2	33	61	92	122	153	183	214	245	275	306	336
3	3	34	62	93	123	154	184	215	246	276	307	337
4	4	35	63	94	124	155	185	216	247	277	308	338
5	5	36	64	95	125	156	186	217	248	278	309	339
6	6	37	65	96	126	157	187	218	249	279	310	340
7	7	38	66	97	127	158	188	219	250	280	311	341
8	8	39	67	98	128	159	189	220	251	281	312	342
9	9	40	68	99	129	160	190	221	252	282	313	343
10	10	41	69	100	130	161	191	222	253	283	314	344
11	11	42	70	101	131	162	192	223	254	284	315	345
12	12	43	71	102	132	163	193	224	255	285	316	346
13	13	44	72	103	133	164	194	225	256	286	317	347
14	14	45	73	104	134	165	195	226	257	287	318	348
15	15	46	74	105	135	166	196	227	258	288	319	349
16	16	47	75	106	136	167	197	228	259	289	320	350
17	17	48	76	107	137	168	198	229	260	290	321	351
18	18	49	77	108	138	169	199	230	261	291	322	352
19	19	50	78	109	139	170	200	231	262	292	323	353
20	20	51	79	110	140	171	201	232	263	293	324	354
21	21	52	80	111	141	172	202	233	264	294	325	355
22	22	53	81	112	142	173	203	234	265	295	326	356
23	23	54	82	113	143	174	204	235	266	296	327	357
24	24	55	83	114	144	175	205	236	267	297	328	358
25	25	56	84	115	145	176	206	237	268	298	329	359
26	26	57	85	116	146	177	207	238	269	299	330	360
27	27	58	86	117	147	178	208	239	270	300	331	361
28	28	59	87	118	148	179	209	240	271	301	332	362
29	29		88	119	149	180	210	241	272	302	333	363
30	30		89	120	150	181	211	242	273	303	334	364
31	31		90		151		212	243		304		365

JIP-test parameters extracted from the fast chl a fluorescence OKJIP transient. F refers to prompt fluorescence; RC: active (Q_A reducing) reaction centre. According to STRASSER *et al.* (2010) and STIRBET & GOVINDJEE (2011).

Data extracted from the recorded fluorescence transient

F_t	Fluorescence at the time t
$F_{50\mu s}$	First reliable recorded fluorescence at 50 μ s
$F_{300\mu s} \equiv F_K$	Fluorescence intensity at the K-step (300 μ s)
$F_{2ms} \equiv F_J$	Fluorescence intensity at the J-step (2 ms)
$F_{30ms} \equiv F_I$	Fluorescence intensity at the I-step (30 ms)
F_P	Maximal recorded fluorescence intensity at the transient

Fluorescence parameters derived from the extracted data

$F_0 \equiv F_{50\mu s}$	Minimal fluorescence, when all RCs are open
$F_m (=F_P)$	Maximal fluorescence, when all RCs are closed
$F_v \equiv F_m - F_0$	Maximal variable fluorescence
$V_t \equiv (F_t - F_0) / (F_m - F_0)$	Variable fluorescence at the time t
$\Delta V_{IP} = 1 - V_I$	Relative amplitude of the I-P phase
$V_{OJ300\mu s} = (F_K - F_{50\mu s}) / (F_J - F_{50\mu s})$	Relative amplitude of the K-step
$M_0 \equiv [(\Delta F / \Delta t)_0] / (F_m - F_{50\mu s})$ $\equiv 4 (F_{300\mu s} - F_{50\mu s}) / (F_m - F_{50\mu s})$	Approximated initial slope (in ms^{-1}) of the fluorescence transient normalized on the maximal variable Fluorescence F_v

Biophysical parameters derived from the fluorescence parameters

$\phi_{P0} \equiv F_v / F_m$	Maximum quantum yield of primary photochemistry / PSII. Efficiency / probability that an absorbed photon leads to a reduction of Q_A .
$\psi_{E0} \equiv 1 - V_J$	Efficiency / probability that an electron moves further than Q_A^-
$\phi_{D0} \equiv 1 - \phi_{P0}$	Efficiency / probability that the energy of an absorbed photon is dissipated as heat.
$RC/ABS = \phi_{P0} (V_J / M_0)$	Q_A reducing RCs per PSII antenna Chl [reciprocal of $ABS/RC = \text{Absorption flux (of antenna Chls) per RC}$ (Also a measure of PSII apparent antenna size)]
$PI_{abs} \equiv RC/ABS \phi_{P0} / (1 - \phi_{P0}) \psi_{E0} / (1 - \psi_{E0})$	Performance Index (potential) for energy conservation from photons absorbed by PSII to the reduction of intersystem electron acceptors

Appendix II

Best-fit coefficient values of empirical species-specific polynomial (POLY) and homographic (HOMG) model for area based chlorophyll content to SPAD-readings. CI: 90% confidence interval.

Polynomial 2. Order (POLY) $y = A + BX + CX^2$	A			B			C		
	mean	±	CI	mean	±	CI	mean	±	CI
<i>Q. frainetto</i>	12,36	±	26,62	2,95	±	2,13	0,12	±	0,04
<i>Q. ilex</i>	-10,22	±	201,65	3,87	±	11,42	0,13	±	0,16
<i>Q. pubescens</i>	14,07	±	38,18	2,08	±	2,78	0,17	±	0,05
<i>Q. robur</i>	34,58	±	30,89	1,65	±	2,46	0,17	±	0,05
<i>Q. rubra</i>	22,47	±	29,22	2,34	±	2,33	0,16	±	0,04
<i>Q. cerris</i>	2,88	±	253,15	1,12	±	14,39	0,18	±	0,20
<i>Q. suber</i>	~-3124	±	very wide	~-153,6	±	very wide	~-1,630	±	very wide
<i>Q. x hispanica</i>	84,93	±	590,90	-5,72	±	34,93	0,34	±	0,49
<i>Q. x turneri</i>	99,23	±	110,14	-5,34	±	8,44	0,30	±	0,15
All species	25,950	±	20,587	1,413	±	1,440	0,174	±	0,025

Homographic (HOMG) $y = AX (B-x)^{-1}$	A			B		
	mean	±	CI	mean	±	CI
<i>Q. frainetto</i>	569,9	±	176,45	109,5	±	21,72
<i>Q. ilex</i>	597,4	±	220,45	107,6	±	23,37
<i>Q. pubescens</i>	470,7	±	92,95	91,45	±	10,35
<i>Q. robur</i>	542,6	±	135,35	99,44	±	15,86
<i>Q. rubra</i>	495,9	±	100,4	94,16	±	11,54
<i>Q. cerris</i>	357,2	±	83,7	84,22	±	10,40
<i>Q. suber</i>	616,6	±	751,5	101,6	±	85,88
<i>Q. x hispanica</i>	357,9	±	192,65	77,02	±	17,77
<i>Q. x turneri</i>	295,1	±	86,55	72,88	±	10,34
All species	498,7	±	53,3	95,8	±	5,9

Developmental parameters estimated from the time-course of chlorophyll-content alterations. SD: standard deviation of the mean; n: number of samples; doy: day of the year. For parameter estimation, see Figure 5. Data of time-course 2013. Different letters indicate that means of a parameter are significantly different on the species-level (one-way ANOVA with Tukey's post test).

Parameter	Unit	mean	SD		n
<i>Q. frainetto</i>					
Rate of increase	[SPAD-units/wk]	4,8	± 1,1	a/b	22
End of development	[doy]	161,9	± 7,0	a	22
Duration of Plateau	[days]	105,5	± 26,3	a/b	22
Begin of senescence	[doy]	267,0	± 26,9	a/b	22
Rate of decline	[SPAD-units/wk]	-6,1	± 3,8	a	22
<i>Q. ilex</i>					
Rate of increase	[SPAD-units/wk]	5,5	± 1,4	a	19
End of development	[doy]	177,3	± 11,0	b	19
Duration of Plateau	[days]	n.M	± n.M	-	0
Begin of senescence	[doy]	n.M	± n.M	-	0
Rate of decline	[SPAD-units/wk]	n.M	± n.M	-	0
<i>Q. pubescens</i>					
Rate of increase	[SPAD-units/wk]	4,1	± 1,4	b	24
End of development	[doy]	159,5	± 7,8	a	24
Duration of Plateau	[days]	128,4	± 36,08	a	21
Begin of senescence	[doy]	282,0	± 13,0	a	21
Rate of decline	[SPAD-units/wk]	-2,8	± 2,4	b	21
<i>Q. robur</i>					
Rate of increase	[SPAD-units/wk]	4,1	± 1,0	b	21
End of development	[doy]	166,8	± 8,3	a	21
Duration of Plateau	[days]	88,9	± 30,1	b	18
Begin of senescence	[doy]	255,0	± 30,4	b	18
Rate of decline	[SPAD-units/wk]	-4,7	± 3,2	a/b	18
<i>Q. rubra</i>					
Rate of increase	[SPAD-units/wk]	3,0	± 0,9	c	23
End of development	[doy]	164,7	± 13,8	a	23
Duration of Plateau	[days]	103,5	± 15,6	a	17
Begin of senescence	[doy]	271,0	± 11,9	a/b	17
Rate of decline	[SPAD-units/wk]	-6,6	± 4,3	a	17

Morphological leaf traits in mature leaves of different *Quercus* taxa. SE: Standard error of the mean; CI: 90% confidence interval; doy: day of the year. Different letter indicate that means are significantly different (One-way ANOVA with Tukey post test for multiple comparison).

Morphological Leaf Trait	<i>Q. cerris</i>	<i>Q. frainetto</i>	<i>Q. ilex</i> current year	<i>Q. ilex</i> previous year
<i>Leaf Dry Matter Content</i>				
LDMC [mg _{DW} g _{FW} ⁻¹]	e	a	c	d
mean ± SE	481,3 ± 3,5	431,0 ± 3,1	510,3 ± 2,5	536,4 ± 1,9
90% CI	475,4 – 487,2	425,9 – 436,2	506,1 – 514,5	533,2 – 539,6
<i>Specific Leaf Area</i>				
SLA _{DW} [m ² kg _{DW} ⁻¹]	e	a	d	d
mean ± SE	11,5 ± 0,4	15,3 ± 0,3	7,8 ± 0,1	7,6 ± 0,1
90% CI	10,8 – 12,2	14,8 – 15,7	7,6 – 8,0	7,5 – 7,8
SLA _{FW} [m ² kg _{FW} ⁻¹]	d	a	c/f	c/f
mean ± SE	5,5 ± 0,2	6,5 ± 0,1	4,0 ± 0,1	4,1 ± 0,0
90% CI	5,2 – 5,8	6,4 – 6,7	3,9 – 4,1	4,0 – 4,2
<i>Leaf Mass per Area</i>				
LMA _{DW} [g _{DW} m ⁻²]	d	b	c/e	c/f
mean ± SE	90,4 ± 3,1	67,1 ± 1,0	129,7 ± 2,3	133,2 ± 1,6
90% CI	85,2 – 95,6	65,4 – 68,8	125,8 – 133,7	130,6 – 135,8
LMA _{FW} [g _{FW} m ⁻²]	e	a/b	d	d
mean ± SE	187,7 ± 6,1	155,6 ± 2,1	254,4 ± 4,6	248,4 ± 2,9
90% CI	177,2 – 198,1	152,1 – 159,2	246,8 – 262,0	243,6 – 253,2
<i>Leaf Water Content</i>				
LWC _{FW} [mg _{H2O} g _{FW} ⁻¹]	e	a	c	d
mean ± SE	518,7 ± 3,5	569,0 ± 3,1	489,7 ± 2,5	463,6 ± 1,9
90% CI	512,8 – 524,6	563,8 – 574,1	485,5 – 493,9	460,4 – 466,8
LWC _{DW} [mg _{H2O} g _{DW} ⁻¹]	e	a	c	d
mean ± SE	1081 ± 15,2	1331 ± 18,4	962,6 ± 9,6	866,8 ± 6,7
90% CI	1055 – 1107	1301 – 1362	946,4 – 978,7	855,6 – 877,9
LWC _A [g _{H2O} m ⁻²]	e	a	c	d
mean ± SE	97,3 ± 3,2	88,5 ± 1,3	124,6 ± 2,4	115,2 ± 1,5
90% CI	91,8 – 102,7	86,3 – 90,7	120,7 – 128,6	112,7 – 117,7
Number of Samples	31	87	62	101
Sampling Times (2013)	doy 309	doy 164-312	doy 207-312	doy 141-312

Morphological Leaf Trait	<i>Q. pubescens</i>	<i>Q. robur</i>	<i>Q. rubra</i>	<i>Q. suber</i>
<i>Leaf Dry Matter Content</i>				
LDMC [mg _{DW} g _{FW} ⁻¹]	b	a	a	c
mean ± SE	464,3 ± 2,3	438,5 ± 2,4	436,5 ± 3,2	507,0 ± 2,9
90% CI	460,4 – 468,1	434,4 – 442,5	431,2 – 441,7	502,0 – 511,9
<i>Specific Leaf Area</i>				
SLA _{DW} [m ² kg _{DW} ⁻¹]	b	c	c	d
mean ± SE	13,6 ± 0,1	16,2 ± 0,2	16,9 ± 0,3	7,7 ± 0,2
90% CI	13,4 – 13,9	15,8 – 16,6	16,4 – 17,5	7,4 – 8,0
SLA _{FW} [m ² kg _{FW} ⁻¹]	a	b	b	c/e
mean ± SE	6,3 ± 0,1	7,1 ± 0,1	7,3 ± 0,1	3,9 ± 0,1
90% CI	6,2 – 6,4	6,9 – 7,2	7,2 – 7,5	3,7 – 4,0
<i>Leaf Mass per Area</i>				
LMA _{DW} [g _{DW} m ⁻²]	a	b	b	c/e
mean ± SE	74,2 ± 0,8	62,8 ± 0,8	60,8 ± 1,1	132,5 ± 3,3
90% CI	72,8 – 75,6	61,4 – 64,1	58,9 – 62,6	126,8 – 138,1
LMA _{FW} [g _{FW} m ⁻²]	a	b/c	c	d
mean ± SE	159,8 ± 1,6	143,0 ± 1,6	139,1 ± 2,2	261,2 ± 6,2
90% CI	157,2 – 162,4	140,3 – 145,7	135,4 – 142,8	250,6 – 271,8
<i>Leaf Water Content</i>				
LWC _{FW} [mg _{H2O} g _{FW} ⁻¹]	b	a	a	c
mean ± SE	535,7 ± 2,3	561,5 ± 2,4	563,5 ± 3,2	493,0 ± 2,9
90% CI	531,9 – 539,6	557,5 – 565,6	558,3 – 568,8	488,1 – 498,0
LWC _{DW} [mg _{H2O} g _{DW} ⁻¹]	b	a	a	c
mean ± SE	1158 ± 10,7	1287 ± 12,9	1301 ± 16,6	975 ± 11,6
90% CI	1141 – 1176	1265 – 1308	1274 – 1329	955 – 994,1
LWC _A [g _{H2O} m ⁻²]	a/b	b	b	c
mean ± SE	85,6 ± 0,9	80,3 ± 0,9	78,3 ± 1,3	128,7 ± 3,1
90% CI	84,1 – 87,1	78,7 – 81,8	76,2 – 80,5	123,4 – 133,9
Number of Samples	85	88	86	31
Sampling Times (2013)	doy 164-312	doy 164-312	doy 164-312	doy 309

Morphological leaf traits

Appendix V

Morphological Leaf Trait	<i>Q. x hispanica</i>	<i>Q. x turneri</i>
<i>Leaf Dry Matter Content</i>		
LDMC [mg _{DW} g _{FW} ⁻¹]	b/e	b/e
mean ± SE	465,1 ± 2,2	475,4 ± 2,7
90% CI	461,3 – 468,9	470,8 – 479,9
<i>Specific Leaf Area</i>		
SLA _{DW} [m ² kg _{DW} ⁻¹]	d	f
mean ± SE	7,3 ± 0,2	9,5 ± 0,1
90% CI	6,9 – 7,6	9,3 – 9,7
SLA _{FW} [m ² kg _{FW} ⁻¹]	e	f
mean ± SE	3,4 ± 0,1	4,5 ± 0,1
90% CI	3,2 – 3,6	4,4 – 4,6
<i>Leaf Mass per Area</i>		
LMA _{DW} [g _{DW} m ⁻²]	e	f
mean ± SE	140,7 ± 4,6	106,2 ± 1,6
90% CI	133,0 – 148,4	103,5 – 108,9
LMA _{FW} [g _{FW} m ⁻²]	f	g
mean ± SE	302,4 ± 9,5	223,4 ± 3,0
90% CI	286,2 – 318,6	218,2 – 228,5
<i>Leaf Water Content</i>		
LWC _{FW} [mg _{H2O} g _{FW} ⁻¹]	b/e	b/e
mean ± SE	534,9 ± 2,2	524,6 ± 2,7
90% CI	531,1 – 538,7	520,1 – 529,2
LWC _{DW} [mg _{H2O} g _{DW} ⁻¹]	b/e	b/e
mean ± SE	1151 ± 10,5	1106 ± 12,3
90% CI	1134 – 1169	1085 – 1127
LWC _A [g _{H2O} m ⁻²]	f	c/d
mean ± SE	161,7 ± 5,1	117,2 ± 1,7
90% CI	153,1 – 170,4	114,3 – 120,0
Number of Samples	30	32
Sampling Times (2013)	doy 309	doy 309

Bodenform Nr. 1, Bericht vom: 15.05.2012

Bodenformenarchiv: Bodenformen, Punktbeschreibung

Profaufnahme: Wald der Zukunft - Standort Schwanheimer Wald Aufgenommen am 10.05.2012

Zweck der Profilaufnahme: Gutachten / Projekterhebung Grabung
 Beprobungsintensität: Beprobung gesörter Proben - alle Horizonte Erweiterte Profilbeschreibung
 Wasserverhältnisse: nach Auskunft des Revierförsters GW bei > 3 m u. Fl. akt. Grundwasserstand: > 250 cm u Fl

Braunerde aus lössarmem, flugsandführendem Lehmsand (Hauptlage) über tiefem Flussleinsand (Pleistozän) ID = 1

Bodensystematik: *BBn* Stauassestufe: *S0*
 Entw.-Tiefstufe: *groß* Grundnassestufe: *G0*
 Bedeck.-Klasse: *Forst und Wald allgemein* Erhebung: *Friedrich*
 Eff. Wurzelraum: Haftnassestufe: *H0*
Hangnassestufe: *HGO*
 Humusform: *Rohhumusartiger Moder* Erf.-Datum: *14.05.2012*
 Zusatz: *Das frühere Projekt "Wald der Zukunft" heute SHOP (South Hesse Oak Project) steht unter Schirmherrschaft von Umweltministerin Lucia Puttrich und ist eine Kooperation von BIK-F (Biodiversität und Klima Forschungszentrum- Ein Joint Venture aus Uni Frankfurt und Senckenberg), NW-FVA (Nordwestdeutsche Forstwissenschaftliche Versuchsanstalt) StadForst Frankfurt, HLOG, Stadt Rüsselsheim, Hessenwasser und weiteren. Auf 3 Waldflächen in Südhessen (lampertheim, Rüsselsheim, Nähe Trebur und Frankfurt Schwanheim) wurden Eichenpflanzungen vorgenommen. Stieleiche, Flaumeiche, Steineiche, Ungarische Eiche und in Lampertheim zusätzlich 2 Eichenhybriden, Kiefer, Fichte und Roteiche. Hier soll über die nächsten Jahre festgelegt werden, ob diese Baumarten eine Alternative zu den bis dato eingesetzten Baumarten auf trockenen Standorten sein könnten.*

Projekt und Vertraulichkeit: keine Einschränkung, Bewertung: hoher Standard
 Raumbezug: TK25: 5917, RH: 3469167,71/5548613,038, (Ortung mit GPS-Handgerät, möglicher Fehler 10 - 1 m), Schwanheimer Wald, Waldabteilung 258 A 4
 Höhenangaben: 96 m NN (aus der Karte abgelesen, möglicher Fehler 10 - 1 m)

Reliefsituation: nicht geneigt

Auflage: L: -5 cm (von -3,5 cm bis -6 cm) (Mächt. 1 cm), Lagerungsart: locker, Streuart: Gemenge aus Blatt- und Nadelstreu
 Of: -4 cm (von -3 cm bis -5 cm) (Mächt. 3 cm), Lagerungsart: vermetzt (Nadelforma), unscharfer Übergang; Zusatz: extreme Mächtigkeitsunterschiede durch Deilen und Fahrspuren in denen sich die Streu sammelt (örtlich bis 10 cm Of)
 Oh: -1 cm (von 0 cm bis -2 cm) (Mächt. 1 cm), Lagerungsart: lose, scharfer Übergang

I, 75 cm unter GOF (Mächt. 75 cm), Lehmsand, Hauptlage, Bildungsprozess: solifluktuiv
 äol. Komponente: Lösssubstrat, arm an Komponente
 Flugsandsubstrat, deutlicher Komponentenanteil

Ah: 2 cm (2 cm bis 5 cm) u. GOF (Mächt. 2 cm), schwach schluffiger Sand, stark humos, carbonatfrei, pt2, Packungsdichte gering; Horizontgrenze deutlich, wellig, Hohlräumenanteil mittel
 Bhv: 50 cm (45 cm bis 55 cm) u. GOF (Mächt. 48 cm), schwach schluffiger Sand, sehr schwach Grus -haltig, schwach humos (h1 bis h2), carbonatfrei, pt2, Packungsdichte gering; Horizontgrenze deutlich, wellig, Hohlräumenanteil mittel

Bv: 75 cm u. GOF (Mächt. 25 cm), schwach schluffiger Sand, sehr schwach Grus -haltig, sehr schwach humos (h0 bis h1), carbonatfrei, pt3, Packungsdichte mittel; Horizontgrenze deutlich, wellig, Hohlräumenanteil mittel

II, 230 cm unter GOF (Mächt. 155 cm), Reinsand, Pleistozän, Bildungsprozess: fluviatil, (Geschiebefracht)
 Bv+ilCv: 95 cm (90 cm bis 100 cm) u. GOF (Mächt. 20 cm), Mittelsand, sehr schwach Grus -haltig, humusfrei (h0 bis h1), carbonatfrei, pt3, Packungsdichte mittel; Horizontgrenze deutlich, wellig, Hohlräumenanteil mittel

ilCv: 230 cm u. GOF (Mächt. 135 cm), grobsandiger Mittelsand (von mS bis gS), sehr schwach Grus -haltig, humusfrei, carbonatfrei, pt3, Packungsdichte deutlich, wellig, Hohlräumenanteil mittel

Lebenslauf

Persönliche Daten

Stefan Koller

Diplom Biologe

Geboren am: 12.08.1982 in Frankfurt am Main
Staatsangehörigkeit: Deutsch
Familienstand: verheiratet
1 Kind (*27.11.2014)

Adresse: An den Postwiesen 36
60488 Frankfurt am Main

Telefon: 069 17521520
Handy: 0172 6558282
E-Mail: stefankoller@web.de

Führerschein: BCE

Ausbildung

01/2011–2015

Promotion an der Goethe Universität Frankfurt
Institut für Ökologie & Evolution,
Abt. Ökophysiologie der Pflanzen, AK Brüggemann
Thema: *Ecophysiological monitoring of native and foreign Oaks in Central Europe, introduced in the framework of climate change mitigation.*

01/2011–2015

Graduiertenkolleg GRADE, Goethe Universität Frankfurt

2004–2009

Studium der Biologie (Diplom)
Goethe Universität, Frankfurt am Main

Schwerpunktfächer Hauptstudium:

- Ökologie und Evolution der Pflanzen
- Biochemie und Physiologie der Pflanzen
- Ökologie und Evolution der Tiere

07/2009

Diplom, Note: 1,1

Diplomarbeit, Note: 1,3

Dt. Zentrum für Marine Biodiversitätsforschung, Wilhelmshaven
Thema: *Untersuchungen zur Taxonomie und zum Vorkommen der Zosimidae Seifried (Copepoda: Harpacticoida) der Großen Meteorbank (Nordöstlicher Atlantik)*

10/2006

Vordiplom

07/2003–04/2004

Wehrdienst. 4/ Lazarettregiment 21. Rennerod.
BCE Führerschein, KfAusbZentr Birkenfeld (10/2003–11/2003)

1993–2003

Bettinagymnasium, Frankfurt am Main

07/2003

Abitur, Note: 1,6

1999–2000

Akademischer Austausch USA: Rome High School, Rome GA
(1 Jahr)

Forschungserfahrung

- 09/2014–02/2015 Goethe Universität, Frankfurt
Institut für Ökologie & Evolution, Abt. Ökophysiologie der Pflanzen AK. Brüggemann
Wissenschaftlicher Mitarbeiter (50%) im BMBF Projekt: *Wildgerste als genetische Ressource für abiotische Stresstoleranz unter Bedingungen des Klimawandels*
- 01/2011–07/2014 Biodiversität und Klima Forschungszentrum, Frankfurt
Wissenschaftlicher Mitarbeiter (50%) im Projekt: *Reaktionen von Waldökosystemen auf Klimawandel*
Monitoring von Chlorophyllgehalt und Chlorophyll a Fluoreszenz
Experimente im Bereich Trocken-, Hitze- und Kältestress
- 07/2013–08/2013 Nordsee, Deutsche AWZ. Monitoring an Bord FK Senckenberg
Marine Zoology, Sektion Crustacea, Prof. Dr. M. Türkay
Beprobung: Benthos und Wassersäule
- 06/2013 Baku, Aserbaidshan
Teilnahme an Konferenz: Photosynthesis Research for Sustainability
Auszeichnung mit einem „Best Poster“ Award
- 07/2011 Mongolei, Ulan Bator und Khentai Gebirge
Summer School: Ökologie und Ökophysiologie
Vegetationsaufnahmen und Ökophysiologisches Monitoring
- 07/2010–08/2010 Nordsee, Doggerbank. Monitoring an Bord FK Senckenberg
Marine Zoology, Sektion Crustacea, Prof. Dr. M. Türkay
Beprobung: Benthos und Wassersäule
- 06/2010 Nordsee, Jade. Monitoring an Bord FK Senckenberg
Marine Zoology, Sektion Crustacea, Prof. Dr. M. Türkay
Beprobung: Plankton und Benthos und Wassersäule
- 10/2009–01/2010 Goethe Universität Frankfurt, Inst. für Ökologie und Evolution.
Dr. O. Tackenberg. Wissenschaftliche Hilfskraft.
Sammlung von Pflanzenmaterial *Ambrosia artemisiifolia* L. in den USA. (Südstaaten und Teile des mittleren Westens (6000 km)

- 12/200903/2010 Senckenberg, Frankfurt. Abt. Paläobiologie der Wirbeltiere
Funktionelle Morphologie. Prof. Dr. F. Schrenk.
Wissenschaftliche Hilfskraft
Kursbetreuung im anatomischen Praktikum und Segmentierung
von Mikro-CT Daten mit AMIRA 5
- 10/2009 Census of the Diversity of Marine Abyssal Life (CeDAMar)
Wissenschaftliche Beschreibung einer unbekanntes *Zosime* Art
der Tiefsee (Crustacea: Copepoda: Harpacticoida)
- 05/2009 Seamount Expedition P384 an Bord FS Poseidon. Atlantik
Dt. Zentrum für Marine Biodiversitätsforschung, Senckenberg am
Meer, Wilhelmshaven. Prof. Dr. M. Türkay, Dr. K.-H. George

Publikationen

- 2014 Koller S., Jedmowski C., Kamm K., Brüggemann W.
The South Hesse Oak Project (SHOP): *Species- and site-specific efficiency of the photosynthetic apparatus of Mediterranean and Central European Oaks*. Plant Biosystems
- 2014 Holland V., Koller S., Brüggemann W.
Insight into the photosynthetic apparatus in evergreen and deciduous European oaks during autumn senescence using OJIP fluorescence transient analysis. Plant Biology
- 2013 Koller S., Holland V., Brüggemann W.
Effects of drought stress on the evergreen Quercus ilex L., the deciduous Q. robur L. and their hybrid Q. x turneri Willd. Photosynthetica
- 2011 Koller S. & George K.H.
Description of a new species of Zosime Boeck, 1872 (Copepoda: Harpacticoida: Zosimeidae) from the Great Meteor Seamount, representing one of the few eurybathic Harpacticoida among the distinct plateau and deep-sea assemblages. Meiofauna Marina

Danksagung

Mein Dank gilt Herrn Prof. Dr. Wolfgang Brüggemann für die Möglichkeit meine Arbeit im Bereich Ökophysiologie der Pflanzen durchführen zu dürfen und für das Vertrauen, das mir im Hinblick auf das Verfolgen meiner eigenen Forschungsinteressen im Projekt entgegen gebracht wurde. Ebenso danke ich Prof. Dr. Imke Schmitt, für die Zweitbetreuung meiner Arbeit.

Danke an Dr. Ahmed Ashoub, Ulrike Feickert, Renate Pathe und Roswitha Caps, die jederzeit ein offenes Ohr für neue Ideen hatten, sich um mein Wohlbefinden gesorgt und mich stets motiviert haben.

Vielen Dank an meine Kollegen Vera Holland, Tanja Jungcurt, Katharina Kamm und Christoph Jedmowski, auf die man nicht nur im Arbeitsalltag, sondern auch bei der Feldarbeit und auf Expeditionen immer zählen kann. Wir waren ein tolles Team! Jederzeit wieder!

Danke an unsere Partner im South Hesse Oak Project und die Mitarbeiter des Botanischen Gartens der Uni Frankfurt für die gute Zusammenarbeit.

Vielen Dank an David Russel, Barbara Jaeschke und Sebastian Moll des Senckenberg Museums für Naturkunde Görlitz für die Ermöglichung und Unterstützung bei der Messung der Stickstoffgehalte.

Ein Besonderer Dank gilt meiner Familie und meinen Freunden

Meinen Eltern, meiner Schwester, meinen Schwiegereltern, meiner Schwägerin und besonders meiner Frau Anne. Ich habe das großes Glück, Euch stets an meiner Seite zu wissen!

Ich widme diese Arbeit meiner Familie und meiner kleinen Juliane!